EMBEDDING THIOLS INTO CHOLINE PHOSPHATE POLYMER ZWITTERIONS: SYNTHESIS AND INTEGRATION INTO BIOMOLECULAR MATERIALS

EMBEDDING THIOLS INTO CHOLINE PHOSPHATE POLYMER ZWITTERIONS: SYNTHESIS AND INTEGRATION INTO BIOMOLECULAR MATERIALS

A Dissertation Presented

By

DEBORAH JOY CASSARO-SNYDER

Submitted to the Graduate School of the
University of Massachusetts Amherst in partial fulfillment
of the requirements for the degree of

DOCTOR OF PHILOSOPHY

May 2024

Polymer Science and Engineering

EMBEDDING THIOLS INTO CHOLINE PHOSPHATE POLYMER ZWITTERIONS: SYNTHESIS AND INTEGRATION INTO BIOMOLECULAR MATERIALS

A Dissertation Presented

By

DEBORAH JOY CASSARO-SNYDER

Approved as to style and content by:

_____
Todd Emrick, Chair

_____
David Hoagland, Member

_____
Peter Beltramo, Member

_____
Alfred Crosby, Department Head
Polymer Science & Engineering

DEDICATION

To the One who works all things together for the good of those who love Him.

ACKNOWLEDGMENTS

First and foremost, I would like to thank Dr. Todd Emrick for the pivotal role that he has played in my academic and scientific growth. He has pushed me to my limits and beyond, challenging me and what I thought I could achieve. I also want to thank the other members of my thesis committee, Dr. David Hoagland and Dr. Peter Beltramo, for their unique perspectives on my research. Your support has been invaluable and greatly appreciated.

I want to additionally thank my collaborators, Dr. Weiguo Hu and Gabrielle Ho, for their insight into NMR solution dynamics. I gained a deeper understanding and appreciation of NMR spectroscopy, and a greater appreciation for Dr. Hu's key contributions to the department. I enjoyed our academic and life discussions together and am thankful for your wisdom.

I also want to thank Dr. Timothy Anderson (TTA), Director of the UMass-Minutemen Marching Band, for always having a seat for me in the UMass Concert Band.

Although the science is important, so are the individuals behind the scenes. I am very grateful to the PSE Staff for their crucial administrative role in helping me obtain my degree and keeping the building running for all of our experiments and research. This includes Lisa Groth, Lisa McNamara, Cheryl Kehoe, Lindy Orr, Jessica Skrocki and Maria Farrington. I also want to thank John Nicholson, Jack Hirsch, Glenda Pons, Dr. Alex Ribbe, Dr. Weiguo Hu, and Andre Melcuk for their contributions in keeping the characterization facilities up and running safely. I am also grateful for Dr. James Chambers and Dr. Steve Eyles at IALS for their insights/help to my early research. Thank you.

Equally important are the funding sources which paid for my research and thesis projects. I am grateful for the financial support for research in biomolecular materials from the Department of Energy, Office of Basic Energy Science (DE-SC0008876). I am also appreciative of the GAANN Fellowship and the NIH BTP trainee fellowships that supported me during the early years of my PhD.

I want to thank the members of the Emrick Research Group for their intellectual and emotional support during this journey, especially Dr. Liz Stubbs, Dr. Le Zhou, Dr. Jing Zhao, Dr. Zhefei Yang, Dr. Dylan Barber, and Steve Rosa. I am also thankful for the current ERG members and our daily interactions and commiserating: Eva Morgenthaler, Cornelia Messner, Hong-Gyu Seong, Grace Leone, Carla Steppan, Jordan Varma, Chris Cueto, Krishna Murthy, Kyoungwon Lee, Isha Farook, Dupyo Jeon, and Imani Page.

None of the work in this thesis would have been possible without the support of family and friends, encouraging me to continue and to see the silver lining during this incredibly arduous journey. First, I would like to thank my nerdy DnD friends: Dr. Demi Moed, Brandon Clarke, Dr. Jerred Wassgren, Eva Morgenthaler, Dr. Dylan Barber, Dr. Walter Young, Tomoko Yamazaki, and Mary-Kate Jutze. It was a pleasure to spend time watching movies and going on amazing fantasy adventures together. I additionally want to thank Kayla Koch for being a supportive friend and teaching me the importance of self-confidence. Next, I want to thank my church friends, who supported my spiritual journey over the past five years (and other wedding shenanigans): Hannah & Ryan Evini, Bree & Bruce McAlister, Meagan & Shannon Mitchell, Clara Culver, Renee Villines, Orphée Meledje, Bénédicte Miagoto, Flora Koussemian, Benjamin Tan, Christian Courchesne, Mike & Fab Courchesne, Sanjoy Mazumdar, Jaret Barrows, Dan O'Shea, and Colman

Culver. I also want to thank Daniel Kroll, my Minnesota friend, for his down-to-earth conversations and sarcasm. I especially want to thank Hannah, Bree, and Demi for being great friends and role models as we walked through difficult situations and experiences. It is an honor to do life together.

As for my family, I want to thank my parents, Georgette (Gigi) & Gary Snyder for their constant support and love in every circumstance, from helping me move to talking me off ledges. I am also very grateful for my godmother, Julia Daniel, for all her prayers, mentorship, and encouragement. I would also like to thank Jerod and April DeSicy for being role models in faith and marriage. I am also grateful for the support of my grandmother, Sandra DeSicy, my aunt, Laurie Snyder (and her partner, Janet Collins), and my late aunt, Julie Fire; thank you for your loving kindness and for instilling in me the importance of family. I am also thankful for my uncle, Jason DeSicy, and my brother, John Snyder, for their unspoken, long-distance support.

And finally, I want to thank my husband, Dominic Cassaro, for being an amazing and ridiculous teammate over the past five years. Ever since our flirtatious Star Wars beginnings, it has been such an incredible saga together, and I would not have wanted to share the highs and lows with anyone else. Your love and emotional cookie support has been greatly appreciated and words cannot express how thankful I am to have you by my side for the rest of my life.

ABSTRACT

EMBEDDING THIOLS INTO CHOLINE PHOSPHATE POLYMER ZWITTERIONS: SYNTHESIS AND INTEGRATION INTO BIOMOLECULAR MATERIALS

MAY 2024

DEBORAH JOY CASSARO-SNYDER

B.S. UNIVERSITY OF MINNESOTA TWIN CITIES

M.S., UNIVERSITY OF MASSACHUSETTS AMHERST

PH.D., UNIVERSITY OF MASSACHUSETTS AMHERST

Directed by: Professor Todd Emrick

The compositional scope of polymer zwitterions has grown significantly in recent years and now offers designer synthetic materials that are broadly applicable across numerous areas, including supracolloidal structures, electronic materials interfaces, and macromolecular therapeutics. Among recent developments in polymer zwitterion syntheses are those that allow insertion of reactive functionality directly into the zwitterionic moiety, yielding new monomer and polymer structures that hold potential for maximizing the impact of zwitterions on the macromolecular materials chemistry field. This dissertation describes the preparation of zwitterionic choline phosphate (CP) methacrylates containing either aromatic or aliphatic thiols embedded directly into the zwitterion. The polymerization of these functional CP methacrylates by reversible addition-fragmentation chain-transfer (RAFT) methodology yields polymeric zwitterionic thiols (**PZTs**) containing protected thiol functionality in the zwitterionic units. After polymerization, the protected thiols are liberated to yield thiol-rich polymer zwitterions

which serve as precursors to subsequent reactions that produce polymer networks as well as polymer-protein bioconjugates through reversible disulfide formation or by permanent addition mechanisms. Moreover, the aromatic **PZTs** are found to stabilize oil-in-water interfaces when evaluated by pendant drop tensiometry. Overall, **PZTs** represent a novel and versatile materials platform to access a variety of properties and chemistries with wide ranging potential applications in the macromolecular field, from stimuli-responsive surfactants to polymer-protein therapeutics.

TABLE OF CONTENTS

Page

ACKNOWLEDGEMENTS ..... **v**
ABSTRACT ..... **viii**
LIST OF TABLES ..... **xii**
LIST OF FIGURES ..... **xiv**
CHAPTER
1 INTRODUCTION **1**
1.1 Overview of Biomolecular Materials 1
1.2 Polymer Zwitterions 4
1.3 Thiols in Polymer Chemistry 8
1.4 Thesis Outline 11
1.5 References. 12
2 SYNTHESIS OF CHOLINE PHOSPHATE ZWITTERION MONOMERS & POLYMERS WITH EMBEDDED THIOLS **26**
2.1 Introduction 26
2.2 Synthesis of Embedded Thiol CP Zwitteiron Monomers 29
2.3 Synthesis of Embedded Thiol CP Zwitterion Polymers 35
2.4 Synthesis of Polymer Zwitterion Thiols (PZTs) 44
2.5 Summary 50
2.6 References 51
3 POLYMERIC ZWITTERIONIC THIOLS: SYNTHESIS, REACTIVITY, AND PROPERTIES **55**
3.1 Introduction 55
3.2 PZT Post-Polymerization Modifications 57
3.3 Interfacial Activity of PZTs 60
3.4 PZTs in Hydrogel Formation 64
3.5 Summary 68
3.6 References 68
4 POLYMERIC ZWITTERIONIC THIOLS IN POLYMER-PROTEIN BIOCONJUGATION **71**
4.1 Introduction 71
4.2 Disulfide Bioconjugation Mechanism 74
4.3 Vinyl Sulfone Bioconjugation Mechanism 82
4.4 Summary 87
4.5 References 87
5 CONLCUDING REMARKS **98**
6 EXPERIMENTAL METHODS **100**
6.1 Materials 100
6.2 General Methods 102
6.3 CP Zwitterion Monomer Synthesis 103

6.4 RAFT Copolymerization of CP Zwitterion Monomers 107
6.5 RAFT Homopolymerization of CP Zwitterion Monomers.....110
6.6 PZT Post-Polymerization Thiol Functionalization 111
6.7 Synthesis of Thiol-terminated Poly(MPC) 113
6.8 Ellman's Assay 114
6.9 Pendant Drop Tensiometry 115
6.10 Oil-in-Water Emulsion Formation.....115
6.11 Hydrogels.....116
6.12 Polymer-Protein Bioconjugation 117
6.13 References
.....
119**.....**
APPENDIX.....119
A: Tyrosinase-Mediated Oxidative-Addition for Polymer-Protein Bioconjugation
.....120
B: Probing Solution Dynamics, Configuration, and Molecular Weight of
Poly(MPC) by DOSY NMR.....134
BIBLIOGRAPHY.....141

LIST OF TABLES

Table **Page**

2-1. Sample reaction conditions of the ring-opening step (**Figure 2-3b**) to produce CP methacrylates **3a** and **3b** **30**

2-2. Sample reaction conditions for the ring-opening step (**Figure 2-3c**) to produce CP methacrylates **3c** and **3d**..... **33**

2-3. Representative reaction conditions and characterization results for the RAFT copolymerization of embedded thiol CP methacrylates **3a** and **3b** at various mole percents with comonomer MPC..... **39**

2-4. Molecular weight estimations by GPC analysis in TFE or aqueous eluents of RAFT copolymers **4a** and **4b** **39**

2-5. Representative reaction conditions and characterization results for the RAFT copolymerization of embedded thiol CP methacrylates **3c** and **3d** at various mole percents with comonomer MPC..... **42**

2-6. Molecular weight estimations by GPC analysis in TFE or aqueous eluents of RAFT copolymers **4c** and **4d**. **42**

2-7. Optimization of RAFT homopolymerization conditions for embedded thiol CP methacrylates **3a** **43**

2-8. Amount of free thiol (SH/chain and mol% SH) in **5a-20**, **5b-20**, **5c-20**, and **5d-20** copolymers as determined by Ellman's Assay by measuring absorbance (A_{412})..... **47**

3-1. Functional group incorporation (mol%) into **PZT** copolymers containing 20 mol% CP content as determined by ^{1}H NMR spectroscopy following post-polymerization modification..... **59**

3-2. Optimization of hydrogel formation conditions formed *via* UV-catalyzed thiol-Michael addition using **5a-20** copolymer and PEG diacrylate solutions at various wt% polymer and VA-044 initiator concentrations. All polymer molecular weights were calculated by ^{1}H NMR end group analysis or GPC analysis (*) in TFE eluents **62**

3-3. Optimization of hydrogel formation conditions formed *via* disulfide formation using **5a-20** copolymer at various wt% in 0.1 M PBS buffer (1 mM EDTA) with PEG1000 dithiol as crosslinker. All polymer

molecular weights were calculated by ^{1}H NMR end group analysis or GPC analysis (+) in TFE eluents **63**

4-1. Amount of free thiol per protein (native or reduced), as determined following an Ellman's assay procedure. **75**

4-2. List of buffer conditions (1-24) utilized in bioconjugation reactions between **5b-20** or thiol-terminated PMPC and reduced BSA *via* disulfide formation..... **78**

LIST OF FIGURES

Figure **Page**

1-1. Chemically tunable polymer surfactants provide access to triggered stimulus response and cell-like structures. (**a**) Polymer zwitterion-amine (PZA) surfactants form sticky emulsion droplets that can be printed into supracolloidal fibers at basic pHs; upon exposure to acidic environments, the droplets become non-sticky and collapse.[26] (**b**) *Tert*-butyl methacrylate terpolymer films can be converted into hydrophobic or hydrophilic mesoscale polymer ribbons (MSPs) through embedded coumarin and photoacid generator moieties, which control crosslinking and *tert*-butyl deprotection, respectively. The resulting MSPs are surface active at oil-water interfaces and can form structures (arms) that extend into solution.[28] **2**

1-2. Integrating proteins into biomolecular assemblies. (**a**) Simulations of microcapsule assembly driven by enzyme catalysis: the immobilized enzyme (on the dark green patch) generates concentration gradients that develop into local fluid flows that direct assembly of the microcapsules into towers. Reproduced with permission.[49] Copyright 2018, American Chemical Society. (**b**) Cowpea mosaic virus, which stabilizes oil-in-water emulsions droplets, forms robust capsules (*left*) that maintain their integrity after drying and rehydration steps (*right*) following glutaraldehyde crosslinking. Adapted under terms of the CC-BY-4.0 license.[52] Copyright 2005, the Authors, Wiley-VCH **3**

1-3. (**a**) Schematic of the phospholipid bilayer found in cell membranes, including the chemical structure of an individual phospholipid whose polar head group (pink) contains a zwitterion. (**b**) Structures of the most common polymer zwitterions, such as poly(MPC), which most closely resembles the phospholipid head groups of cell membranes **5**

1-4. Examples of thiol reaction partners encompassing a variety of chemistries and coupling mechanisms **9**

2-1. (**a**) Competing endo- and exo-cyclic synthetic pathways in ring-opening of substituted ECPs, with comparison to the synthesis of MPC. (**b**) Functional CP zwitterionic monomers synthesized previously (in italics), including reactive CP-based alkenes and alkynes, CP benzophenone, and CP disulfide dimethacrylate.. ..... **27**

2-2. Embedded thiol choline phosphate zwitterion (**a**) monomers and (**b**) polymers synthesized in this chapter **29**

2-3. Synthesis of *S*-trityl-protected CP zwitterion monomers by ring-opening the (**a**) precursor phospholanes **2a** or **2b** with (**b**) dimethylamino methacrylate to give **3a** and **3b** or (**c**) vinylbenzyl dimethylamine to obtain **3c** and **3d**..... **30**

2-4. (**a**) ^{1}H and ^{31}P NMR (inset) spectra of CP methacrylate **3a** in MeOD-*d4*, including the (**b**) ESI spectrum in positive ion mode **31**

2-5. (**a**) ^{1}H and ^{31}P NMR (inset) spectra of CP methacrylate **3b** in MeOD-*d4*, including the (**b**) ESI spectrum in positive ion mode **32**

2-6. (**a**) ^{1}H and ^{31}P NMR (inset) spectra of CP styrene **3c** in MeOD-*d4*, including (**b**) ESI spectrum in positive ion mode. **33**

2-7. (**a**) ^{1}H and ^{31}P NMR (inset) spectra of CP styrene **3d** in MeOD-*d4*, including (**b**) ESI spectrum in positive ion mode. **34**

2-8. Synthesis of random copolymer zwitterions incorporating (**a**) CP methacrylates **4a** and **4b** or (**b**) CP styrenes **4c** and **4d** *via* RAFT conditions in the presence of a dithiobenzoate chain transfer agent (CTA) and azo initiator (ACVA). **35**

2-9. Depletion of the vinyl proton resonances of CP methacrylate monomers (denoted $\mathbf{H_1}$) and MPC (denoted $\mathbf{H_2}$) for the RAFT copolymerization of (**a**) aromatic **3a** or (**b**) aliphatic **3b** with MPC, as monitored by ^{1}H NMR spectroscopy in MeOD-*d4*. The five spectra were recorded from aliquots taken from the polymerizations at t = 2h (red), 4h (orange), 6h (yellow), 8h (green), and 24h (blue)..... **36**

2-10. (**a**) Structure of random copolymer zwitterion **4a** containing 20 mol % **3a** following RAFT copolymerization with MPC. (**b**) ^{1}H and (**c**) ^{31}P NMR spectra in MeOD-*d4* of **4a-20** and (**c**) representative GPC traces, including estimated molecular weight and PDI values, in TFE and aqueous eluents **37**

2-11. (**a**) Structure of random copolymer zwitterion **4b** containing 20 mol % **3b** following RAFT copolymerization with MPC. (**b**) ^{1}H and (**c**) ^{31}P NMR spectra in MeOD-*d4* of **4b-20** and (**c**) representative GPC traces, including estimated molecular weight and PDI values, in TFE and aqueous eluents **38**

2-12. (**a**) Synthesis random copolymer zwitterion **4c** *via* RAFT conditions in the presence of a dithiobenzoate chain transfer agent (CTA) and azo initiator (ACVA). (**b**) ^{1}H and (**c**) ^{31}P NMR spectra in MeOD-*d4* and (**c**) representative GPC traces, including estimated molecular weight and PDI values, in TFE and aqueous eluents for copolymer **4c** containing 20 mol % **3c** with MPC..... **40**

2-13. (**a**) Synthesis random copolymer zwitterion **4d** *via* RAFT conditions in the presence of a dithiobenzoate chain transfer agent (CTA) and azo initiator (ACVA). (**b**) ^{1}H and (**c**) ^{31}P NMR spectra in MeOD-*d4* and (**c**) representative GPC traces, including estimated molecular weight and PDI values, in TFE and aqueous eluents for copolymer **4d** containing 20 mol % **3d** with MPC..... **41**

2-14. (**a**) Structure of homopolymer zwitterion **3a** and its (**b**) ^{1}H and (*inset*) ^{31}P NMR spectra in DMSO-*d6*..... **43**

2-15. General reaction scheme for deprotection of embedded thiol CP polymer zwitterions to yield CP polymer zwitterion thiols (**PZTs**). **45**

2-16. (**a**) Structure of **PZT 5a** following TFA deprotection. (**b**) ^{1}H NMR spectra of **5a-20** in MeOD-*d4* and (**c**) ^{31}P NMR spectra of **5a-20** compared to **4a-20** in MeOD-*d4*, including (**d**) representative GPC traces of **4a-20** versus **5a-20** in TFE eluents and (**e**) associated GPC molecular weight estimates and PDI values for both TFE and aqueous eluents. **46**

2-17. (**a**) Structure of **PZT 5b** following TFA deprotection. (**b**) ^{1}H NMR spectra of **5b-20** in MeOD-*d4* and (**c**) ^{31}P NMR spectra of **5b-20** compared to **4b-20** in MeOD-*d4*, including (**d**) representative GPC traces of **4b-20** versus **5b-20** in TFE eluents and (**e**) associated GPC molecular weight estimates and PDI values for both TFE and aqueous eluents. **47**

2-18. (**a**) ^{31}P NMR spectrum of **5a-20** copolymers in 0.1 M PBS pH 8 with 10% D_2O as is (bottom line), after addition of 10 mM TCEP (middle line), and after exposure to 0.8 M hydrogen peroxide for 30 minutes (top line). (**b**) ^{31}P NMR spectrum of **5a-20** copolymers in MeOD-*d4* as is (bottom line), after addition of 10 mM TCEP (middle line), and after exposure to 0.8 M hydrogen peroxide for 30 minutes (top line). **48**

2-19. (**a**) Structure of **PZT 5c** following TFA deprotection. (**b**) ^{1}H NMR spectra of **5c-20** in MeOD-*d4* and (**c**) ^{31}P NMR spectra of **5c-20** compared to **4c-20** in MeOD-*d4*, including (**d**) representative GPC traces

of **4c-20** versus **5c-20** in TFE eluents and (**e**) associated GPC molecular weight estimates and PDI values for both TFE and aqueous eluents. **49**

2-20. (**a**) Structure of **PZT 5d** following TFA deprotection. (**b**) ^{1}H NMR spectra of **5d-20** in MeOD-*d4* and (**c**) ^{31}P NMR spectra of **5d-20** compared to **4d-20** in MeOD-*d4*, including (**d**) representative GPC traces of **4d-20** versus **5d-20** in TFE eluents and (**e**) associated GPC molecular weight estimates and PDI values for both TFE and aqueous eluents. **50**

3-1. General reaction scheme for post-polymerization modifications of **PZTs** with dipyridyl disulfide and divinyl sulfone **57**

3-2. (**a**) Structure of VS-modified copolymer zwitterion **6a**. (**b**) ^{1}H and (**c**) ^{31}P NMR spectra in MeOD-*d4* and (**d**) representative GPC traces, including (**e**) estimated molecular weight and PDI values, in aqueous and TFE eluents. **58**

3-3. (**a**) Structure of VS-modified copolymer zwitterion **6b**. (**b**) ^{1}H and (**c**) ^{31}P NMR spectra in MeOD-*d4* and (**d**) representative GPC traces, including (**e**) estimated molecular weight and PDI values, in TFE and aqueous eluents **58**

3-4. (**a**) Structure of DPDS-modified copolymer zwitterion **7a-20**. (**b**) ^{1}H and (**c**) ^{31}P NMR spectra in MeOD-*d4* and (**d**) representative GPC traces, including estimated (**e**) molecular weight and dispersity values, in TFE and aqueous eluents **59**

3-5. (**a**) Structure of DPDS-modified copolymer zwitterion **7b-20**. (**b**) ^{1}H and (**c**) ^{31}P NMR spectra in MeOD-*d4* and (**d**) representative GPC traces, including estimated (**e**) molecular weight and dispersity values, in TFE eluents **60**

3-6. (**a**) Schematic of hydrogel formation using **PZTs** with difunctional crosslinkers. (**b**) Photographs of hydrogels (600 mg scale) formed *via* UV-catalyzed thiol-Michael addition between **5a-20** copolymers (at 10 wt%) and PEG700 diacrylate (acrylate-to-thiol ratio = 5.1) in the presence of VA-044 initiator (2 wt%). (**c**) Optical images of hydrogels (900 mg scale) formed *via* disulfide formation between PEG1000 dithiol (acrylate-to-thiol ratio = 5.4) and **5a-20** copolymers (20 wt%) in 0.1 M PBS pH 8 buffer with 28 M H_2O_2. Addition of TCEP leads to cleavage of disulfides, resulting in hydrogel dissolution, which re-forms upon exposure to 28 M H_2O_2. The swelling over time of **5a-20** hydrogels (50-

100 µL scale) created from (**d**) thiol-Michael (acrylate-to-thiol ratio = 5.6, 13 wt% polymer) or (**e**) disulfide mechanisms (acrylate-to-thiol ratio = 2.0, 32 wt% polymer). Scale bar = 0.45 cm. **61**

3-7. (**a**) Interfacial tension curves (mN/m) from pendant drop tensiometry evaluation of aromatic **PZT**s **4a-20** and **4a-50** (protected), and **5a-20** and **5a-50** (deprotected), including aliphatic **PZTs 4b-20** and **5b-20**, at 0.5 mg/mL (drop phase = TCB; aqueous phase = DI water). (**b**) Photographs of the corresponding oil-in-water emulsions stabilized by aromatic (**4a-20**, **4a-50**) or aliphatic (**4b-20**) protected **PZTs** (*top*), and by aromatic (**5a-20**, **5a-50**) or aliphatic (**5b-20**) deprotected **PZTs** (*bottom*), on a **PZT** concentration range of 0.5 to 10 mg/mL..... **65**

3-8. Photographs of oil-in-water emulsion droplets stabilized by protected (**4a-20**) or deprotected (**5a-20**) **PZTs** at 0.5 mg/mL prepared using various continuous phases, aged 16 hours. Encapsulated phase = TCB. Asterisks (*) designate emulsions that are stable for months..... **66**

3-9. Photographs of oil-in-water emulsions stabilized by aromatic protected (**4c-20**) and deprotected (**5c-20**) or aliphatic protected (**4d-20**) and deprotected (**5d-20**) **SPZTs** on a concentration range of 0.5 to 10 mg/mL (oil phase = TCB; aqueous phase = DI water)..... **67**

4-1. Schematic of (**a**) mono-/bi-functional PEGs with limited functionality at the chain ends relative to (**b**) multi-functional **PZTs**, where the functional groups are pendent to the polymer backbone. (**c**) Scheme depicting formation of polymer-protein bioconjugates in this chapter using **5a-20** or **6a-20 PZT** copolymers **73**

4-2. SDS-PAGE gels of the bioconjugation reaction of **5a-20** with reduced protein (CAT, BSA, and GOX) utilizing a disulfide mechanism after 24 hours incubation in 0.1 M PBS buffer at various pH values (7-9), (**a**) before and (**b**) after pre-treatment with reducing agent (TCEP). Lane 1 is the molecular weight protein ladder, lane 2 is the polymer control, and lane 3 is the protein control. Lanes 4-6 are the BSA experimental conditions, at pH 7, 8 and 9, respectively. Size-exclusion FPLC chromatograms of reduced **5a-20** bioconjugates od (**c**) BSA or (**d**) CAT from lanes 4, 5, and 6 (BSA) or lanes 8, 9 and 10 (CAT) in (**a**) and (**b**). Mobile phase is 0.1 M PBS pH 7.4 (0.14 M NaCl, 2.7 mM KCl) **76**

4-3. SDS-PAGE gels of the bioconjugation reaction of **5a-20** with native BSA utilizing a disulfide mechanism after 24 hours incubation in 0.1 M PBS

buffer (0.14 M NaCl, 2.7 mM KCl) at various pH values (7-9), (**a**) before and (**b**) after pre-treatment with reducing agent (TCEP). Lane 1 is the molecular weight protein ladder, lane 2 is the polymer control, and lane 3 is the protein control. Lanes 4-6 are the BSA experimental conditions, at pH 7, 8 and 9, respectively. (**c**) Size-exclusion FPLC chromatograms of BSA and **5a-20**-BSA bioconjugates from lanes 4, 5, and 6 in (**a**). Mobile phase is 0.1 M PBS pH 7.4 (0.14 M NaCl, 2.7 mM KCl) **77**

4-4. SDS-PAGE gels of the bioconjugation reaction of **5b-20** with reduced protein (BSA, HRP or LYS) utilizing a disulfide mechanism after 24 hours incubation in 0.1 M PBS buffer (0.14 M NaCl, 2.7 mM KCl) at various pH values (7-9). Lane 1 is the molecular weight protein ladder, lane 2 is the polymer control, and lane 3 is the protein control. Lanes 2, 7, and 11 represent the BSA, HRP and LYS protein controls, respectively. Lanes 4-6 are the BSA experimental conditions at pH 7, 8 and 9, respectively; and lanes 8-10 and lanes 12-14 are the HRP and LYS experimental conditions, respectively..... **78**

4-5. SDS-PAGE gels of the bioconjugation reactions between **5b-20** or thiol-terminated PMPC (**PCSH**) and reduced BSA in a disulfide mechanism after 24 hours incubation in the various buffer conditions (1-24) outlined in **Table 4-2**. For each gel, lane 1 is the molecular weight protein ladder. For (**a**), lane 2 is the polymer control and lane 3 is the reduced BSA control. Lanes 4, 6, 8, 10, 12, and 14 are the experimental conditions for **5b-20** reactions in for reaction conditions 1-6. Lanes 5, 7, 9, 11, 13, and 15 are the experimental conditions for **PCSH** reactions in for reaction conditions 1-6. For (**b-c**), lanes 2, 4, 6, 8, 10, 12, and 14 are the experimental conditions for **5b-20** reactions in conditions 7-20. Lanes 3, 5, 7, 9, 11, 13, and 15 are the experimental conditions for **PCSH** reactions in conditions 7-20. For (**d**), lanes 2, 4, 6, and 8 are the experimental conditions for **5b-20** reactions in conditions 21-24. Lanes 3, 5, 7, and 9 are the experimental conditions for **PCSH** reactions in conditions 21-24. The white arrows indicate lanes demonstrating bioconjugation **79**

4-6. (**a**) Reaction scheme to obtain thiol-terminated poly(MPC). (**b**) ^{1}H NMR spectrum in D_2O of poly(MPC) (*top*) and poly(MPC)-SH (*bottom*) showing loss of aromatic resonances following base-catalyzed hydrolysis of the dithiobenzoate chain end. (**c**) Representative GPC traces of poly(MPC) in TFE eluents before and after base hydrolysis, including (**d**) estimated molecular weight and PDI values, and (**e**)

estimated free thiol per polymer chain as determined *via* Ellman's Assay **80**

4-7. SDS-PAGE gels of the bioconjugation reactions between **7b-20** and (**a,b**) reduced BSA or (**c**) reduced LYS in an activated disulfide mechanism after 5 days incubation in the various buffer conditions outlined in **Table 4-2**. For each gel, lane 1 is the molecular weight protein ladder. For (**a**), lane 2 is the polymer control and lane 3 is the reduced BSA control. Lanes 4-15 are the experimental conditions 1-6, 10-12, and 25-26. For (**b**), lanes 2-10 are the experimental conditions 7 and 15-24. For (**c**), lane 2 is the polymer control and lane 3 is the reduced LYS control. Lanes 4-15 are the experimental conditions 1-4, 7, 10, 16, 18-21, and 23-23. The white arrow indicates a lane that exhibits broadening of the protein band and thus possible bioconjugation; however, no changes in retention time were observed by FPLC characterization **81**

4-8. SDS-PAGE gels of the bioconjugation reactions between (**a**) **5c-20** or (**b**) **5d-20** and reduced protein (BSA, CAT) or native BSA utilizing a disulfide mechanism after 24 hours in 0.1 M PBS buffer at various pH values (7-9). Lane 1 is the molecular weight protein ladder; lane 2 is the polymer control; and lanes 3, 7, and 11 are the protein controls. Lanes 4-6 are the BSA experimental conditions, at pH 7, 8 and 9, respectively. Lanes 8-10 are the reduced BSA experimental conditions, at pH 7, 8 and 9, respectively. Lanes 12-14 are the reduced CAT experimental conditions, at pH 7, 8 and 9, respectively **81**

4-9. SDS-PAGE gels of the bioconjugation reactions between VS-modified **PZT 6a** and (**a**) BSA, (**b**) GOX, (**c**) LYS, and (**d**) HRP in various buffer conditions after 24 hours. Lane 1 is the molecular weight ladder, lane 2 is the polymer control, and lane 3 is the protein control. Lanes 4-8 are the **PZT 6a** experimental conditions, with each lane representing a different buffer condition. Condition a: 0.15 M PBS; Condition b: Certipur Borate; Condition c: 0.1 M Sodium Bicarbonate; Condition d: 0.15 M HEPES; Condition e: 0.15 M Tris. All conditions were at pH 9.2, 1 mM EDTA **83**

4-10. (**a**) SDS-PAGE of bioconjugation reactions between the VS-modified **PZT 6a** and reduced or native BSA and GOX after 16 hours in Certipur Borate buffer pH 9.2 with 1 mM EDTA. Lane 1 is the molecular weight protein ladder, lane 2 is the polymer control, and lanes 3 and 6 are the protein controls. Lanes 4 and 7 are the **6a-20** experimental conditions with native protein while lanes 5 and 8 are with reduced protein. (**b**)

SDS-PAGE of bioconjugation reactions between VS-modified **PZT 6a** and BSA, GOX, HRP, and LYS after 16 hours with or without reducing agent (TCEP) in Certipure Borate buffer pH 9.2 with 1 mM EDTA. Lane 1 is the molecular weight protein ladder and lanes 3, 6, 9, and 12 are the protein controls. Lanes 4, 7, 10, and 13 are the **PZT 6a** experimental conditions without TCEP; lanes 5, 8, 11, and 14 have TCEP. **84**

4-11. Size-exclusion FPLC chromatograms of **PZT 6a**-protein conjugates for (**a**) BSA, (**b**) LYS or (**c**) HRP. Each bioconjugate formed from condition a-e is denoted with a different colored line: Condition a: 0.15 M PBS (red); Condition b: Certipur Borate; Condition (green); c: 0.1 M Sodium Bicarbonate (thin purple); Condition d: 0.15 M HEPES (pink); Condition e: 0.15 M Tris (orange). All conditions were at pH 9.2, 1 mM EDTA. Mobile phase is 0.1 M PBS pH 7.4 (0.14 M NaCl, 2.7 mM KCl) **85**

4-12. SDS-PAGE gels of attempted bioconjugation reactions between **PZT 6b** and (**a**) BSA, (**b**) GOX, (**c**) LYS, and (**d**) HRP in various buffer conditions after 24 hours. Lane 1 is the molecular weight ladder, lane 2 is the polymer control, and lane 3 is the protein control. Lanes 4-8 are the **6b-20** experimental conditions with each lane representing a different buffer condition. Condition a: 0.15 M PBS; Condition b: Certipur Borate; Condition c: 0.1 M Sodium Bicarbonate; Condition d: 0.15 M HEPES; Condition e: 0.15 M Tris. All conditions were at pH 9.2, 1 mM EDTA..... **86**

CHAPTER ONE:
INTRODUCTION

1.1 Overview of Biomolecular Materials

Biomolecular materials merge synthetic and biological concepts from the materials/biology interface, with potential to create innovative, new materials with hybrid properties that extend beyond their constituents alone. This has been especially evident in fields where out-of-equilibrium processes govern biological response, which are critical for sensing and adapting to changes in local environment,[1-2] and are driving new discoveries in numerous research areas, such as in synthetic cells development.[1-4] While a variety of synthetic cell-like structures have been described–from polymersomes and vesicles to nanoparticles and coacervates–emulsion droplets are an attractive soft matter system since their surfactant-stabilized interface offers control over structure and function.[3,6-8] More specifically, droplet movements mimicking cellular motion were achieved by creating surface tension differentials or instabilities that give rise to Marangoni forces at the droplet interface[1,9-14] through chemical reactions (*i.e.*, hydrolysis,[15-16] surfactant generation,[17-18] light isomerization,[19-20] *etc*.) and internalized active components (*e.g.*, actin[21]). Emulsion droplets are also capable of chasing prey[22] and following surfactant[14], substrate[23] or salt[24] concentrations, a form of motion referred to as chemotaxis.

Polymer surfactants are especially interesting for accessing responsive emulsion droplets, in part due to their chemical tunability *via* functional groups that may impart pre-programmed stimulus response. Functional polymer surfactants can therefore control interfacial properties and subsequent behaviors of the oil-in-water droplet, from phase inversion to self-replication.[25] For instance, oil-in-water droplets stabilized by polymer zwitterion surfactants with cationic comonomers form extrudable, sticky fibers (i.e.,

droplet assemblies) at basic pH as a result of electrostatic attractions of droplet interfaces; however, the droplets undergo triggered coalescence when those interactions are disrupted under acidic conditions (**Figure 1-1a**).[26] Sulfothetin polymer surfactants can additionally be utilized to create supracolloidal droplet fibers that, when prepared with toluene as the oil phase, exhibit sefl-driven motion at the air-water interface due to Marangoni forces that arise as polymer surfactant migrates from the oil-water interface to the air-water interface.[27] Alternatively, mesoscale polymer ribbons, derived from *tert*-butyl methacrylate terpolymers containing crosslinking units and photo-switchable wetting properties, are interfacially active and form extendable arm-like structures that reach past the droplet interface into solution, akin to dendritic cells (**Figure 1-1b**).[28-29] Biological self-healing

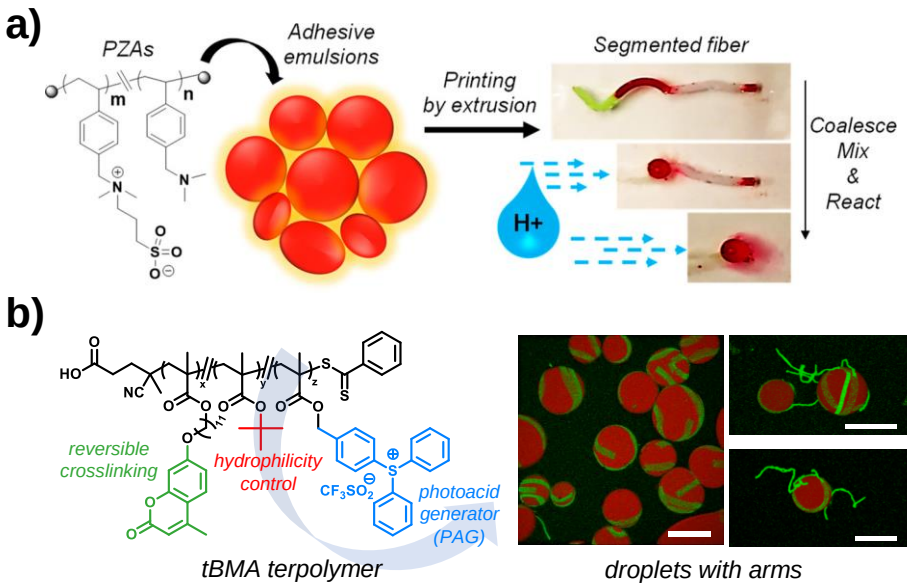

Figure 1-1. Chemically tunable polymer surfactants provide access to triggered stimulus response and cell-like structures. (**a**) Polymer zwitterion-amine (PZA) surfactants form sticky emulsion droplets that can be printed into supracolloidal fibers at basic pHs; upon exposure to acidic environments, the droplets become non-sticky and collapse.[26] (**b**) *Tert*-butyl methacrylate terpolymer films can be converted into hydrophobic or hydrophilic mesoscale polymer ribbons (MSPs) through embedded coumarin and photoacid generator moieties, which control crosslinking and *tert*-butyl deprotection, respectively. The resulting MSPs are surface active at oil-water interfaces and can form structures (arms) that extend into solution.[28]

mechanisms, as exemplified by the role of osteoclast cells in bone repair,[30] have likewise been replicated.[31-37] Fundamental research pioneered by Kratz, *et al.* generated oil-in-water droplets capable of delivering nanoparticles (NPs) to damaged sites of substrates, thereby restoring mechanical integrity.[32,35-36] Critical to substrate repair were the carboxylate groups of the copolymer surfactants, which reversibly bound to the SiO_2 NPs via electrostatic interactions.[36]

Biomolecular materials often incorporate biological entities (i.e., proteins, viruses, etc.) into hybrid materials system through chemistry and/or structure, including enzyme-powered microswimmers,[38-40] intrinsically disordered protein biomaterials,[41-43] and polymer-decorated drug carriers.[44-46] For instance, immobilizing enzymes onto sheets rather than spheres results in chemically propelled structures that demonstrate inchworm-like motion along both smooth and rough surfaces.[47] However, coating immobile substrates with enzymes instead converts the chemical potential energy of the enzymes into mechanical fluid flows, which pump solute throughout the chamber and can result in particle assembly (**Figure 1-2a**).[48-50] Polymer-protein hybrid materials can also create new

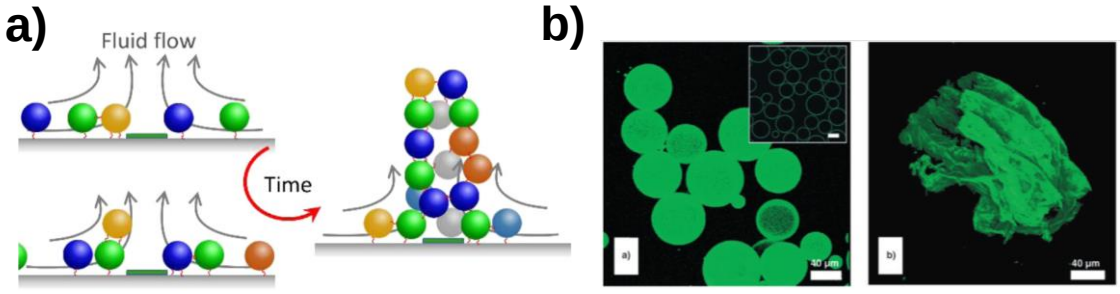

Figure 1-2. Integrating proteins into biomolecular assemblies. (**a**) Simulations of microcapsule assembly driven by enzyme catalysis: the immobilized enzyme (on the dark green patch) generates concentration gradients that develop into local fluid flows that direct assembly of the microcapsules into towers. Reproduced with permission.[49] Copyright 2018, American Chemical Society. (**b**) Cowpea mosaic virus, which stabilizes oil-in-water emulsions droplets, forms robust capsules (*left*) that maintain their integrity after drying and rehydration steps (*right*) following glutaraldehyde crosslinking. Adapted under terms of the CC-BY-4.0 license.[52] Copyright 2005, the Authors, Wiley-VCH.

assemblies and structures, as seen for ferritin-polymer conjugates. Prepared using grafting-to or grafting-from techniques, poly(MPC)- and poly(ethylene glycol methacrylate)-coated ferritin NPs were found to selectively segregate to the PEO domains of PS-*b*-PEO block copolymer films, which increased the PEO domain size while inhibiting protein adsorption.[51] Moreover, protein alone can be used to create hybrid structures as in the case of cowpea mosaic viral particles, which act as bionanoparticle surfactants at the perfluorodecalin-water interface and, when crosslinked with glutaraldehyde, form mechanically robust capsules or films (**Figure 1-2b**).[52]

These biological and materials examples and concepts form a core motivation underpinning this thesis work on novel polymer zwitterion synthesis, functional interfaces, hydrogels, and polymer-protein bioconjugates. **Section 1.2** introduces a class of bioinspired polymers known as polymer zwitterions, including their recent synthetic advances and challenges, while **Section 1.3** describes the role of thiols in accessing dynamic behaviors and structures resembling biological systems. Integrating thiols into polymer zwitterions thus enables the creation of polymers containing enzyme-like functionality while simultaneously opening routes to tunable and responsive macromolecular systems.

1.2 Polymer Zwitterions

The complex processes and behaviors of biological systems have informed numerous breakthroughs in synthetic materials design, significantly impacting application areas such as drug delivery, sustainability, and sensing.[53] Described as “bioinspired” or “biomimetic”, these innovations have led to novel materials that constitute biological

chemistries or motifs, and/or replicate biological structures or behaviors. Polymer zwitterions, which are inspired by the phospholipid headgroups of the cell membrane bilayer, are one such example (**Figure 1-3**).[54-55] Zwitterions contain two oppositely charged ions within one molecular subunit and are abundant in biology, notably in the amino acids comprising proteins, which have key roles in signal processing and catalysis.[56-58] Likewise, when zwitterions are integrated into polymer structures, each macromolecule contains multiple ion pairs. The zwitterion unit can adopt a variety of configurations depending on its synthesis, including linear, branched, or pendent structures,[59-60] and in contrast to proteins or polypeptides, polymer zwitterions remain net neutral across a wide pH range.[61-62] Incorporation of zwitterions into polymer structures gives the resultant polymers significant hydrophilicity, thus leading to impacts in medicine and surface modification.[61-68] The first synthesis of zwitterionic monomer 2-methacryloyloxyethyl phosphorylcholine methacrylate, more commonly known as MPC, was reported in 1977 by Nakai, *et al.*[69] Initial studies revealed that poly(MPC) coatings reduced protein absorption and minimized blood thrombogenicity, which was attributed to its extreme hydrophilicity.[69-71] Carboxybetaine and sulfobetaine zwitterions were also developed around this time and

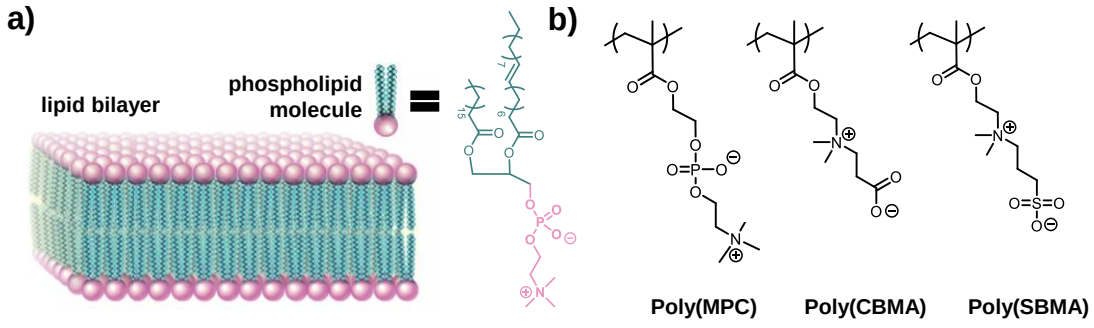

Figure 1-3. (**a**) Schematic of the phospholipid bilayer found in cell membranes, including the chemical structure of an individual phospholipid whose polar head group (pink) contains a zwitterion. (**b**) Structures of the most common polymer zwitterions, such as poly(MPC), which most closely resembles the phospholipid head groups of cell membranes.

likewise have been studied extensively as non-fouling coasting, for example by Jiang and coworkers.[72-77] The cumulative results of these research efforts eventually led to polymer zwitterions being key components of consumer products, such as contact lenses and medical devices.[61, 78-79]

The properties of polymer zwitterions are typically controlled by the selection of anion-cation pair. Sulfobetaine (SB), carboxybetaine (CB), and phosphorylcholine (PC) zwitterions (**Figure 1-3b**), all of which contain an ammonium group, accompanied by either a sulfonate, carbonate or phosphate anion, respectively, are among the most extensively utilized zwitterions.[62-63,68,76] Recent work by Brown, *et al.* and Chalarca, *et al.* in Todd Emrick's group at UMass Amherst, has expanded the zwitterion library and its properties by introducing sulfonate zwitterions containing phosphonium or sulfonium cations.[80-82] For example, phosphonium sulfonate (PS) zwitterions impart organic solubility to the resulting polymer and provide routes to interfacial stabilization oil-in-water droplets, similar to sulfonium sulfonate polymer zwitterions.[80-82] Moreover, when copolymerized with MPC, the PS copolymers function as amphiphiles and self-assemble into polymeric micelles; depending on the solution conditions, the PS groups are solvent-exposed in the corona or form the micelle core.[80]

One way to modulate polymer zwitterion properties by through addition of functional groups adjacent to the zwitterion subunit.[83] Specific to CP polymer zwitterions, functionality is incorporated through substitution of functional alcohols onto ethylene chlorophosphate (ECP), which can then be ring-opened to give the desired CP zwitterion monomer. However, this crucial ring-opening step limits advances in CP zwitterion synthesis since phospholane ring intermediate has two sites available for nucleophilic

attack: either the *endo* methylene position to yield the desired zwitterion, or the *exo* position to produce the unwanted salt.[83] Nevertheless, a limited number of polymer zwitterions has been produced following this method, with initial synthetic efforts incorporating aliphatic chains (i.e., methyl, isopropyl, butyl, etc.) adjacent to the zwitterion and pendent to the main chain;[83-85] interestingly, *n*-butyl substituents were found to form aggregated solution structures while remaining biocompatible.[85] More recently, as reported by Zhou, *et al.*, incorporation of fluorinated moieties to give fluorinated polymer zwitterions did not reduce the biocompatibility of the resultant polymers, even though per- and polyfluoroalkylated substances (PFAS) are typically toxic to humans and the environment, and they resisted biofouling against bovine serum albumin and lysozyme proteins more effectively than poly(MPC).[86-87] Outside of CP zwitterions, Brown *et al.* have demonstrated that changing the substituents on the ammonium cation of inverted sulfobetaine polymers (i.e., the sulfonate is positioned nearer the polymer backbone) results in unique solution behaviors, such as chain aggregation and complex emulsion formation.[88] Likewise, changing the ammonium substituents of sulfobetaine copolymers can electronically alter the work function of monolayer graphene.[89]

An alternate strategy to expand the polymer zwitterion library is by introducing of reactive groups amenable to post-polymerization modification. Such reactive handles provide a route to tunable structures and properties, which further improving the versatility of polymer zwitterions. To-date, only four reactive groups (alkyne, alkene, disulfide, and benzophenone) have been incorporated into SB or CP zwitterions.[90-93] However, even this limited selection of reactive groups enables a variety of reactions and applications.[90,93-95] For example, SB and CP alkynes were used in copper-catalyzed azide-alkyne click

chemistries to create crosslinked polymer capsules or camptothecin-containing macromolecular therapeutics, while SB and PC alkenes yielded hydrogels and nanoparticles *via* thiol-ene click chemistry.[90,93-95] On the other hand, benzophenone-substituted CP provided a route to photocrosslinkable PMPC polymer brushes while CP disulfide served as a biodegradable crosslinker for zwitterionic hydrogels.[91-92] This dissertation continues to expand the reactive functionality available to polymer zwitterions by embedding thiols into CP methacrylate monomers. The resulting thiol-substituted polymer zwitterions have their own unique properties and potential applications as zwitterion hydrogels, oil-in-water emulsions, and polymer-protein bioconjugates.

1.3 Role of Thiols in Polymer Chemistry

Sulfur and its various forms are abundant in biology, and have an important role in regulating processes crucial to living systems.[96-98] Small molecule thiols, such as glutathione, are known to regulate oxidative stress, disease, and metabolic pathways, whereas the amino acid cysteine is essential to protein folding and function.[96,99-100] Harnessing sulfur chemistry in functional monomers and polymers has led to innovation in macromolecular science, from the integral component of chain-transfer agents in reversible addition-fragmentation chain transfer (RAFT) polymerization to applications in drug delivery and optical materials.[100-101] Incorporating thiols into polymers has been particularly attractive because of the versatility of the thiol handle, which can participate in a variety of reactions including thiol-Michael, thiol-ene, thiol-yne, and disulfide formation (**Figure 1-4**).[100,102-103] Moreover, these bonds can be reversible or irreversible, depending on the reaction conditions, and can approach the quantitative and site-selective

criteria typical of click chemistries.[102,104-108] Due to these properties, thiols have risen to prominence for their utility in covalent adaptable networks and dynamic covalent chemistry, which has proven useful for stimuli responsive applications such as self-healing, drug delivery and shape memory.[104-120] However, thiols have additionally had a key role in the development of polymer therapeutics and polymer-protein bioconjugates, where their biodegradable properties and sensitivity to reducing environments are key to polymer renal clearance or therapeutic drug release.[121-125] Moreover, the interactions between thiols and gold produced the field of self-assembled monolayers (SAMs) and other surface coatings.[126-130]

Most reported thiol-based chemistries rely on aliphatic thiols to achieve dynamic and responsive polymer properties. Though less explored due to solubility challenges,[131-135] aromatic thiols can also be employed. For example, reprocessable rubbers are formed

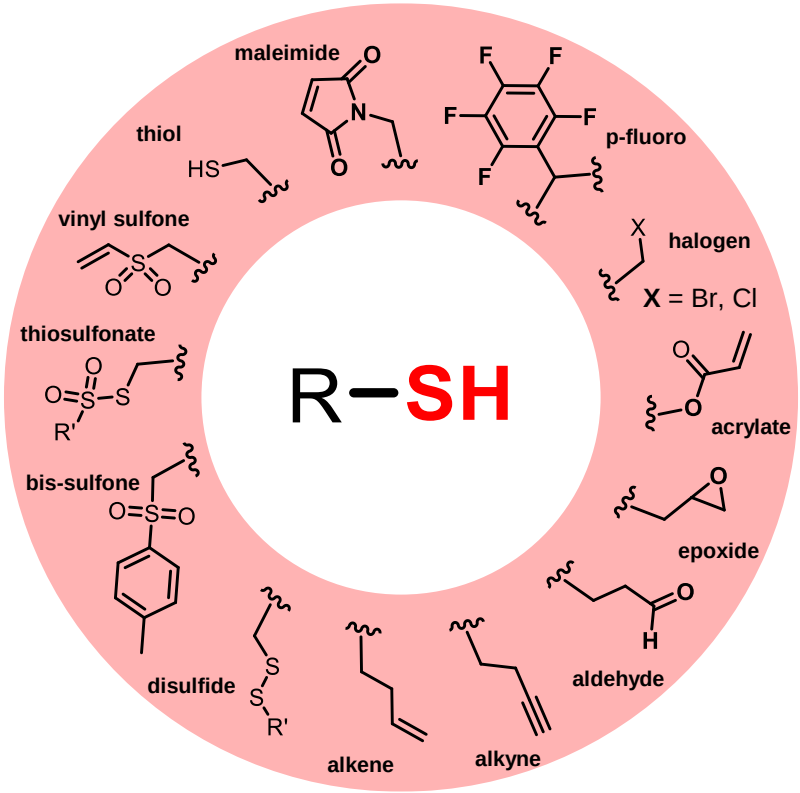

Figure 1-4. Examples of thiol reaction partners encompassing a variety of chemistries and coupling mechanisms.

by integrating aromatic thiols into the polymer backbone of poly(urea-urethane)s: the embedded aromatic disulfides undergo radical-mediated [2+1] disulfide metathesis at room temperature to produce autonomously healing polymer films.[136-137] Alternatively, embedding aromatic disulfides in epoxy networks creates re-shapable and reusable vitrimer networks while retaining epoxy mechanical properties.[136,138] In bio-centric settings, aromatic thiols are good leaving groups and can activate a polymer towards cysteine bioconjugation, for pyridyl disulfide-containing polymers;[121] dithiobenzyls can additionally promote self-immolation fragmentation in *p*-dithiobenzyl carbamate linkers for drug release.[139] Likewise, aromatic thiols form reversible bonds with maleimide functional groups, which Kiick and coworkers used to create glutathione-responsive hydrogels for controlled degradation and cargo release.[140-141] When incorporated as pendent groups in poly(ethyleneimine) (PEI) copolymers bearing deoxycholic acid, the thiophenol was found to bind thiol-siRNA *via* disulfide bond formation in siRNA-PEI polyplexes, which improved the delivery and release of siRNA in tumor cells relative to unmodified siRNA polyplexes.[142] Other examples utilizing aromatic thiols have led to the formation of self-crosslinking hydrogels and nanoparticles.[143-144]

Polymer zwitterions, which are well-known for their biocompatibility and anti-fouling properties,[54,64-67,70-71] have been integrated into thiol-containing structures to improve hydrophilicity and biocompatibility of the macromolecular system (*i.e.*, drug carriers, hydrogels, surface coatings).[38,91,95,145-152] For example, Sae-ung, *et al.* integrated lipoic acid into PC polymer zwitterions to create tunable anti-fouling surfaces,[146] whereas Sonu, *et al.* incorporated lipoic acid into SB copolymers containing pendent alkene moieties, which allowed formation of an adaptable secondary network to create strain-

stiffening hydrogels.[95] Alternatively, Iwasaki and coworkers synthesized disulfide CP dimethacrylates as crosslinker, with the disulfides adjacent to the CP zwitterion moiety, to yield tough hydrogels that are degradable in reducing environments.[91] However, synthetic routes to thiol-containing polymer zwitterions typically include (1) chain-end functionalization, (2) polymerization with a protected thiol comonomer, or (3) post-polymerization modification.[38,95,145-153] To-date, there are no reported polymer zwitterions with pendant thiols (i.e., where the zwitterion unit is adjacent to the free thiol). By integrating thiol units into zwitterions, a variety of properties and reactions not previously available to zwitterions become accessible, without addition of comonomers. Moreover, it primes polymer zwitterions for interaction with biology in biologically relevant environments. This work expands the polymer zwitterion library to this new class of polymer zwitterions and explores their fundamental properties and versatility in various thiol chemistries.

1.4 Thesis Outline

This thesis describes the synthesis of embedded thiol CP zwitterion monomers and polymers and their incorporation into biomolecular materials, specifically as hydrogels, polymer-protein bioconjugates, and surface-active agents, harnessing the versatility of the pendant thiol in various post-polymerization strategies. **Chapter 2** describes the synthesis of embedded thiol CP methacrylates and styrenes, and their incorporation into copolymers using reversible addition-fragmentation chain-transfer (RAFT) polymerization. CP-substituted methacrylates and styrenes are synthesized by ring-opening substituted phospholanes containing *S*-trityl-protected mercaptoethanol (aliphatic) and

mercaptophenol (aromatic) groups with dimethylaminoethyl methacrylate or vinylbenzyl dimethylamine. The copoymerization of CP methacrylates or CP styrenes with MPC to give protected thiol CP copolymers are described, including subsequent acid deprotection to yield water-soluble polymeric zwitterionic thiols (**PZTs**). In **Chapter 3**, the versatility of aromatic and aliphatic **PZTs** are explored by probing fundamental properties at oil-water interfaces, in post-polymerization reactions, and in hydrogel formation. The interfacial activity of protected and deprotected **PZTs** are examined using pendant drop tensiometry while monitoring the long-term stability of the resultant emulsions under various solution conditions. The reactivity of the **PZT** thiols is then analyzed in post-polymerization reactions with divinyl sulfone (DVS) and dipyridyl disulfide (DPDS). Moreover, the **PZTs** are utilized to create hydrogels *via* Michael addition and disulfide bond formation. **Chapter 4** describes **PZTs** in polymer-protein bioconjugation, in which thiol chemistries have a prominent role in creating polymer therapeutics. The aromatic and aliphatic **PZTs** are first evaluated in bioconjugation using disulfide formation mechanisms for a variety of proteins, including several enzymes. The polymer-protein conjugation reactions yielding polymer-protein bioconjugates are characterized with gel electrophoresis and fast protein-liquid chromatography. Bioconjugation reactions between **PZTs** modified with vinyl sulfone or dipyridyl disulfide groups will additionally be examined.

1.5 References

1. Lach, S.; Yoon, S. M.; Gryzbowski, B. A. Tactic, Reactive, and Functional Droplets Outside of Equilibrium. *Chem. Soc. Rev.* **2016**, *45*, 4766–4796.

2. Wang. L.; Song, S.; van Hest, J.; Abdelmohsen, L. K. E. A.; Huang, X.; Sanchez, S. Biomimicry of Cellular Motility and Communication Based on Synthetic Soft-Architectures. *Small* **2020**, *16*, 1907680, 19 pages.

3. Maass, C. C.; Krüger, C.; Herminghaus, S.; Bahr, C. Swimming Droplets. *Annu. Rev. Condens. Matter Phys.* **2015**, *7*, 171–193.

4. Nijemeisland, M.; Abdelmohsen, L. K. E. A.; Huck, W. T. S.; Wilson, D. A.; van Hest, J. C. M. A Compartmentalized Out-of-Equilibrium Enzymatic Reaction Network for Sustained Autonomous Movement. *ACS Cent. Sci.* **2016**, *2* (11), 843–849.

5. Elani, Y. Interfacing Living and Synthetic Cells as an Emerging Frontier in Synthetic Biology. *Angew. Chem.* **2020**, *133* (11), 5662–5671.

6. Rideau, E.; Dimova, R.; Schwille, P.; Wurm, F.R.; Landfester, K. Liposomes and Polymersomes: A Comparative Review towards Cell Mimicking. *Chem. Soc. Rev.* **2018**, *47*, 8572–8610.

7. Jiang, W.; Wu, Z.; Gao, Z.; Wan, M.; Zhou, M.; Mao, C.; Shen, J. Artificial Cells: Past, Present and Future. *ACS Nano* **2022**, *16* (10), 15705–15733.

8. Cook, A. B.; Novosedlik, S.; van Hest, J. C. M. Complex Coacervate Materials as Artificial Cells. *Acc. Mater. Res.* **2023**, *4* (3), 287–298

9. Lin, Y.; Wang, L.; Huang, X. Dynamic Behaviour in Microcompartments. *Chem. Eur. J.* **2019**, *25*, 16440–16450.

10. Santiago, I.; Simmel, F. C. Self-Propulsion Strategies for Artificial Cell-Like Compartments. *Nanomaterials* **2019**, *9*, 1680, 14 pages.

11. Suematsu, N. J.; Nakata, S. Evolution of Self-Propelled Objects: From the Viewpoint of Nonlinear Science. *Chem. Eur. J.* **2018**, *24* (24), 6308–6324.

12. Toyota, T.; Sugiyama, H.; Hiroi, S.; Ito, H.; Kitahata, H. Chemically Artificial Rovers Based on Self-Propelled Droplets in Micrometer-Scale Environment. *Curr. Opin. Colloid Interface Sci.* **2020**, *49*, 60–68.

13. Maass, C. C.; Krüger, C.; Herminghaus, S.; Bahr, C. Swimming Droplets. *Annu. Rev. Condens. Matter Phys.* **2015**, *7*, 171–193.

14. Jin, C.; Krüger, C.; Maass, C. Chemotaxis and Autochemotaxis of Self-Propelling Droplet Swimmers. *PNAS* **2017**, *114* (20), 5089–5094.

15. Hanczyc, M. M.; Toyota, T.; Ikegami, T.; Packard, N.; Sugawara, T. Fatty Acid Chemistry at the Oil-Water Interface: Self-Propelled Oil Droplets. *J. Am. Chem. Soc.* **2007**, *129* (30), 9386–9391.

16. Banno, T.; Asami, A.; Ueno, N.; Kitahata, H.; Koyano, Y.; Asakura, K.; Toyota, T. Deformable Self-Propelled Micro-Object Comprising Underwater Oil Droplets. *Sci. Rep.* **2016**, *6*, 31292, 9 pages.

17. Nagasaka, Y.; Tanaka, S.; Nehira, T.; Amimoto, T. Spontaneous Emulsification and Self-Propulsion of Oil Droplets Induced by the Synthesis of Amino Acid-Based Surfactants. *Soft Matter* **2017**, *37*, 6450–6457.

18. Kasuo, Y.; Kitahata, H.; Koyano, Y.; Takinoue, M.; Asakura, K.; Banno, T. Start of Micrometer-Sized Oil Droplet Motion through Generation of Surfactants. *Langmuir* **2019**, *35* (41), 13351–13355.

19. Suzuki, K.; Sugawara, T. Phototaxis of Oil Droplets Comprising a Caged Fatty Acid Tightly Linked to Internal Convection. *ChemPhysChem.* **2016**, *17* (15), 2300–2303.

20. Zarghami, S.; Xiao, Y.; Wagner, P.; Florea, L.; Diamond, D.; Officer, D.; Wagner, K. Dual Droplet Functionality: Phototaxis and Photopolymerization. *ACS Appl. Mater. Interfaces* **2019**, *11* (34), 31484–31489.

21. Haller, B.; Jahnke, K.; Weiss, M; Göpfrich, K.; Platzman, I.; Spatz, J. Autonomous Directional Motion of Actin-Containing Cell-Sized Droplets. *Adv. Intell. Syst.* **2021**, *3*, 2000190, 8 pages.

22. Meredith, C. H.; Moerman, P. G.; Groenewold, J.; Chiu, Y.-J.; Kegel, W. K.; van Blaaderen, A.; Zarzar, L. D. Predator–Prey Interactions Between Droplets Driven by Non-Reciprocal Oil Exchange. *Nat. Chem.* **2020**, *12*, 1136–1142.

23. Somasundar, A.; Ghosh, S.; Mohajerani, F.; Massenburg, L.; Yang, T.; Cremer, P.; Velegol, D.; Sen, A. Positive and Negative Chemotaxis of Enzyme-Coated Liposome Motors. *Nat. Nanotechnol.* **2019**, *14*, 1129–1134.

24. Čejková, J.; Novák, M.; Štěpánek, F.; Hanczyc, M. Dynamics of Chemotactic Droplets in Salt Concentration Gradients. *Langmuir* **2014**, *30* (40), 11937–11944.

25. Yang, Z.; Snyder, D.; Sathyan, A.; Balazs, A.C.; Emrick, T. Smart Droplets Stabilized by Designer Surfactants: from Biomimicry to Active Motion to Materials Healing. *Adv. Funct. Mater.* **2023**, 2306819, 31 pages.

26. Zhao, J.; Pan, Z.; Snyder, D.; Stone, H. A.; Emrick, T. Chemically Triggered Coalescence and Reactivity of Droplet Fibers. *J. Am. Chem. Soc.* **2021**, *143* (14), 5558–5564.

27. Zhao, J.; Chalarca, C. F. S.; Nunes, J. K.; Stone, H. A.; Emrick, T. Self-Propelled Supracolloidal Fibers from Multifunctional Polymer Surfactants and Droplets. *Macromol. Rapid Commun.* **2020**, *41*, 2000334, 7 pages.

28. Yang, Z.; Snyder, D.; Pagaduan, J. N.; Waldman, A.; Crosby, A. J.; Emrick, T. Mesoscale Polymer Surfactants: Photolithographic Production and Localization at Droplet Interfaces. *J. Am. Chem. Soc.* **2022**, *144* (48), 22059–22066.

29. Lagaraine, C.; Hoarau, C.; Chabot, V.; Velge-Roussel, F.; Lebranchu, Y. *Int. Immunol.* **2005**, *17*, 351–363.

30. Raggatt, L. J.; Partridge, N. C. Cellular and Molecular Mechanisms of Bone Remodeling. *J. Biol. Chem.* **2010,** *285* (33), 25103–25108.

31. Zarghami, S.; Xiao, Y.; Wagner, P.; Florea, L.; Diamond, D.; Officer, D.; Wagner, K. Dual Droplet Functionality: Phototaxis and Photopolymerization. *ACS Appl. Mater. Interfaces* **2019**, *11* (34), 31484–31489.

32. Kratz, K.; Narasimhan, A.; Tangirala, R.; Moon, S.; Revanur, R.; Kundu, S.; Kim, H. S.; Crosby, A. J.; Russell, T. P.; Emrick, T.; Kolmakov, G.; Balazs, A. C. Probing and Repairing Damaged Surfaces with Nanoparticle-Containing Microcapsules. *Nat. Nanotechnol.* **2012**, *7*, 87– 90.

33. Kosif, I.; Chang, C. C.; Bai, Y.; Ribbe, A. E.; Balazs, A. C.; Emrick, T. Picking up Nanoparticles with Functional Droplets. *Adv. Mater. Interfaces* **2014**, *1*, 1400121, 6 pages.

34. Bai, Y.; Chang, C.-C.; Choudhary, U.; Bolukbasi, I.; Crosby, A. J.; Emrick, T. Functional Droplets that Recognize, Collect, and Transport Debris on Surfaces. *Sci. Adv.* **2016**, *2*, e1601462, 7 pages.

35. Bai, Y.; Chang, C.-C.; Zhao, X.; Ribbe, A.; Bolukbasi, I.; Szyndler, M. J.; Crosby, A. J.; Emrick, T. Mechanical Restoration of Damaged Polymer Films by "Repair-and-Go". *Adv. Funct. Mater.* **2016**, *26*, 857–863.

36. Sathyan, A.; Yang, Z.; Bai, Y.; Kim, H.; Crosby, A. J.; Emrick, T. Simultaneous "Clean-and-Repair" of Surfaces Using Smart Droplets. *Adv. Funct. Mater.* **2019**, *29*, 1805219, 6 pages.

37. Yang, Z.; Zhao, J.; Emrick, T. Functional Polymer Zwitterions as Reactive Surfactants for Nanoparticle Capture. *ACS Appl. Mater. Interfaces* **2021**, *13* (18), 21898–21904.

38. Dey, K. K.; Zhao, X.; Tansi, B. M.; Méndez-Oritz, W. J.; Córdova-Figueroa, U. M. Golestanian, R.; Sen, A. Micromotors Powered by Enzyme Catalysis. *Nano Lett.* **2015**, *15* (12), 8311–8315.

39. Patino, T.; Porchetta, A.; Jannasch, A.; Lladó, A.; Stumpp, T.; Schäffer, E.; Ricci, F.; Sánchez, S. Self-Sensing Enzyme-Powered Micromotors Equipped with pH-Responsive DNA Nanoswitches. *Nano Lett.* **2019**, *19* (6), 3440–3447.

40. Kovacs, E. W.; Hooker, J. M.; Romanini, D. W.; Holder, P. G.; Berry, K. E.; Francis, M. B. Dual-Surface-Modified Bacteriophage MS2 as an Ideal Scaffold for a Viral Capsid-Based Drug Delivery System. *Bioconjugate Chem.* **2007**, *18* (4), 1140–1147.

41. Strader, R. L.; Shmidov, Y.; Chilkoti, A. Encoding Structure in Intrinsically Disordered Protein Biomaterials. *Acc. Chem. Res.* **2024**. DOI: 10.1021/acs.accounts.3c00624

42. Muiznieks, L. D.; Keeley, F. W. Biomechanical Design of Elastic Protein Biomaterials: A Balance of Protein Structure and Conformational Disorder. *ACS Biomater. Sci. Eng.* **2017**, *3* (5), 661–679.

43. Gagner, J. E.; Kim, W.; Chaikof, E. L. Designing Protein-Based Biomaterials for Medical Applications. *Acta Biomater.* **2014**, *10* (4), 1542–1557.

44. Raja, K. S.; Wang, Q.; Gonzalez, M. J.; Manchester, M.; Johnson, J. E.; Finn, M. G. Hybrid Virus−Polymer Materials. 1. Synthesis and Properties of PEG-Decorated Cowpea Mosaic Virus. *Biomacromolecules* **2003**, *4* (3), 472–476.

45. Crooke, S. N.; Zheng, J.; Ganewatta, M. S.; Guldberg, S. M.; Reineke, T. M.; Finn, M. G. Immunological Properties of Protein–Polymer Nanoparticles. *ACS Appl. Bio Mater.* **2019**, *2* (1), 93–103.

46. Steinmetz, N. F.; Manchester, M. PEGylated Viral Nanoparticles for Biomedicine: The Impact of PEG Chain Length on VNP Cell Interactions In Vitro and Ex Vivo. *Biomacromolecules* **2009**, *10* (4), 784–792.

47. Laskar, A.; Shklyaev, O. E.; Balazs, A. C. Designing Self-Propelled, Chemically Active Sheets: Wrappers, Flappers, and Creepers. *Sci. Adv.* **2018**, *4* (12), eaav1745, 11 pages.

48. Shklyaev, O. E.; Shum, H.; Sen, A.; Balazs, A. C. Harnessing Surface-Bound Enzymatic Reactions to Organize Microcapsules in Solution. *Sci. Adv.* **2016**, *2* (3), e150183, 13 pages.

49. Shum, H.; Balazs, A. C. Flow-Driven Assembly of Microcapsules into Three-Dimensional Towers. *Langmuir* ***2018***, *34* (8), 2890–2899.

50. Maiti, S.; Shklyaev, O. E.; Balazs, A. C.; Sen, A. Self-Organization of Fluids in a Multi-enzymatic Pump System. *Langmuir* **2019**, *35*, 3724–3732.

51. Hu, Y.; Samanta, D.; Parelkar, S. S.; Hong, S. W.; Wang, Q.; Russell, T. P.; Emrick, T. Ferritin–Polymer Conjugates: Grafting Chemistry and Integration into Nanoscale Assemblies. *Adv. Funct. Mater.* **2010**, *20* (20), 3603–3612.

52. Russell, J. T.; Lin, Y.; Böker, A.; Su, L.; Carl, P.; Zettl, H.; He, J.; Sill, K.; Tangirala, R.; Emrick, T.; Littrell, K.; Thiyagarajan, P.; Cookson, D.; Fery, A.; Wang, Q.; Russell, T. P. Self-Assembly and Cross-Linking of Bionanoparticles at Liquid–Liquid Interfaces. *Angew. Chem.* **2005**, *117* (16), 2472–2478.

53. Lurie-Luke, E. Product and Technology Innovation: What can Biomimicry Inspire? *Biotechnol. Adv.* **2014**, *32*, 1494–1505.

54. Ishihara, K.; Ueda, T.; Nakabayashi, N. Preparation of Phospholipid Polymers and Their Properties as Polymer Hydrogel Membranes. *Polym. J.* **1990**, *22* (5), 355–360.

55. Nakai, S.; Nakaya, T.; Imoto, M. Polymeric Phospholipid Analog, 10*): Synthesis and Polymerization of 2-(Methacryloyloxy)ethyl 2-Aminoethyl Hydrogen Phosphate. *Makromol. Chem.* **1977**, *178*, 2963–2967.

56. Fried, S. D.; Boxer, S. G. Electric Fields and Enzyme Catalysis. *Annu. Rev. Biochem.* **2017**, *86*, 387-415.

57. Alfonso, I.; Solà, J. Molecular Recognition of Zwitterions with Artificial Receptors. *Chem. Asian J.* **2020**, *15* (7), 986–994.

58. Roskoski, R. A Historical Overview of Protein Kinases and Their Targeted Small Molecule Inhibitors. *Pharmacol. Res.* **2015**, *100*, 1–23.

59. Laschewsky, A.; Rosenhahn. A. Molecular Design of Zwitterionic Polymer Interfaces: Searching for the Difference. *Langmuir* **2019**, *35* (5), 1056–1071.

60. Liu, Y., Sheri, M., Cole, M. D., Emrick, T. & Russell, T. P. Combining Fullerenes and Zwitterions in Non-Conjugated Polymer Interlayers to Raise Solar Cell Efficiency. *Angew. Chem. Int. Ed.* **2018**, *57*, 9675–9678.

61. Ishihara, K. Highly Lubricated Polymer Interfaces for Advanced Artificial Hip Joints Through Biomimetic Design. *Polym. J.* **2015**, *47*, 585–597.

62. Li, Q.; Wen, C.; Yang, J. Zhou, X.; Zhu, Y.; Zheng, J.; Cheng, G.; Bai, J.; Xu, T.; Ji, J.; Jiang, S.; Zhang, L.; Zhang, P. Zwitterionic Biomaterials. *Chem. Rev.* **2022**, *122* (23), 17073–17154.

63. Venault, A.; Chang, Y. Designs of Zwitterionic Interfaces and Membranes. *Langmuir* **2019**, *35* (5), 1714–1726.

64. Mi, L.; Jiang, S. Integrated Antimicrobial and Nonfouling Zwitterionic Polymers. *Angew. Chem. Int. Ed.* **2014**, *53*, 1746–1754.

65. Li, D.; Wei, Q.; Wu, C.; Zhang, X.; Xue, Q.; Zheng, T.; Cao, M. Superhydrophilicity and Strong Salt-Affinity: Zwitterionic Polymer Grafted Surfaces in Biological Systems. *Adv. Colloid Interface Sci.* **2020**, *278*, 102141, 18 pages.

66. Jin, Q.; Chen, Y.; Wang, Y.; Ji, J. Zwitterionic Drug Nanocarriers: A Biomimetic Strategy for Drug Delivery. *Colloids Surf. B: Biointerfaces* **2014**, *124*, 80–86.

67. Iwasaki, Y.; Ishihara, K. Phosphorylcholine-Containing Polymers for Biomedical Applications. *Anal. Bioanal. Chem.* **2005**, 381, 534–546.

68. Baggerman, J.; Smulders, M. M. J.; Zuilhof, H. Romantic Surfaces: A Systematic Overview of Stable, Biospecific, and Antifouling Zwitterionic Surfaces. *Langmuir* **2019**, *35* (5), 1072–1084.

69. Ishihara, K.; Oshida, H.; Endo, Y.; Ueda, T.; Watanabe, A.; Nakabayashi, N. Hemocompatibility of Human Whole Blood on Polymers with a Phospholipid Polar Group and its Mechanism. *J. Biomed. Mater. Res.* **1992**, *26*, 1543–1552.

70. Ishihara, K.; Tsuji, T.; Kurosaki, T.; Nakabayashi, N. Hemocompatibility on Graft Copolymers Composed of Poly(2-methacryloyloxyethyl phosphorylcholine) Side Chain and Poly(n-butyl methacrylate) Backbone. *J. Biomed. Mater. Res.* **1994**, *28*, 225–232.

71. Ishihara, K.; Nomura, H.; Mihara, T.; Kurita, K.; Iwasaki, Y.; Nakabayashi, N. Why do Phospholipid Polymers Reduce Protein Adsorption? *J. Biomed. Mater. Res.* **1998**, 39, 323–330.

72. Liaw, D.-J.; Huang, C.-C.; Lee, W.-F.; Borbély, J.; Kang, E.-T. Synthesis and Characteristics of the Poly(carboxybetaine)s and the Corresponding Cationic Polymers. *J. Polym. Sci., Part A: Polym. Chem.* **2000**, *35* (16), 3527–3536.

73. Shao, Q.; Jiang, S. Molecular Understanding and Design of Zwitterionic Materials. *Adv. Mater.* **2014**, *27* (1), 15–26.

74. Zhang, Z.; Chao, T.; Chen, S.; Jiang, S. Superlow Fouling Sulfobetaine and Carboxybetaine Polymers on Glass Slides. *Langmuir* **2006**, *22* (24), 10072–10077.

75. Zhang, Z.; Chen, S.; Jiang, S. Dual-Functional Biomimetic Materials: Nonfouling Poly(carboxybetaine) with Active Functional Groups for Protein Immobilization. *Biomacromolecules* **2006**, *7* (12), 3311–3315.

76. Lalani, R.; Liu, L. Electrospun Zwitterionic Poly(Sulfobetaine Methacrylate) for Nonadherent, Superabsorbent, and Antimicrobial Wound Dressing Applications. *Biomacromolecules* **2012**, *13* (6), 1853–1863.

77. Lowe, A. B.; Billingham, N. C.; Armes, S. P. Synthesis and Properties of Low-Polydispersity Poly(sulfopropylbetaine)s and Their Block Copolymers. *Macromolecules* **1999**, *32* (7), 2141–2148.

78. Kim, Y. H.; Her, A.-Y.; Rha, S.-W.; Choi, B. G.; Choi, S. Y. ; Byun, J. K. ; Park, Y. ; Kang, D. O.; Jang, W. Y.; Kim, W.; Choi, W. G.; Kang, T. S.; Ahn, J.; Park, S.-H.; Park, J. Y.; Lee, M-H.; Choi, C. U.; Park, C. G.; Seo, H. S. Three-Year Major Clinical Outcomes of Phosphorylcholine Polymer- vs Biolinx Polymer-Zotarolimus-Eluting Stents. *Medicine (Baltimore)* **2019**, *98* (32), e16767, 10 pages.

79. Young, G.; Bowers, R.; Hall, B.; Port, M. Clinical Comparison of Omafilcon A with Four Control Materials. *CLAO J.* **1997**, *23* (4), 249–58.

80. Brown, M. U.; Triozzi, A.; Emrick, T. Polymer Zwitterions with Phosphonium Cations. *J. Am. Chem. Soc.* **2021**, *143* (17), 6528–6532.

81. Brown, M. U.; Seong, H.; Russell, T. P.; Emrick, T. Zwitterionic Sulfonium Sulfonate Polymers: Impacts of Substituents and Inverted Dipole. *Macromolecules* **2023**, *56*, 1105–1110.

82. Chalarca, C. F. S.; Emrick, T. Reactive Polymer Zwitterions: Sulfonium Sulfonates. *J. Polym. Sci. A. Polym. Chem.* **2017**, *55*, 83–92.

83. Hu, G. J.; Parelkar, S. S.; Emrick, T. A Facile Approach to Hydrophilic, Reverse Zwitterionic, Choline Phosphate Polymers. *Polym. Chem.* **2015**, *6* (4), 525–530.

84. Yu, X.; Yang, X.; Horte, S.; Kizhakkedathu, J. N.; Brooks, D. E. ATRP Synthesis of Poly(2-(methacryloyloxy)ethyl choline phosphate): A Multivalent Universal Biomembrane Adhesive. *Chem. Commun.* **2013**, *49*, 6831–6833.

85. Chen, T.-M.; Wang, Y.-F.; Li, Y.-J.; Nakaya, T.; Sakurai, I. Studies on the Synthesis and Properties of Novel Phospholipid Analogous Polymers. *J. Appl. Polym. Sci.* **1996**, *60* (3), 455–464.

86. Zhou, L.; Triozzi, A.; Figueiredo, M.; Emrick, T. Fluorinated Polymer Zwitterions: Choline Phosphates and Phosphorylcholines. *ACS Macro Lett.* **2021**, *10*, 1204–1209.

87. Zhou, L.; Yang, Z.; Pagaduan, J. N.; Emrick, T. Fluorinated Zwitterionic Polymers as Dynamic Surface Coatings. *Polym. Chem.* **2023**, *14*, 32–36.

88. Brown, M. U.; Seong, H.-G.; Margossian, K. O.; Bishop, L.; Russell, T. P.; Muthukumar, M.; Emrick, T. Zwitterionic Ammonium Sulfonate Polymers: Synthesis and Properties in Fluids. *Macromol. Rapid Commun.* **2022**, *43*, 2100678, 7 pages.

89. Pagaduan, J. N.; Hight-Huf, N.; Datar, A.; Nagar, Y.; Barnes, M.; Naveh, D.; Ramasubramaniam, A.; Katsumata, R.; Emrick, T. Electronic Tuning of Monolayer Graphene with Polymeric "Zwitterists". *ACS Nano* **2021**, *15* (2), 2762–2770.

90. Hu, G.; Emrick, T. Functional Choline Phosphate Polymers. *J. Am. Chem. Soc.* **2016**, *138*, 1828–1831.

91. Nguyen, H. N.; Ngo, T. L. H.; Iwasaki, Y.; Huang, C.-J. Biodegradable Phosphocholine Cross-Linker with Ion-Pair Design for Tough Zwitterionic Hydrogel. *Adv. Mater. Interfaces* **2022**, *9* (33), 2201002, 11 pages.

92. Nakano, H.; Noguchi, Y.; Kakinoki, S.; Yamakawa, M; Osaka, I.; Iwasaki, Y. Highly Durable Lubricity of Photo-Cross-Linked Zwitterionic Polymer Brushes Supported by Poly(ether ether ketone) Substrate. *ACS Appl. Bio Mater*. **2020**, *3* (2), 1071–1078.

93. Chang, C.-C.; Letteri, R.; Hayward, R. C.; Emrick, T. Functional Sulfobetaine Polymers: Synthesis and Salt-Responsive Stabilization of Oil-in-Water Droplets. *Macromolecules* **2015**, *48* (21), 7843–7850.

94. Skinner, M.; Johnston, B. M.; Liu, Y.; Hammer, B.; Selhorst, R.; Xenidou, I.; Perry, S. L.; Emrick, T. Synthesis of Zwitterionic Pluronic Analogs. *Biomacromolecules* **2018**, *19* (8), 3377–3389.

95. Sonu, K. P.; Zhou, L.; Biswas, S.; Klier, J.; Balazs, A. C.; Emrick, T.; Peyton, S. R. Strain-Stiffening Hydrogels with Dynamic, Secondary Cross-Linking. *Langmuir* **2023**, *39* (7), 2659–2666.

96. Toohey, J. I.; Cooper, A. J. L. Thiosulfoxide (Sulfane) Sulfur: New Chemistry and New Regulatory Roles in Biology. *Molecules* **2014**, *19* (8), 12789–12813.

97. Beinert, H. A Tribute to Sulfur. *Eur. J. Biochem.* **2001**, *267* (18), 5657–5664.

98. Leimkühler, S.; Ogunkola, M. O. 10 - Sulfur Transferases in the Pathways of Molybdenum Cofactor Biosynthesis and tRNA Thiolation in Humans. In *Foundations and Frontiers in Enzymology, Sulfurtransferases* [Online]; Nagahara, N., Ed.; Academic Press: 2023, 207–236.

99. Poole, L. B. The Basics of Thiols and Cysteines in Redox Biology and Chemistry. *Free Radic. Biol. Med.* **2014**, *0*, 148–157.

100. Beaupre, D. M.; Weiss, R. G. Thiol- and Disulfide-Based Stimulus-Responsive Soft Materials and Self-Assembling Systems. *Molecules* **2021**, *26* (11), 3332, 44 pages.

101. Mutlu, H.; Ceper, E. B.; Li. X.; Yang, J.; Dong, W.; Ozmen, M. M.; Theato, P. Sulfur Chemistry in Polymer and Materials Science. *Macromol. Rapid. Comm*. **2019**, *40*, 1800650, 51 pages.

102. Le Neindre, M.; Nicolaÿ, R. Polythiol Copolymers with Precise Architectures: A Platform for Functional Materials. *Polym. Chem.* **2014**, *5* (16), 4601–4611.

103. Le Neindre, M.; Nicolaÿ, R. One-pot Deprotection and Functionalization of Polythiol Copolymers via Six Different Thiol–X Reactions. *Polym. Int.* **2013**, *63* (5), 887–893.

104. Hoyle, C. E.; Lowe, A.; Bowman, C. N. Thiol-Click Chemistry: A Multifaceted Toolbox for Small Molecule and Polymer Synthesis. *Chem. Soc. Rev*. **2010**, *4*, 1355–1387.

105. Li, M.; De, P.; Gondi, S. R.; Sumerlin, B. S. End Group Transformations of RAFT-Generated Polymers with Bismaleimides: Functional Telechelics and Modular Block Copolymers. *Polym. Sci. A. Polym. Chem.* **2008**, *46* (15), 5093–5100.

106. Konkolewicz, D.; Gray-Weale, A.; Perrier, S. Hyperbranched Polymers by Thiol−Yne Chemistry: From Small Molecules to Functional Polymers. *J. Am. Chem. Soc*. **2009**, *131* (50), 18075–18077.

107. Yang, R.; Liu, X.; Ren, Y.; Xue, W.; Liu, S.; Wang, P.; Zhao, M.; Xu, H.; Chi, B. Injectable Adaptive Self-Healing Hyaluronic Acid/Poly (γ-glutamic acid) Hydrogel for Cutaneous Wound Healing. *Acta Biomaterialia* **2021**, *127*, 102–115.

108. Canadell, J.; Goossens, H.; Klumperman, B. Self-Healing Materials Based on Disulfide Links. *Macromolecules* **2011**, *44* (8), 2536–2541.

109. Chakma, P.; Konkolewicz, D. Dynamic Covalent Bonds in Polymeric Materials. *Angew. Chem. Int. Ed.* **2019**, *58* (29), 9682–9695.

110. Zhang, Q.; Qu, D.-H.; Feringa, B. L.; Tian. H. Disulfide-Mediated Reversible Polymerization toward Intrinsically Dynamic Smart Materials. *J. Am. Chem. Soc.* **2022**, *144* (5), 2022–2033.

111. Canadell, J.; Goossens, H.; Klumperman, B. Self-Healing Materials Based on Disulfide Links. *Macromolecules* **2011**, *44* (8), 2536–2541.

112. Xiang, H.; Yin, J.; Lin, G.; Liu, X.; Rong, M.; Zhang, M. Photo-Crosslinkable, Self-Healable, and Reprocessable Rubbers. *Chem. Eng. J.* **2019**, *358*, 878–890.

113. Kloxin, C. J.; Bowman, C. N. Covalent Adaptable Networks: Smart, Reconfigurable and Responsive Network Systems. *Chem. Soc. Rev.* **2013**, *42*, 7161–7173.

114. Yoon, J. A.; Kamada, J.; Koynov, K.; Mohin, J.; Nicolaÿ, R.; Zhang, Y.; Balazs, A. C.; Kowalewski, T.; Matyjaszewski, K. Self-Healing Polymer Films Based on Thiol-Disulfide Exchange Reactions and Self-Healing Kinetics Measured Using Atomic Force Microscopy. *Macromolecules* **2012**, *45* (1), 142–149.

115. Otsuka, H.; Nagano, S.; Kobashi, Y.; Maeda, T.; Takahara, A. A Dynamic Covalent Polymer Driven by Disulfide Metathesis under Photoirradiation. *Chem. Comm.* **2010**, *7*, 1150–1152.

116. Azcune, I.; Odriozola, I. Aromatic Disulfide Crosslinks in Polymer Systems: Self-Healing, Reprocessability, Recyclability and more. *Eur. Polym. J.* **2016**, *84*, 147–160.

117. Michal, B. T.; Jaye, C. A.; Spencer, E. J.; Rowan, S. J. Inherently Photohealable and Thermal Shape-Memory Polydisulfide Networks. *ACS Macro Lett.* **2013**, *2* (8), 694–699.

118. Altinbasak, I.; Arslan, M.; Sanyal, R.; Sanyal, A. Pyridyl disulfide-based thiol–disulfide exchange reaction: shaping the design of redox-responsive polymeric materials. *Polym. Chem.* **2020**, *11* (48), 7603–7624.

119. Wojtecki, R. J.; Jones, G. O.; Yuen, A. Y.; Chin, W.; Boday, D. J.; Nelson, A.; García, J. M.; Yang, Y. Y.; Hedrick, J. Developments in Dynamic Covalent Chemistries from the Reaction of Thiols with Hexahydrotriazines. *J. Am. Chem. Soc.* **2015**, *137* (45), 14248–14251.

120. Fuoco, T.; Finne-Wistrand, A.; Pappalardo, D. A Route to Aliphatic Poly(ester)s with Thiol Pendant Groups: From Monomer Design to Editable Porous Scaffolds. *Biomacromolecules* **2016**, *17* (4), 1383–1394.

121. Altinbasak, I.; Arslan, M.; Sanyal, R.; Sanyal, A. Pyridyl disulfide-based thiol–disulfide exchange reaction: shaping the design of redox-responsive polymeric materials. *Polym. Chem.* **2020**, *11* (48), 7603–7624.

122. Summonte, S.; Racaniello, G. F.; Lopedota, A.; Denora, N.; Bernkop-Schnürch, A. Thiolated Polymeric Hydrogels for Biomedical Application: Cross-Linking Mechanisms. *J. Control. Release* **2021**, *330* (10), 470–482.

123. Lee, M. H.; Sessler, J. L.; Kim, J. S. Disulfide-Based Multifunctional Conjugates for Targeted Theranostic Drug Delivery. *Acc. Chem. Res.* **2015**, *48* (11), 2935–2946.

124. Zhang, P.; Wu, J.; Xiao, F.; Zhao, D.; Luan, Y. Disulfide Bond Based Polymeric Drug Carriers for Cancer Chemotherapy and Relevant Redox Environments in Mammals. *Med. Res. Rev.* **2018**, *38* (5), 1485–1510.

125. Huo, M.; Yuan, J.; Tao, L.; Wei, Y. Redox-Responsive Polymers for Drug Delivery: From Molecular Design to Applications. *Polym. Chem.* **2014**, *5*, 1519–1528.

126. Chen, X.; Lawrence, J.; Parelkar, S.; Emrick, T. Novel Zwitterionic Copolymers with Dihydrolipoic Acid: Synthesis and Preparation of Nonfouling Nanorods. *Macromolecules* **2013**, *46* (1), 119–127.

127. Frederix, F.; Bonroy, K.; Laureyn, W.; Reekmans, G.; Campitelli, A.; Dehaen, W.; Maes, G. Enhanced Performance of an Affinity Biosensor Interface Based on Mixed Self-Assembled Monolayers of Thiols on Gold. *Langmuir* **2003**, *19* (10), 4351–4357.

128. Frasconi, M.; Mazzei, F.; Ferri, T. Protein Immobilization at Gold-Thiol Surfaces and Potential for Biosensing. *Anal. Bioanal. Chem.* **2010**, *398*, 1545–1564.

129. Xue, Y.; Li, X.; Li, H.; Zhang, W. Quantifying Thiol-Gold Interactions Towards the Efficient Strength Control. *Nat. Commun.* **2014**, *5*, 4348, 9 pages.

130. Bain, C. D.; Evall, J.; Whitesides, G. M. Formation of Monolayers by the Coadsorption of Thiols on Gold: Variation in the Head Group, Tail Group, and Solvent[1]. *J. Am. Chem. Soc.* **1989**, *111* (18), 7155–7164.

131. Li, J.; Richardson, J. J.; Ejima, H. Synthesis of Dithiocatechol-Pendant Polymers. *J. Am. Chem. Soc.* **2022**, *144* (6), 2450–2454.

132. Kihara, N.; Kanno, C.; Fukutomi, T. Synthesis and Properties of Microgel Bearing a Mercapto Group. *J. Polym. Sci. A. Polym. Chem.* **1997**, *35* (8), 1443–1451.

133. Gregor, H. P.; Dolar, D.; Hoeschele, G. K. Polythiolstyrene-A New Oxidation-Reduction Ion Exchange Resin. *J. Am. Chem. Soc.* **1955**, *77* (13), 3675–3675.

134. Overberger, C. G.; Lebovits, A. The Synthesis of Poly-p-thiostyrene, An Oxidation Reduction Polymer. *J. Am. Chem. Soc.* **1955**, *77* (13), 3675–3676.

135. Overberger, C. G.; Lebovits, A. Preparation of p-Vinylphenyl Thioacetate,[1] its Polymers, Copolymers and Hydrolysis Products. Water-Soluble Copolymers Containing Sulfhydryl Groups[2]. *J. Am. Chem. Soc.* **1956**, *78* (18), 4792–4797.

136. Azcune, I.; Odriozola, I. Aromatic Disulfide Crosslinks in Polymer Systems: Self-Healing, Reprocessability, Recyclability and more. *Eur. Polym. J.* **2016**, *84*, 147–160.

137. Rekondo, A.; Martin, R.; de Luzuriaga, A. R.; Cabañero, G.; Grande, H. J.; Odriozola, I. Catalyst-Free Room-Temperature Self-Healing Elastomers Based on Aromatic Disulfide Metathesis. *Mater. Horiz.* **2014**, *1* (2), 237–240.

138. Martin, R.; Rekondo, A.; de Luzuriaga, A. R.; Santamaria, A.; Odriozola, I. Mixing the Immiscible: Blends of Dynamic Polymer Networks. *RCS Adv.* **2015**, *5* (23), 17514–17518.

139. Deng, Z.; Hu, J.; Liu, S. Disulfide-Based Self-Immolative Linkers and Functional Bioconjugates for Biological Applications. *Macromol. Rapid Commun.* **2019**, *41* (1), 1900531, 14 pages.

140. Kharkar, P. M.; Kloxin, A. M.; Kiick, K. L. Dually Degradable Click Hydrogels for Controlled Degradation and Protein Release. *J. Mater. Chem. B* **2014**, *2* (34), 5511–5521.

141. Lang, Y.; Kiick, K. L. Liposome-Cross-Linked Hybrid Hydrogels for Glutathione-Triggered Delivery of Multiple Cargo Molecules. *Biomacromolecules* **2016**, *17* (2), 601–614.

142. Yin, Y.; Lee, J. E.; Kim, N. W.; Lee, J. H.; Lim, S. Y.; Kim, E. S.; Park, J. W.; Lee, M. S.; Jeong, J. H. Inhibition of Tumor Growth via Systemic siRNA Delivery Using Reducible Bile Acid-Conjugated Polyethylenimine. *Polymers* **2018**, *10* (9), 953, 16 pages.

143. Bracchi, M. E.; Dura, G.; Fulton, D. A. The Synthesis of Poly(aryl thiols) and Their Utilization in the Preparation of Cross-Linked Dynamic Covalent Polymer Nanoparticles and Hydrogels. *Polym. Chem.* **2019**, *10* (10), 1258–1267.

144. Tuten, B. T.; Chao, D.; Lyon, C. K.; Berda, E. B. Single-Chain Polymer Nanoparticles via Reversible Disulfide Bridges. *Polym. Chem.* **2012**, *3* (11), 3068–3071.

145. Page, S. M.; Martorella, M.; Parelkar, S.; Kosif, I.; Emrick, T. Disulfide Cross-Linked Phosphorylcholine Micelles for Triggered Release of Camptothecin. *Mol. Pharmaceutics* **2013**, *10* (7), 2684–2692.

146. Sae-ung, P.; Kolewe, K. W.; Bai, Y.; Rice, E. W.; Schiffman, J. D.; Emrick, T.; Hoven, V. P. Antifouling Stripes Prepared from Clickable Zwitterionic Copolymers. *Langmuir* **2017**, *33* (28), 7028–7035.

147. Shahkaramipour, N.; Lai, C. K.; Venna, S. R.; Sun, H.; Cheng, C.; Lin, H. Membrane Surface Modification Using Thiol-Containing Zwitterionic Polymers via Bioadhesive Polydopamine. *Ind. Eng. Chem. Res.* ***2018***, *57* (6), 2336–2345.

148. Macková, H.; Plichta, Z.; Hlídková, H.; Sedláček, O.; Konefal, R.; Sadakbayeva, Z.; Dušková-Smrčková, M.; Horák, D.; Kubinová, S. Reductively Degradable Poly(2-hydroxyethyl methacrylate) Hydrogels with Oriented Porosity for Tissue Engineering Applications. *ACS Appl. Mater. Interfaces* **2017**, *9*, 10544–10553.

149. Khunsuk, P.; Chawalitpong, S.; Sawutdeechaikul, P.; Palaga, T.; Hoven, V. P. Gold Nanorods Stabilized by Biocompatible and Multifunctional Zwitterionic Copolymer for Synergistic Cancer Therapy. *Mol. Pharmaceutics* **2018**, *15*, 164–174.

150. Macková, H.; Hlídková, H.; Kaberova, Z.; Proks, V.; Kučka, J.; Patsula, V.; Vetrik, M.; Janoušková, O.; Podhorská, B.; Pop-Georgievski, O.; Kubinová, S.; Horák, D. Thioated Poly(2-hydroxyethyl methacrylate) Hydrogels as a Degradable Biocompatible Scaffold for Tissue Engineering. *Mater. Sci. Eng. C* **2021**, *131*, 112500, 11 pages.

151. Li, J.-Y.; Qiu, L.; Xu, X.-F.; Pan, C.-Y.; Hong, C.-Y.; Zhang, W.-J.; Photo-Responsive Camptothecin-Based Polymeric Prodrug Coated Silver Nanoparticles for Drug Release Behaviour Tracking *via* the Nanomaterial Surface Energy Transfer (NSET) Effect. *J. Mater. Chem. B* **2018**, *6*, 1678-1687.

152. Lin, W.; Ma, G.; Kampf, N.; Yuan, Z.; Chen, S. Development of Long-Circulating Zwitterionic Cross-Linked Micelles for Active-Targeted Drug Delivery. *Biomacromolecules* **2016**, *17* (6), 2010–2018.

153. Bulmus, V.; RAFT Polymerization Mediated Bioconjugation Strategies. *Polym. Chem*. **2011**, *2*, 1463–1472.

CHAPTER TWO:
SYNTHESIS OF CHOLINE PHOSPHATE ZWITTERION MONOMERS & POLYMERS WITH EMBEDDED THIOLS

2.1 Introduction

Polymer zwitterions are charge neutral polymers containing both a cationic (e.g., ammonium, phosphonium, or sulfonium) and an anionic (e.g., phosphonate or sulfonate) group within each monomer subunit along the polymer backbone.[1-4] This characteristic structural motif, reflected for example in poly(methacryloyloxyethyl phosphorylcholine) (polyMPC), generates their widely appreciated hydrophilicity, biocompatibility, and anti-fouling properties.[1-3,5-7] More recent synthetic advances have produced new types of polymer zwitterions (*e.g.*, choline phosphates, sulfothetins, and phosphonium sulfonates), many of which embed useful functionality directly within the zwitterionic moieties, including hydrocarbons, fluorocarbons, and reactive functional groups.[4,8-16] These novel zwitterionic structures impart unusual properties to the corresponding polymers,[6-22] including solubility in non-polar organic solvents,[4,12] self-association at fluid-fluid interfaces (*i.e.*, affording sticky droplets),[13,15-16,21,23] and the ability to participate in high-yielding, versatile chemical reactions such as azide-alkyne cycloaddition.[9,20,22]

One impediment to more rapid synthetic progress in functional zwitterions specific to choline phosphate (CP) structures is associated with complications in the essential phospholane ring-opening step illustrated in **Figure 2-1a**. When nucleophilic attack favors the exocyclic bimolecular substitution, the undesired ammonium phosphonate salt forms, whereas the desired endocyclic ring-opening pathway produces the zwitterionic product.[8] Changing the nucleophile, charged groups, or their substituents all impact the outcome of this reaction, though in ways not understood systematically at present, which has limited

functional group integration into CP polymer zwitterions. The small library of CP polymer zwitterions is further limited: to-date, the only reactive functional groups are alkenes and alkynes, with recent work by Iwasaki and coworkers introducing CP benzophenone and CP disulfides (**Figure 2-1b**).[9-10,13,15-16] Such groups are useful, for example, since alkene and alkyne functionalities in CP zwitterions enable their participation in thiol-ene and azide-alkyne cycloaddition, thus opening opportunities to prepare prodrugs, chemically tailored surfactants, hydrogels, and other structures.[9,15-16,20]

Our interest in integrating thiols into zwitterionic structures stems from their relevance in numerous fundamental organic reactions, including Michael addition, thiol-ene coupling, and disulfide formation, with potential extension to protein conjugation, where

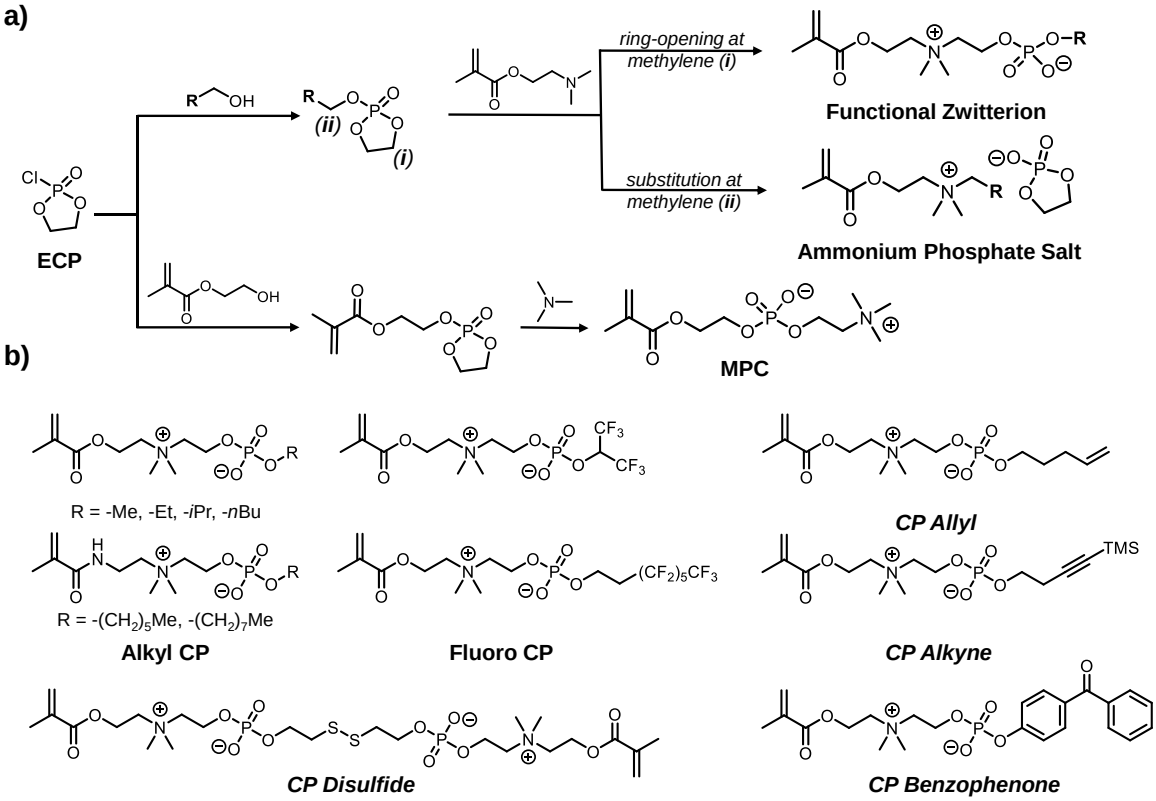

Figure 2-1. (**a**) Competing endo- and exo-cyclic synthetic pathways in ring-opening of substituted ECPs, with comparison to the synthesis of MPC. (**b**) Functional CP zwitterionic monomers synthesized previously (in italics), including reactive CP-based alkenes and alkynes, CP benzophenone, and CP disulfide dimethacrylate.

polymers play an important role such as in improved biological therapeutics (i.e., PEGylation and related derivatives).[24-25] Such thiol-embedded CP structures have the potential to greatly expand the polymer zwitterion library through post-polymerization reactions, stemming from the versatile thiol reactive handle. In general, thiol-containing polymers are recognized as valuable for affording entry into dynamic, self-healing, and/or stimuli-responsive materials.[26-37] Such dynamic properties and applications are often accessed by introducing aliphatic thiols into the polymer structure as disulfides embedded in the polymer backbone[31] or in crosslinking agents,[29-30,32] as chain ends,[35] or as pendent groups,[36,38-40] the latter being particularly useful for post-polymerization modifications[41] and hydrogel formation.[36,42] Notably, much less examined are polymers with thiophenol pendent groups, due in part to their instability and tendency to gel upon attempted preparation and isolation.[43-44] Examples of the successful utility of aryl thiols include the integration of 4-aminophenyl disulfide crosslinks into polymer backbones to yield reprocessable epoxy networks and self-healing urethane thermosets,[34,45-46] and the participation of aryl thiol-terminated PEG in retro-thiol-Michael addition under biologically relevant conditions (i.e., the reducing environment of glutathione).[46-48] When incorporated as pendent groups, aryl thiols can yield self-immolative crosslinked micelles[49] and single-chain polymer nanoparticles,[50] utilizing mechanisms involving disulfides and metathesis. For example, Fulton and coworkers prepared pendant aryl thiol copolymers from a pentafluorophenyl acrylate polymer precursor, where the presence of the aryl thiols gave access to polymer nanoparticle and hydrogel formation *via* self-crosslinking disulfide formation.[51] By integrating thiol group directly into the zwitterion subunit, we anticipate that the hydrophilicity of the zwitterionic groups, combined with the reactive thiol

moieties, will prove useful in a variety of applications where aqueous solubility, biocompatibility, and tunable functionality are crucial, such as in hydrogels, drug delivery, and surfactant design.

In **Chapter 1**, we describe the synthesis of embedded thiol CP zwitterions and their preparation as embedded thiol polymer zwitterions through controlled free radical methods, either as copolymers with MPC or as homopolymers, in which thiol functionality is embedded directly into the zwitterionic subunit (**Figure 2-2**). Following acid deprotection, aromatic and aliphatic polymer zwitterion thiols with methacrylate (**PZTs**) or styrene backbones (**SPZTs**) are obtained with free thiol content characterized by Ellman's Assay and NMR spectroscopic methods.

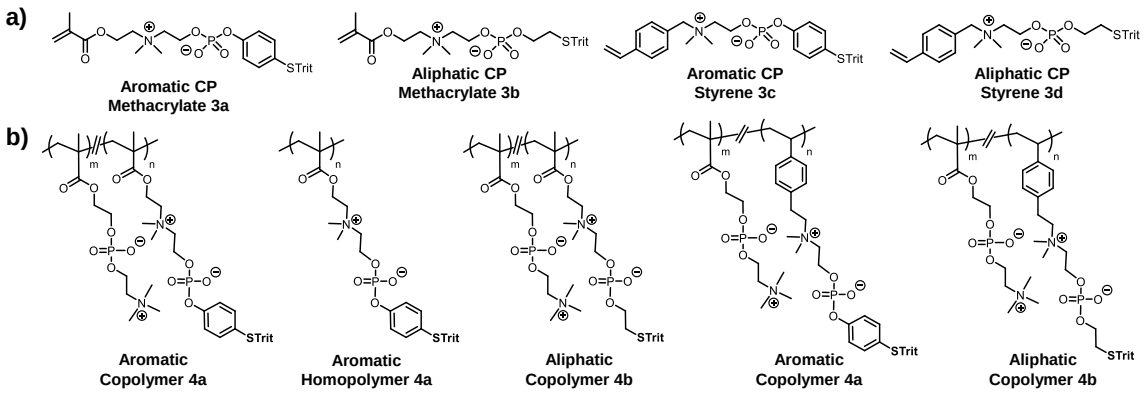

Figure 2-2. Embedded thiol choline phosphate zwitterion (**a**) monomers and (**b**) polymers synthesized in this chapter.

2.2 Synthesis of Embedded Thiol CP Zwitterion Monomers

Following the general strategy described in **Figure 2-1a**, embedded thiol CP methacrylates **3a** and **3b**, and CP styrenes **3c** and **3d**, containing either protected aromatic or protected aliphatic thiols, were prepared as illustrated in **Figure 2-3**. To begin, 4-mercaptophenol and 2-mercaptoethanol were protected as their S-trityl derivatives **1a** and

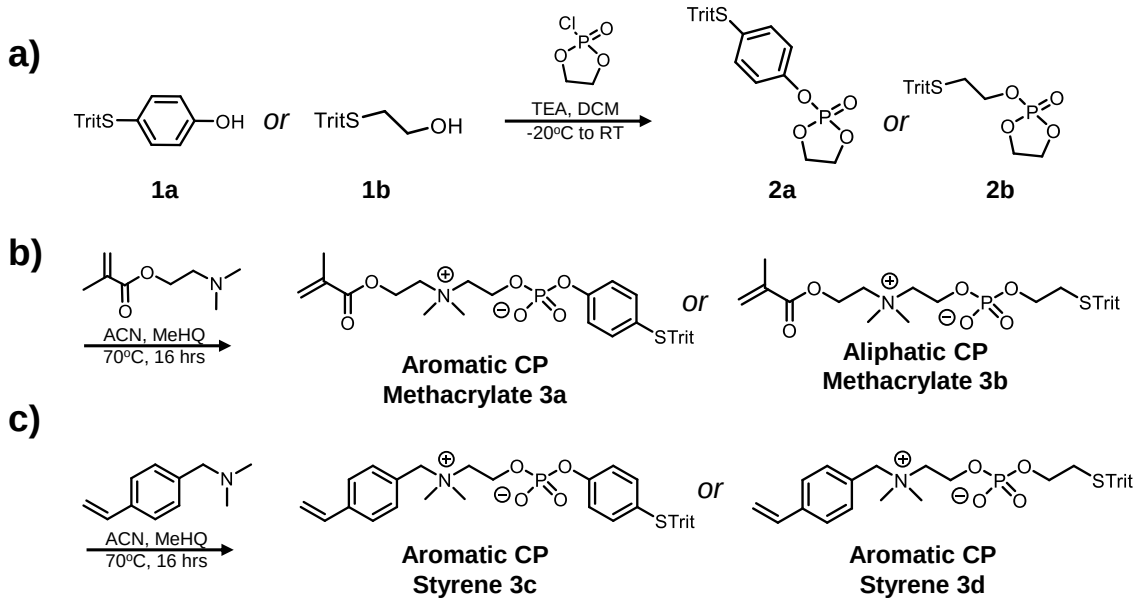

Figure 2-3. Synthesis of *S*-trityl-protected CP zwitterion monomers by ring-opening the (**a**) precursor phospholanes **2a** or **2b** with (**b**) dimethylamino methacrylate to give **3a** and **3b** or (**c**) vinylbenzyl dimethylamine to obtain **3c** and **3d**.

1b, since performing the monomer or polymer syntheses in the presence of the free thiols (*i.e.*, which can serve as nucleophile or chain transfer agent) would be problematic. Reacting the hydroxyl groups of these protected thiols with ethylene chlorophosphate (ECP) gave quantitative isolated yields (> 90%) of phospholane intermediates **2a** and **2b**

Table 2-1. Sample reaction conditions of the ring-opening step (**Figure 2-3b**) to produce CP methacrylates **3a** and **3b**.

Monomer	Trial	Scale (g)	DMAEMA (eq)	Concentration (M)	Conversion (%)‡	Yield (g, %)
3a	1	5.4	4.9	0.2	100	1.5 (21)
	2	12.4	1.4	0.2	100	1.8 (18)
	3	27.1	1.6	0.1	*	10.5 (30)
3b	1	8.1	1.4	0.3	60	2.5 (12)
	2	5.2	1.9	0.2	58	2.5 (36)
	3	32.3	0.9	0.5	57	3.1 (7)

‡*qualitative by ^{31}P NMR*

**product precipitated out of solution before conversion could be assessed*

on multi-gram scales, noting that high ECP conversion at this stage was key for maximizing yields of subsequent steps. Ring-opening of **2a** and **2b** was accomplished with a slight excess of dimethylaminoethyl methacrylate (DMAEMA) in 60-95% conversion to afford CP methacrylates **3a** and **3b** as white or off-white solids, though in modest isolated yields (up to 40%), noting that **3a** precipitated out of solution while cooling to room temperature (**Table 2-1**, **3a**, Trial 3) unlike **3b**, which precipitated upon addition of diethyl ether and contained significant amounts of the triethylammonium chloride by-product (**Table 2-1**). As a result, higher isolated yields (20-30%) were consistently achieved for the aromatic CP methacrylate **3a**, while the high conversion (~100%) of the **3a** ring-opening step was likely due to the absence of an exocyclic methylene group for nucleophilic attack (**Figure**

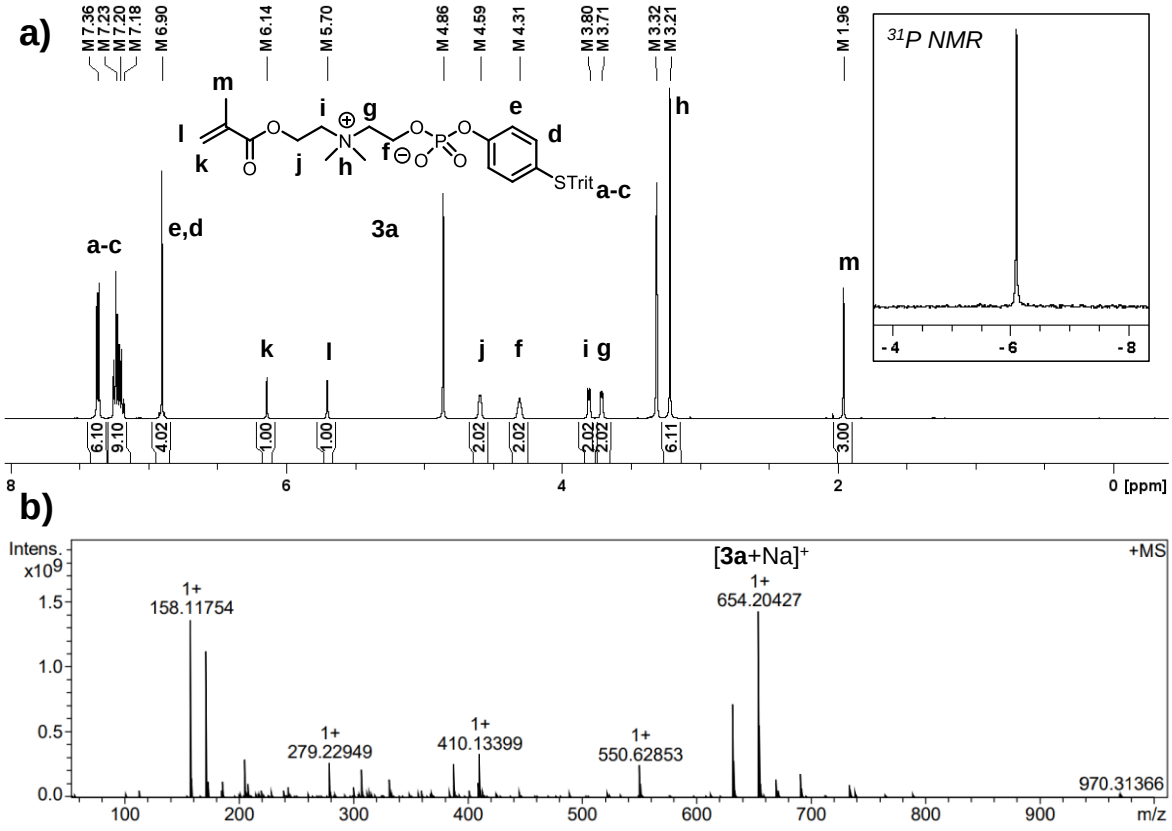

Figure 2-4. (**a**) ^{1}H and ^{31}P NMR (inset) spectra of CP methacrylate **3a** in MeOD-*d4*, including the (**b**) ESI spectrum in positive ion mode.

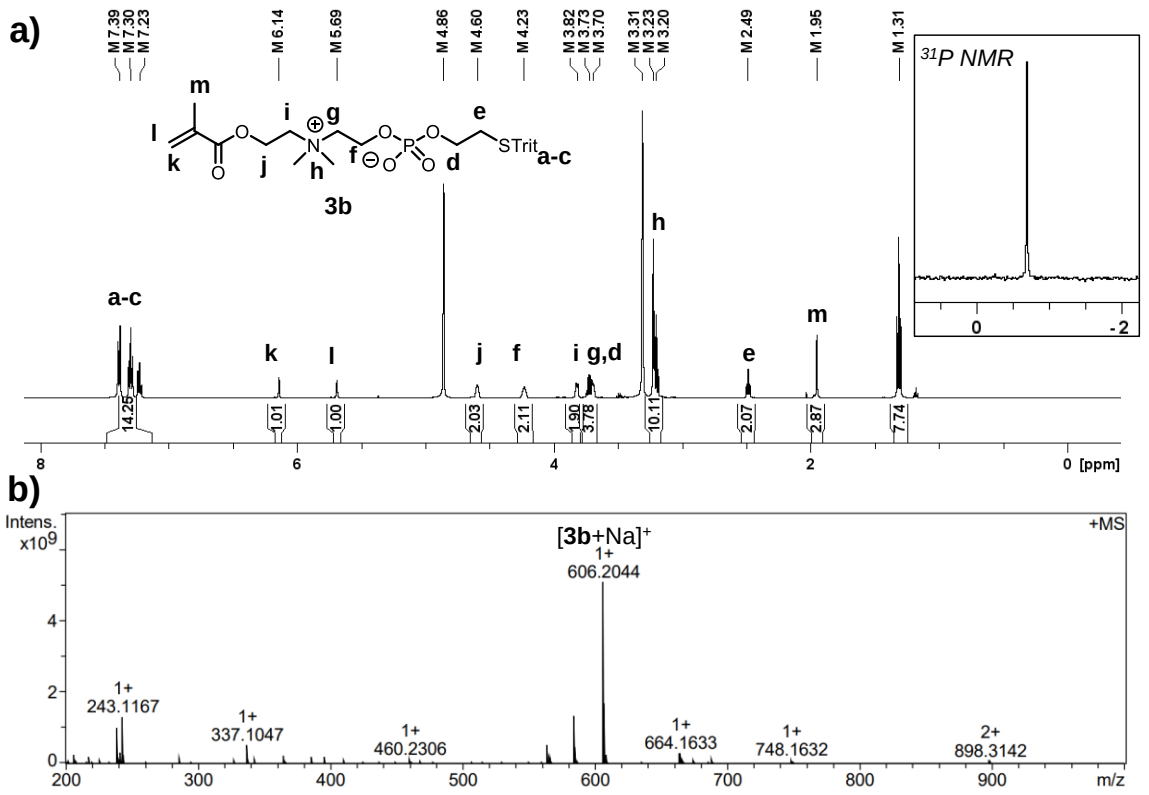

Figure 2-5. (**a**) ^{1}H and ^{31}P NMR (inset) spectra of CP methacrylate **3b** in MeOD-*d4*, including the (**b**) ESI spectrum in positive ion mode.

2-1a). Nevertheless, although increasing the yield of the ring-opening reaction remains an outstanding challenge, multigram quantities of both monomers were obtained. ^{1}H NMR spectroscopy in MeOD-*d4* solution revealed aromatic protons at 6.9 ppm for **3a** (**Figure 2-4a**), and methylene protons at 2.5 ppm for **3b** (**Figure 2-5a**), indicative of successful incorporation of the S-trityl-protected components into the CP monomers. ^{31}P NMR signals (insets of **Figure 2-4a**, **2-5a**) were found at -0.7 ppm for **3a** and -6.1 ppm for **3b**, demonstrating successful ring-opening, with resonances well upfield of that expected for the undesired salt (~18 ppm[8]). Mass spectral analysis by electrospray ionization (ESI) analysis (**Figure 2-4b**, **2-5b**) confirmed the expected molecular weights of the CP-methacrylate monomers, with *m/z* values obtained for the sodium adducts of each (**3a**, $C_{35}H_{38}NO_6PS$: 631.21 g/mol; **3b**, $C_{31}H_{38}NO_6PS$: 583.21 g/mol). Interestingly, monomer

Table 2-2. Sample reaction conditions for the ring-opening step (**Figure 2-3c**) to produce CP methacrylates **3c** and **3d**.

Monomer	Trial	Scale (g)	VBDMA (eq)	Concentration (M)	Conversion (%)‡	Yield (g, %)	Product Purity (%)‡
3c	1	3.8	5.5	0.2	100	1.7 (34)	56
	2	0.8	3.1	0.2	100	0.6 (56)	51
	3	4.1	1.1	0.2	90	0.6 (12)	100
3d	1	6.4	1.1	0.3	40	0.7 (8)	100

‡*qualitative by ^{31}P NMR*

3a was soluble only in MeOH, chloroform, and DMSO, while monomer **3b** dissolved in a wide range of polar organic solvents but not water.

To synthesize CP styrenes **3c** and **3d**, the phospholane intermediates **2a** and **2b** were ring-opened with vinylbenzyl dimethylamine (VBDMA) (**Figure 2-3c**). The resulting CP

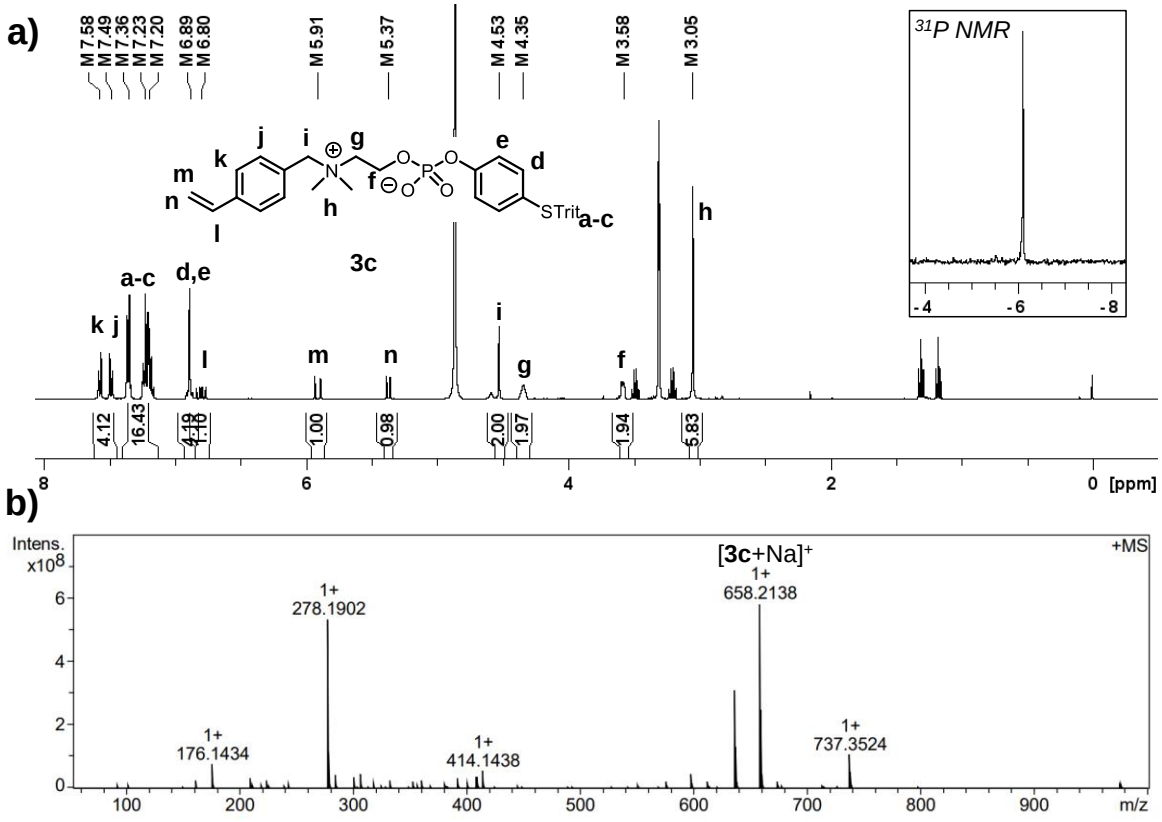

Figure 2-6. (**a**) ^{1}H and ^{31}P NMR (inset) spectra of CP styrene **3c** in MeOD-*d4*, including (**b**) ESI spectrum in positive ion mode.

styrenes **3c** and **3d** were obtained as white solids in low isolated yields (~10%), despite moderate-to-high conversion (40-100%), finding that limiting excess VBDMA to ~1.1 eq. during the ring-opening step was crucial to minimizing by-product formation (**Table 2-2**). ^{1}H NMR spectroscopy in MeOD-*d4* solution revealed aromatic protons at 6.9 ppm for **3c** (**Figure 2-6a**), and methylene protons at 2.5 ppm for **3d** (**Figure 2-7a**), with characteristic aromatic styrene peaks observed at 7.6 and 7.5 ppm, indicative of successful incorporation of the S-trityl-protected components into the CP styrenes. ^{31}P NMR signals (insets of **Figure 2-6a**, **2-7a**) were also found at -0.8 ppm for **3c** and -6.1 ppm for **3d**, confirming that the desired CP styrenes were synthesized and not the corresponding salt (~18 ppm[8]). Mass spectral analysis by electrospray ionization (ESI) analysis (**Figure 2-6b**, **2-7b**) confirmed the expected molecular weights of the CP-styrene monomers, with *m/z* values

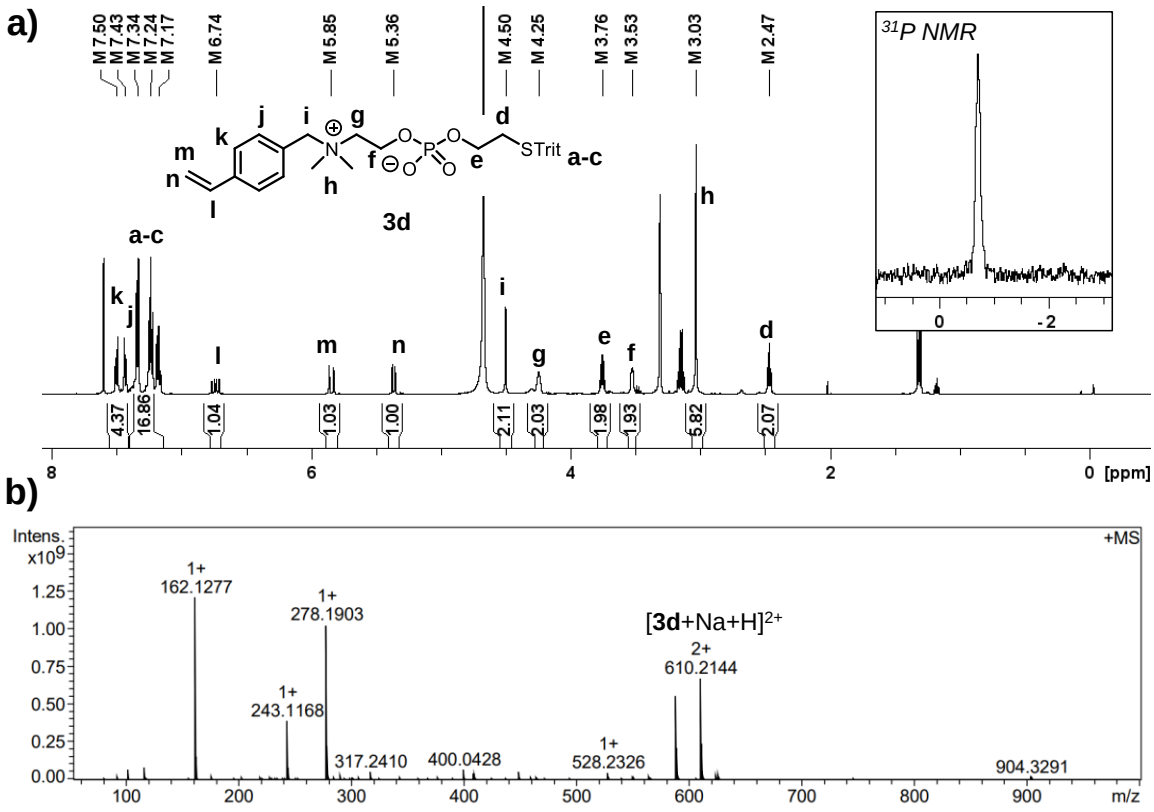

Figure 2-7. (**a**) ^{1}H and ^{31}P NMR (inset) spectra of CP Styrene **3d** in MeOD-*d4*, including (**b**) ESI spectrum in positive ion mode.

obtained for the sodium adducts of each (**3c**, $C_{36}H_{38}NO_4PS$: 635.23 g/mol; **3d**, $C_{32}H_{38}NO_4PS$: 587.23 g/mol).

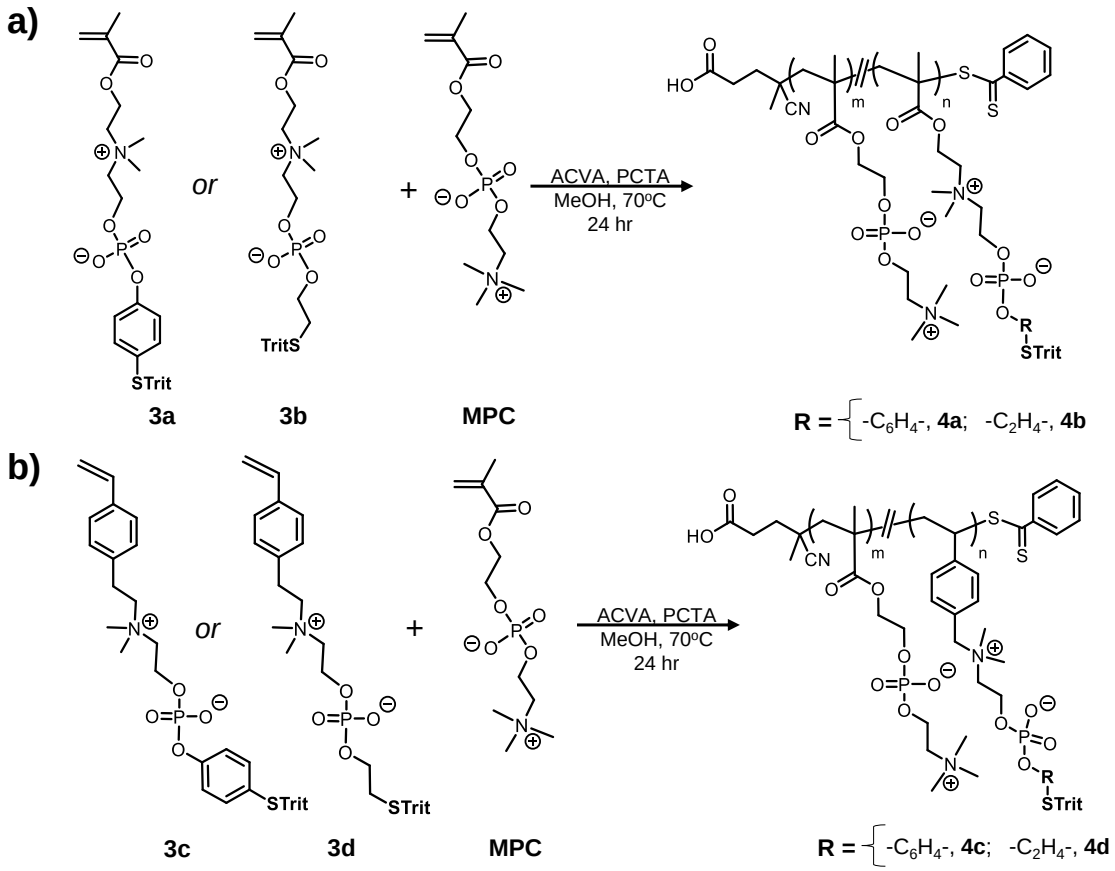

Figure 2-8. Synthesis of random copolymer zwitterions containing (**a**) CP methacrylates **4a** and **4b** or (**b**) CP styrenes **4c** and **4d** and MPC *via* RAFT polymerization in the presence of a dithiobenzoate chain transfer agent (CTA) and azo initiator (ACVA).

2.3 Synthesis of Embedded Thiol CP Zwitterion Polymers

2.3.1 RAFT Copolymerization with MPC

CP methacrylate monomers **3a** and **3b** were used as monomer precursors to fully zwitterionic copolymers with pendent thiols. Considering the hydrophobicity of their trityl protecting groups, we focused first on suitable conditions for copolymerization with MPC, finding effective polymerization in MeOH solutions using reversible addition-

fragmentation chain transfer (RAFT) conditions with dithiobenzoate as chain transfer agent (CTA) and 4,4'-azobis(4-cyanopentanoic acid) (ACVA) as initiator as shown in **Figure 2-8a**. ^{1}H NMR analysis of aliquots removed during the polymerization showed the intensity

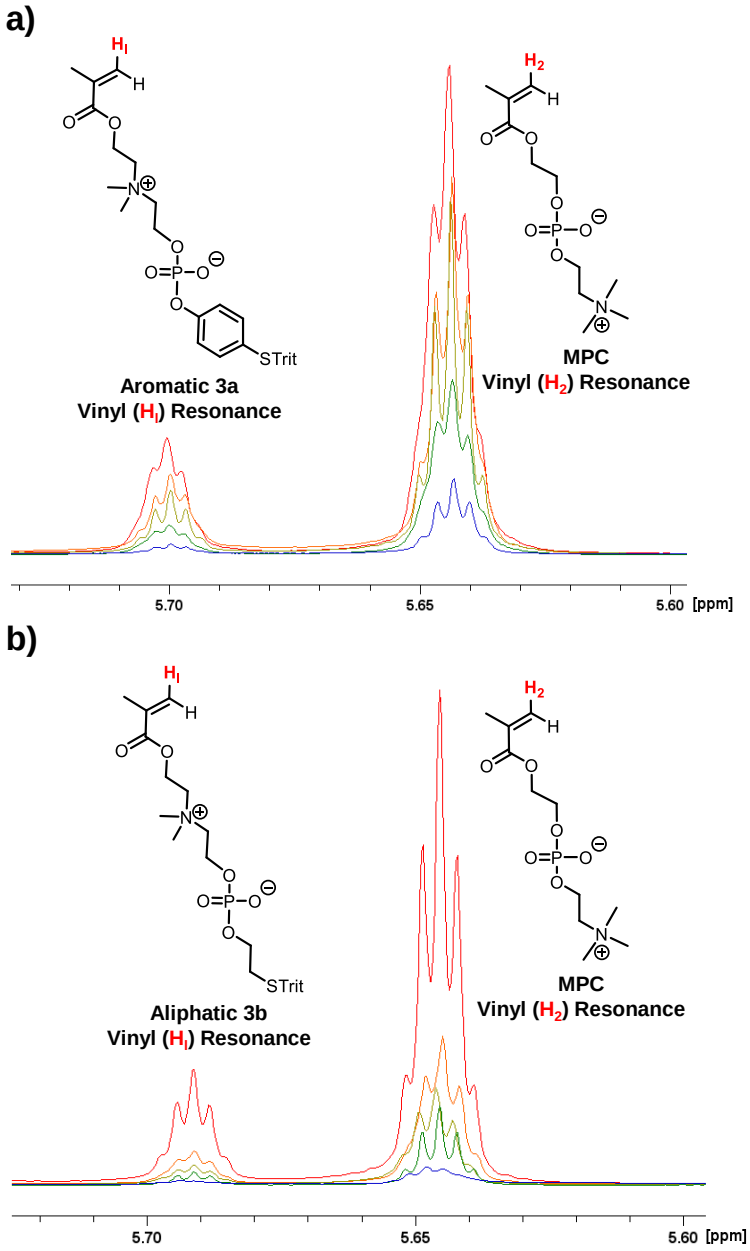

Figure 2-9. Depletion of the vinyl proton resonances of CP methacrylate monomers (denoted $\mathbf{H_I}$) and MPC (denoted $\mathbf{H_2}$) for the RAFT copolymerization of (**a**) aromatic **3a** or (**b**) aliphatic **3b** with MPC, as monitored by ^{1}H NMR spectroscopy in MeOD-*d4*. The five spectra were recorded from aliquots taken from the polymerizations at t = 2h (red), 4h (orange), 6h (yellow), 8h (green), and 24h (blue).

of vinyl resonances of both MPC and **3a** or **3b** to diminish at similar rates, suggesting the formation of a generally random copolymer microstructure (**Figures 2-10a, 2-11a**). About 80% overall monomer conversion was reached in 36 hours, with ^{1}H NMR analysis of the polymer products (**Figures 2-10b**, **2-11b**) indicating good agreement between monomer feed ratio and incorporation into the polymer as shown in **Table 2-3**, which additionally includes theoretical *v.* experimental molecular weights by end-group analysis and GPC estimations, as will be discussed later. The appearance of two distinct resonances in the ^{31}P NMR spectra of copolymers of type **4a** (**Figure 2-10c**) and **4b** (**Figure 2-11c**) confirmed successful integration of both the PC (-0.5 ppm) and CP (-1.0 for **3a** and -6.0 ppm for **3b**) subunits in the copolymers. A maximum of 50 mol% of monomer **3a** was targeted and

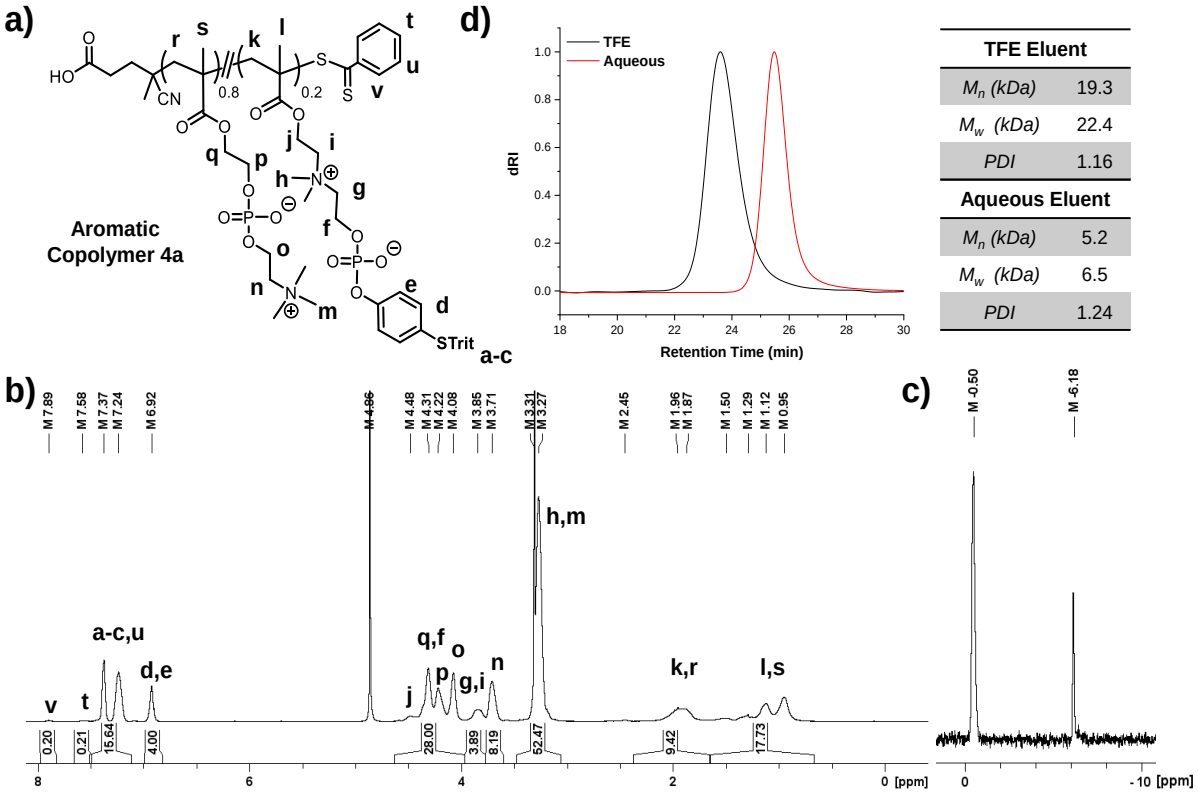

Figure 2-10. (**a**) Structure of random copolymer zwitterion **4a** containing 20 mol % **3a** following RAFT copolymerization with MPC. (**b**) ^{1}H and (**c**) ^{31}P NMR spectra in MeOD-*d4* of **4a-20** and (**c**) representative GPC traces, including estimated molecular weight and PDI values, in TFE and aqueous eluents.

incorporated into the copolymer **4a** whereas a maximum of 20 mol% monomer **3b** was incorporated into copolymer **4b**. Going forward, CP methacrylate copolymers with MPC will be denoted **copolymer-mol% CP** (*e.g.*, copolymer **4a**, with 20 mol% CP methacrylate, is **4a-20**).

Copolymers of type **4a**, containing 10-50 mol% of **3a**, were isolated in 50-80% yield after purification by dialysis against water, with ^{1}H NMR end-group analysis (using the aromatic methyne signal of the CTA at ~8.0 ppm) giving number-average molecular weight (M_n) values in the ~16-42 kDa range against molecular weight targets of ~10-20 kDa. GPC characterization for copolymers of type **4a** using TFE or aqueous mobile phases showed moderate-to-low dispersity values of ~1.1-1.4 (**Figure 2-10d, Table 2-3**), with

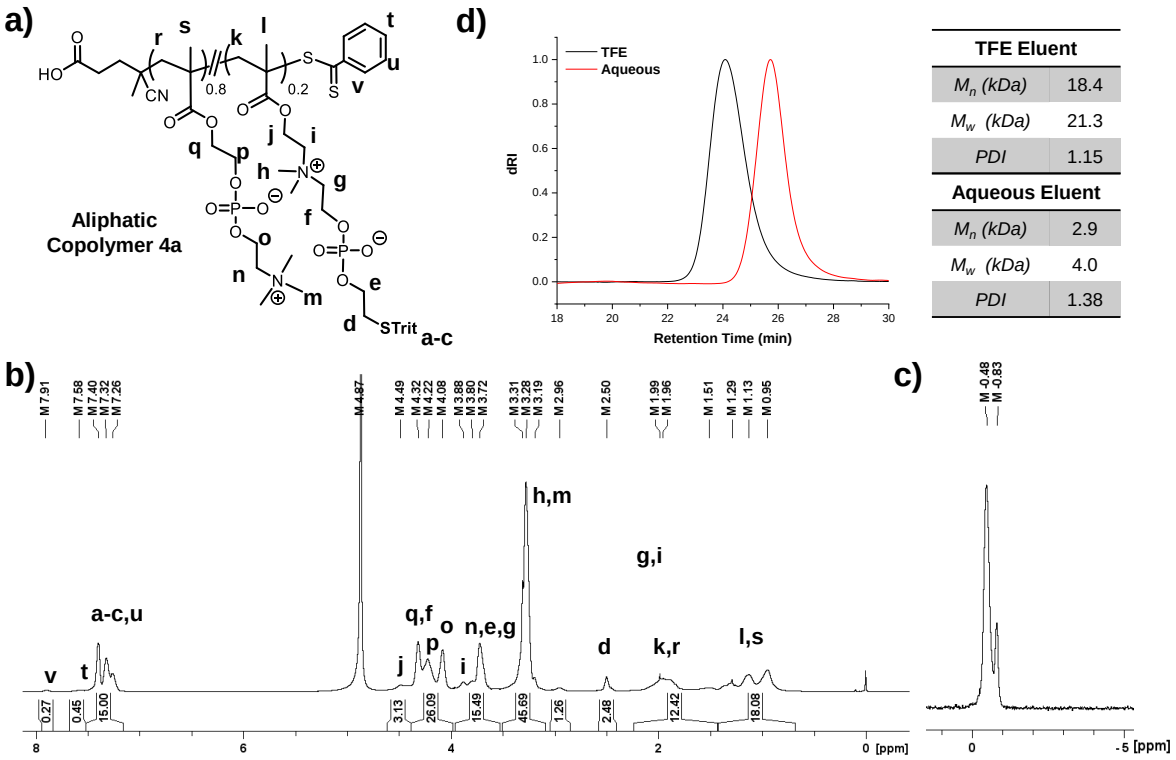

Figure 2-11. (**a**) Structure of random copolymer zwitterion **4b** containing 20 mol % **3b** following RAFT copolymerization with MPC. (**b**) ^{1}H and (**c**) ^{31}P NMR spectra in MeOD-*d4* of **4b-20** and (**c**) representative GPC traces, including estimated molecular weight and PDI values, in TFE and aqueous eluents.

estimated M_n values of ~11-19 kDa in TFE eluents and ~3-6 kDa in aqueous conditions (80% water, 20% acetonitrile) (**Table 2-4**). While the inaccurate molecular weight estimates in aqueous eluents are in part a result of using PEO calibration standards, GPC analysis in both eluents significantly underestimated molecular weight. This is more likely a result of the collapsed conformation that the CP methacrylates adopt in order to shield the large hydrophobic groups from the polar mobile phase environments.

Copolymers of type **4b**, containing the aliphatic CP monomer, were obtained in 40-75% isolated yield following dialysis (which also removes residual triethylammonium chloride), with incorporation of 10-25 mol% **3b** and PDI values of 1.2 or less (**Figure 2-**

Table 2-3. Representative reaction conditions and characterization results for the RAFT copolymerization of embedded thiol CP methacrylates **3a** and **3b** at various mole percents with comonomer MPC.

Trial	Scale (g)	PC:CP Ratio		Concentration (M)*	Conversion (%)	Yield (mg, %)	Molecular Weight by ^{1}H NMR (kDa)	
		Theo.	*Exp.*				*Theo.*	*Exp.*
4a-50	0.3	50:50	45:55	1.5	50	150 (48)	13.2	24.3
4a-30	0.6	70:30	72:28	1.3	80	265 (46)	10.0	34.0
4a-20	2.3	80:20	82:18	0.9	85	1860 (80)	12.0	19.0
4a-10	0.4	90:10	91:9	1.1	80	283 (75)	9.9	42.0
4b-20	0.8	85:15	88:12	0.6	80	531 (71)	16.5	17.9
4b-10	0.3	90:10	94:6	0.5	90	120 (40)	9.6	21.4

** all reactions took place in MeOH with a 3:1 CTA:ACVA ratio*

Table 2-4. Molecular weight estimations by GPC analysis in TFE or aqueous eluents of RAFT copolymers **4a** and **4b**.

Trial	Molecular Weight by TFE GPC (kDa)*			Molecular Weight by Aqueous GPC (kDa)‡		
	M_n	M_w	*PDI*	M_n	M_w	*PDI*
4a-50	11.6	10.2	1.09	3.6	5.0	1.39
4a-30	13.3	16.6	1.24	3.7	5.2	1.40
4a-20	14.2	11.3	1.18	6.0	7.0	1.17
4a-10	18.5	22.4	1.21	5.0	6.4	1.26
4b-20	12.3	15.7	1.28	5.5	6.5	1.18
4b-10	13.6	14.4	1.04	6.8	7.9	1.16

**calibrated against PMMA standards*
‡calibrated against PEO standards

11b, Table 2-3). Interestingly, attempts to copolymerize **3b** at larger scales led to higher PDI values (> 1.2), so smaller scales (~300 mg) were generally used. Copolymers of type **4a** and **4b** were soluble in water, and at high levels in MeOH and TFE.

CP styrene monomers **3c** and **3d** were likewise incorporated into MPC copolymers *via* RAFT polymerization in MeOH solutions using a dithiobenzoate CTA and ACVA as the initiator (**Figure 2-8b**). ^{1}H NMR analysis of the reaction mixture after ~24 hours revealed full conversion of the CP styrene monomers, as indicated by complete loss of the styrenic vinyl proton resonances at 7.4-7.6 ppm, relative to MPC, which only achieved ~70-90% conversion. Following precipitation in diethyl ether and purification by dialysis against water, copolymer products **4c** (**Figure 12a**) and **4d** (**Figure 13a**) were obtained as

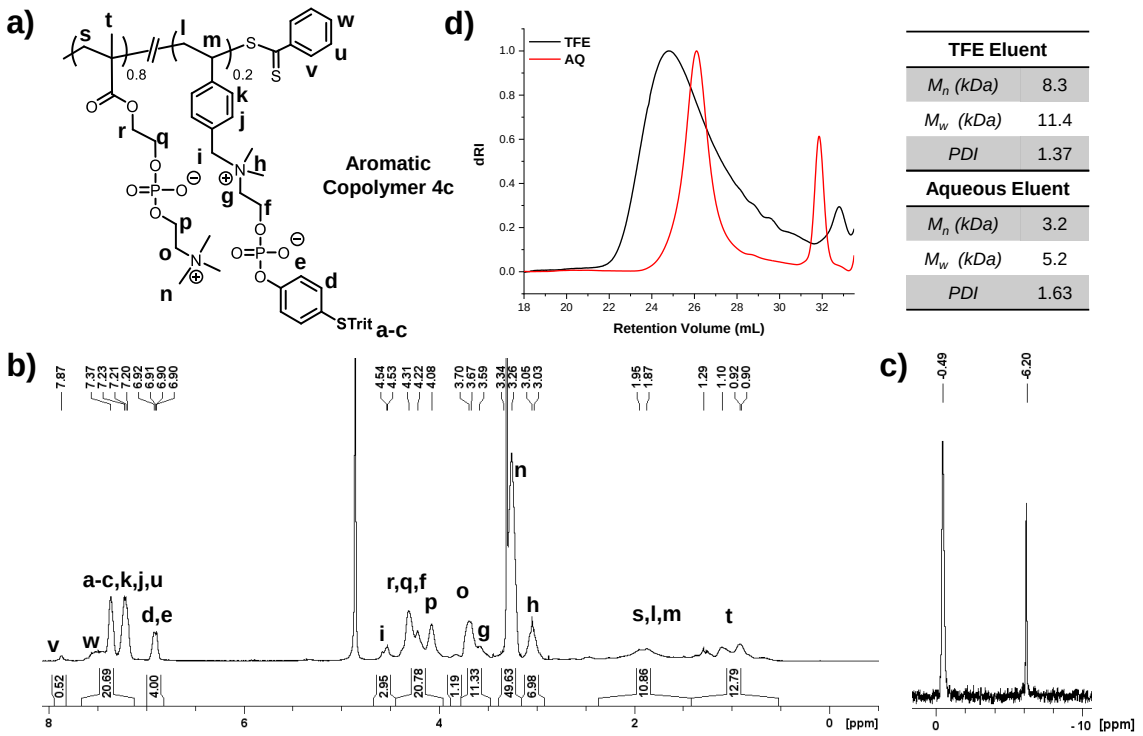

Figure 2-12. (**a**) Synthesis random copolymer zwitterion **4c** *via* RAFT conditions in the presence of a dithiobenzoate chain transfer agent (CTA) and azo initiator (ACVA). (**b**) ^{1}H and (**c**) ^{31}P NMR spectra in MeOD-*d4* and (**c**) representative GPC traces, including estimated molecular weight and PDI values, in TFE and aqueous eluents for copolymer **4c** containing 20 mol % **3c** with MPC.

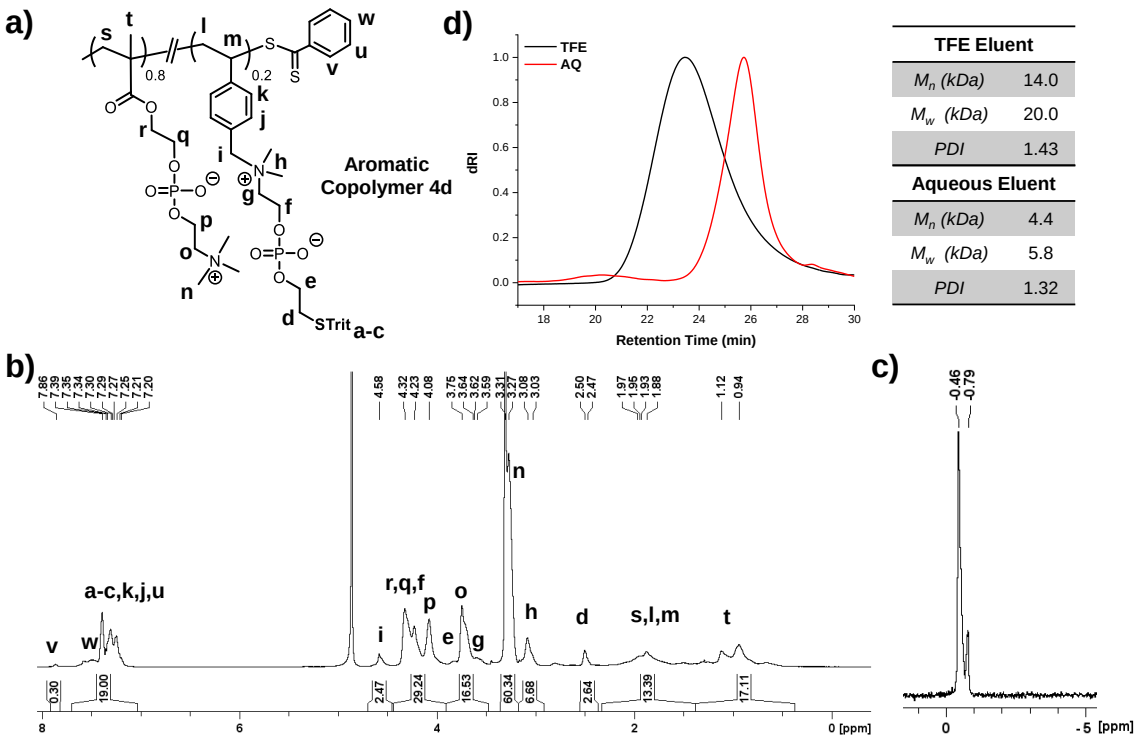

Figure 2-13. (**a**) Synthesis random copolymer zwitterion **4d** *via* RAFT conditions in the presence of a dithiobenzoate chain transfer agent (CTA) and azo initiator (ACVA). (**b**) ^{1}H and (**c**) ^{31}P NMR spectra in MeOD-*d4* and (**c**) representative GPC traces, including estimated molecular weight and PDI values, in TFE and aqueous eluents for copolymer **4d** containing 20 mol % **3d** with MPC.

pink solids in 45-60% isolated yield. ^{1}H NMR end group analysis of both **4c** (**Figures 2-12b**) and **4d** (**Figure 2-13b**) indicated good agreement between theoretical (~10 kDa) *v.* experimental molecular weights (6-13 kDa), as well as between monomer feed ratio and incorporation (**Table 2-5**). To-date, only a maximum of 20 mol% of CP styrenes **3c** or **3d** has been targeted and incorporated into the corresponding copolymers. The appearance of two distinct resonances in the ^{31}P NMR spectra of copolymers of type **4c** (**Figure 2-12c**) and **4d** (**Figure 2-13c**) additionally confirmed successful integration of both the PC (-0.5 ppm) and CP (-0.8 for **3a** and -6.2 ppm for **3b**) subunits in the copolymers. GPC analysis of **4c** copolymers using TFE eluents gave an M_n of ~8 kDa, which resembled the molecular weight calculated by end group analysis (~6 kDa). Similarly, GPC molecular weight

estimations of **4d** copolymers in a TFE mobile phase gave M_n of ~14 kDa which matched M_n values (~13 kDa) determined by end group analysis. Both **4c** and **4d** copolymers had moderate polydispersity values (~1.4), which was likely a result of copolymerizing both styrene and methacrylate monomers. As had been the case for **4a** and **4b** copolymers, GPC characterization of **4c** and **4d** copolymers in aqueous eluents gave M_n estimates that were much smaller (**Table 2-6**).

Table 2-5. Representative reaction conditions and characterization results for the RAFT copolymerization of embedded thiol CP methacrylates **3c** and **3d** at various mole percents with comonomer MPC.

Trial	Scale (g)	PC:CP Ratio		Concentration (M)*	Conversion (%)	Yield (mg, %)	Molecular Weight by ^{1}H NMR (kDa)	
		Theo.	*Exp.*				*Theo.*	*Exp.*
4c-20	0.3	80:20	73:27	0.5	70	106 (45)	9.8	6.0
4d-20	0.6	80:20	80:20	0.5	90	130 (57)	10.0	12.7

Table 2-6. Molecular weight estimations by GPC analysis in TFE or aqueous eluents of RAFT copolymers **4c** and **4d**.

Trial	Molecular Weight by TFE GPC (kDa)*			Molecular Weight by Aqueous GPC (kDa)‡		
	M_n	M_w	*PDI*	M_n	M_w	*PDI*
4c-20	8.3	11.4	1.37	3.2	5.2	1.63
4d-20	14.0	20.0	1.43	4.4	5.8	1.32

**calibrated against PMMA standards*
‡calibrated against PEO standards

2.3.2 RAFT Homopolymerization

In addition to copolymerization, the RAFT homopolymerization of aromatic CP monomer **3a** (**Figure 2-14a**) proceeded effectively to 80% conversion (**Table 2-7**) with a trithiocarbonate CTA and ACVA initiator in methanol solutions, judging from monomer disappearance by ^{1}H NMR analysis. The resultant CP homopolymer **3a** was soluble only in DMF and DMSO, and was isolated in up to 60% yield following purification by dialysis

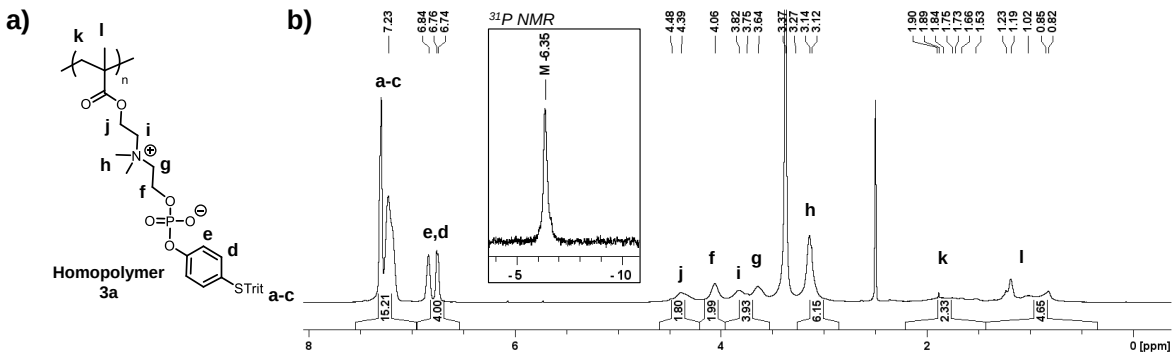

Figure 2-14. (**a**) Structure of homopolymer zwitterion **3a** and its (**b**) ^{1}H and (*inset*) ^{31}P NMR spectra in DMSO-*d6*.

in MeOH: DMSO (1:1), which effectively removed residual monomer, and precipitation into water:MeOH mixtures (**Figure 2-14a**). ^{31}P NMR spectroscopy analysis (in DMSO-*d6*) showed one resonance at -6.32 ppm (**Figure 2-14b,** *inset*) while ^{1}H NMR analysis showed broadened CP monomer resonances (**Figure 2-14b**), as anticipated for the CP homopolymer structure. However, molecular weight characterization *via* GPC or end-group analysis to-date has been unrealized due to mobile phase refractive index matching

Table 2-7. Optimization of RAFT homopolymerization conditions for embedded thiol CP methacrylates **3a**.

Trial	CTA	Solvent	Concentration (M)	Conversion (%)*	Yield (mg, %)
1	PCTA	MeOH	0.5	70	230 (75) ‡
2		MeOH	1.0	50	157 (52) ‡
3		TFE	1.0	0	-
4		MeOH/CHCl3	0.5	65	263 (88) ‡
5		DMSO/MeOH	0.24	50	82 (27) ‡
6		DMSO/DMF/MeOH	0.24	68	0
7	YCTA	MeOH	0.5	79	248 (81) ‡
8		MeOH/DMSO	0.4	54	200 (66) ‡
9		MeOH/DMF	0.4	54	241 (79) ‡
10		MeOH	0.5	75	174 (58)

‡*impurity remains from monomer*
**estimated from relative ratios of monomer to polymer integrations by ^{1}H and ^{31}P NMR*

and overlapping CTA proton resonances, respectively. Attempts to homopolymerize CP monomers **3b**, **3c** or **3d**, on the other hand, have been met with limited success due to the formation of unknown reaction products observed in ^{31}P NMR during polymerization.

2.3.3 RAFT Block Copolymerization with MPC

Although random copolymer and homopolymer structures were successfully achieved for the RAFT polymerization of CP methacrylate **3a**, obtaining block copolymer structures has not yet been realized. Attempted routes to block copolymers containing CP methacrylate **3a** included the following strategies: (1) the synthesis of PMPC as macro chain transfer agent (macroCTA), followed by chain extension with **3a**; and (2) the synthesis of **3a** homopolymers (see *section 2.3.2*) to serve as macroCTAs, with chain extension by MPC. In both cases, GPC analysis of the crude polymerization mixtures in TFE or aqueous eluents revealed the presence of two polymer species, indicative that chain extension of the macroCTA from was incomplete. It is believed that the solubility of the nascent polymer chain is limiting block copolymer synthesis since homopolymers of **3a** are only soluble in DMSO and DMF, in which PMPC is insoluble.

2.4 Synthesis of Polymeric Zwitterionic Thiols (PZTs)

With synthetic routes to embedded thiol polymer zwitterions established, the protected thiols in zwitterionic copolymers **4a** and **4b** were liberated by stirring in aqueous solutions of trifluoroacetic acid (TFA) at room temperature (**Figure 2-15**), affording copolymer zwitterions **5a** (**Figure 2-16a**) and **5b** (**Figure 2-17a**), with successful deprotection indicated in their ^{1}H NMR spectra that lacked any aromatic (trityl) signals (~7.0-7.5 ppm) (**Figure 2-16b**, **2-17b**). However, an Ellman's assay of the deprotected copolymers

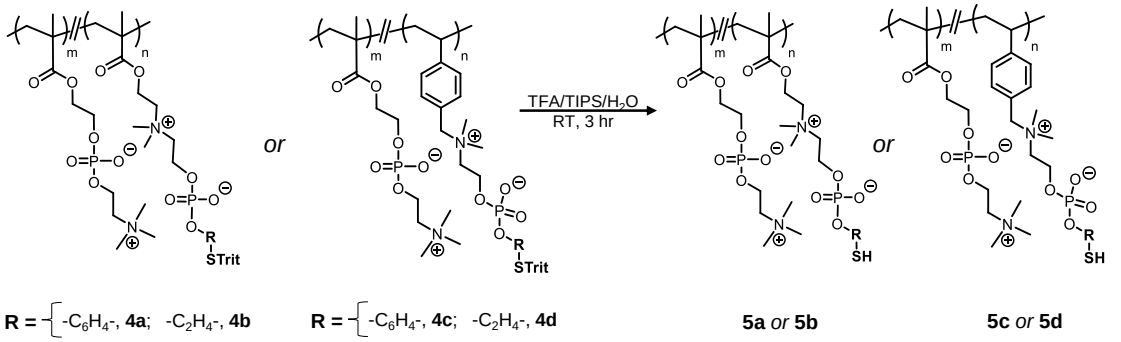

Figure 2-15. General reaction scheme for deprotection of embedded thiol CP polymer zwitterions to yield CP polymer zwitterion thiols (**PZTs**).

revealed a free thiol content of, at most, 80% of the theoretical maximum (**Table 2-8**). For copolymer **5a**, organic solubility (e.g., in MeOH or TFE) often required adding trace amounts of tris(2-carboxyethyl)phosphine hydrochloride (TCEP), which may reduce any disulfides that had formed. ^{31}P NMR spectroscopy proved useful for characterizing the free thiol *vs*. disulfide content in the polymers. For example, copolymer **5a-20** in 0.1 M PBS pH 8.2, 1 mM EDTA buffer (and 10% D_2O) showed phosphorus resonances at -4.9 ppm and -5.6 ppm, while the PC phosphorus signal remained unchanged at -0.5 ppm (**Figure 2-16c**). Treatment with TCEP increased the peak intensity and sharpness of the -4.9 ppm resonance, accompanied by appearance of a signal at 57.5 ppm for the TCEP phosphine and 17.0 ppm for the oxidized TCEP product. Then, adding 50 wt% H_2O_2 to the polymer solutions in PBS buffer resulted in a single, broader resonance at -5.6 ppm (**Figure 2-18a**). Two ^{31}P resonances were likewise observed in MeOD (-5.7 ppm and -6.0 ppm), with addition of TCEP resulting in one dominant signal at -5.7 ppm (**Figure 2-18b**). The sharper, more upfield phosphorus resonance in both D_2O and MeOD is attributed to the presence of free sulfhydryl in the **5a-20** copolymer, in contrast to the downfield resonances which is indicative of disulfide bonds. Despite the apparent disulfide formation, the copolymer solution remained visually homogeneous at all stages (i.e., without evident

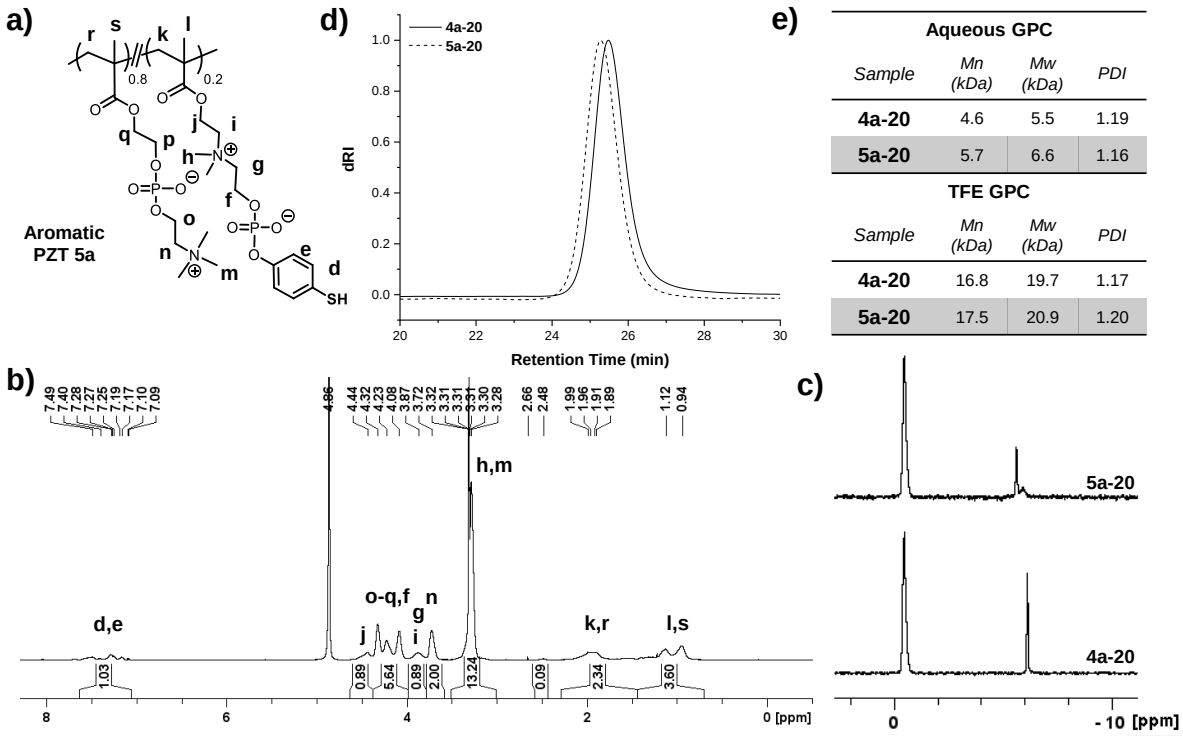

Aqueous GPC

Sample	*Mn (kDa)*	*Mw (kDa)*	*PDI*
4a-20	4.6	5.5	1.19
5a-20	5.7	6.6	1.16

TFE GPC

Sample	*Mn (kDa)*	*Mw (kDa)*	*PDI*
4a-20	16.8	19.7	1.17
5a-20	17.5	20.9	1.20

Figure 2-16. (**a**) Structure of **PZT 5a** following TFA deprotection. (**b**) ^{1}H NMR spectra of **5a-20** in MeOD-*d4* and (**c**) ^{31}P NMR spectra of **5a-20** compared to **4a-20** in MeOD-*d4*, including (**d**) representative GPC traces of **4a-20** versus **5a-20** in TFE eluents and (**e**) associated GPC molecular weight estimates and PDI values for both TFE and aqueous eluents.

precipitation or gelation), which may indicate the formation of intramolecular disulfides under these conditions (<10 mg/mL). Moreover, after trityl deprotection, GPC characterization of copolymers **5a-20** showed little-to-no change in molecular weight or PDI from their protected version, both in aqueous and TFE mobile phases (**Figure 2-16d,e**), suggestive that the aromatic CP content controls polymer conformation in polar solvents more than trityl groups.

In contrast to the aromatic CP polymers, the aliphatic copolymers of type **5b** did not require addition of TCEP to promote solubilization. The characteristic phosphorous CP resonance in **5b** was observed at -0.1 ppm, distinct from the MPC phosphorus resonance at -0.5 ppm (**Figure 2-17c**). Molecular weight characterization by GPC, eluting in TFE,

revealed an increase post-deprotection from ~12-14 kDa to ~19 kDa, likely a result of improved solvation in TFE solvents following loss of hydrophobic trityl groups, while retaining a similar PDI around ~1.1. In an aqueous mobile phase, PDI values remained

Table 2-8. Amount of free thiol (SH/chain and mol% SH) in **5a-20**, **5b-20**, **5c-20**, and **5d-20** copolymers as determined by Ellman's Assay by measuring absorbance (A_{412}).

Polymer	Trial	SH/chain			mol% SH		
		Exp.	*Theo.*	*%*	*Exp.*	*Theo.*	*%*
	5	7	10	68	13	20	68
5a-20	6	4.7	10	47	9	20	47
	8	10	13	80	15	20	80
5b-20	1	<1	8	7	1	20	7
5c-20	1	0.6	3	20	6	30	20
5d-20	1	0.3	7	4	0.8	20	4

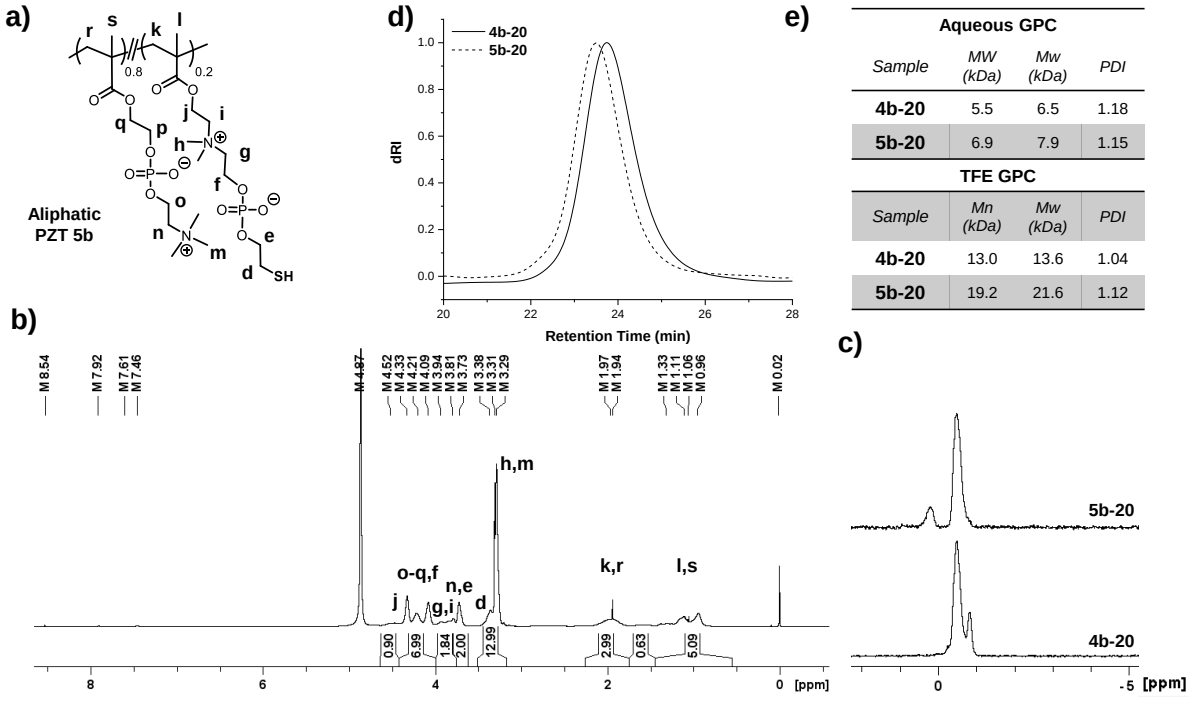

Figure 2-17. (**a**) Structure of **PZT 5b** following TFA deprotection. (**b**) ^{1}H NMR spectra of **5b-20** in MeOD-*d4* and (**c**) ^{31}P NMR spectra of **5b-20** compared to **4b-20** in MeOD-*d4*, including (**d**) representative GPC traces of **4b-20** versus **5b-20** in TFE eluents and (**e**) associated GPC molecular weight estimates and PDI values for both TFE and aqueous eluents.

unchanged (~1.2) accompanied by minimal molecular weight changes (~5-7 kDa to ~4-6 kDa) (**Figure 2-17d,e**).

In some cases, the GPC trace in TFE eluents of both **PZTs 5a** and **5b** showed a small shoulder at lower retention time (higher molecular weight, about twice the peak-average molecular weight (M_p) of the primary peak) and a corresponding increase in PDI (from 1.04 to 1.20), which may reflect some extent of inter-chain coupling. However, no such shoulders were observed in polymer solutions prepared with TCEP.

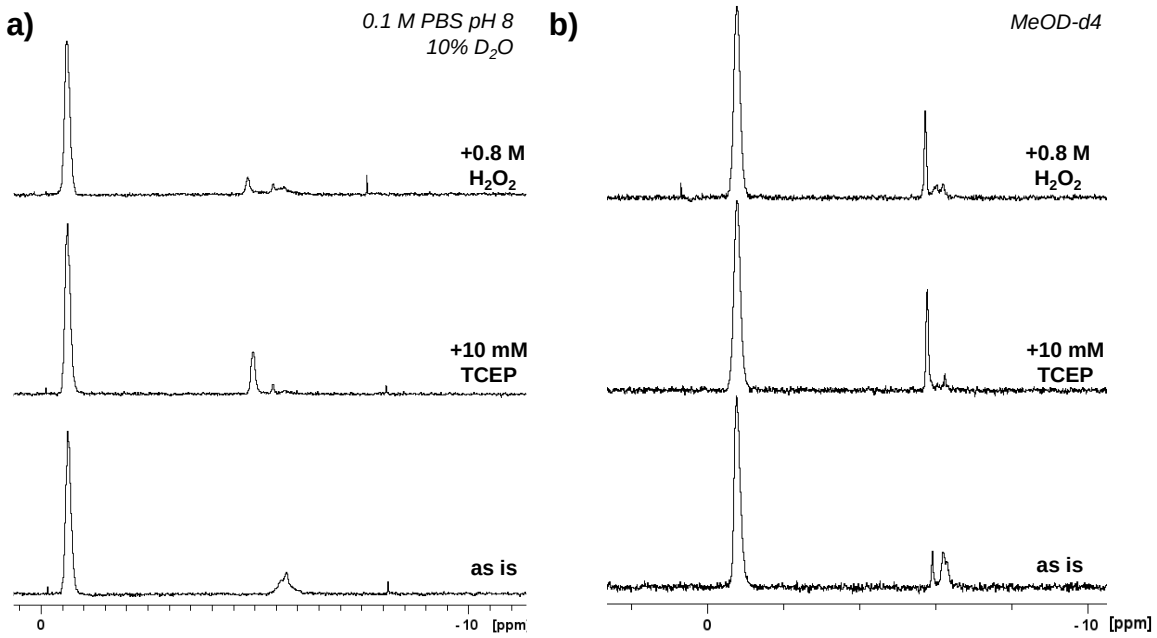

Figure 2-18. (**a**) ^{31}P NMR spectrum of **5a-20** copolymers in 0.1 M PBS pH 8 with 10% D_2O as is (bottom line), after addition of 10 mM TCEP (middle line), and after exposure to 0.8 M hydrogen peroxide for 30 minutes (top line). (**b**) ^{31}P NMR spectrum of **5a-20** copolymers in MeOD-*d4* as is (bottom line), after addition of 10 mM TCEP (middle line), and after exposure to 0.8 M hydrogen peroxide for 30 minutes (top line).

Trityl-protected CP styrene-based copolymer zwitterions were also deprotected in aqueous solutions of trifluoroacetic acid (TFA) at room temperature (**Figure 2-15**), affording styrenic copolymer zwitterions (**SPZTs**) **5c** (**Figure 2-19a**) and **5d** (**Figure 2-20a**) as white solids in 50% yield. Successful deprotection was indicated in their ^{1}H NMR spectra that lacked any trityl signals (~7.0-7.5 ppm) (**Figure 2-19b**, **2-20b**). Moreover, the

characteristic phosphorous CP resonance for **5c** (**Figure 2-19c**) shifted downfield and broadened from -6.2 to -5.3 ppm, while the CP resonance of **5d** copolymers similarly broadened and shifted downfield from -0.8 to 0.3 ppm (**Figure 2-20c**); both CP resonances were distinct from the MPC phosphorus resonance at -0.5 ppm. An Ellman's assay of the deprotected copolymers revealed a maximum free thiol content of 20% (**Table 2-8**) and did not require reducing agents to promote organic solubility. After trityl deprotection, GPC characterization of copolymer **5c-20** in TFE eluents showed a significant increase in molecular weight whereas in aqueous eluents, the PDI showed a significant increase (**Figure 2-19d,e**). In contrast, GPC characterization of copolymers **5c-20** showed little-to-no change in molecular weight or PDI from their protected version, both in aqueous and TFE mobile phases (**Figure 2-20d,e**).

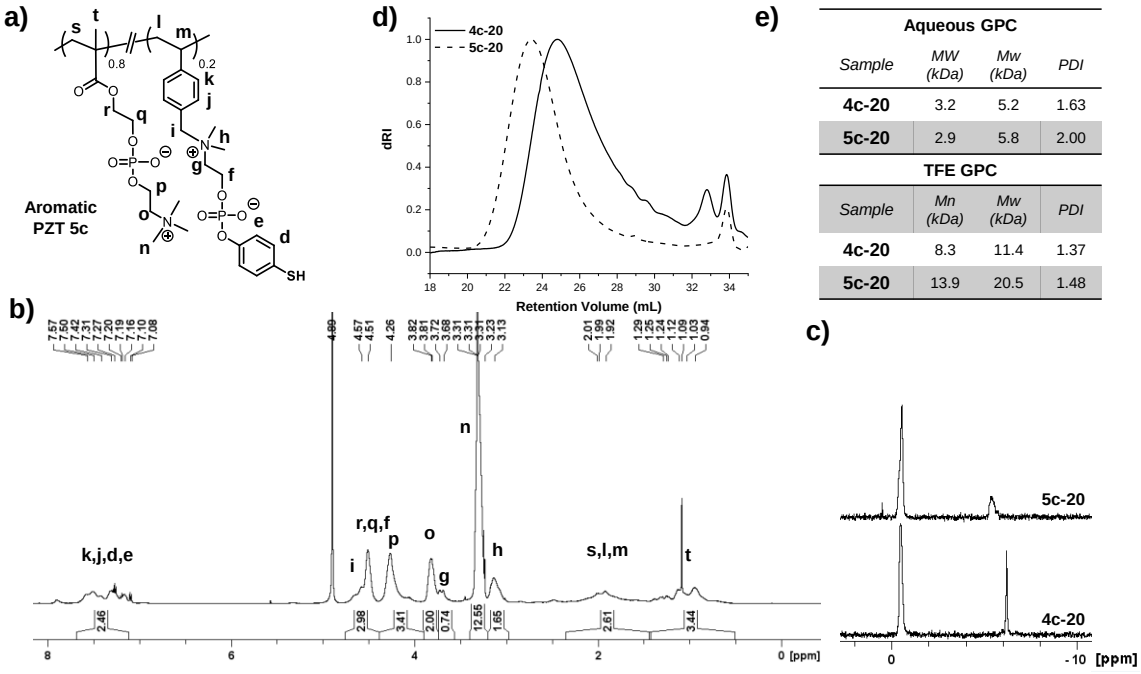

Aqueous GPC

Sample	*MW (kDa)*	*Mw (kDa)*	*PDI*
4c-20	3.2	5.2	1.63
5c-20	2.9	5.8	2.00

TFE GPC

Sample	*Mn (kDa)*	*Mw (kDa)*	*PDI*
4c-20	8.3	11.4	1.37
5c-20	13.9	20.5	1.48

Figure 2-19. (**a**) Structure of **SPZT 5c** following TFA deprotection. (**b**) ^{1}H NMR spectra of **5c-20** in MeOD-*d4* and (**c**) ^{31}P NMR spectra of **5c-20** compared to **4c-20** in MeOD-*d4*, including (**d**) representative GPC traces of **4c-20** versus **5c-20** in TFE eluents and (**e**) associated GPC molecular weight estimates and PDI values for both TFE and aqueous eluents.

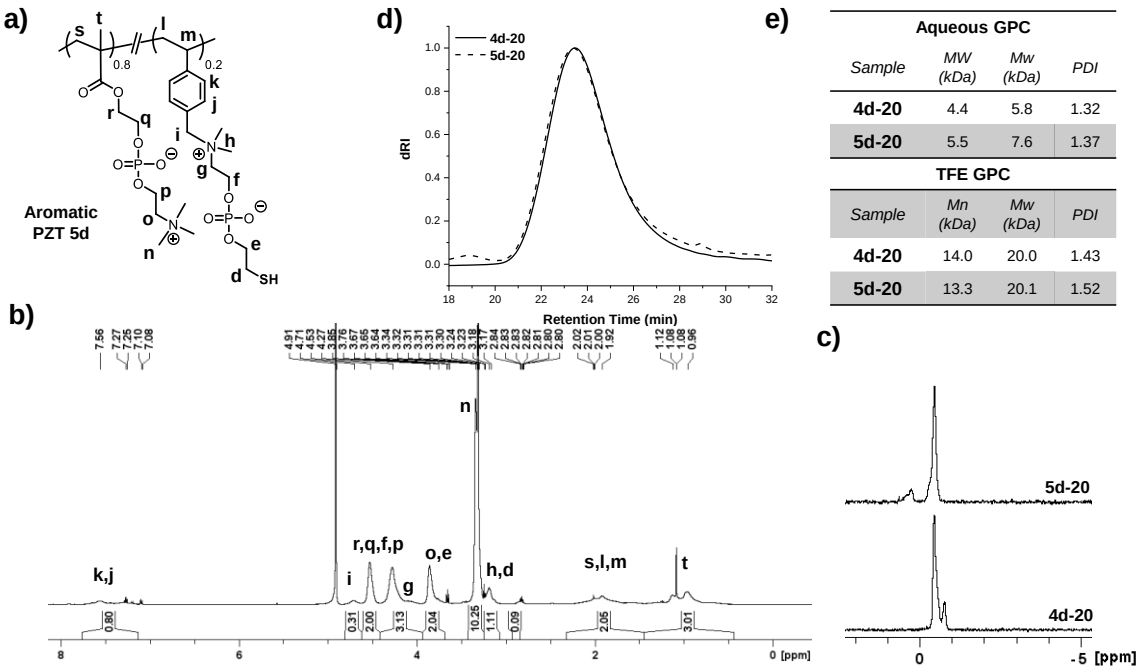

Aqueous GPC

Sample	*MW (kDa)*	*Mw (kDa)*	*PDI*
4d-20	4.4	5.8	1.32
5d-20	5.5	7.6	1.37

TFE GPC

Sample	*Mn (kDa)*	*Mw (kDa)*	*PDI*
4d-20	14.0	20.0	1.43
5d-20	13.3	20.1	1.52

Figure 2-20. (**a**) Structure of **SPZT 5d** following TFA deprotection. (**b**) ^{1}H NMR spectra of **5d-20** in MeOD-*d4* and (**c**) ^{31}P NMR spectra of **5d-20** compared to **4d-20** in MeOD-*d4*, including (**d**) representative GPC traces of **4d-20** versus **5d-20** in TFE eluents and (**e**) associated GPC molecular weight estimates and PDI values for both TFE and aqueous eluents.

2.5 Summary

Chapter 2 describes the synthesis of embedded thiol CP methacrylates and styrenes from their S-trityl protected mercaptophenol (aromatic) and mercaptoethanol (aliphatic) starting reagents and their incorporation into copolymers using RAFT controlled polymerization with MPC as comonomer. The thiol moieties of the embedded thiol copolymers were liberated with acid to give aromatic and aliphatic with methacrylate (**PZTs**) or styrene backbones (S**PZTs**), thereby expanding the functional and reactive polymer zwitterion library to include zwitterions with pendent thiols. The fundamental properties of these novel **PZTs** in hydrogel formation, interfacial stabilization, and polymer-protein bioconjugation are further explored in **Chapters 3** and **4**.

2.6 References

1. Ishihara, K.; Ueda, T.; Nakabayashi, N. Preparation of Phospholipid Polymers and Their Properties as Polymer Hydrogel Membranes. *Polym. J.* **1990**, *22* (5), 355–360.

2. Li, D.; Wei, Q.; Wu, C.; Zhang, X.; Xue, Q.; Zheng, T.; Cao, M. Superhydrophilicity and Strong Salt-Affinity: Zwitterionic Polymer Grafted Surfaces in Biological Systems. *Adv. Colloid Interface Sci.* **2020**, *278*, 102141, 18 pages.

3. Jin, Q.; Chen, Y.; Wang, Y.; Ji, J. Zwitterionic Drug Nanocarriers: A Biomimetic Strategy for Drug Delivery. *Colloids Surf. B: Biointerfaces* **2014**, *124*, 80–86.

4. Brown, M. U.; Triozzi, A.; Emrick, T. Polymer Zwitterions with Phosphonium Cations. *J. Am. Chem. Soc.* **2021**, *143* (17), 6528–6532.

5. Ishihara, K., Nomura, H., Mihara, T., Kurita, K., Iwasaki, Y., and Nakabayashi, N. Why do Phospholipid Polymers Reduce Protein Adsorption? *J. Biomed. Mater. Res.* **1998**, *39*, 323–330.

6. Mi, L.; Jiang, S. Integrated Antimicrobial and Nonfouling Zwitterionic Polymers. *Angew. Chem. Int. Ed.* 2014, *53*, 1746–1754.

7. Iwasaki, Y.; Ishihara, K. Phosphorylcholine-Containing Polymers for Biomedical Applications. *Anal. Bioanal. Chem.* **2005**, *381*, 534–546.

8. Hu, G. J.; Parelkar, S. S.; Emrick, T. A Facile Approach to Hydrophilic, Reverse Zwitterionic, Choline Phosphate Polymers. *Polym. Chem.* **2015**, *6* (4), 525–530.

9. Hu, G.; Emrick, T. Functional Choline Phosphate Polymers. *J. Am. Chem. Soc.* **2016**, *138*, 1828–1831.

10. Chalarca, C. F. S.; Emrick, T. Reactive Polymer Zwitterions: Sulfonium Sulfonates. *J. Polym. Sci. A. Polym. Chem.* **2017**, *55*, 83–92.

11. Zhou, L.; Triozzi, A.; Figueiredo, M.; Emrick, T. Fluorinated Polymer Zwitterions: Choline Phosphates and Phosphorylcholines. *ACS Macro Lett.* **2021**, *10*, 1204–1209.

12. Brown, M. U.; Seong, H.-G.; Margossian, K. O.; Bishop, L.; Russell, T. P.; Muthukumar, M.; Emrick, T. Zwitterionic Ammonium Sulfonate Polymers: Synthesis and Properties in Fluids. *Macromol. Rapid Commun.* **2022**, *43*, 2100678, 7 pages.

13. Chang, C.-C.; Letteri, R.; Hayward, R. C.; Emrick, T. Functional Sulfobetaine Polymers: Synthesis and Salt-Responsive Stabilization of Oil-in-Water Droplets. *Macromolecules* **2015**, *48* (21), 7843–7850.

14. Chen, T.-M.; Wang, Y.-F.; Li, Y.-J.; Nakaya, T.; Sakurai, I. Studies on the Synthesis and Properties of Novel Phospholipid Analogous Polymers. *J. Appl. Polym. Sci.* **1996**, *60* (3), 455–464.

15. Nguyen, H. N.; Ngo, T. L. H.; Iwasaki, Y.; Huang, C.-J. Biodegradable Phosphocholine Cross-Linker with Ion-Pair Design for Tough Zwitterionic Hydrogel. *Adv. Mater. Interfaces* **2022**, *9* (33), 2201002, 11 pages.

16. Nakano, H.; Noguchi, Y.; Kakinoki, S.; Yamakawa, M; Osaka, I.; Iwasaki, Y. Highly Durable Lubricity of Photo-Cross-Linked Zwitterionic Polymer Brushes Supported by Poly(ether ether ketone) Substrate. *ACS Appl. Bio Mater.* **2020**, *3* (2), 1071–1078.

17. Letteri, R. A.; Chalarca, C. F. S.; Bai, Y.; Hayward, R. C.; Emrick, T. Forming Sticky Droplets from Slippery Polymer Zwitterions. *Adv. Mater.* **2017**, *29*, 17002921, 8 pages.

18. Zhao, J.; Chalarca, C. F. S.; Nunes, J. K.; Stone, H. A.; Emrick, T. Self-Propelled Supracolloidal Fibers from Multifunctional Polymer Surfactants and Droplets. *Macromol. Rapid Commun.* **2020**, *41*, 2000334, 7 pages.

19. Yang, Z.; Zhao, J.; Emrick, T. Functional Polymer Zwitterions as Reactive Surfactants for Nanoparticle Capture. *ACS Appl. Mater. Interfaces* **2021**, *13* (18), 21898–21904.

20. Skinner, M.; Johnston, B. M.; Liu, Y.; Hammer, B.; Selhorst, R.; Xenidou, I.; Perry, S. L.; Emrick, T. Synthesis of Zwitterionic Pluronic Analogs. *Biomacromolecules* **2018**, *19* (8), 3377–3389.

21. Zhao, J.; Pan, Z.; Snyder, D.; Stone, H. A.; Emrick, T. Chemically Triggered Coalescence and Reactivity of Droplet Fibers. *J. Am. Chem. Soc.* **2021**, *143* (14), 5558–5564.

22. Sonu, K. P.; Zhou, L.; Biswas, S.; Klier, J.; Balazs, A. C.; Emrick, T.; Peyton, S. R. Strain-Stiffening Hydrogels with Dynamic, Secondary Cross-Linking. *Langmuir* **2023**, *39* (7), 2659–2666.

23. Chalarca, C. F. S.; Letteri, R. A.; Perazzo, A.; Stone, H. A.; Emrick, T. Building Supracolloidal Fibers from Zwitterion-Stabilized Adhesive Emulsions. *Adv. Funct. Mater.* **2018**, *28*, 1804325, 10 pages.

24. Kolate, A.; Baradia, D.; Patil, S.; Vhora, I.; Kore, G.; Misra, A. PEG — A Versatile Conjugating Ligand for Drugs and Drug Delivery Systems. *J. Cont. Release* **2014**, *192*, 67–81.

25. Alconcel, S. N. S.; Baas, A. A.; Maynard, H. D. FDA-Approved Poly(ethylene glycol)–Protein Conjugate Drugs. *Polym. Chem.* **2011**, *2*, 1442–1448.

26. Chakma, P.; Konkolewicz, D. Dynamic Covalent Bonds in Polymeric Materials. *Angew. Chem. Int. Ed.* **2019**, *58* (29), 9682–9695.

27. Mutlu, H.; Ceper, E. B.; Li. X.; Yang, J.; Dong, W.; Ozmen, M. M.; Theato, P. Sulfur Chemistry in Polymer and Materials Science. *Macromol. Rapid. Comm*. **2019**, *40*, 1800650, 51 pages.

28. Zhang, Q.; Qu, D.-H.; Feringa, B. L.; Tian. H. Disulfide-Mediated Reversible Polymerization toward Intrinsically Dynamic Smart Materials. *J. Am. Chem. Soc.* **2022**, *144* (5), 2022–2033.

29. Canadell, J.; Goossens, H.; Klumperman, B. Self-Healing Materials Based on Disulfide Links. *Macromolecules* **2011**, *44* (8), 2536–2541.

30. Xiang, H.; Yin, J.; Lin, G.; Liu, X.; Rong, M.; Zhang, M. Photo-Crosslinkable, Self-Healable, and Reprocessable Rubbers. *Chem. Eng. J.* **2019**, *358*, 878–890.

31. Kloxin, C. J.; Bowman, C. N. Covalent Adaptable Networks: Smart, Reconfigurable and Responsive Network Systems. *Chem. Soc. Rev.* **2013**, *42*, 7161–7173.

32. Yoon, J. A.; Kamada, J.; Koynov, K.; Mohin, J.; Nicolaÿ, R.; Zhang, Y.; Balazs, A. C.; Kowalewski, T.; Matyjaszewski, K. Self-Healing Polymer Films Based on Thiol-Disulfide Exchange Reactions and Self-Healing Kinetics Measured Using Atomic Force Microscopy. *Macromolecules* **2012**, *45* (1), 142–149.

33. Otsuka, H.; Nagano, S.; Kobashi, Y.; Maeda, T.; Takahara, A. A Dynamic Covalent Polymer Driven by Disulfide Metathesis under Photoirradiation. *Chem. Comm.* **2010**, *7*, 1150–1152.

34. Azcune, I.; Odriozola, I. Aromatic Disulfide Crosslinks in Polymer Systems: Self-Healing, Reprocessability, Recyclability and more. *Eur. Polym. J.* **2016**, *84*, 147–160.

35. Michal, B. T.; Jaye, C. A.; Spencer, E. J.; Rowan, S. J. Inherently Photohealable and Thermal Shape-Memory Polydisulfide Networks. *ACS Macro Lett.* **2013**, *2* (8), 694–699.

36. Altinbasak, I.; Arslan, M.; Sanyal, R.; Sanyal, A. Pyridyl disulfide-based thiol–disulfide exchange reaction: shaping the design of redox-responsive polymeric materials. *Polym. Chem.* **2020**, *11* (48), 7603–7624.

37. Wojtecki, R. J.; Jones, G. O.; Yuen, A. Y.; Chin, W.; Boday, D. J.; Nelson, A.; García, J. M.; Yang, Y. Y.; Hedrick, J. Developments in Dynamic Covalent Chemistries from the Reaction of Thiols with Hexahydrotriazines. *J. Am. Chem. Soc.* **2015**, *137* (45), 14248–14251.

38. Le Neindre, M.; Nicolaÿ, R. Polythiol Copolymers with Precise Architectures: A Platform for Functional Materials. *Polym. Chem.* **2014**, *5* (16), 4601–4611.

39. Fuoco, T.; Finne-Wistrand, A.; Pappalardo, D. A Route to Aliphatic Poly(ester)s with Thiol Pendant Groups: From Monomer Design to Editable Porous Scaffolds. *Biomacromolecules* **2016**, *17* (4), 1383–1394.

40. Chen, X.; Lawrence, J.; Parelkar, S.; Emrick, T. Novel Zwitterionic Copolymers with Dihydrolipoic Acid: Synthesis and Preparation of Nonfouling Nanorods. *Macromolecules* **2013**, *46* (1), 119–127.

41. Le Neindre, M.; Nicolaÿ, R. One-pot Deprotection and Functionalization of Polythiol Copolymers via Six Different Thiol–X Reactions. *Polym. Int.* **2013**, *63* (5), 887–893.

42. Summonte, S.; Racaniello, G. F.; Lopedota, A.; Denora, N.; Bernkop-Schnürch, A. Thiolated Polymeric Hydrogels for Biomedical Application: Cross-Linking Mechanisms. *J. Control. Release* **2021**, *330* (10), 470–482.

43. Li, J.; Richardson, J. J.; Ejima, H. Synthesis of Dithiocatechol-Pendant Polymers. *J. Am. Chem. Soc.* **2022**, *144* (6), 2450–2454.

44. Kihara, N.; Kanno, C.; Fukutomi, T. Synthesis and Properties of Microgel Bearing a Mercapto Group. *J. Polym. Sci. A. Polym. Chem.* **1997**, *35* (8), 1443–1451.

45. Rekondo, A.; Martin, R.; de Luzuriaga, A. R.; Cabañero, G.; Grande, H. J.; Odriozola, I. Catalyst-Free Room-Temperature Self-Healing Elastomers Based on Aromatic Disulfide Metathesis. *Mater. Horiz.* **2014**, *1* (2), 237–240.

46. Martin, R.; Rekondo, A.; de Luzuriaga, A. R.; Santamaria, A.; Odriozola, I. Mixing the Immiscible: Blends of Dynamic Polymer Networks. *RCS Adv.* **2015**, *5* (23), 17514–17518.

47. Kharkar, P. M.; Kloxin, A. M.; Kiick, K. L. Dually Degradable Click Hydrogels for Controlled Degradation and Protein Release. *J. Mater. Chem. B* **2014**, *2* (34), 5511–5521.

48. Lang, Y.; Kiick, K. L. Liposome-Cross-Linked Hybrid Hydrogels for Glutathione-Triggered Delivery of Multiple Cargo Molecules. *Biomacromolecules* **2016**, *17* (2), 601–614.

49. Deng, Z.; Yuan, S.; Xu, R. S.; Liang, H.; Liu, S. Reduction-Triggered Transformation of Disulfide-Containing Micelles at Chemically Tunable Rates. *Angew. Chem. Int. Ed.* **2018**, *57* (29), 8896–8900.

50. Bracchi, M. E.; Dura, G.; Fulton, D. A. The Synthesis of Poly(aryl thiols) and Their Utilization in the Preparation of Cross-Linked Dynamic Covalent Polymer Nanoparticles and Hydrogels. *Polym. Chem.* **2019**, *10* (10), 1258–1267.

51. Tuten, B. T.; Chao, D.; Lyon, C. K.; Berda, E. B. Single-Chain Polymer Nanoparticles via Reversible Disulfide Bridges. *Polym. Chem.* **2012**, *3* (11), 3068–3071.

CHAPTER THREE:
POLYMERIC ZWITTERIONIC THIOLS: SYNTHESIS, REACTIVITY, AND PROPERTIES

3.1 Introduction

Recent synthetic advances have expanded the range of applications and properties accessible to polymer zwitterions beyond that of conventional poly(MPC)–which cannot undergo further transformations and is well-known for being hydrophilic and biologically inert[1-2]–through inclusion of functional groups.[3-13] For example, polymer zwitterions comprised of sulfothetin or sulfobetaine groups can stabilize oil-in-water interfaces and create emulsion droplets that are "sticky", *i.e.* can be utilized form supracolloidal structures as a result of inter-chain interactions, [14-15,17] which can additionally self-propel in solution through Marangoni forces arising at the air-water interface.[16] The sticky emulsions and structures also exhibit stimulus response in the presence of salt or acid, which shields or disrupts inter-droplet interactions, causing droplets to become non-sticky and coalesce.[14-15,17] On the other hand, the novel phosphonium sulfonate polymer zwitterions reported by Brown *et al.*, are soluble in dichloromethane and, when incorporated into block copolymers with MPC, form assembled micelles that have switchable solution behavior in organic *v.* aqueous solutions.[3]

More than tuning solution properties, an equally sought after synthetic target has been the integration of reactive groups that undergo post polymerization transformations, which gives access to designer zwitterion materials.[5-6,10,12-14,18-20] One of the first reported examples describes the synthesis of functional sulfobetaine polymer zwitterions with pendent alkene or protected alkyne groups: when crosslinked at the oil-in-water interface of emulsion droplets, polymer capsules were created.[10] Pendent alkenes and alkynes have

likewise led to the preparation of CP-based polymer zwitterions hydrogels[5] and nanoparticles[18] *via* thiol-ene or thiol-yne reactions whereas copper azide-alkyne chemistries have been utilized to attach therapeutic drugs and fluorophores.[5] More recently, Iwasaki and coworkers incorporated benzophenone groups into CP zwitterions to create crosslinkable structures, such as surface lubricating polymer brushes;[13] in contrast, the synthesis and inclusion of embedded disulfide dimethacrylate CP zwitterion crosslinking groups led to degradable, anti-fouling zwitterionic hydrogels.[12] The aromatic and aliphatic **PZTs** described in **Chapter 2** likewise place the functional moiety adjacent to the zwitterion and pendent to the polymer backbone, making it readily available for further modification utilizing standard thiol chemistries, such as thiol-Michael addition and disulfide formation. Moreover, the **PZTs** are water-soluble and therefore amenable to thiol transformations under biologically relevant conditions.

In **Chapter 3**, we explore the fundamental properties of **PZTs** at oil-in-water interfaces and in functional group transformations including crosslinking to yield **PZT** hydrogels. We find that with thiophenol pendent groups, the normally ultra-hydrophilic polymer zwitterions assume surfactant properties, seen in long-term droplet stability assessed by interfacial tension measurements. Additionally, the free thiols of **PZTs** are amenable to post-polymerization modification with divinyl sulfone or dipyridyl disulfide to yield functional **PZTs**. We further demonstrate that **PZTs** form hydrogels with bifunctional PEG crosslinkers *via* UV-catalyzed thiol-Michael addition, with the thiophenol-containing **PZTs** also producing gels through disulfide formation.

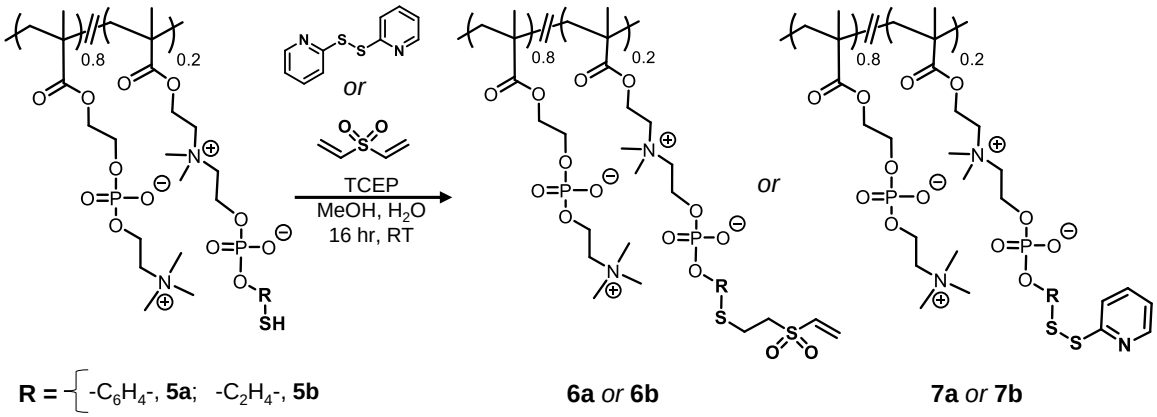

Figure 3-1. General reaction scheme for post-polymerization modifications of **PZTs** with dipyridyl disulfide and divinyl sulfone.

3.2 PZT Post-Polymerization Modifications

Deprotected **PZTs 5a** and **5b** are available to reactions using the thiol groups, which were examined for the cases of divinylsulfone (DVS) and dipyridyl disulfide (DPDS) modification, each selected for the amenability of the products to undergo further transformations (**Figure 3-1**). For vinyl sulfone (VS) modification, adding a large excess of DVS to the polymers in 1:1 MeOH: PBS buffer (pH ~ 7.4-9.1) followed by dialysis against water yielded VS-modified **PZT** products **6a** and **6b** as white solids (50-90% yield). Spectroscopic analysis indicated a modest integration of VS into the aromatic **PZTs** (**Figure 3-2**), while the aliphatic version showed minimal VS incorporation (**Figure 3-3**). In contrast, modification of **PZTs** with DPDS proceeded in excellent conversion for both the aromatic **7a** (**Figure 3-4**) and aliphatic **7b** (**Figure 3-5**) cases, finding that the addition of TCEP to the aromatic **PZTs** was helpful for producing high functional group incorporation, as determined by ^{1}H NMR spectroscopy. Interestingly, as shown in **Table 3-1**, the pyridyl integrations of **7a-5 PZTs** with 5 mol% DPDS changed depending on the solution conditions. For example, **7a-5** in deuterated TFE resulted in a small increase in

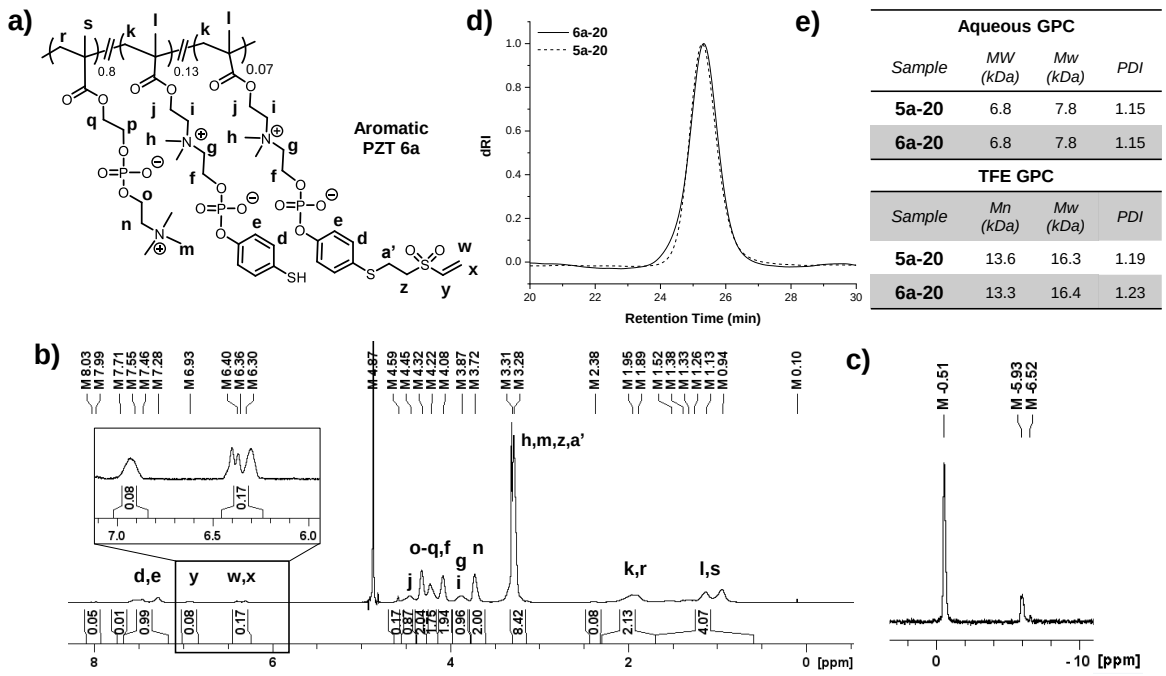

Aqueous GPC			
Sample	*MW (kDa)*	*Mw (kDa)*	*PDI*
5a-20	6.8	7.8	1.15
6a-20	6.8	7.8	1.15

TFE GPC			
Sample	*Mn (kDa)*	*Mw (kDa)*	*PDI*
5a-20	13.6	16.3	1.19
6a-20	13.3	16.4	1.23

Figure 3-2. (**a**) Structure of VS-modified copolymer zwitterion **6a**. (**b**) ^{1}H and (**c**) ^{31}P NMR spectra in MeOD-*d4* and (**d**) representative GPC traces, including (**e**) estimated molecular weight and PDI values, in aqueous and TFE eluents.

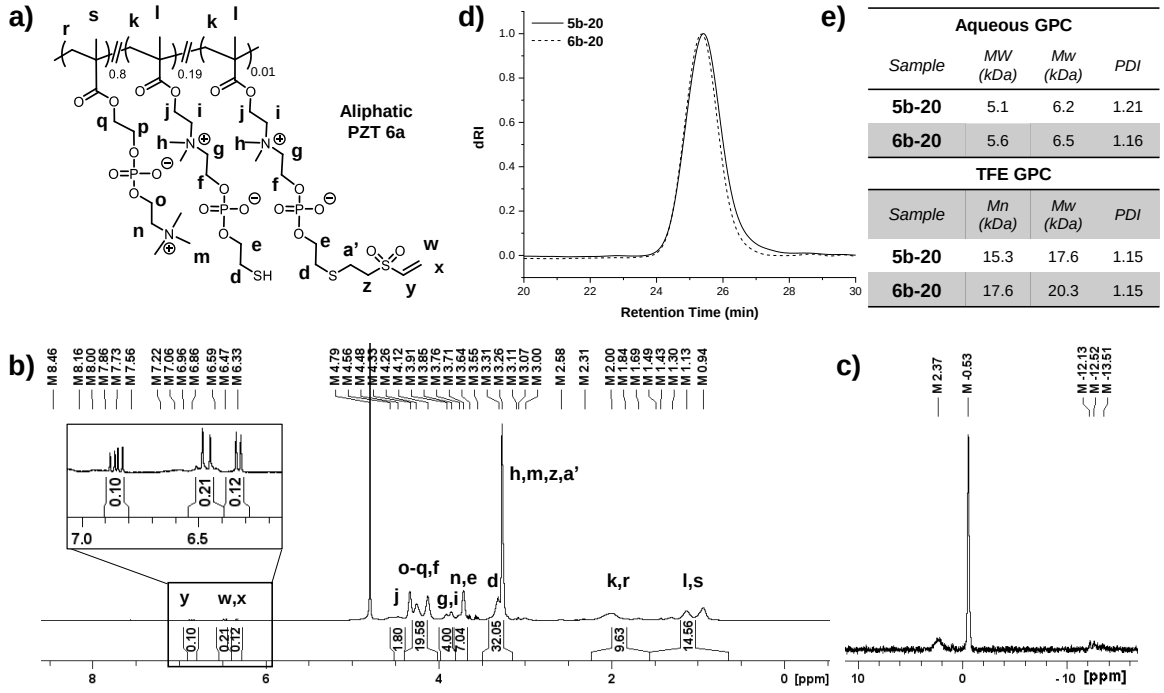

Aqueous GPC			
Sample	*MW (kDa)*	*Mw (kDa)*	*PDI*
5b-20	5.1	6.2	1.21
6b-20	5.6	6.5	1.16

TFE GPC			
Sample	*Mn (kDa)*	*Mw (kDa)*	*PDI*
5b-20	15.3	17.6	1.15
6b-20	17.6	20.3	1.15

Figure 3-3. (**a**) Structure of VS-modified copolymer zwitterion **6b**. (**b**) ^{1}H and (**c**) ^{31}P NMR spectra in MeOD-*d4* and (**d**) representative GPC traces, including (**e**) estimated molecular weight and PDI values, in TFE and aqueous eluents.

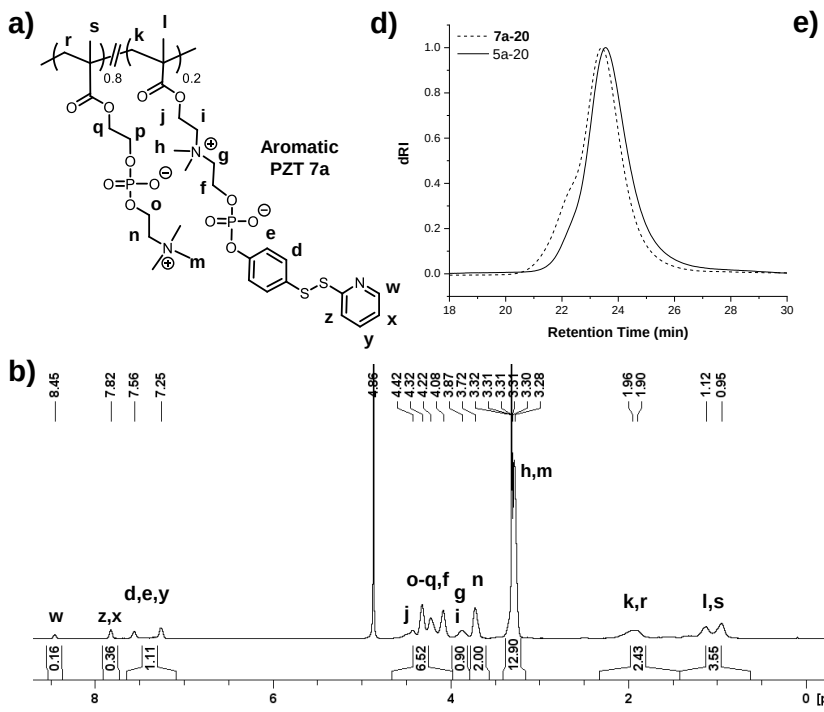

e)

Aqueous GPC

Sample	*Mn (kDa)*	*Mw (kDa)*	*PDI*
5a-20	6.8	7.8	1.15
7a-20	4.3	6.0	1.38

TFE GPC

Sample	*Mn (kDa)*	*Mw (kDa)*	*PDI*
5a-20	17.7	20.3	1.14
7a-20	19.9	24.1	1.21

Figure 3-4. (**a**) Structure of DPDS-modified copolymer zwitterion **7a-20**. (**b**) ^{1}H and (**c**) ^{31}P NMR spectra in MeOD-*d4* and (**d**) representative GPC traces, including estimated (**e**) molecular weight and dispersity values, in TFE and aqueous eluents.

pyridyl integration to 7 mol% whereas acidic deuterated water solutions (0.1 M HCl) reduced pyridyl integration to 2 mol%. These results show that the hydrophobic pyridyl resonances are being partially shielded in aqueous environments (**Table 3-1**) and may indicate the formation of structures in solution, similar to the solution switching behaviors

Table 3-1. Functional group incorporation (mol%) into **PZT** copolymers containing 20 mol% CP content as determined by ^{1}H NMR spectroscopy following post-polymerization modification.

Sample	*Solvent*	*mol% CP*	*mol% modified*
6a-20	MeOD-*d4*	20	7
6b-20	MeOD-*d4*	20	1
7a-20	MeOD-*d4*	20	20
	MeOD-*d4*	20	5
	TFE-d3	20	7
	0.1 M HCl in D_2O	20	2
7b-20	MeOD-*d4*	20	20

similar to those observed for phosphonium sulfonate polymer zwitterions.[3] GPC analysis in aqueous and/or TFE eluents for both VS- and DPDS-modified **PZTs** demonstrated minimal changes in molecular weight and dispersity post-functionalization, although a high molecular weight shoulder was occasionally observed and attributed to interchain coupling. A summary of all successful thiol functionalization can be found in **Table 3-1**.

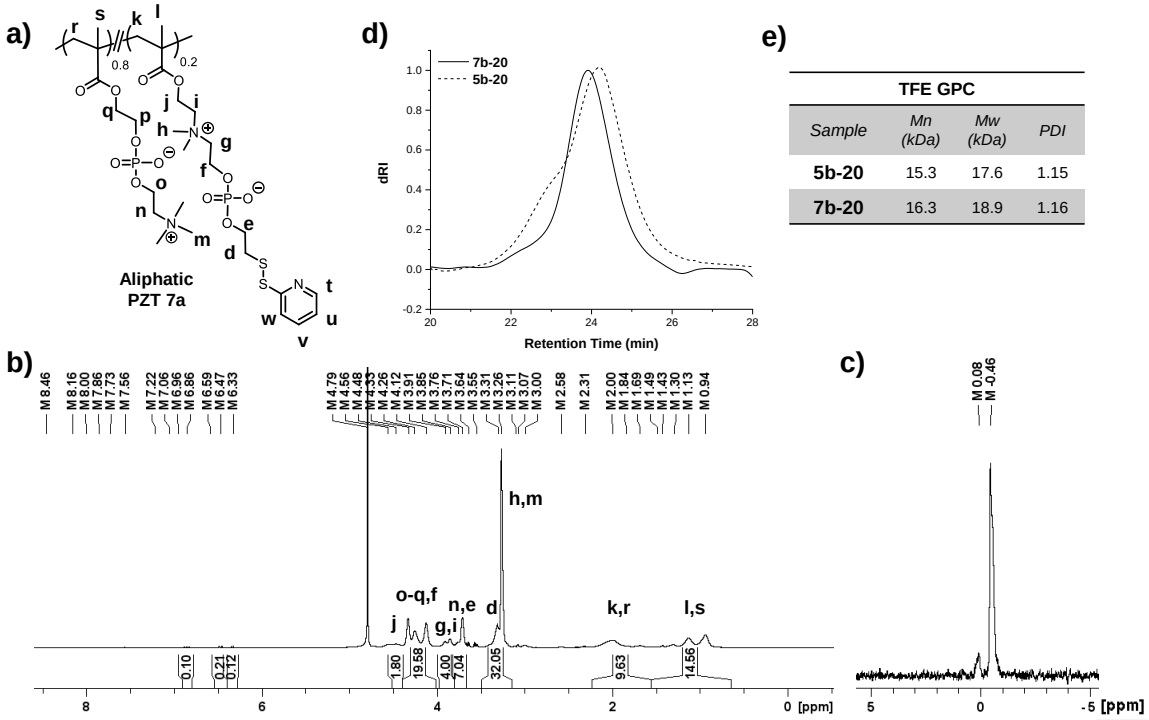

TFE GPC			
Sample	*Mn (kDa)*	*Mw (kDa)*	*PDI*
5b-20	15.3	17.6	1.15
7b-20	16.3	18.9	1.16

Figure 3-5. (**a**) Structure of DPDS-modified copolymer zwitterion **7b-20**. (**b**) ^{1}H and (**c**) ^{31}P NMR spectra in MeOD-*d4* and (**d**) representative GPC traces, including estimated (**e**) molecular weight and dispersity values, in TFE eluents.

3.3 PZTs in Hydrogel Formation

The pendent thiols of **PZTs** can serve also as precursors to hydrogels through disulfide and thiol-Michael addition mechanisms, as illustrated in **Figure 3-6a**. For example, in UV-catalyzed Michael addition, copolymer **5a-20** (M_w ~15-20 kDa) was added to a DI water or buffer (0.1 M PBS, pH 8) solution containing PEG diacrylate (M_n ~ 235, 575, and 700

Da) and water soluble azo-initiator VA-044 at various polymer and crosslinker wt %, with differing acrylate-to-thiol molar ratios (**Table 3-2**). Interestingly, the hydrogel precursor solutions demonstrated varying degrees of opacity in aqueous solutions, often appearing more opaque in DI water than buffer solutions, which may indicate the formation of solution structures or existing disulfide in solution (**Figure 2-18**) and their disruption in

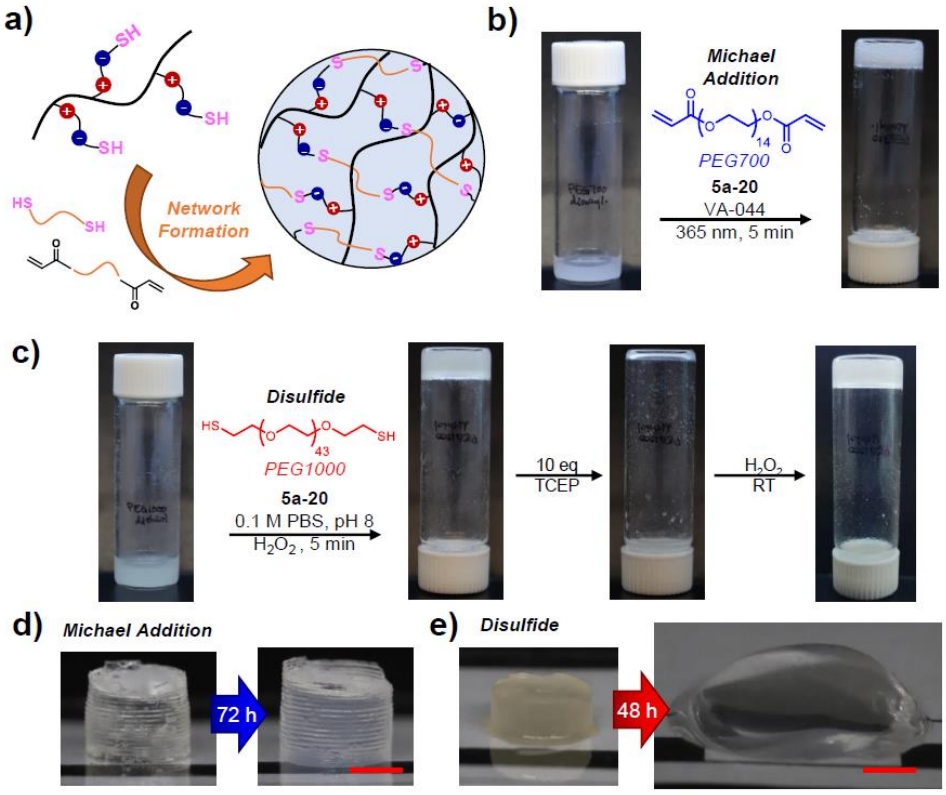

Figure 3-6. (**a**) Schematic of hydrogel formation using **PZTs** with difunctional crosslinkers. (**b**) Photographs of hydrogels (600 mg scale) formed *via* UV-catalyzed thiol-Michael addition between **5a-20** copolymers (at 10 wt%) and PEG700 diacrylate (acrylate-to-thiol ratio = 5.1) in the presence of VA-044 initiator (2 wt%). (**c**) Optical images of hydrogels (900 mg scale) formed *via* disulfide formation between PEG1000 dithiol (acrylate-to-thiol ratio = 5.4) and **5a-20** copolymers (20 wt%) in 0.1 M PBS pH 8 buffer with 28 M H_2O_2. Addition of TCEP leads to cleavage of disulfides, resulting in hydrogel dissolution, which re-forms upon exposure to 28 M H_2O_2. The swelling over time of **5a-20** hydrogels (50-100 µL scale) created from (**d**) thiol-Michael (acrylate-to-thiol ratio = 5.6, 13 wt% polymer) or (**e**) disulfide mechanisms (acrylate-to-thiol ratio = 2.0, 32 wt% polymer). Scale bar = 0.45 cm.

the presence of salt/buffer (see **Figure 3-8**) or reducing agent (e.g., TCEP) (**Figure 2-18a**). The degassed aqueous solutions were then subjected to 365 nm UV irradiation for 5 minutes to yield stiff and brittle gels (**Figure 3-6b**). It was found that acrylate-to-thiol ratios greater than ~2 typically resulted in complete network formation when 20 wt% **PZT** was employed. However, at 10 wt% **PZT**, either partial or no gelation was observed unless the acrylate-to-thiol ratio was at least ~5, whereas hydrogels produced at >20 wt % needed a minimum ratio of 1. The swelling ratios of successful hydrogel formulations, which were determined from the mass of each swollen and dry hydrogel, were found to between 250-500% in water (**Figure 3-6d**).

Attempts at forming hydrogels with base-catalyzed thiol-Michael addition, on the other hand, were met with limited success, finding network formation only with triethylamine at high base concentrations (2.5 M) and acrylate-to-thiol values (~2.5).

Table 3-2. Optimization of hydrogel formation conditions formed *via* UV-catalyzed thiol-Michael addition using **5a-20** copolymer and PEG diacrylate solutions at various wt% polymer and VA-044 initiator concentrations. All polymer molecular weights were calculated by ^{1}H NMR end group analysis or GPC analysis (*) in TFE eluents.

Trial	Polymer MW (Da)	Theoretical DP_{SH}	Crosslinker MW (Da)	Polymer (wt%)	Crosslinker (wt%)	Initiator (wt%)	Acrylate:Thiol Ratio	Hydrogel Formation?	Swelling Ratio (%)
1	18.0*	9.5	235	23	5	2	2.2	N	-
2	15.6*	5.6		19	9	2	11.9	N	-
3	29.2	15.2	575	24	11	3	3.3	Y	-
4	29.2	15.2		11	11	5	7.2	Y	-
5	29.2	15.2	700	22	17	3	5.6	N	-
6	15.6*	5.6		20	5	2	6.9	N	-
7	15.6*	5.6		20	5	1	2.0	N	-
8	18.0*	9.5		27	7	1	1.4	Y	275
9	15.6*	5.6		11	5	3	4.0	N	-
10	15.6*	5.6		18	9	2	4.0	Partial	-
11	18.0*	9.5		33	4	2	0.7	Partial	-
12	19.3	9.8		10	7	2	4.0	N	-
13	19.3	9.8		10	10	2	5.7	Y	390
14	19.3	9.8		5	10	2	11.3	Y	500
15	19.3	9.8		20	10	2	2.8	Y	280
16	18.0*	9.5		22	9	2	2.2	Y	260
17	18.0*	5.6		18	9	0.1	4.0	Y	142

Similarly, the aliphatic **PZTs** were only amenable to hydrogel formation *via* UV-catalyzed thiol-Michael addition and were thus not pursued further.

Disulfide formation was evaluated as another route to **PZT** networks by combining **5a-20** copolymers with PEG dithiol (M_n ~ 1000 Da) in 0.1 M PBS pH 8 buffer (1 mM EDTA) at various ratios of crosslinker thiol to polymer functionality at 20-40 wt% copolymer (**Table 3-3**). While soft, flexible hydrogels were achieved under ambient conditions after several hours, gels formed quickly (~15 min) and reproducibly in the presence of H_2O_2. Once formed, the **5a-20** hydrogels could be solubilized upon addition of reducing agent (e.g., TCEP) and then reformed following H_2O_2 oxidation (**Figure 3-6c**), demonstrating the reversible nature of disulfide-induced gels for at least one reduction-oxidation cycle. Further optimization revealed that for 10 wt% **5a-20** copolymer solutions, crosslinker-to-polymer thiol molar ratios greater than ~4 were typically required to achieve gelation whereas low thiols ratios (around ~1) gave hydrogels only at **PZT** concentrations

Table 3-3. Optimization of hydrogel formation conditions formed *via* disulfide formation using **5a-20** copolymer at various wt% in 0.1 M PBS buffer (1 mM EDTA) with PEG1000 dithiol as crosslinker. All polymer molecular weights were calculated by ^{1}H NMR end group analysis or GPC analysis (+) in TFE eluents.

Trial	Polymer MW (kDa)	Theoretical DP_{SH}	Polymer (wt%)	Crosslinker (wt%)	Crosslinker: Polymer Thiol Ratio	pH	Oxidant (M)	Hydrogel Formation?	Swelling Ratio (%)	Time (h)
1	18.0$^+$	9.5	21	5	0.9	8	H_2O_2 (2.8)	Y	68	16-24
2	18.0$^+$	9.5	21	11	2.0	8		Y	220	
3	19.0	9.6	20	10	2.0	8^		Y	11800	
4	19.0	9.6	10	10	4.0	8^		Y	300	
5	18.8	9.5	20	15	3.0	8		Y	28100	<1
6						8*		Partial	-	>1
7						8	FeCl3 (0.1)	N	-	-
8						7	H_2O_2 (2.3)	Y	6500	<1
9						9		N	-	-
10			10	13	5.0	8	H_2O_2 (2.8)	N	-	<1‡
11						8*		N	-	>1‡
12			38	47		8		Y	-	<1

**indicates hydrogel solutions that initially formed complete networks before redissolving into solution*
^contains 1 mM TCEP in buffer solution

greater than 20 wt%. In contrast to hydrogels formed by thiol-Michael addition, swelling the disulfide hydrogels in water resulted in large swelling ratios and/or dissolution (**Figure 3-6e**). Self-gelation of **PZTs** (i.e., no added crosslinker) was additionally explored but ultimately did not yield hydrogels across a variety of oxidation conditions and polymer wt%. Moreover, attempts at using aliphatic **5b-20 PZTs** in disulfide crosslinking have likewise been unsuccessful to-date.

Overall, despite the high thiol content of the **PZTs** developed in this dissertation, forming crosslinked hydrogels has been a challenge, in contrast to other thiol-containing polymers which tend to slowly oxidize and self-crosslink over time,[22-23] which is likely a result of the lower pKa of thiophenol and its poorer nucleophilicity.

3.4 Interfacial Activity of PZTs

Unlike conventional polyMPC, which is not surface active due to its extreme hydrophilicity,[21] functional zwitterions such as **PZTs** offer the opportunity to localize functionality at fluid interfaces *via* droplet stabilization.[65] We anticipated surfactant properties to arise from trityl-protected **PZTs** due to their aromatic groups, with the potential to alter interfacial properties upon deprotection. To probe interfacial properties, protected **PZTs 4a** and **4b** were evaluated by pendant drop tensiometry, using trichlorobenzene (TCB) as the oil (drop) phase in a continuous aqueous (DI water) phase containing 0.5 mg/mL polymer (**Figure 3-7a**). The aromatic **PZT 4a-20** was found to significantly stabilize the o/w interface, reducing the interfacial tension (γ) of TCB-water from 34 mN/m to < 5 mN/m, whereas higher CP content in the copolymer (i.e., **4a-50**) yielded higher γ values of ~8 mN/m. The protected aliphatic **4b-20** performed similarly,

with γ reaching ~8-9 mN/m. To further evaluate oil-water interfacial stabilization by **PZT** surfactants, oil-in-water emulsions were prepared by vortexing aqueous solutions of **PZTs 4a-20** and **4b-20** at various concentrations in DI water (0.5 to 10 mg/mL) with TCB for ~1 min. As illustrated in **Figure 3-7b**, the protected aromatic CP polymers **4a-20** and **4a-50** provided longer-term droplet stability (e.g., months) compared to those generated from **4b-**

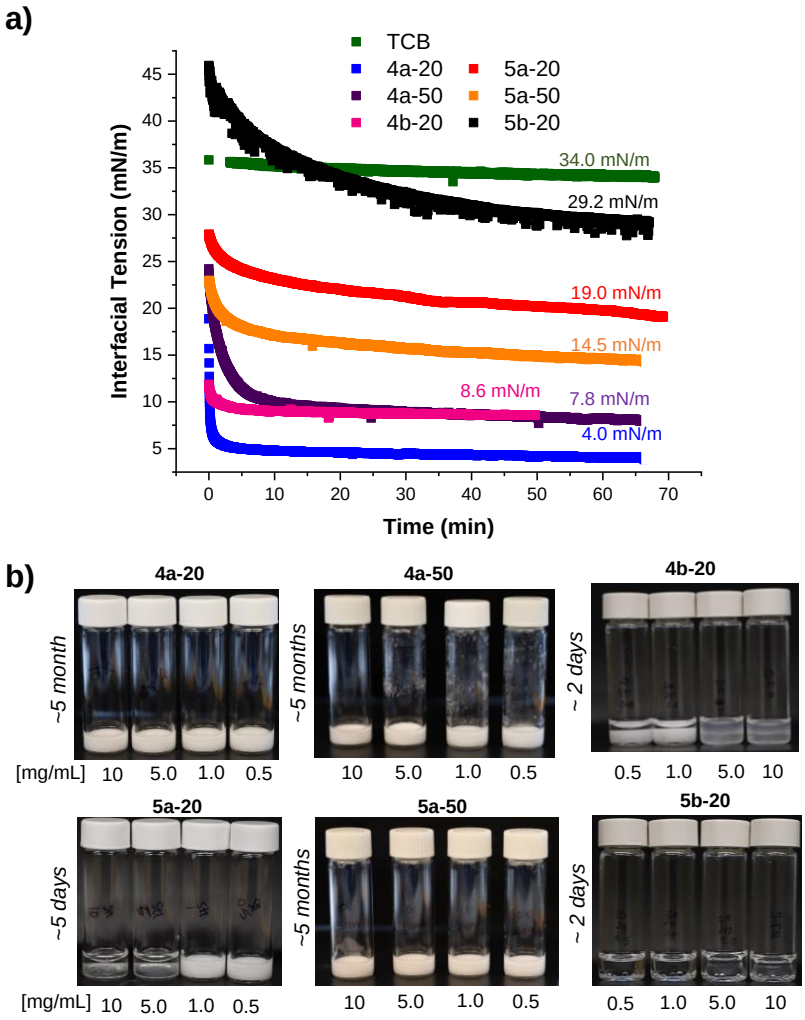

Figure 3-7. (**a**) Interfacial tension curves (mN/m) from pendant drop tensiometry evaluation of aromatic **PZT**s **4a-20** and **4a-50** (protected), and **5a-20** and **5a-50** (deprotected), including aliphatic **PZTs 4b-20** and **5b-20**, at 0.5 mg/mL (drop phase = TCB; aqueous phase = DI water). (**b**) Photographs of the corresponding oil-in-water emulsions stabilized by aromatic (**4a-20**, **4a-50**) or aliphatic (**4b-20**) protected **PZTs** (*top*), and by aromatic (**5a-20**, **5a-50**) or aliphatic (**5b-20**) deprotected **PZTs** (*bottom*), on a **PZT** concentration range of 0.5 to 10 mg/mL.

20 copolymers, which collapsed quickly (at 5.0 and 10 mg/mL) or over the course of days (at 0.5 and 1.0 mg/mL) despite similar γ values (~8 mN/m), likely a result of the higher hydrophobic content of aromatic **5b-20** copolymers. Moreover, **4a**-stabilized droplets were stable under a variety of conditions, including in presence of different aqueous buffers, salt, and pH values, resisting complete collapse over a period of months (**Figure 3-8**). We attribute this interfacial salt stability of the **4a** copolymers to the impact of the bulky trityl groups that likely interrupt extensive inter-zwitterion pairing at the droplet interface. The pH-stability is also the expected consequence of the zwitterion composition, with the low pKa of the phosphonate anion and the fully alkylated ammonium cation.

Upon trityl deprotection, the pendent thiophenols of **PZT 5a** imparted significant surfactant character, reducing TCB/water γ values to ~19 mN/m, while the deprotected aliphatic **PZT 5b** displayed no appreciable γ reduction, much like poly(MPC) (**Figure 3-7a**). Moreover, emulsions prepared from copolymers **5a-20** and **5a-50** were stable for months at low polymer concentrations (0.5 and 1.0 mg/mL) (**Figure 3-7b**). For these droplets, in contrast to the trityl-protected system, rapid coalescence was observed upon

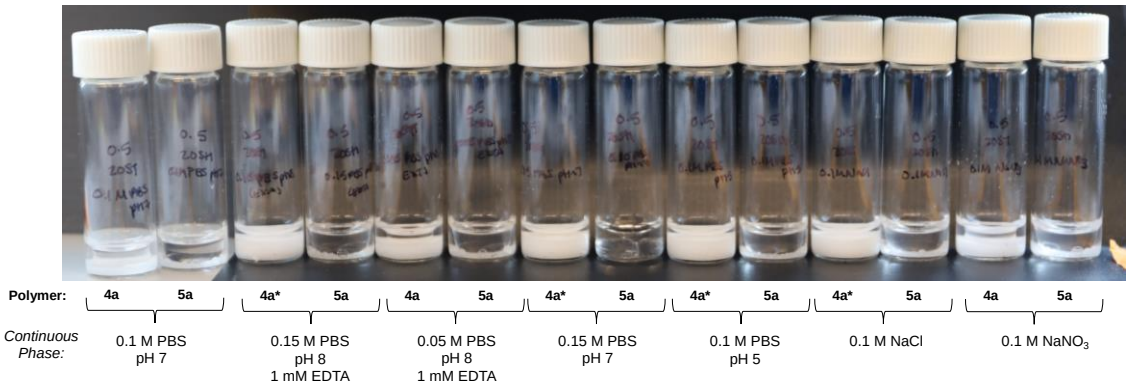

Figure 3-8. Photographs of oil-in-water emulsion droplets stabilized by protected (**4a-20**) or deprotected (**5a-20**) **PZTs** at 0.5 mg/mL prepared using various continuous phases, aged 16 hours. Encapsulated phase = TCB. Asterisks (*) designate emulsions that are stable for months.

addition of salt (e.g., 0.1 M NaCl) (**Figure 3-8**), which suggests that the smaller thiophenol group (relative to S-trityl) allows inter-zwitterion interactions at interfaces, which then are amenable to triggered disruption. The different interfacial behavior between the trityl-protected and deprotected systems suggests the possibility for *in situ* droplet transformations.[19] This was tested by dropwise addition of 5 M TFA into **4a-20**- and **4b-20**-stabilized o/w droplets at a 0.5 mg/mL polymer concentration, triggering rapid coalescence. In contrast, droplets stabilized at 5-10 mg/mL **PZT**, when subjected to TFA, resulted in aggregation and inter-droplet adhesion, suggesting the potential role of thiols in inter-droplet interactions *via* disulfide formation or other mechanisms.

Initial evaluation of oil-in-water stabilization of emulsions prepared using protected aromatic **SPZTs 4c-20** gave droplets that were stable for weeks at all concentrations. In contrast, aliphatic **SPZTs 4d-20** emulsions started coalescing after two weeks (at 0.5 to 10

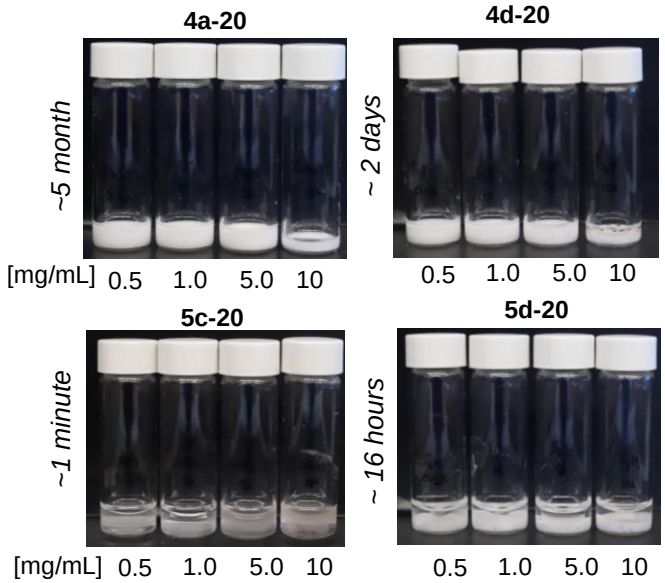

Figure 3-9. Photographs of oil-in-water emulsions stabilized by aromatic protected (**4c-20**) and deprotected (**5c-20**) or aliphatic protected (**4d-20**) and deprotected (**5d-20**) **SPZTs** on a concentration range of 0.5 to 10 mg/mL (oil phase = TCB; aqueous phase = DI water).

mg/mL) or a few days (at 5.0 and 10 mg/mL). Similarly, the deprotected **PZTs 5c** and **5d** were incapable of stabilizing oil-in-water droplets, which collapsed within hours-to-minutes (**Figure 3-9**). Interestingly, the more hydrophobic backbone of **5c-20** and **5d-20** did not improve surfactantcy of the **PZTs** and, as such, were not further evaluated.

3.5 Summary

Chapter 3 explored the fundamental properties of **PZTs** in post polymerization transformations, hydrogel formation, and oil-water interfacial stabilization. The thiols of both aromatic and aliphatic **PZTs** were completely converted to pyridyl groups whereas low-to-moderate vinyl sulfone functionalization was achieved. The aromatic **PZTs** were likewise found to participate in crosslinking reactions to form hydrogels using thiol-Michael addition (base- or UV-catalyzed) or disulfide formation, in contrast to aliphatic **PZTs**, which yielded hydrogels only through UV-catalyzed thiol-Michael addition. The protected **PZTs** were also found to capably stabilize the TCB-water interface, although only the aromatic **PZTs** could provide interfacial stabilization following deprotection. The proclivity of **PZTs** to interact with proteins will be further explored in **Chapter 4**.

3.6 References

1. Li, D.; Wei, Q.; Wu, C.; Zhang, X.; Xue, Q.; Zheng, T.; Cao, M. Superhydrophilicity and Strong Salt-Affinity: Zwitterionic Polymer Grafted Surfaces in Biological Systems. *Adv. Colloid Interface Sci.* **2020**, *278*, 102141, 18 pages.

2. Ishihara, K., Nomura, H., Mihara, T., Kurita, K., Iwasaki, Y., and Nakabayashi, N. Why do Phospholipid Polymers Reduce Protein Adsorption? *J. Biomed. Mater. Res.* **1998**, *39*, 323–330.

3. Brown, M. U.; Triozzi, A.; Emrick, T. Polymer Zwitterions with Phosphonium Cations. *J. Am. Chem. Soc.* **2021**, *143* (17), 6528–6532.

4. Hu, G. J.; Parelkar, S. S.; Emrick, T. A Facile Approach to Hydrophilic, Reverse Zwitterionic, Choline Phosphate Polymers. *Polym. Chem.* **2015**, *6* (4), 525–530.

5. Hu, G.; Emrick, T. Functional Choline Phosphate Polymers. *J. Am. Chem. Soc.* **2016**, *138*, 1828–1831.

6. Chalarca, C. F. S.; Emrick, T. Reactive Polymer Zwitterions: Sulfonium Sulfonates. *J. Polym. Sci. A. Polym. Chem.* **2017**, *55*, 83–92.

7. Zhou, L.; Triozzi, A.; Figueiredo, M.; Emrick, T. Fluorinated Polymer Zwitterions: Choline Phosphates and Phosphorylcholines. *ACS Macro Lett.* **2021**, *10*, 1204–1209.

8. Brown, M. U.; Seong, H.-G.; Margossian, K. O.; Bishop, L.; Russell, T. P.; Muthukumar, M.; Emrick, T. Zwitterionic Ammonium Sulfonate Polymers: Synthesis and Properties in Fluids. *Macromol. Rapid Commun.* **2022**, *43*, 2100678, 7 pages.

9. Brown, M. U.; Seong, H.; Russell, T. P.; Emrick, T. Zwitterionic Sulfonium Sulfonate Polymers: Impacts of Substituents and Inverted Dipole. *Macromolecules* **2023**, *56*, 1105–1110.

10. Chang, C.-C.; Letteri, R.; Hayward, R. C.; Emrick, T. Functional Sulfobetaine Polymers: Synthesis and Salt-Responsive Stabilization of Oil-in-Water Droplets. *Macromolecules* **2015**, *48* (21), 7843–7850.

11. Chen, T.-M.; Wang, Y.-F.; Li, Y.-J.; Nakaya, T.; Sakurai, I. Studies on the Synthesis and Properties of Novel Phospholipid Analogous Polymers. *J. Appl. Polym. Sci.* **1996**, *60* (3), 455–464.

12. Nguyen, H. N.; Ngo, T. L. H.; Iwasaki, Y.; Huang, C.-J. Biodegradable Phosphocholine Cross-Linker with Ion-Pair Design for Tough Zwitterionic Hydrogel. *Adv. Mater. Interfaces* **2022**, *9* (33), 2201002, 11 pages.

13. Nakano, H.; Noguchi, Y.; Kakinoki, S.; Yamakawa, M; Osaka, I.; Iwasaki, Y. Highly Durable Lubricity of Photo-Cross-Linked Zwitterionic Polymer Brushes Supported by Poly(ether ether ketone) Substrate. *ACS Appl. Bio Mater.* **2020**, *3* (2), 1071–1078.

14. Letteri, R. A.; Chalarca, C. F. S.; Bai, Y.; Hayward, R. C.; Emrick, T. Forming Sticky Droplets from Slippery Polymer Zwitterions. *Adv. Mater.* **2017**, *29*, 17002921, 8 pages.

15. Chalarca, C. F. S.; Letteri, R. A.; Perazzo, A.; Stone, H. A.; Emrick, T. Building Supracolloidal Fibers from Zwitterion-Stabilized Adhesive Emulsions. *Adv. Funct. Mater.* **2018**, *28*, 1804325, 10 pages.

16. Zhao, J.; Chalarca, C. F. S.; Nunes, J. K.; Stone, H. A.; Emrick, T. Self-Propelled Supracolloidal Fibers from Multifunctional Polymer Surfactants and Droplets. *Macromol. Rapid Commun.* **2020**, *41*, 2000334, 7 pages.

17. Zhao, J.; Pan, Z.; Snyder, D.; Stone, H. A.; Emrick, T. Chemically Triggered Coalescence and Reactivity of Droplet Fibers. *J. Am. Chem. Soc.* **2021**, *143* (14), 5558–5564.

18. Skinner, M.; Johnston, B. M.; Liu, Y.; Hammer, B.; Selhorst, R.; Xenidou, I.; Perry, S. L.; Emrick, T. Synthesis of Zwitterionic Pluronic Analogs. *Biomacromolecules* **2018**, *19* (8), 3377–3389.

19. Yang, Z.; Zhao, J.; Emrick, T. Functional Polymer Zwitterions as Reactive Surfactants for Nanoparticle Capture. ACS Appl. Mater. Interfaces **2021**, *13* (18), 21898–21904.

20. Sonu, K. P.; Zhou, L.; Biswas, S.; Klier, J.; Balazs, A. C.; Emrick, T.; Peyton, S. R. Strain-Stiffening Hydrogels with Dynamic, Secondary Cross-Linking. *Langmuir* **2023**, *39* (7), 2659–2666.

21. Ishihara, K.; Mu, Mingwei, M.; Konno, T.; Inoue, Y.; Fukazawa, K. The Unique Hydration State of Poly(2-methacryloyloxyethyl phosphorylcholine). *J. Biomater. Sci. Polym. Ed.* **2017**, *28* (10-12), 884–899.

22. Le Neindre, M.; Nicolaÿ, R. Polythiol Copolymers with Precise Architectures: A Platform for Functional Materials. *Polym. Chem.* **2014**, *5* (16), 4601–4611.

23. Le Neindre, M.; Nicolaÿ, R. One-pot Deprotection and Functionalization of Polythiol Copolymers via Six Different Thiol–X Reactions. *Polym. Int.* **2013**, *63* (5), 887–893.

CHAPTER FOUR:
POLYMERIC ZWITTERIONIC THIOLS IN POLYMER-PROTEIN BIOCONJUGATION

4.1 Introduction

Synthetic polymers have had an increasingly important role in biomedical applications and the field of polymer therapeutics is no exception, notably with the inception of PEGylation, or the attachment of polyethylene glycol (PEG) to therapeutic drugs.[1-2] While studies as early as 1955 reported the synthesis of polymer-drug conjugates,[3-6] Abuchowski *et al.* reported the first example of PEGylated protein in the late 1970s using bovine liver catalase and bovine serum albumin, finding that the PEGylation extended protein circulation time in rabbit models while minimizing immune response relative to protein controls.[7-8] In the decades that followed, seminal concepts and research by Ringsdorf,[9-10] Kopeček,[11-13] Maeda,[14-17] Duncan,[18-21] and others,[22-26] established that PEGylation improves the pharmacokinetic properties (*i.e.*, half-life) of polymer-conjugated drugs in the body/bloodstream, with PEG conferring aqueous solubility, stability, biocompatibility, and stealth characteristics. [13,25,27-30] As a result of these discoveries, the first FDA-approved polymer-protein drug known as Adagen, a PEG-adenosine deaminase conjugate, was released on the market in 1990 for the treatment of severe combined immunodeficiency disease.[27-28] Since then, the number of FDA-approved polymer-modified therapeutics has grown over the years, with many more in clinical trials, resulting in improved therapeutic outcomes for a variety of conditions and diseases.[2,28,31]

While PEGylation continues to dominate the field of polymer therapeutics and FDA-approved drug lists, several major limitations persist. For example, recent studies have identified anti-PEG antibodies promoting an immune response against PEG-

containing drugs or drug carriers,[34-38] a concern that received global attention during the development of the COVID-19 vaccine.[39] Accompanying immune response, PEGylated therapeutics have likewise been documented to undergo accelerated blood clearance (ABC), a process by which the PEGylated drug is rapidly cleared from the body due to attenuated immune recognition, thereby limiting its therapeutic effect.[13,32,38] Furthermore, PEG contains limited functional sites (i.e., at the polymer chain ends) for attachment to the therapeutic. For PEGylated protein drugs, which make up a majority of FDA approved polymer therapeutics,[2] only one chain end hydroxyl group is utilized in bioconjugation (**Figure 4-1a**).

Advances in polymer chemistry have since created new macromolecular platforms that improve upon PEGylation and offer routes to polymers with tunable and modular designs. Modification of polymer architecture (*i.e.*, linear, comb, dendrimer),[18,39-43] composition (*i.e.*, poly(oxazolines), HPMA, polypeptides),[11,42,44-48] and embedded functionality (*i.e.*, maleimide, NHS-ester, click chemistries)[22-23,43,49-55] allow control over crucial components of the polymer therapeutic, such as size, immune response, solubility, and drug loading, all of which impact therapeutic efficiency. Polymer zwitterion-based therapeutics such as poly(MPC) are of particular interest because their zwitterion subunits are hydrated by a greater number of water molecules than PEG, conferring improved stealth capabilities of the polymer therapeutic; to-date, poly(MPC) has not been observed to elicit an immune response.[56-58] In addition to poly(MPC), other polymer zwitterions such as carboxybetaine and sulfobetaine have been shown to be biocompatible on numerous occasions in biological applications,[59-68,56] including polymer therapeutics.[69-82] Moreover, owing to their synthesis, polymer zwitterions can have multiple functional groups, pendent

to the main chain, integrated into the final polymer structure, which translates into multiple conjugation sites to therapeutic drug. In this way, each polymer chain can have multiple points of attachment to one protein and/or multiple proteins attached to one polymer chain (**Figure 4-1b**).

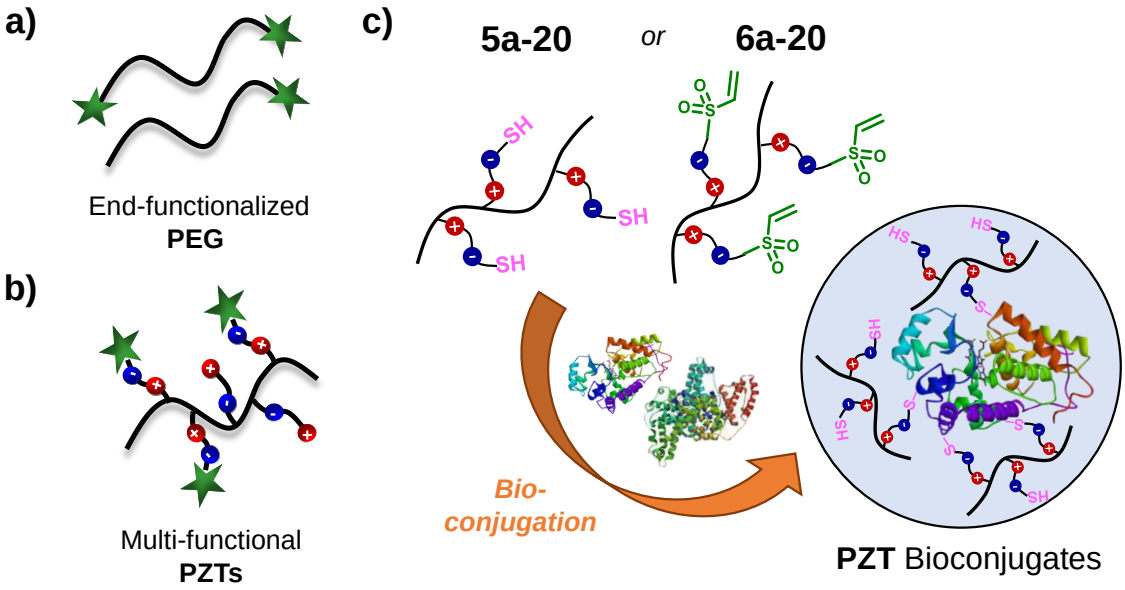

Figure 4-1. Schematic of (**a**) mono-/bi-functional PEGs with limited functionality at the chain ends relative to (**b**) multi-functional **PZTs**, where the functional groups are pendent to the polymer backbone. (**c**) Scheme depicting formation of polymer-protein bioconjugates in this chapter using **5a-20** or **6a-20 PZT** copolymers.

We envision that the **PZTs** developed in **Chapters 2** and **3** will be advantageous over conventional PEGylation through integration of multiple reactive conjugation sites while complementing previously reported functional polymer zwitterions.[83-86] Thiol groups or activated disulfides have been extensively explored in therapeutic applications and are especially useful in polymer-protein conjugation strategies since they can conjugate directly with cysteine residues in protein without the need for protein modification.[57,87-90] Moreover, they can be reversibly cleaved: disulfides embedded in the polymer backbone or as pendent groups lead to biodegradable polymers and/or mechanisms for drug release under reduction-triggered cleavage in physiological conditions.[91-95] However, thiols can be

utilized to make irreversible or "clickable" bonds using thiol-ene, thiol-Michael, *etc*. chemistries,[96-99] which adds to the versatility of thiols in the bioconjugation toolbox. The VS-modified **PZTs**, on the other hand, create irreversible polymer-protein bonds that are superior in hydrolytic stability to maleimide or NHS-ester chemistries,[51,100-102] and offer selectivity for nucleophilic cysteine residues at physiological pHs (i.e., since few proteins have cysteine).[100-101,103-104]

Given these considerations, **Chapter 4** describes the utility of **PZTs** in polymer-protein bioconjugation. The aromatic and aliphatic **PZTs** and **SPZTs** developed in **Chapter 2**, including DPDS-modified aliphatic **PZTs** of **Chapter 3** are first evaluated in bioconjugation utilizing disulfide mechanisms with bovine serum albumin (BSA) as model protein, and then extended to catalytic enzymes including horseradish peroxidase (HRP), catalase (CAT), lysozyme (LYS), and glucose oxidase (GOX) (**Figure 4-1c**). The VS-modified **PZTs** of **Chapter 3** are additionally explored in bioconjugation through electrophilic addition to protein residues such as lysine, histidine, or cysteine. The success of the bioconjugation reactions is assessed using SDS-PAGE gel electrophoresis and, for conditions producing bioconjugates, are further analyzed with FPLC.

4.2 Disulfide Bioconjugation Mechanism

The potential for the thiol groups of **5a** or **5b PZTs** to participate in bioconjugation was first evaluated with catalase (CAT), bovine serum albumin (BSA), and glucose oxidase (GOX) following pre-treatment of the proteins with TCEP, which produced numerous free thiols per enzyme as judged by Ellman's assay (~16 for CAT, ~14 for BSA, and ~1 for GOX) (**Table 4-1**). Incubation of the reduced CAT and BSA proteins (~2-6 μM) with aromatic **PZT 5a-20** (~200 eq. with respect to thiol functionality) for 5 hours in 0.1 M PBS

at various pH values (7.4, 8.0, and 9.1) led to a visible band by SDS-PAGE analysis at higher molecular weight than that of the reduced protein (**Figure 4-2a**), corresponding to ~1 polymer chain per protein; no bioconjugation was observed for GOX. Even without TCEP, BSA-**PZT** conjugation was observed, noting that native BSA contains one available thiol for conjugation (**Figure 4-3a**).[105-106] As shown in **Figures 4-2b** and **4-3b**, SDS-PAGE analysis of the bioconjugation reactions after incubation in reducing conditions (*i.e.*, mercaptoethanol or glutathione) revealed no high molecular weight band, as would be anticipated for a disulfide-based bioconjugate.

To complement SDS-PAGE analysis, size-exclusion fast protein liquid chromatography (FPLC) was used to characterize the polymer-protein bioconjugates through their elution profiles. For this, the bioconjugation reaction mixtures were subjected to centrifugal dialysis against 0.1 M PBS buffer (pH 7.4) to remove unreacted polymer (**Figure 4-2c,d**, **Figure 4-3c**). The reduced BSA bioconjugates from lanes 4-5 of **Figure 4-2a** eluted at similar retention volumes of ~16.5 mL, slightly earlier than the reduced BSA control (~17 mL), and as monomodal peaks (**Figure 4-2c**). In contrast, lane 6 showed a slight increase in retention volume and a low molecular weight shoulder consistent with residual polymer. The native BSA (**Figure 4-3c**) and reduced CAT (**Figure 4-2d**) bioconjugates, on the other hand, demonstrated an increase in retention volume post-

Table 4-1. Amount of free thiol per protein (native or reduced), as determined following an Ellman's assay procedure.

Enzyme	Enzyme Concentration (μM)	Free Thiol (μM)	SH/enzyme
BSA	2.5	35.5	14
native BSA	33.6	13.3	0.4
CAT	2.1	33.1	16
GOX	5.6	6.2	1
HRP	6.8	0	-
LYS	72.3	19.0	0.3

bioconjugation. An increase in retention volume post-bioconjugation, though uncommon, has been reported to occur, which the authors attributed to attractive interactions between the polymer-decorated bioconjugate surface and the column.[107] The residual unreacted protein that was observed by SDS-PAGE (**Figure 4-2a, 4-3a**) was not detected by FPLC (**Figure 4-2c,d**, **Figure 4-3c**), which is unsurprising considering the ng detection levels of Coomassie Blue stain.

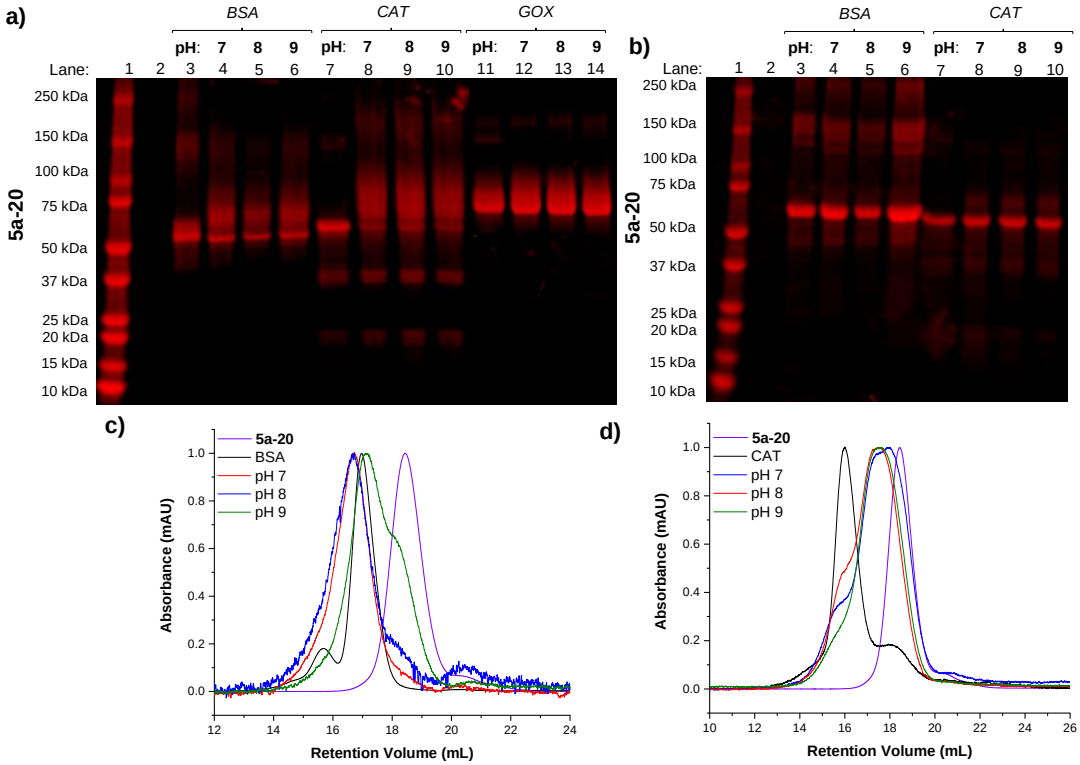

Figure 4-2. SDS-PAGE gels of the bioconjugation reaction of **5a-20** with reduced protein (CAT, BSA, and GOX) utilizing a disulfide mechanism after 24 hours incubation in 0.1 M PBS buffer at various pH values (7-9), (**a**) before and (**b**) after pre-treatment with reducing agent (TCEP). Lane 1 is the molecular weight protein ladder, lane 2 is the polymer control, and lane 3 is the protein control. Lanes 4-6 are the BSA experimental conditions, at pH 7, 8 and 9, respectively. Size-exclusion FPLC chromatograms of reduced **5a-20** bioconjugates od (**c**) BSA or (**d**) CAT from lanes 4, 5, and 6 (BSA) or lanes 8, 9 and 10 (CAT) in (**a**) and (**b**). Mobile phase is 0.1 M PBS pH 7.4 (0.14 M NaCl, 2.7 mM KCl).

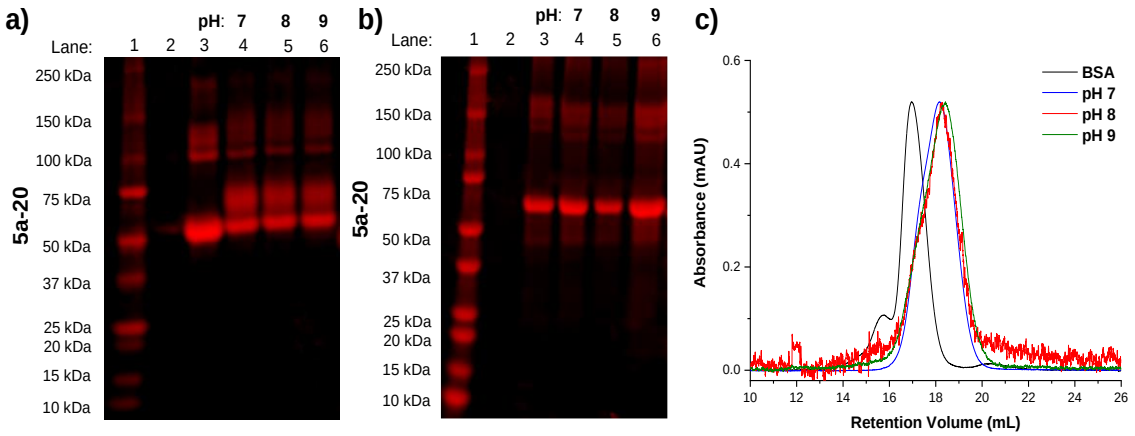

Figure 4-3. SDS-PAGE gels of the bioconjugation reaction of **5a-20** with native BSA utilizing a disulfide mechanism after 24 hours incubation in 0.1 M PBS buffer (0.14 M NaCl, 2.7 mM KCl) at various pH values (7-9), (**a**) before and (**b**) after pre-treatment with reducing agent (TCEP). Lane 1 is the molecular weight protein ladder, lane 2 is the polymer control, and lane 3 is the protein control. Lanes 4-6 are the BSA experimental conditions, at pH 7, 8 and 9, respectively. (**c**) Size-exclusion FPLC chromatograms of BSA and **5a-20**-BSA bioconjugates from lanes 4, 5, and 6 in (**a**). Mobile phase is 0.1 M PBS pH 7.4 (0.14 M NaCl, 2.7 mM KCl).

Despite the success of aromatic **5a PZTs** in bioconjugation, attempts at bioconjugation using aliphatic **5b-20** copolymers have been unsuccessful to-date in a variety of buffer conditions (**Table 4-2**) with reduced lysozyme (LYS) and horseradish peroxidase (HRP) (**Figure 4-4**), and with reduced BSA (**Figure 4-4, 4-5**) compared to a thiol-terminated poly(MPC) control (**Figure 4-6**). As can be observed in **Figure 4-6**, none of the buffer conditions attempted led to bioconjugation with **6b-20** copolymers unlike thiol-terminated poly(MPC), where high molecular weight streaking above the BSA protein band was observed for several conditions. In an attempt to promote bioconjugation, the free thiols of **5b-20 PZTs** were functionalized with dipyridyl disulfide to create activated disulfide copolymer **7b-20** (see **Section 3-3**).[91,105-106] Since **7b-20** copolymers were insoluble in aqueous solutions, bioconjugation attempts either (*i*) increased reaction

Table 4-2. List of buffer conditions (1-24) utilized in bioconjugation reactions between **5b-20** or thiol-terminated PMPC and reduced BSA *via* disulfide formation.

Trial	Condition			Trial	Condition		
	Buffer	*pH*	*[EDTA]*		*Buffer*	*pH*	*[EDTA]*
1	Certipur Borate	7	7	**14**	DI H_2O/MeOH	-	1
2		9		**15**	0.15 M HEPES	7	1
3		8	5	**16**		8	
4	0.1 M $NaHCO_3$	7	7	**17**		8	5
5		9		**18**		9	1
6		8	5	**19**	0.05 M HEPES	8	1
7	0.15-0.25 M $NaHCO_3$	8	1	**20**	0.15 M TRIS	7	1
8	0.15 M PBS	8	5	**21**		8	
9			1	**22**		8	5
10		6.7		**23**		9	1
11	0.2-0.5 M PBS	8	1	**24**	0.05 M TRIS	8	1
12	0.15 M PBS	8	1	**25**	50 mM PBS	8	1
13	DI H_2O-	-	1	**26**	150 mM PBS	9	1

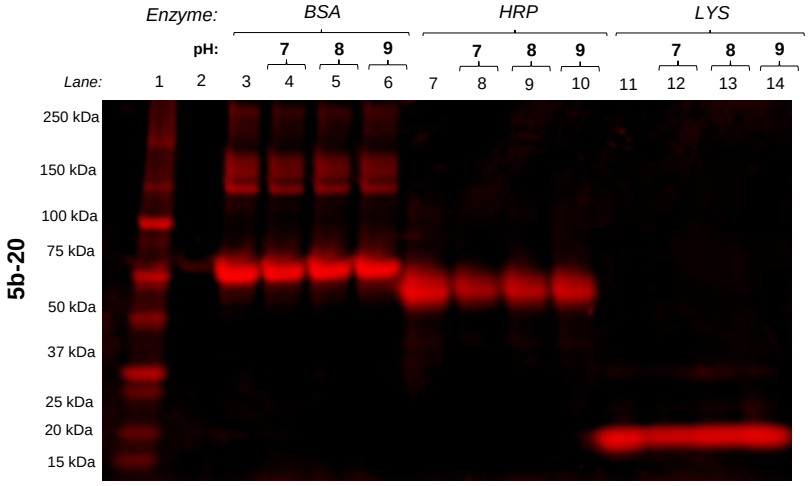

Figure 4-4. SDS-PAGE gels of the bioconjugation reaction of **5b-20** with reduced protein (BSA, HRP or LYS) utilizing a disulfide mechanism after 24 hours incubation in 0.1 M PBS buffer (0.14 M NaCl, 2.7 mM KCl) at various pH values (7-9). Lane 1 is the molecular weight protein ladder, lane 2 is the polymer control, and lane 3 is the protein control. Lanes 2, 7, and 11 represent the BSA, HRP and LYS protein controls, respectively. Lanes 4-6 are the BSA experimental conditions at pH 7, 8 and 9, respectively; and lanes 8-10 and lanes 12-14 are the HRP and LYS experimental conditions, respectively.

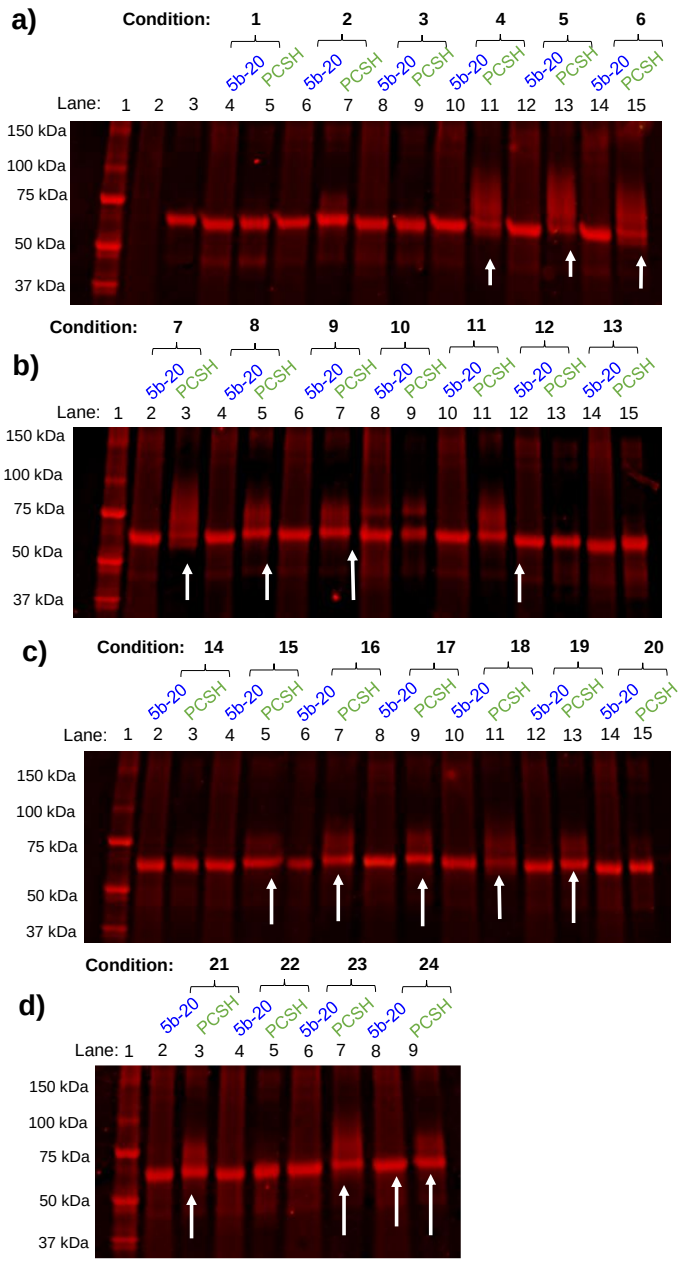

Figure 4-5. SDS-PAGE gels of the bioconjugation reactions between **5b-20** or thiol-terminated PMPC (**PCSH**) and reduced BSA in a disulfide mechanism after 24 hours incubation in the various buffer conditions (1-24) outlined in **Table 4-2**. For each gel, lane 1 is the molecular weight protein ladder. For (**a**), lane 2 is the polymer control and lane 3 is the reduced BSA control. Lanes 4, 6, 8, 10, 12, and 14 are the experimental conditions for **5b-20** reactions in for reaction conditions 1-6. Lanes 5, 7, 9, 11, 13, and 15 are the experimental conditions for **PCSH** reactions in for reaction conditions 1-6. For (**b-c**), lanes 2, 4, 6, 8, 10, 12, and 14 are the experimental conditions for **5b-20** reactions in conditions 7-20. Lanes 3, 5, 7, 9, 11, 13, and 15 are the experimental conditions for **PCSH** reactions in conditions 7-20. For (**d**), lanes 2, 4, 6, and 8 are the experimental conditions for **5b-20** reactions in conditions 21-24. Lanes 3, 5, 7, and 9 are the experimental conditions for **PCSH** reactions in conditions 21-24. The white arrows indicate lanes demonstrating bioconjugation.

time to 5-7 days or (*ii*) were conducted in 50% MeOH to promote solubilization. Unfortunately, the activated **7b-20** copolymer did not improve bioconjugation across the range of conditions tested for BSA or for LYS (**Figure 4-7**). Moreover, initial attempts at bioconjugation using **SPZTs 5c** and **5d** were likewise unsuccessful (**Figure 4-8**).

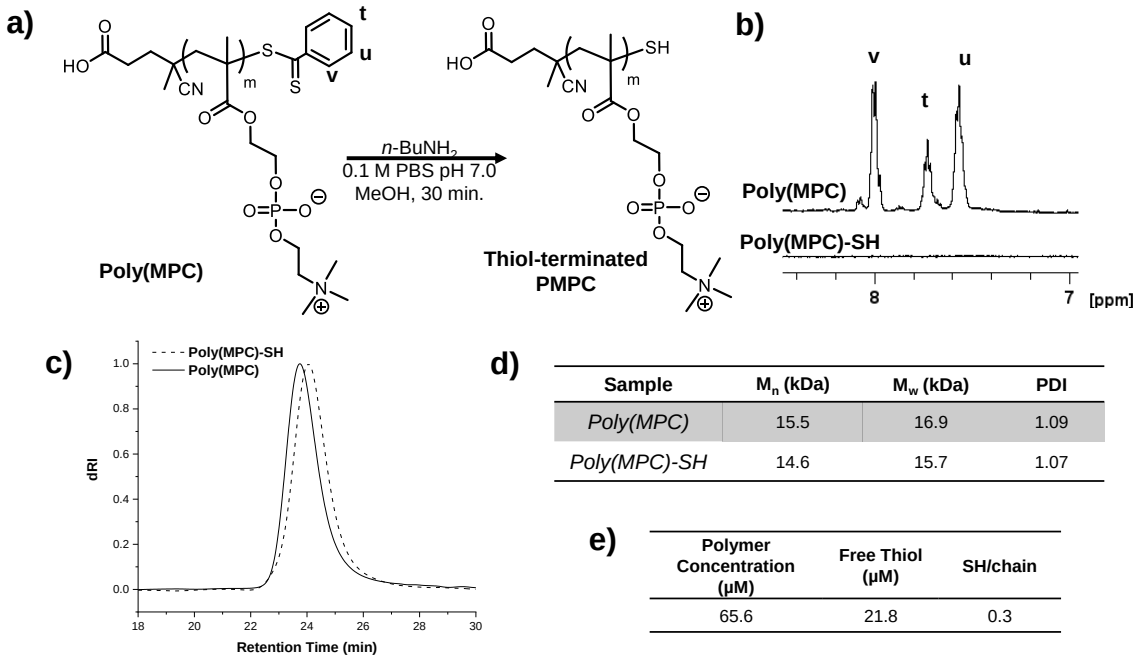

Sample	M_n (kDa)	M_w (kDa)	PDI
Poly(MPC)	15.5	16.9	1.09
Poly(MPC)-SH	14.6	15.7	1.07

Polymer Concentration (μM)	Free Thiol (μM)	SH/chain
65.6	21.8	0.3

Figure 4-6. (**a**) Reaction scheme to obtain thiol-terminated poly(MPC). (**b**) ^{1}H NMR spectrum in D_2O of poly(MPC) (*top*) and poly(MPC)-SH (*bottom*) showing loss of aromatic resonances following base-catalyzed hydrolysis of the dithiobenzoate chain end. (**c**) Representative GPC traces of poly(MPC) in TFE eluents before and after base hydrolysis, including (**d**) estimated molecular weight and PDI values, and (**e**) estimated free thiol per polymer chain as determined *via* Ellman's Assay.

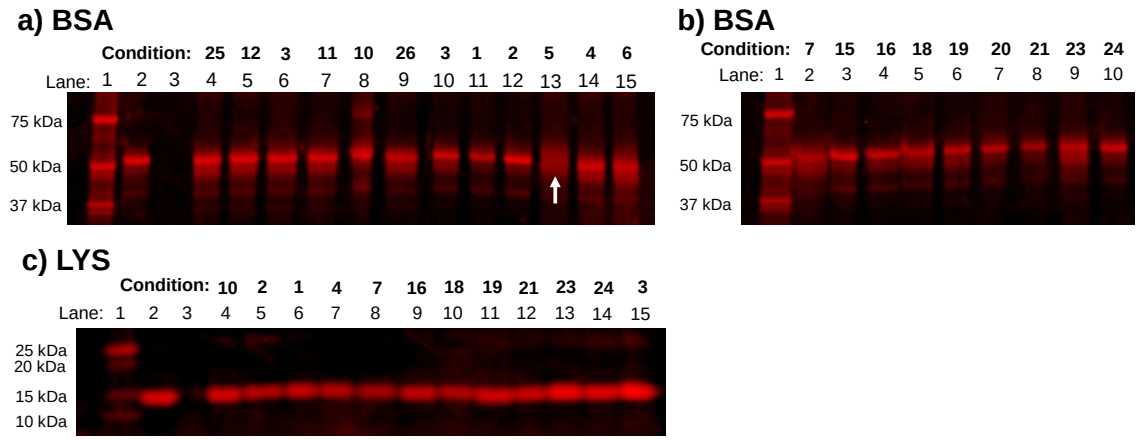

Figure 4-7. SDS-PAGE gels of the bioconjugation reactions between **7b-20** and (**a,b**) reduced BSA or (**c**) reduced LYS in an activated disulfide mechanism after 5 days incubation in the various buffer conditions outlined in **Table 4-2**. For each gel, lane 1 is the molecular weight protein ladder. For (**a**), lane 2 is the polymer control and lane 3 is the reduced BSA control. Lanes 4-15 are the experimental conditions 1-6, 10-12, and 25-26. For (**b**), lanes 2-10 are the experimental conditions 7 and 15-24. For (**c**), lane 2 is the polymer control and lane 3 is the reduced LYS control. Lanes 4-15 are the experimental conditions 1-4, 7, 10, 16, 18-21, and 23-23. The white arrow indicates a lane that exhibits broadening of the protein band and thus possible bioconjugation; however, no changes in retention time were observed by FPLC characterization.

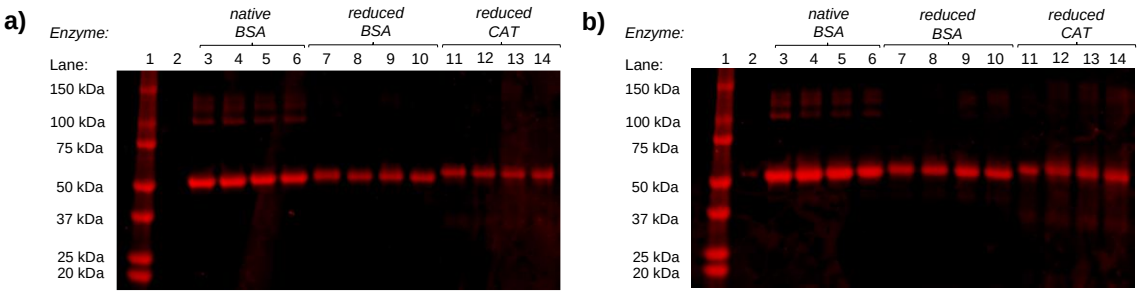

Figure 4-8. SDS-PAGE gels of the bioconjugation reactions between (**a**) **5c-20** or (**b**) **5d-20** and reduced protein (BSA, CAT) or native BSA utilizing a disulfide mechanism after 24 hours in 0.1 M PBS buffer at various pH values (7-9). Lane 1 is the molecular weight protein ladder; lane 2 is the polymer control; and lanes 3, 7, and 11 are the protein controls. Lanes 4-6 are the BSA experimental conditions, at pH 7, 8 and 9, respectively. Lanes 8-10 are the reduced BSA experimental conditions, at pH 7, 8 and 9, respectively. Lanes 12-14 are the reduced CAT experimental conditions, at pH 7, 8 and 9, respectively.

4.3 Vinyl Sulfone Bioconjugation Mechanism

Our conversion of **PZTs** to VS-substituted polymer zwitterions as described in **Section 3.2** presents an additional route to bioconjugation through VS reaction with nucleophilic lysine, histidine, or cysteine protein residues.[100,103-104] Several proteins were examined in VS-modified **PZT** conjugation, including BSA, GOX, LYS, and HRP, in each case pre-mixing the enzymes in buffer (pH 9) with 1 mM TCEP. A 1 mg/μL (~3 mM) copolymer solution in DI water was then incubated in the protein solution (~3-70 μM), testing a variety of buffer conditions at pH 9 for 6-24 h. SDS-PAGE analysis of the bioconjugation reactions as shown in **Figure 4-9** suggests successful bioconjugation of the VS-modified **PZT 6a** with BSA, LYS and HRP, noting the high molecular weight streak relative to the free protein band. Control experiments using reduced protein (GOX and BSA) did not improve the extent of bioconjugation (**Figure 4-10a**); however, experiments without TCEP (i.e., using native protein) led to nearly quantitative conversion of protein to polymer-protein bioconjugate, confirming that the VS moieties react with nucleophilic amine residues, in addition to thiols (**Figure 4-10b**). Regardless, the extensive streaking in the gels likely indicates a breadth of molecular weight populations (e.g., polymers per protein).

Following centrifugal dialysis, FPLC characterization of the **PZT 6a**-BSA bioconjugates showed peaks at lower retention times relative to the unmodified proteins, with several high molecular weight shoulders, indicative of a significant molecular weight increase and, potentially, multiple molecular weight populations (**Figure 4-11a**) that may occur when the bioconjugate consists, on average, of more than one polymer chain per protein. **PZT 6a**-LYS bioconjugates likewise displayed an increase in retention volume

relative to the LYS protein control (**Figure 4-11b**), whereas HRP bioconjugates occasionally demonstrated a decrease in retention volume for several conditions (**Figure 4-11c**). Excepting some residual protein, LYS and HRP bioconjugates typically displayed

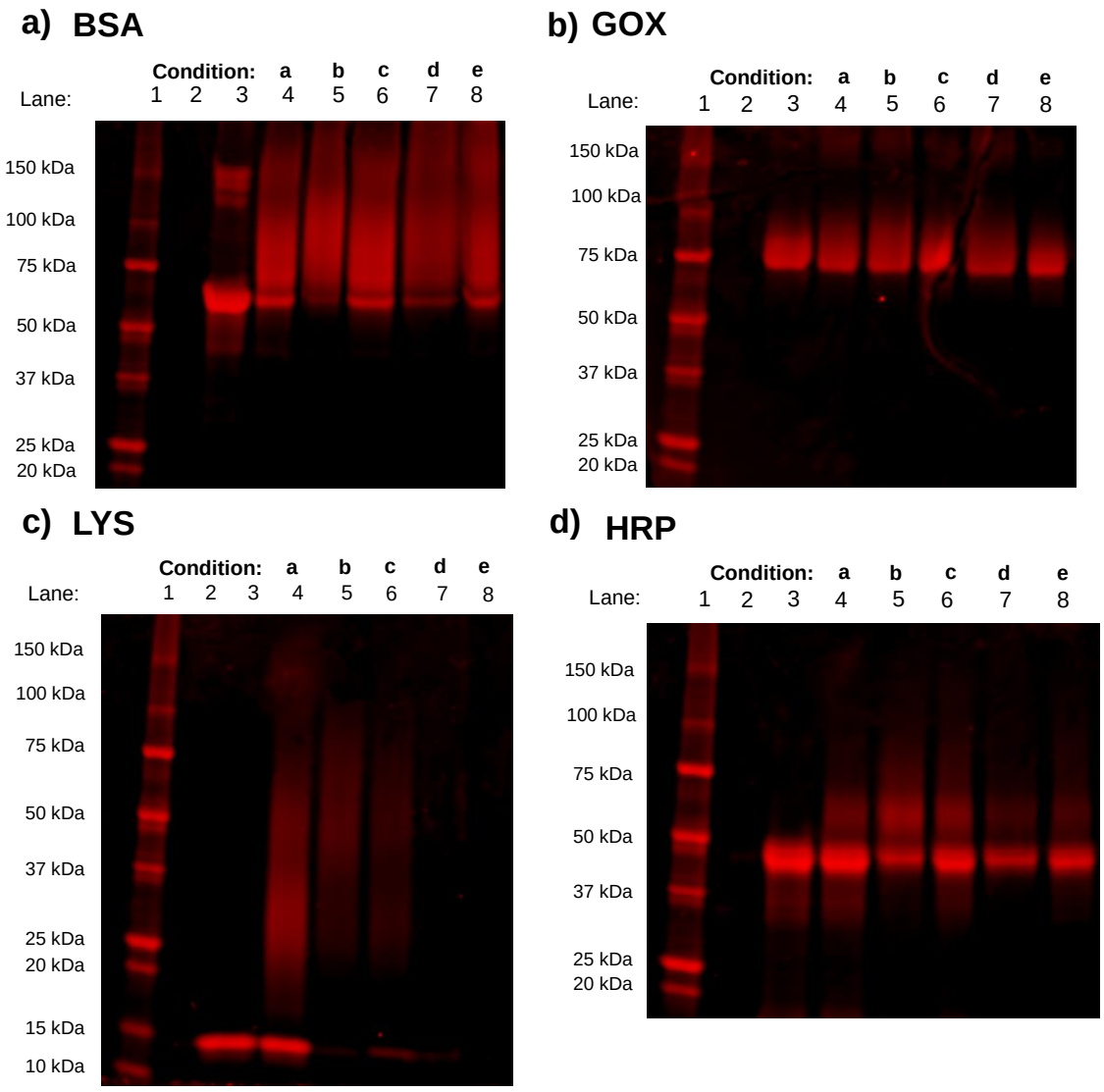

Figure 4-9. SDS-PAGE gels of the bioconjugation reactions between VS-modified **PZT 6a** and (**a**) BSA, (**b**) GOX, (**c**) LYS, and (**d**) HRP in various buffer conditions after 24 hours. Lane 1 is the molecular weight ladder, lane 2 is the polymer control, and lane 3 is the protein control. Lanes 4-8 are the **PZT 6a** experimental conditions, with each lane representing a different buffer condition. Condition a: 0.15 M PBS; Condition b: Certipur Borate; Condition c: 0.1 M Sodium Bicarbonate; Condition d: 0.15 M HEPES; Condition e: 0.15 M Tris. All conditions were at pH 9.2, 1 mM EDTA.

one monomodal peak. Unfortunately, attempts at using VS-modified aliphatic **PZT 6b** have not been successful to-date (**Figure 4-12**).

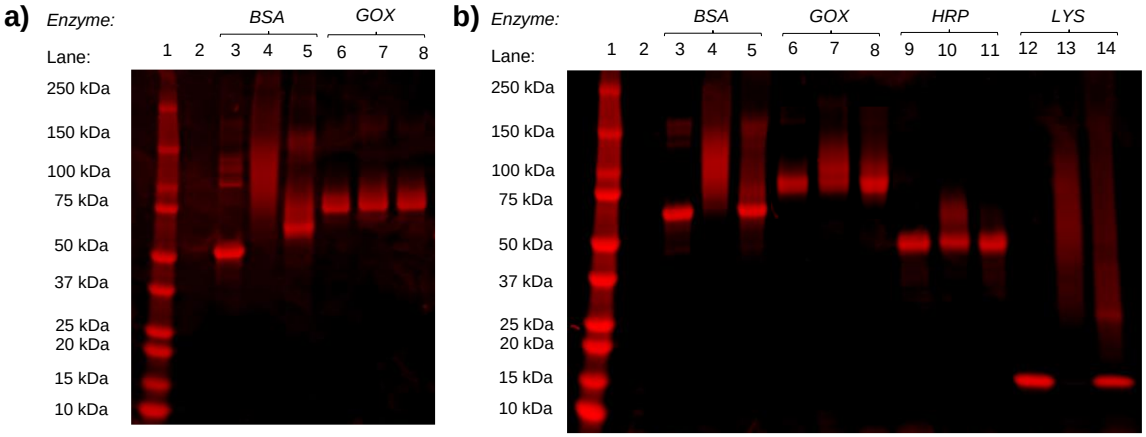

Figure 4-10. (**a**) SDS-PAGE of bioconjugation reactions between the VS-modified **PZT 6a** and reduced or native BSA and GOX after 16 hours in Certipur Borate buffer pH 9.2 with 1 mM EDTA. Lane 1 is the molecular weight protein ladder, lane 2 is the polymer control, and lanes 3 and 6 are the protein controls. Lanes 4 and 7 are the **6a-20** experimental conditions with native protein while lanes 5 and 8 are with reduced protein. (**b**) SDS-PAGE of bioconjugation reactions between VS-modified **PZT 6a** and BSA, GOX, HRP, and LYS after 16 hours with or without reducing agent (TCEP) in Certipure Borate buffer pH 9.2 with 1 mM EDTA. Lane 1 is the molecular weight protein ladder and lanes 3, 6, 9, and 12 are the protein controls. Lanes 4, 7, 10, and 13 are the **PZT 6a** experimental conditions without TCEP; lanes 5, 8, 11, and 14 have TCEP.

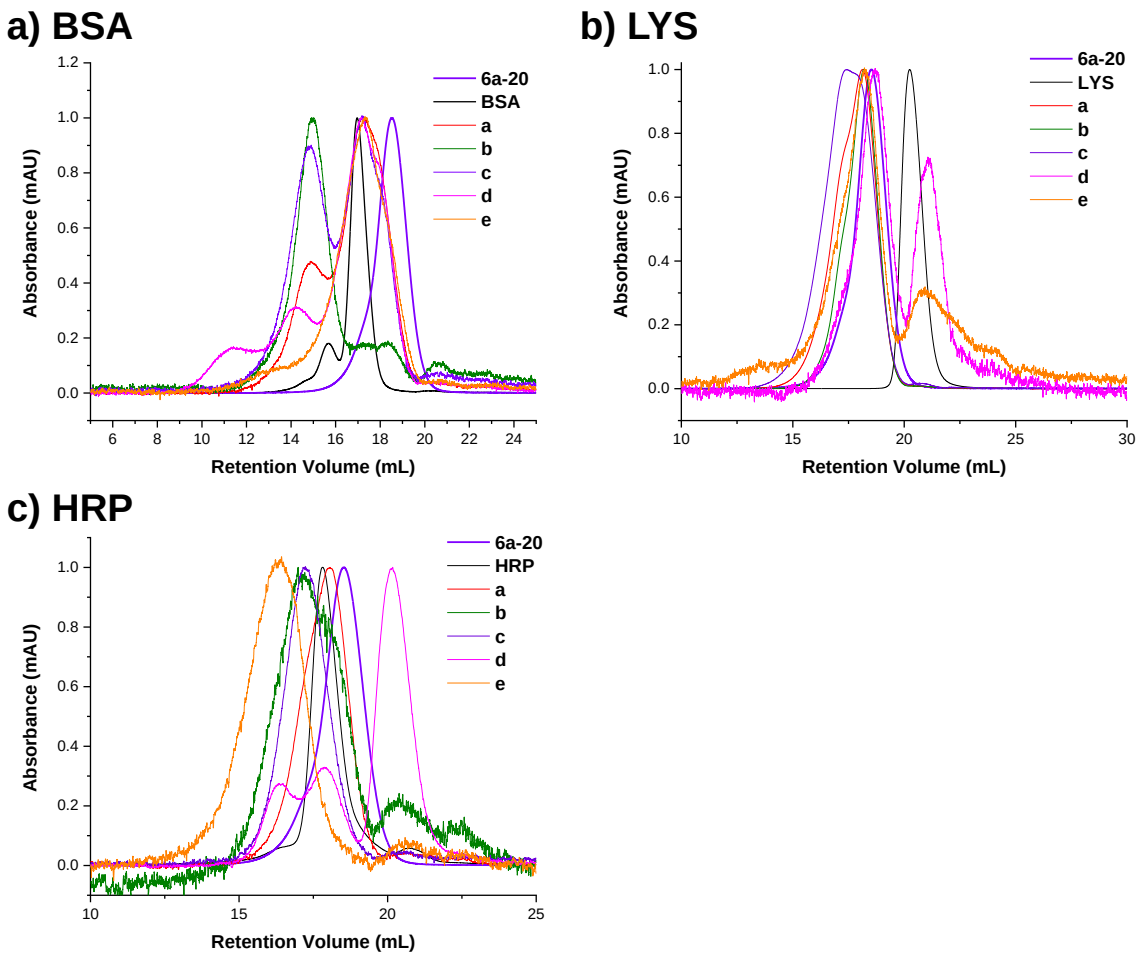

Figure 4-11. Size-exclusion FPLC chromatograms of **PZT 6a**-protein conjugates for (**a**) BSA, (**b**) LYS or (**c**) HRP. Each bioconjugate formed from condition a-e is denoted with a different colored line: Condition a: 0.15 M PBS (red); Condition b: Certipur Borate; Condition (green); c: 0.1 M Sodium Bicarbonate (thin purple); Condition d: 0.15 M HEPES (pink); Condition e: 0.15 M Tris (orange). All conditions were at pH 9.2, 1 mM EDTA. Mobile phase is 0.1 M PBS pH 7.4 (0.14 M NaCl, 2.7 mM KCl).

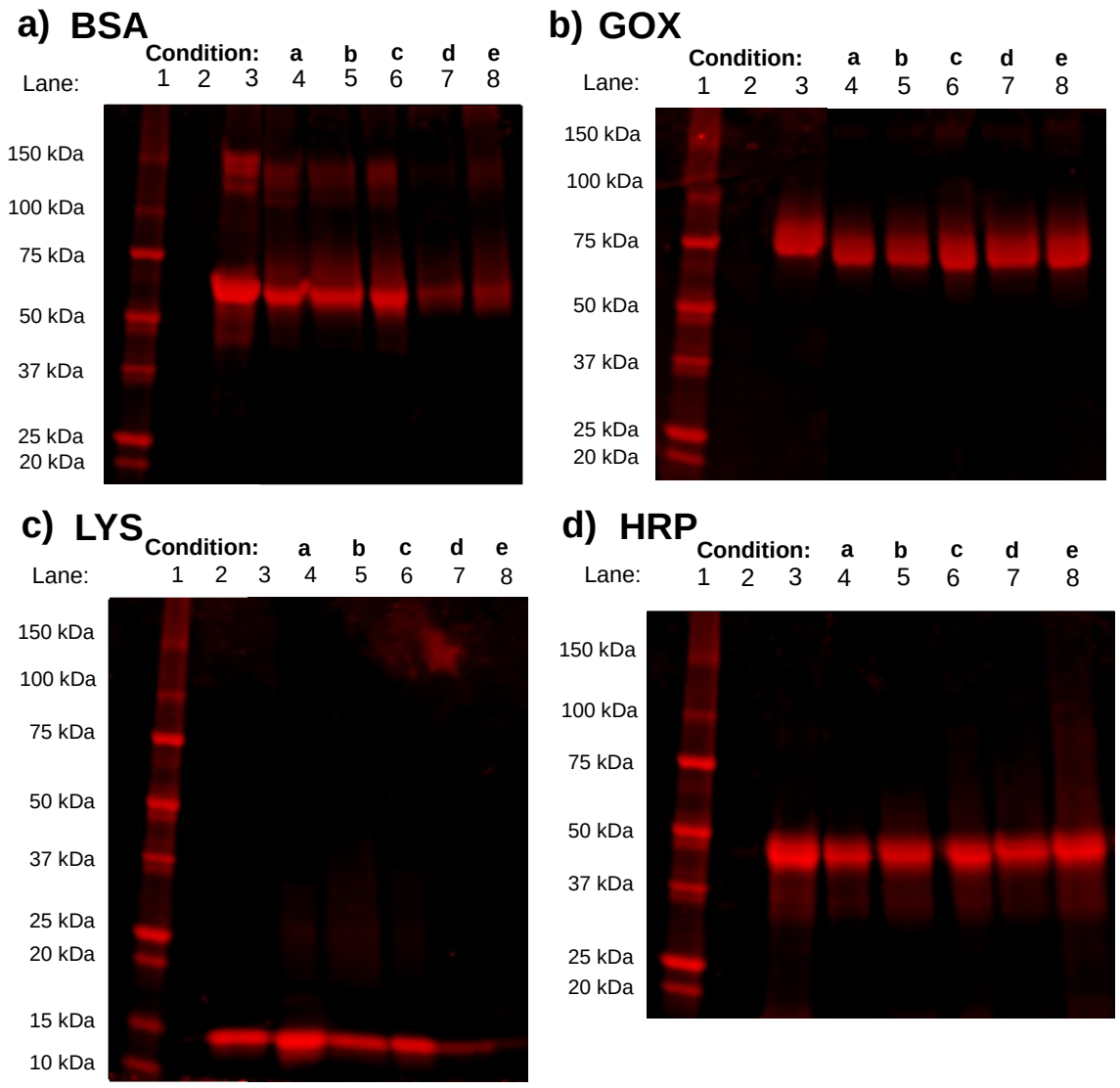

Figure 4-12. SDS-PAGE gels of attempted bioconjugation reactions between **PZT 6b** and (**a**) BSA, (**b**) GOX, (**c**) LYS, and (**d**) HRP in various buffer conditions after 24 hours. Lane 1 is the molecular weight ladder, lane 2 is the polymer control, and lane 3 is the protein control. Lanes 4-8 are the **6b-20** experimental conditions with each lane representing a different buffer condition. Condition a: 0.15 M PBS; Condition b: Certipur Borate; Condition c: 0.1 M Sodium Bicarbonate; Condition d: 0.15 M HEPES; Condition e: 0.15 M Tris. All conditions were at pH 9.2, 1 mM EDTA.

4.4 Summary

Chapter 4 demonstrated the utility of aromatic **PZTs** in polymer-protein bioconjugation *via* disulfide formation and electrophilic addition with both native and reduced proteins, such as BSA, CAT, and LYS, finding that VS-modified **PZTs** significantly improved conjugation efficiency across a variety of conditions. In contrast, bioconjugates comprising aliphatic **PZTs** or aromatic and aliphatic **SPZTs** have not yet been realized for either mechanism.

4.5 References

1. Veronese, F. M.; Pasut, G. PEGylation, Successful Approach to Drug Delivery. *Drug Discov. Today* **2005**, *10* (21), 1451-1458.

2. Gao, Y.; Joshi, M.; Zhao, Z.; Mitragotri, S. PEGylated Therapeutics in the Clinic. *Bioeng. Transl. Med.* **2020**, *9* (1), e10600, 28 pages.

3. Jatzkewitz, H. Peptamin (Glycyl-L-leucyl-mescaline) Bound to Blood Plasma Expander (Polyvinylpyrrolidone) as a New Depot form of a Biologically Active Primary Amine (Mescaline) *Z. Naturforsch.* **1955**, *10b*, 27–31.

4. Mathé, G.; Loc, T. B.; Bernard, J. Effet sur la leucémie 1210 de la Souris d'une combinaison par diazotation d'**A**-méthopterine et de γ-globulines de hamsters porteurs de cette leucémie par hétérogreffe. *C R Hebd. Seances Acad. Sci.* **1958**, *246* (10), 1626-1628.

5. Givetal, N. I.; Ushakov, S. N.; Panarin, E. F.; Popova, G. O. Experimental Studies on Penicillin Polymer Derivatives (in Russian). *Antibiotiki* **1965**, *10*, 701-706.

6. Panarin, E. F.; Ushakov, S. N. Synthesis of Polymer Salts and Aminopenicillins (in Russian). *Khim. Pharm. Zhur.* **1968**, *2*, 28-31.

7. Abuchowski, A.; McCoy, J. R.; Palczuk, N. C.; van Es, T.; Davis, F. F. Effect of Covalent Attachment of Polyethylene Glycol on Immunogenicity and Circulating Life of Bovine Liver Catalase. *J. Biol. Chem.* **1977**, *252* (11), 3582–3586.

8. Abuchowski, A.; van Es, T.; Palczuk, N. C.; Davis, F. F. Alteration of Immunological Properties of Bovine Serum Albumin by Covalent Attachment of Polyethylene Glycol. *J. Biol. Chem.* **1977**, *252* (11), 3578–3581.

9. Ringsdorf, H. Structure and Properties of Pharmacologically Active Polymers. J. Polym. Sci., Polym. Symp. **1975**, *51*, 135–153.

10. Bader, H.; Ringsdorf, H.; Schmidt, B. Watersoluble Polymers in Medicine. *Angew. Makromol. Chem.* **1984**, *123*, 457–485.

11. Kopeček, J.; Kopečková, P.; Minko, T.; Lu, Z.-R. HPMA Copolymer–Anticancer Drug Conjugates: Design, Activity, and Mechanism of Action. *Eur. J. Pharm. Biopharm*. **2000**, *50* (1), 61–81.

12. Nori, A.; Kopeček, J. Intracellular Targeting of Polymer-Bound Drugs for Cancer Chemotherapy. *Adv. Drug Deliv. Rev.* **2005**, *57* (4), 609–636.

13. Kopeček, J. Polymer–Drug Conjugates: Origins, Progress To-Date and Future Directions. *Adv. Drug Deliv. Rev.* **2013**, *65* (1), 49–59.

14. Matsumura, Y.; Maeda, H. A New Concept for Macromolecular Therapeutics in Cancer Chemotherapy: Mechanism of Tumoritropic Accumulation of Proteins and the Antitumor Agent smancs. *Cancer Res.* **1986**, *46* (12:1), 6387–6392.

15. Maeda, H.; Seymour, L. W.; Miyamoto, Y. Conjugates of Anticancer Agents and Polymers: Advantages of Macromolecular Therapeutics In Vivo. *Bioconjugate Chem.* **1992**, *3* (5), 351–362.
16. SMANCS and Polymer-conjugated Macromolecular Drugs: Advantages in Cancer Chemotherapy. *Adv. Drug Deliv. Rev.* **2001**, *46* (1–3), 169–185.

17. Fang, J.; Sawa, T.; Akaike, T.; Akuta, T.; Sahoo, S. K.; Khaled, G.; Hamada, A.; Maeda, H. In Vivo Antitumor Activity of Pegylated Zinc Protoporphyrin: Targeted Inhibition of Heme Oxygenase in Solid Tumor. *Cancer Res.* **2003**, *63* (13), 3567–3574.

18. Malik, N.; Evagorou, E. G.; Duncan, R. Dendrimer-Platinate: A Novel Approach to Cancer Chemotherapy. *Anti-Cancer Drugs* **1999**, *10* (8), 767–776.

19. Veronese, F. M.; Schiavon, O.; Pasut, G.; Mendichi, R.; Andersson, L.; Tsirk, A.; Ford, J.; Wu, G.; Kneller, S.; Davies, J.; Duncan, R. PEG−Doxorubicin Conjugates: Influence

of Polymer Structure on Drug Release, in Vitro Cytotoxicity, Biodistribution, and Antitumor Activity. *Bioconjugate Chem.* **2005**, *16* (4), 775–784.

20. Duncan, R. The Dawning Era of Polymer Therapeutics. *Nat. Rev. Drug Discov.* **2003**, *2*, 347–360.

21. Duncan, R.; Vicent, M. J. Polymer Therapeutics-Prospects for 21st Century: The End of the Beginning. *Adv. Drug Deliv. Rev.* **2013**, *65* (1), 60–70.

22. Hong, V.; Presolski, S. I.; Ma, C.; Finn, M. G. Analysis and Optimization of Copper-Catalyzed Azide–Alkyne Cycloaddition for Bioconjugation. *Angew. Chem.* **2009**, *121*, 10063 –10067.

23. Sen Gupta, S.; Kuzelka, J.; Singh, P.; Lewis, W. G.; Manchester, M.; Finn, M. G. Accelerated Bioorthogonal Conjugation: A Practical Method for the Ligation of Diverse Functional Molecules to a Polyvalent Virus Scaffold. *Bioconjugate Chem.* **2005**, *16* (6), 1572–1579.

24. Pokorski, J. K.; Breitenkamp, K.; Liepold, L. O.; Qazi, S.; Finn, M. G. Functional Virus-Based Polymer–Protein Nanoparticles by Atom Transfer Radical Polymerization. *J. Am. Chem. Soc.* **2011**, *133* (24), 9242–9245.

25. Fontana, A.; Spolaore, B.; Mero, A.; Veronese, F. M. Site-specific Modification and PEGylation of Pharmaceutical Proteins Mediated by Transglutaminase. *Adv. Drug Deliv. Rev.* **2008**, *60* (1), 13–28.

26. Shaunak, S.; Godwin, A.; Choi, J.-W.; Balan, S.; Pedone, E.; Vijayarangam, D.; Heidelberger, S.; Teo, I.; Zloh, M.; Brocchini, S. Site-Specific PEGylation of Native Disulfide Bonds in Therapeutic Proteins. *Nat. Chem. Biol.* **2006**, *2*, 312-313.

27. Ekladious, I.; Colson, Y. L.; Grinstaff, M. W. Polymer–Drug Conjugate Therapeutics: Advances, Insights and Prospects. *Nat. Rev. Drug Discov.* **2019**, *18*, 273–294.

28. Alconcel, S. N. S.; Baas, A. A.; Maynard, H. D. FDA-approved Poly(ethylene glycol)–Protein Conjugate Drugs. *Polym. Chem.* **2011**, *2*, 1442–1448.

29. Caliceti, P.; Veronese, F. M. Pharmacokinetic and Biodistribution Properties of Poly(ethylene glycol)–Protein Conjugates. *Adv. Drug Deliv. Rev.* **2003**, *55*, 1261–1277.

30. Harris, J. M.; Chess, R. B. Effect of PEGylation on Pharmaceuticals. *Nat. Rev. Drug Discov.* **2003**, *2*, 214-221.

31. Park, H.; Otte, A.; Park, K. Evolution of Drug Delivery Systems: From 1950 to 2020 and Beyond. *J. Cont. Release* **2022**, *342*, 53-65.

32. Yang, Q.; Lai, S. K. Anti-PEG Immunity: Emergence, Characteristics, and Unaddressed Questions. *WIREs Nanomed. Nanobiotechnol.* **2015**, *7*, 655–677.

33. Kozma, G. T.; Shimizu, T.; Ishida, T.; Szebeni, J. Anti-PEG Antibodies: Properties, Formation, Testing and Role in Adverse Immune Reactions to PEGylated Nano-biopharmaceuticals. *Adv. Drug Deliv. Rev.* **2020**, *154-155*, 163–175.

34. Zhang, P.; Sun, F.; Liu, S.; Jiang, S. Anti-PEG Antibodies in the Clinic: Current Issues and Beyond PEGylation. *J. Cont. Release* **2016**, *244* (B), 184–193.

35. Stone, C. A.; Yiwei Liu, Y.; Relling, M. V.; Krantz, M. S.; L. Pratt, A. L.; Abreo, A.; Hemler, J. A.; Phillips, E. J. Immediate Hypersensitivity to Polyethylene Glycols and Polysorbates: More Common Than We Have Recognized. *J. Allergy Clin. Immunol. Pract*. **2019**, *7* (5), 1533–1540.e8.

36. Shi, D.; Beasock, D.; Fessler, A.; Szebeni, J.; Ljubimova, J. Y.; Afonin, K. A.; Dobrovolskaia, M. A. To PEGylate or not to PEGylate: Immunological Properties of Nanomedicine's Most Popular Component, Polyethylene Glycol and its Alternatives. *Adv. Drug Deliv. Rev.* **2022**, *180*, 114079, 22 pages.

37. Nilsson, L.; Csuth, Á.; Storsaeter, J.; Garvey, L. H.; Jenmalm, M. C. Vaccine Allergy: Evidence to Consider for COVID-19 Vaccines. *Curr. Opin. Allergy Clin. Immunol*. **2021**, *21* (4), 401-409.

38. Chen, B.-M.; Cheng, T.-L.; Roffler, S. R. Polyethylene Glycol Immunogenicity: Theoretical, Clinical, and Practical Aspects of Anti-Polyethylene Glycol Antibodies. *ACS Nano* **2021**, *15* (9), 14022–14048.

39. Ozer, I.; Tomak, A.; Zareie, H. M.; Baran, Y.; Bulmus. Effect of Molecular Architecture on Cell Interactions and Stealth Properties of PEG. *Biomacromolecules* **2017**, *18* (9), 2699–2710.

40. Barz, M.; Luxenhofer, R.; Zentel, R.; Vincent, M. Overcoming the PEG-Addiction: Well-Defined Alternatives to PEG, from Structure–Property Relationships to Better Defined Therapeutics. *Polym. Chem.* **2011**, *2*, 1900-1918.

41. Deng, B.; Burns, E.; McNelles, S. A.; Sun, J.; Ortega, J.; Adronov, A. Molecular Sieving with PEGylated Dendron-Protein Conjugates. *Bioconjugate Chem.* **2023**, *34* (8), 1467–1476.

42. Kostka, L.; Kotrchová, L.; Šubr, V.; Libánská, A.; Ferreira, C. A.; Malátová, I.; Lee, H. J.; Barnhart, T. E.; Engle, J. W.; Cai, W.; Šírová, M.; Etrych, T. HPMA-based Star Polymer Biomaterials with Tuneable Structure and Biodegradability Tailored for Advanced Drug Delivery to Solid Tumours. *Biomaterials* **2020**, *235*, 119728, 14 pages.

43. Bays, E.; Tao, L.; Chang, C.-W.; Maynard, H. D. Synthesis of Semitelechelic Maleimide Poly(PEGA) for Protein Conjugation By RAFT Polymerization. *Biomacromolecules* **2009**, *10* (7), 1777–1781.

44. Yang, J.; Kopeček, J. The Light at the End of the Tunnel—Second Generation HPMA Conjugates for Cancer Treatment. *Curr. Opin. Colloid. Interface Sci.* **2017**, *31*, 30–42.

45. Luxenhofer, R.; Han, Y.; Schulz, A.; Tong, J.; Kabanov, A. V.; He, Z.; Jordan, R. Poly(2-oxazoline)s as Polymer Therapeutics. *Macromol. Rapid Commun.* **2012**, *33* (19), 1613-1631.

46. Viegas, T. X.; Bentley, M. D.; Harris, J. M.; Fang, Z.; Yoon, K.; Dizman, B.; Weimer, R.; Mero, A.; Pasut, G.; Veronese, F. M. Polyoxazoline: Chemistry, Properties, and Applications in Drug Delivery. *Bioconjugate Chem.* **2011**, *22* (5), 976–986.

47. Duro-Castano, A.; Conejos-Sánchez, I.; Vincent, M J. Peptide-Based Polymer Therapeutics. *Polymers* **2014**, *6* (2), 515-551.

48. Duncan, R. Development of HPMA Copolymer–Anticancer Conjugates: Clinical Experience and Lessons Learnt. *Adv. Drug Deliv. Rev.* **2009**, *61* (13), 1131–1148.

49. Ravasco, J. M. J. M.; Faustino, H.; Trindade, A.; Gois, P. M. P. Bioconjugation with Maleimides: A Useful Tool for Chemical Biology. Chem. Eur. J. 2019, 25, 43–59.

50. Kalia, D.; Malekar, P. V.; Parthasarathy, M. Exocyclic Olefinic Maleimides: Synthesis and Application for Stable and Thiol-Selective Bioconjugation. *Angew. Chem. Int. Ed.* **2015**, *55* (4), 1432-1435.

51. Jones, M. W.; Strickland, R. A.; Schumacher, F. F.; Caddick, S.; Baker, J. R.; Gibson, M. I.; Haddleton, D. M. Polymeric Dibromomaleimides as Extremely Efficient Disulfide Bridging Bioconjugation and Pegylation Agents. *J. Am. Chem. Soc.* **2012**, *134* (3), 1847–1852.

52. Lu, Z.-P.; Kopečková, P.; Wu, Z.; Kopeček, J. Functionalized Semitelechelic Poly[N-(2-hydroxypropyl)methacrylamide] for Protein Modification. *Bioconjugate Chem.* **1998**, *9* (6), 793–804.

53. Lele, B. S.; Murata, H.; Matyjaszewski, K.; Russell, A. J. Synthesis of Uniform Protein−Polymer Conjugates. *Biomacromolecules* **2005**, *6* (6), 3380–3387.

54. Turecek, P. L.; Bossard, M. J.; Schoetens, F.; Ivens, I. A. PEGylation of Biopharmaceuticals: A Review of Chemistry and Nonclinical Safety Information of Approved Drugs. *J. Pharm. Sci*. **2016**, *105* (2), 460-475.

55. Ko, J. H.; Maynard, H. D. A Guide to Maximizing the Therapeutic Potential of Protein-Polymer Conjugates by Rational Design. *Chem. Soc. Rev.* **2018**, *47*, 8998-9014.

56. Lewis, A.; Tang, Y.; Brocchini, S.; Choi, J.; Godwin, A. Poly(2-methacryloyloxyethyl phosphorylcholine) for Protein Conjugation. *Bioconjugate Chem*. **2008**, *19* (11), 2144–2155.

57. Ishihara, K.; Mu, M.; Konno, T.; Inoue, Y.; Fukazawa. The Unique Hydration State of Poly(2-methacryloyloxyethyl phosphorylcholine). *J. Biomater. Sci. Polym. Ed.* **2017**, *28* (10-12), 884-899.

58. Liang, S.; Liu, Y.; Jin, X.; Liu, G.; Wen, J.; Zhang, L.; Li, J.; Yuan, X.; Chen, I. S. Y.; Chen, W.; Wang, H.; Shi, L.; Zhu, X.; Lu, Y. Phosphorylcholine Polymer Nanocapsules Prolong the Circulation Time and Reduce the Immunogenicity of Therapeutic Proteins. *Nano Res.* **2016**, *9*, 1022-1031.

59. Ishihara, K. Revolutionary Advances in 2-Methacryloyloxyethyl Phosphorylcholine Polymers as Biomaterials. *J. Biomed. Mater. Res. A* **2019**, *107* (5), 933–943.

60. Jackson, M. A.; Werfel, T. A.; Curvino, E. J.; Yu, F.; Kavanaugh, T. E.; Sarett, S. M.; Dockery, M. D.; Kilchrist, K. V.; Jackson, A. N.; Giorgio, T. D.; Duvall, C. L. Zwitterionic Nanocarrier Surface Chemistry Improves siRNA Tumor Delivery and Silencing Activity Relative to Polyethylene Glycol. *ACS Nano* **2017**, *11* (6), 5680–5696.

61. Keefe, A. J.; Jiang, S. Poly(zwitterionic)protein Conjugates offer Increased Stability without Sacrificing Binding Affinity or Bioactivity. *Nat. Chem.* **2012**, *4*, 59–63.

62. Sun, H.; Chang, M. Y. Z.; Cheng, W.; Wang, Q.; Commisso, A.; Capeling, M.; Wu, Y.; Cheng, C. Biodegradable Zwitterionic Sulfobetaine Polymer and its Conjugate with Paclitaxel for Sustained Drug Delivery. *Acta Biomater.* **2017**, *64*, 290–300.

63. Baggerman, J.; Smulders, M. M. J.; Zuilhof, H. Romantic Surfaces: A Systematic Overview of Stable, Biospecific, and Antifouling Zwitterionic Surfaces. *Langmuir* **2019**, *35* (5), 1072–1084.

64. Cheng, G.; Li, G.; Xue, H.; Chen, S.; Bryers, J. D.; Jiang, S. Zwitterionic Carboxybetaine Polymer Surfaces and their Resistance to Long-term Biofilm Formation. *Biomaterials* **2009**, *30* (28), 5234–5240. DOI: 10.1016/j.biomaterials.2009.05.058

65. Zhang, Z.; Chen, S.; Jiang, S. Dual-Functional Biomimetic Materials: Nonfouling Poly(carboxybetaine) with Active Functional Groups for Protein Immobilization. *Biomacromolecules* **2006**, *7* (12), 3311–3315. DOI: 10.1021/bm060750m

66. Yang, W.; Chen, S.; Cheng, G.; Vaisocherová, H.; Xue, H.; Li, W.; Zhang, J.; Jiang, S. Film Thickness Dependence of Protein Adsorption from Blood Serum and Plasma onto Poly(sulfobetaine)-Grafted Surfaces. *Langmuir* **2008**, *24* (17), 9211–9214. DOI: 10.1021/la801487f

67. Chen, Y.; Li, J.; Li, Q.; Shen, Y.; Ge, Z.; Zhang, W.; Chen, S. Enhanced Water-Solubility, Antibacterial Activity and Biocompatibility upon Introducing Sulfobetaine and Quaternary Ammonium to Chitosan. *Carbohydr. Polym*. **2016**, *143* (5), 246–253.

68. Kuo, W.-H.; Wang, M.-J.; Chien, H.-W.; Wei, T.-C.; Lee, C.; Tsai, W.-B. Surface Modification with Poly(sulfobetaine methacrylate-co-acrylic acid) To Reduce Fibrinogen Adsorption, Platelet Adhesion, and Plasma Coagulation. *Biomacromolecules* **2011**, *12* (12), 4348–4356.

69. Samanta, D.; McRae, S.; Cooper, B.; Hu, Y.; Emrick, T. End-functionalized Phosphorylcholine Methacrylates and their use in Protein Conjugation. *Biomacromolecules* **2008**, *9*, 2891-2897.

70. Chen, XJ.; McRae, S.; Samanta, D.; Emrick, T. Polymer-Protein Conjugation in Ionic Liquids. *Macromolecules* **2010**, *43*, 6261-6263.

71. McRae, S.; Chen, X.; Kratz, K.; Samanta, D.; Henchey, E.; Schneider, S.; Emrick, T. Pentafluorophenyl Ester-Functionalized Phosphorylcholine Polymers: Preparation of Linear, Two-Arm, and Grafted Polymer–Protein Conjugates. *Biomacromolecules* **2012**, *13* (7), 2099–2109.

72. Chen, XJ.; McRae, S.; Parelkar, S.; Emrick, T. Polymeric Phosphorylcholine-Camptothecin Conjugates Prepared by Controlled Free Radical Polymerization and Click Chemistry. *Bioconjugate Chem*. **2009**, *20*, 2331–2341.

73. Wong, K. E.; Mora, M. C.; Skinner, M.; Page, S. M.; Crisi, G. M.; Arenas, R. B.; Schneider, S. S.; Emrick, T. Evaluation of PolyMPC-Dox Prodrugs in a Human Ovarian Tumor Model. *Mol. Pharmaceutics* **2016**, 13(5), 1679–1687

74. McRae Page, S.; Henchey, E.; Chen, X., Schneider, S. and Emrick, T. Efficacy of PolyMPC-DOX Prodrugs in 4T1 Tumor-bearing Mice. *Mol. Pharmaceutics* **2014**, 11(5), 1715–1720.

75. Ward, S.M.; Skinner, M.; Saha, B.; Emrick, T. Polymer - Temozolomide Conjugates as Therapeutics for Treating Glioblastoma. *Mol. Pharmaceutics* **2018**, *15* (11), 5263–5276.

76. Jin, Q.; Chen, Y.; Wang, Y.; Ji, J. Zwitterionic Drug Nanocarriers: A Biomimetic Strategy for Drug Delivery. *Colloids Surf. B Biointerfaces* **2014**, *124*, 80-86.

77. Sun, H.; Yan, L.; Zhang, R.; Lovell, J. F.; Wu, Y.; Cheng, C. A Sulfobetaine Zwitterionic Polymer-Drug Conjugate for Multivalent Paclitaxel and Gemcitabine Co-Delivery. *Biomater. Sci*. **2021**, *9* (14), 5000-5010.

78. Harijan, M.; Singh, M. Zwitterionic Polymers in Drug Delivery: A Review. *J. Mol. Recognit.* **2021**, *35* (1), e2944, 13 pages.

79. Wang, Z.; Ma, G.; Zhang, J.; Lin, W.; Ji, F.; Bernards, M. T.; Chen, S. Development of Zwitterionic Polymer-Based Doxorubicin Conjugates: Tuning the Surface Charge to Prolong the Circulation and Reduce Toxicity. *Langmuir* **2014**, *30* (13), 3764–3774.

80. Zhao, G.; Sun, Y.; Dong, X. Zwitterionic Polymer Micelles with Dual Conjugation of Doxorubicin and Curcumin: Synergistically Enhanced Efficacy against Multidrug-Resistant Tumor Cells. *Langmuir* **2020**, *36* (9), 2383–2395.

81. Zhai, S.; Ma, Y.; Chen, Y.; Li, D.; Cao, J.; Liu, Y.; Cai, M.; Xie, X.; Chen, Y.; Luo, X. Synthesis of an Amphiphilic Block Copolymer Containing Zwitterionic Sulfobetaine as a Novel pH-Sensitive Drug Carrier. *Polym. Chem*. **2014**, 5, 1285-1297.

82. Zeng, Z.; Chen, S.; Chen, Y. Zwitterionic Polymer: A New Paradigm for Protein Conjugation beyond PEG. *ChemMedChem* **2023**, *18* (20), e202300245, 9 pages.

83. Hu, G. J.; Parelkar, S. S.; Emrick, T., A Facile Approach to Hydrophilic, Reverse Zwitterionic, Choline Phosphate Polymers. *Polym. Chem.* **2015**, *6* (4), 525–530.

84. Hu, G.; Emrick, T. Functional Choline Phosphate Polymers. *J. Am. Chem. Soc.* **2016**, *138*, 1828–1831.

85. Chang, C.-C.; Letteri, R.; Hayward, R. C.; Emrick, T. Functional Sulfobetaine Polymers: Synthesis and Salt-Responsive Stabilization of Oil-in-Water Droplets. *Macromolecules* **2015**, *48* (21), 7843–7850.

86. Sonu, K. P.; Zhou, L.; Biswas, S.; Klier, J.; Balazs, A. C.; Emrick, T.; Peyton, S. R. Strain-Stiffening Hydrogels with Dynamic, Secondary Cross-Linking. *Langmuir* **2023**, *39* (7), 2659–2666.

87. Chen, F.-J.; Gao, J. Fast Cysteine Bioconjugation Chemistry. *Chem. Eur. J.* **2022**, *28* (66), e202201843, 15 pages.

88. Liu, J.; Bulmus, V.; Herlambang, D. L.; Barner-Kowollik, C.; Stenzel, M. H.; Davis, T. P. In Situ Formation of Protein–Polymer Conjugates through Reversible Addition Fragmentation Chain Transfer Polymerization. *Angew. Chem. Int. Ed.* **2007**, *46* (17), 3099-3103.

89. Heredia, K. L.; Bontempo, D.; Ly, T.; Byers, J. T.; Halstenberg, S.; Maynard, H. D. In Situ Preparation of Protein−"Smart" Polymer Conjugates with Retention of Bioactivity. *J. Am. Chem. Soc.* **2005**, *127* (48), 16955–16960.

90. Gevrek, T. N.; Cosar, M.; Aydin, D.; Kaga, E.; Arslan, M.; Sanyal, R.; Sanyal, R. Facile Fabrication of a Modular "Catch and Release" Hydrogel Interface: Harnessing Thiol–Disulfide Exchange for Reversible Protein Capture and Cell Attachment. *ACS Appl. Mater. Interfaces* **2018**, *10* (17), 14399–14409.

91. Altinbasak, I.; Arslan, M.; Sanyal, R.; Sanyal, A. Pyridyl Disulfide-Based Thiol–Disulfide Exchange Reaction: Shaping the Design of Redox-Responsive Polymeric Materials. *Polym. Chem.* **2020**, *11* (48), 7603–7624.

92. Summonte, S.; Racaniello, G. F.; Lopedota, A.; Denora, N.; Bernkop-Schnürch, A. Thiolated Polymeric Hydrogels for Biomedical Application: Cross-Linking Mechanisms. *J. Control. Release* **2021**, *330* (10), 470–482.

93. Lee, M. H.; Sessler, J. L.; Kim, J. S. Disulfide-Based Multifunctional Conjugates for Targeted Theranostic Drug Delivery. *Acc. Chem. Res.* **2015**, *48* (11), 2935–2946.

94. Zhang, P.; Wu, J.; Xiao, F.; Zhao, D.; Luan, Y. Disulfide Bond Based Polymeric Drug Carriers for Cancer Chemotherapy and Relevant Redox Environments in Mammals. *Med. Res. Rev.* **2018**, *38* (5), 1485-1510.

95. Huo, M; Yuan, J.; Tao, L.; Wei, Y. Redox-Responsive Polymers for Drug Delivery: From Molecular Design to Applications. *Polym. Chem.* **2014**, *5*, 1519-1528.

96. Hoyle, C. E.; Lowe, A. B.; Bowman, C. N. Thiol-Click Chemistry: A Multifaceted Toolbox for Small Molecule and Polymer Synthesis. *Chem. Soc. Rev.* **2010**, 39, 1355-1387.

97. Hoang, M. V.; Chung, H.-J.; Elias, A. L. Irreversible Bonding of Polyimide and Polydimethylsiloxane (PDMS) Based on a Thiol-Epoxy Click Reaction. *J. Micromech. Microeng.* **2016**, *26*, 105019, 9 pages.

98. Lowe, A. B. Thiol-ene "Click" Reactions and Recent Applications in Polymer and Materials Synthesis: A First Update. *Polym. Chem.* **2014**, *5*, 4820-4870.

99. Nair, D. P.; Podgórski, M.; Chatani, S.; Gong, T.; Xi, W.; Fenoli, C. R.; Bowman, C. N. The Thiol-Michael Addition Click Reaction: A Powerful and Widely Used Tool in Materials Chemistry. *Chem. Mater.* **2014**, *26* (1), 724–744.

100. Morales-Sanfrutos, J.; Lopez-Jaramillo, J.; Ortega-Munoz, M.; Megia-Fernandez, A.; Perez-Balderas, F.; Hernandez-Mateo, F.; Santoyo-Gonzalez, F. Vinyl Sulfone: A Versatile Function for Simple Bioconjugation and Immobilization. Org. Biomol. Chem. 2010, 8 (3), 667–675.

101. Zupancich, J. A.; Bates, F. S.; Hillmyer, M. A. Synthesis and Self-Assembly of RGD-Functionalized PEO-PB Amphiphiles. *Biomacromolecules* **2009**, *10* (6), 1554–1563.

102. Badescu, G.; Bryant, P.; Swierkosz, J.; Khayrzad, F.; Pawlisz, E.; Farys, M.; Cong, Y.; Muroni, M.; Rumpf, N.; Brocchini, S.; Godwin, A. A New Reagent for Stable Thiol-Specific Conjugation. *Bioconjugate Chem.* **2014**, *25* (3), 460–469.

103. Grover, G. N.; Alconcel, S. N. S.; Matsumoto, N. M.; Maynard, H. D. Trapping of Thiol-Terminated Acrylate Polymers with Divinyl Sulfone to Generate Well-Defined Semitelechelic Michael Acceptor Polymers. *Macromolecules* **2009**, *42* (20), 7657–7663.

104. Li, M.; Cheng, F.; Li, H.; Jin, W.; Chen, C.; He, W.; Cheng, W.; Wang, Q. Site-Specific and Covalent Immobilization of His-Tagged Proteins via Surface Vinyl Sulfone–Imidazole Coupling. *Langmuir* **2019**, *35* (50), 16466–16475.

105. Bontempo, D.; Heredi, K. L.; Fish, B. A.; Maynard, H. D. Cysteine-Reactive Polymers Synthesized by Atom Transfer Radical Polymerization for Conjugation to Proteins. *JACS* **2004**, *126* (47), 15372–15373.

106. Liu, J.; Liu, H.; Bulmus, V.; Tao, L.; Boyer, C.; Davis, T. P. J. A Simple Methodology for the Synthesis of Heterotelechelic Protein–Polymer–Biomolecule Conjugates. *Polym. Sci. A. Polym. Chem.* **2010**, *48* (6), 1399–1405.

107. Isarov, S. A.; Lee, P. W.; Pokorski, J. K. "Graft-to" Protein/Polymer Conjugates Using Polynorbornene Block Copolymers. *Biomacromolecules* **2016**, *17* (2), 641–648.

CHAPTER FIVE:
CONLCUDING REMARKS & FUTURE WORK

This thesis described the synthesis of embedded thiol choline phosphate (CP) monomers and their incorporation into biomolecular materials as polymer zwitterion thiols (**PZTs**). *S*-trityl-protected mercaptoethanol and mercaptophenol-based CP thiol monomers were produced on multi-gram scales and then utilized in RAFT copolymerization with MPC (**Chapter 2**). The resultant embedded thiol CP polymer zwitterions had tunable incorporation of CP thiol (targeted up to ~50%), controllable molecular weights, and low polydispersities. Following deprotection, the embedded *S*-trityl groups were liberated to afford **PZTs** with free sulfhydryls, which participated in functional group transformations as well as hydrogel formation *via* photocatalyzed thiol-Michael addition and *via* disulfide crosslinking (**Chapter 3**). The aromatic and protected aliphatic **PZTs** were also found to stabilize the o/water interface using pendant drop tensiometry whereas the deprotected aliphatic **PZTs** displayed no interfacial stabilization. Moreover, the aromatic **PZTs** proved useful in bioconjugation reactions using disulfide formation and vinyl sulfone addition with several proteins, confirmed by SDS-PAGE and FPLC characterization (**Chapter 4**).

While the novel integration of thiols into polymer zwitterions as represented by the **PZTs** developed in this thesis have demonstrated utility across a variety of biomolecular applications, several opportunities for improvement remain. The synthesis of aromatic and aliphatic CP methacrylates, although producing multiple grams of product, gave low-to-moderate percent yields of product, and accessing block copolymer structures and well-defined homopolymers remains an ongoing challenge. Moreover, it is not fully understood why the aromatic **PZTs** outperformed the aliphatic **PZTs**, notably in hydrogel and bioconjugation applications, which may underscore the importance of thiol pKa in **PZT**

properties. The biocompatibility and anti-fouling behavior of the **PZTs** has also not been evaluated, which will be crucial for future biomedical applications.

Despite these limitations, the **PZT** synthesis represents a versatile pathway to biomolecular materials that combine the unique properties of zwitterions and thiols into each pendent group along a polymer backbone. For example, stabilization of oil-in-water interfaces with **PZT** surfactants provides a route to explore the interfacial reactivity of the reactive thiol handle and its impact on droplet interfacial tension or disruption. Alternatively, inter-droplet interactions between free thiol or other interfacially anchored reactive moieties (i.e., protein, crosslinkers, etc.) may provide opportunities to aggregation/assembly or communication. On the other hand, reversible disulfide bonds can be used to create stimuli-responsive **PZT** hydrogels or drug delivery prodrugs/carriers that simultaneously immobilize or embed protein therapeutics, for controlled drug release in the reducing environment of cells. Overall, **PZTs** offer exciting possibilities for designer materials with precision control over properties that will continue to be unveiled, as will a deeper understanding of the biological systems that inspired them.

CHAPTER 6:
EXPERIMENTAL METHODS

6.1 Materials

5,5'-Dithiobis(2-nitrobenzoic acid) (Ellman's Reagent), triisopropylsilane (98%), tris(2-carboxyethyl)phosphine hydrochloride, dimethyl sulfoxide, potassium phosphate monobasic, potassium phosphate dibasic, trifluoroacetic acid (99%), ethylenediaminetetraacetic acid (ACS Reagent, 99.4-100.06%), polyethylene glycol diacrylate (M_n ~700, 535, 235 Da), polyethylene glycol dithiol (M_n ~ 1000 Da), 4,4'-azobis(4-cyanovaleric acid) (≥98.0%T) (ACVA), 4-cyano-4-(phenylcarbonothioylthio)pentanoic acid (PCTA), 4-cyano-4-[(dodecylsulfanylthiocarbonyl) sulfanyl]pentanoic acid (97%, HPLC) (YCTA), dipyridyl disulfide (for synthesis), dimethylamine (40 wt% in water), vinylbenzyl chloride, glucose oxidase from *Aspergillus niger*, >100-250,000 units/mg (G7141), bovine serum albumin, suitable for cell culture (>96%, A8806), horseradish peroxidase, >50 units/mg (P8125), lysozyme from chicken egg white, >40,000 units/mg (>90%, L6876), 2-mercaptoethanol for electrophoresis (>98%), hydrogen peroxide (50 wt% in H_2O, stabilized), pyrogallol (ACS reagent, >99%), trichlorobenzene (ReagentPlus, ≥99%), molecular sieves (3 Å, beads, 4-8 mesh), and Amicon ultra centrifugal filters, regenerated cellulose (3 kDa – 100 kDa MWCO) were purchased from Sigma Aldrich. Triethylamine (>99.5%) and dichloromethane (anhydrous, 99.8%, 40-150 pm amylene inhibitor) were purchased from Sigma Aldrich and distilled over sodium hydride. Acetonitrile (anhydrous, 99.8%) was obtained from Sigma and stored over molecular sieves. 2-methacryloyloxyethyl phosphorylcholine (≤100 ppm MeHQ as inhibitor, 97%) (MPC) from Sigma Aldrich was purified in diethyl ether to remove inhibitor. 2-(dimethylamino)ethyl methacrylate

(contains 700-1000 ppm monomethyl ether hydroquinone as inhibitor, 98%) was obtained from Sigma Aldrich, purified with alumina, and stored over molecular sieves. Certipur borate buffer was purchased from Sigma Aldrich and its pH was adjusted to 9.2 using 5 M NaOH. Glacial acetic acid (certified ACS), hydrochloric acid (certified ACS plus), ethanol (certified ACS), sodium bicarbonate (certified ACS), magnesium sulfate (anhydrous), potassium carbonate (anhydrous), sodium chloride, sodium hydroxide (Certified ACS), Methanol (Certified ACS), and Water (Optima for HPLC) were obtained from Fisher Chemical. 2x Laemmli sample buffer, 10X Tris/Glycine/SDS Buffer, 2-mercaptoethanol, Precision Plus Protein™ unstained protein standards (strep-tagged recombinant), and 4–15% Mini-PROTEAN® TGX™ Precast Protein Gels (15-well, 15 µl) were purchased from BioRad. Triphenylmethyl chloride (98%), diethyl ether (ACS reagent, anhydrous), and 4-mercaptophenol (98%) were obtained from ThermoScientific. Methanol-d4 (99.9%), chloroform-D (99.8%, 0.05% v/v TMS), and deuterium oxide (99.9%) were purchased from Cambridge Isotopes. VA-044 was purchased from Wako Chemicals. Pyridine (anhydrous, 99.5+%) was purchased from Alfa Aesar. 4-methoxyphenol, stabilized (>98%) was purchased from Acros Organics. Brilliant Blue R-250 and divinyl sulfone (≥96.0% GC, stabilized with HQ) were obtained from TCI America. 2--1,3,2-dioxaphospholane 2-oxide (ethylene chlorophosphate, ECP) was obtained from TCI America and purified *via* Kugelrohr distillation. Spectra/Por 3 and 6 dialysis membranes (1 kDa & 3.5 kDa, respectively) were purchased from SpectrumLabs. Standard size glass cuvettes (3.5 mL) were obtained from Cole-Parmer.

6.2 General Methods

Characterization. Multi-nucleus (^{1}H, ^{13}C, and ^{31}P) nuclear magnetic resonance (NMR) spectra were obtained on a 500 MHz Bruker-Avance instrument tuned to 400, 126 and 202 MHz, respectively. The chemical shifts of ^{1}H and ^{13}C spectra were calibrated against the signals from the deuterated NMR solvent employed. Gel permeation chromatography (GPC) was performed using an Agilent 1200 series instrument equipped with three PFG analytical linear M columns (8 × 300 mm, particle size 7 μm), a PFG guard column (8 × 50 mm), an isocratic pump, and an auto sampler. The mobile phase was comprised of trifluoroethanol (0.2 M sodium trifluoroacetate), and its flow rate was 1 mL/min at 40^{o}C. The elution profiles of PMMA standards were measured using the refractive index (RI) detector to create a molecular weight calibration curve. All polymer solutions were prepared at 3 mg/mL and were filtered with a 0.22 μm PTFE syringe filter before being loaded on the TFE GPC. Gel permeation chromatography was additionally conducted with an Agilent 1260 infinite series instrument equipped with three Ultrahydrogel linear columns (7.8 x 300 mm), an Ultrahydrogel DP matrix guard column (6 x 40 mm), and an RI and UV detector. The flow rate was 1 mL/min at 35^{o}C and the aqueous mobile phase contained 20% acetonitrile, 0.1 M $NaNO_3$, and 0.02 wt% NaN_3 in DI water. The aqueous GPC was calibrated against PEO standards. Polymer solutions were prepared at 3 mg/mL and filtered using a 0.45 μm PES syringe filter before being manually loaded onto the GPC. Fast protein liquid chromatography (FPLC) was conducted using an ÄKTA pure 25 M2 (V9-IA, V9-IB V9-C V9-O) instrument from GE equipped with a Superose 6 10/300 GL size exclusion column, a fraction collector (F9-R), and an U9-L UV detector. The mobile phase was 0.1 M phosphate buffered saline PBS (pH 7.4) containing 0.14 M NaCl and 2.7

mM KCl, and its flow rate was 0.5 mL/min. All solutions (concentration maximum of 2 mg/mL) injected manually on the FPLC were pre-filtered with a 0.45 µm PES syringe filter. Electrospray ionization (ESI) was conducted with a Bruker SolariX 7T FTMS mass spectrophotometer. Samples were prepared at 50-100 µM in a 50:50 chloroform: methanol solution and spectra were recorded in positive ion mode. UV-Vis spectroscopy was performed with a Shimadzu UV-2600 spectrophotometer. Optical images were acquired with a Cannon EOS 6D Mark II camera equipped with either a zoom lens EF (24-70 mm) or a macro photo lens MP-E (65mm). A macro twin lite MT-26EX-RT attachment was utilized to obtain fluorescent optical images.

6.3 CP Zwitterion Monomer Synthesis

Vinylbenzyl dimethylamine (VBDMA)

Following a reported procedure,[1] vinylbenzyl chloride (8.5 g, 56 mmol) and dimethylamine (11 mL, 87 mmol, 1.6 eq) were dissolved in 100 mL of an ethanol solution containing 1.5 M potassium carbonate. After being heated for 72 hours at 70^{o}C, the solution turned bright yellow from an initially pale-yellow color, with ^{1}H NMR analysis indicating ~81% conversion. The solution was concentrated under vacuum at room temperature and vacuum-dried overnight to give a dark brown oil, which was subsequently purified using column chromatography with a 3:1 Hexanes: DCM mobile phase containing 4% TEA. Pure product was obtained following concentration at room temperature to give a yellow oil (6.2 g, 71%). ^{1}H NMR (500 MHz), $CDCl_3$, δ (ppm): 7.38-7.36 (d, 2H), 7.27-7.26 (d, 2H), 6.74-6.68 (dd, 1H), 5.76-5.72 (d, 1H), 5.23-5.21 (d, 1H), 3.41 (m, 2H), 2.24 (s, 6H).

*Trityl-protected **1a***

Following a procedure reported in literature,[2] mercaptophenol (12.0 g, 95.0 mmol) and pyridine (7.8 mL, 96.2 mmol) were dissolved in DCM (110 mL) to give a final solution concentration between 0.8 – 1.0 M with respect to mercaptophenol. Trityl chloride (26.6 g, 95.4 mmol) was then added over 30 min, at which point white precipitates formed in solution. The solids were collected *via* vacuum filtration and rinsed with cold DCM before being extracted against water. The organic phase was then washed against brine, dried over $MgSO_4$, and concentrated to give white solid powders that were further dried under vacuum to yield **1a** (23.0 g, 66%). ^{1}H NMR (500 MHz), MeOD, δ (ppm): 7.36 – 7.16 (m, 15H), 6.78-6.75 (m, 2H), 6.44-6.42 (m, 2H)

*Trityl-protected **1b***

Following a procedure reported in literature,[3] mercaptoethanol (3.0 mL, 43 mmol) and trityl chloride (12.05 g, 43.22 mmol) were dissolved in DCM (30 mL). After ~12 hours, the solution was concentrated using a rotary evaporator to give a crystalline yellow solid crude product. Silica gel column chromatography was utilized to purify the crude mixture using a mobile phase gradient from 9:1 DCM: hexanes to pure ethyl acetate. The fractions were collected, concentrated and vacuum dried overnight to yield white solid **1b** (7.0 g, 60%). ^{1}H NMR (500 MHz), MeOD, δ (ppm): 7.41-7.20 (m, 15H), 3.34 (t, 2H), 2.35 (t, 2H)

*Trityl-protected CP thiol methacrylate **3a** and **3b***

Freshly distilled DCM (140 mL) was added to vacuum-dried **1a** (23.0 g, 62.3 mmol) (or **1b**). The solution was brought to -20^{o}C using a MeOH/water bath, at which point the distilled TEA (9.6 mL, 65.4 mmol, 1.05 eq) was added. ECP (8.4 g, 58.9 mmol, 0.95 eq), purified before use *via* Kugelrohr distillation, was then added dropwise to the **1a** (or **1b**)

solution. Over time, white solids precipitated out of solution. The solution was held at -20°C for an additional hour before being filtered under nitrogen through oven-dried celite and concentrated under vacuum to give **2a** (28.0 g, 92%) or **2b** (5.71 g, 95%). Dry ACN (170 mL) and dimethylaminoethyl methacrylate (15 mL, 89.0 mmol, 1.6 eq) were then added to **2a** (or **2b**), along with inhibitor MEHQ (10 mg, 0.8 mmol), to give a final solution concentration of 0.3 M. The solution was placed at 70°C and allowed to react for 16 hours before being precipitated under nitrogen in cold diethyl ether. The solution was placed in a -80°C freezer overnight to further encourage precipitation. The white solids were collected *via* vacuum filtration and dried to give **3a** (10.8 g, 30%) and **3b** (2.5 g, 35%). **2a.** ^{1}H NMR (500 MHz), $CDCl_3$, δ (ppm): 7.40 – 7.17 (m, 15H), 6.96-6.95 (m, 2H), 6.86-6.84 (m, 2H), 4.48-4.39 (m, 2H), 4.19-4.10 (m, 2H); Coupled ^{31}P NMR, $CDCl_3$, δ (ppm): 11.28 (m, 1P); ESI: m/z 497.09 (Na+, 51%). **3a.** ^{1}H NMR (500 MHz), MeOD, δ (ppm): 7.37 – 7.17 (m, 15H), 6.90 (s, 4H), 6.14 (m, 1H), 5.70 (m, 1H), 4.60-4.59 (m, 2H), 4.31-4.30 (m, 2H), 3.81-3.79 (m, 2H), 3.72-3.70 (m, 2H), 3.22 (s, 6H), 1.96 (m, 3H); ^{31}P NMR, MeOD, δ (ppm): -6.11; ^{13}C NMR, CDCl3, δ (ppm): 167.52, 154.49, 154.44, 145.90, 138.11, 136.95, 131.12, 129.38, 128.68, 127.80, 127.38, 120.88, 120.84, 71.90, 65.97, 65.91, 65.10, 60.66, 60.61, 52.86, 18.44; ESI: m/z 654.20 (Na+, 17%), 632.22 (H+, 9%). **2b.** ^{1}H NMR (500 MHz), $CDCl_3$, δ (ppm): 7.43-7.20 (m, 15H), 4.44-4.25 (m, 4H), 3.79 (m, 2H), 2.56 (t, 2H); Coupled ^{31}P NMR, CDCl3, δ (ppm): 17.01 (m, 1P); ESI: m/z 449.09 (Na+, 56%). **3b.** ^{1}H NMR (500 MHz), CDCl3, δ (ppm): 7.42-7.23 (m, 15H), 6.16 (s, 1H), 5.71 (s, 1H), 4.62 (s, 2H), 4.26 (s, 2H), 3.86-3.84 (m, 2H), 3.73-3.72 (m, 2H), 3.34-3.33 (m, 6H), 2.51 (t, 2H), 1.98 (s, 3H); ^{31}P NMR, CDCl3, δ (ppm): -0.75; ^{13}C NMR, CDCl3, δ (ppm): 167.89, 167.53, 146.14, 146.10, 145.87, 136.99, 136.95, 136.93, 130.95, 130.71,

130.51, 128.99, 128.88, 128.02, 127.93, 127.86, 127.79, 127.47, 127.38, 127.32, 67.85, 66.83, 66.77, 66.72, 66.00, 65.98, 65.92, 65.48, 65.43, 65.27, 65.23, 65.02, 60.27, 60.23, 60.06, 59.30, 59.17, 57.27, 54.49, 54.46, 54.42, 47.71, 44.05, 34.11, 34.05, 18.4, 9.21; ESI: m/z 606.20 (Na+, 40%), 584.22 (H+, 11%)

*Trityl-protected CP thiol methacrylate **3c** and **3d***

Freshly distilled DCM (30 mL) was added to vacuum-dried **1a** (5.5 g, 14.9 mmol) (or **1b**). The solution was brought to -20°C using a MeOH/water bath, at which point the distilled TEA (2.2 mL, 15.7 mmol, 1.05 eq) was added. ECP (1.6 g, 11.6 mmol, 0.95 eq), purified before use *via* Kugelrohr distillation, was then added dropwise to the **1a** (or **1b**) solution. Over time, white solids precipitated out of solution. The solution was held at -20°C for an additional hour before being filtered under nitrogen through oven-dried celite and concentrated under vacuum to give **2a** (4.1 g, 74%) or **2b** (6.4 g, 87%). Dry ACN (40 mL) and vinylbenzyl dimethylamine (1.2 mL, 9.1 mmol, 1.1 eq) were then added to **2a** (or **2b**), along with inhibitor MEHQ (10 mg, 0.1 mmol), to give a final solution concentration of 0.3 M. The solution was placed at 70°C and allowed to react for 16 hours before being precipitated under nitrogen in cold diethyl ether. The solution was placed in a -80°C freezer overnight to further encourage precipitation. The white solids were collected *via* vacuum filtration and dried to give **3c** (0.6 g, 12%) and **3d** (0.7 g, 8%). **3c.** ^{1}H NMR (500 MHz), MeOD, δ (ppm): 7.59-7.48 (dd, 4H), 7.37 – 7.16 (m, 15H), 6.90-6.88 (m, 4H), 6.84-6.77 (dd, 1H), 5.93-5.89 (d, 1H), 5.39-5.36 (d, 1H), 4.53 (s, 2H), 4.35-4.34 (m, 2H), 3.60-3.57 (m, 2H), 3.05 (s, 6H); ^{31}P NMR, MeOD, δ (ppm): -6.11. ESI: m/z 658.21 (Na+, 28%), 636.23 (H+, 15%). **3d.** ^{1}H NMR (500 MHz), CDCl3, δ (ppm): 7.42-7.23 (m, 15H), 6.16 (s, 1H), 5.71 (s, 1H), 4.62 (s, 2H), 4.26 (s, 2H), 3.86-3.84 (m, 2H), 3.73-3.72 (m, 2H), 3.34-

3.33 (m, 6H), 2.51 (t, 2H), 1.98 (s, 3H); ^{31}P NMR, CDCl3, δ (ppm): -0.75; ESI: m/z 610.21 (Na+, H+, 12%), 588.23 (H+, 13%)

6.4 RAFT Copolymerization of CP Zwitterion Monomers

*Embedded thiol CP methacrylate copolymers **4a** and **4b***

In a typical procedure to achieve 20 mol% CP methacrylate content, MPC (1.51 g, 5.12 mmol) and **3a** (0.82 mg, 1.29 mmol) (or **3b**) were mixed together in methanol (0.6 M) with appropriate amounts of PCTA (53.7 mg, 192 μmol) and ACVA (16.8 mg, 60.0 μmol) to target a final copolymer molecular weight of 12 kDa. The solution was degassed three hours over ice before undergoing three cycles of freeze-pump-thaw. The solution was placed at 70°C for ~36 hours, at hich point conversion reached >90%. The crude polymer was precipitated in diethyl ether and dialyzed against water (3.5 kDa MWCO) for three days before lyophilization to yield pink solids **4a** (1.69 g, 73%) or **4b** (140 mg, 37%). **4a.** ^{1}H NMR (500 MHz), MeOD, δ (ppm): 7.38-7.22 (br m, -C(C_6H_5)$_3$; 6.93 (br s, -C_6H_4-), 4.48 (br s, -COOCH_2CH$_2$-, CP), 4.31 (br s, -COOCH_2CH$_2$-, PC; -CH$_2$CH_2OPO$_3$-, CP); 4.22 (br s, -COOCH$_2$CH_2, PC); 4.08 (br s, -OPO$_3$CH_2CH$_2$-, PC), 3.86-3.71 (br m, -CH_2CH$_2$OPO$_3$-, -COOCH$_2$CH_2-, CP), 3.57 (br s, -OPO$_3$CH$_2$CH_2-, PC), 3.27 (br s, -N(CH_3)$_2$-, CP; -N(CH_3)$_3$, PC), 1.96-1.83 (br m, -CH_2C(CH$_3$)-, PC and CP), 1.49-0.95 (br m, -CH$_2$C(CH_3)-, PC and CP); ^{31}P NMR, MeOD, δ (ppm): -0.50 (PC), -6.15 (CP). **4b.** ^{1}H NMR (500 MHz), MeOD, δ (ppm): 7.61-7.22 (br m, -C(C_6H_5)$_3$; 4.51 (br s, -COOCH_2CH$_2$-, CP), 4.34-4.25 (br m, -COOCH_2CH_2-, PC; -CH$_2$CH_2OPO$_3$-, CP); 4.10 (br s, -OPO$_3$CH_2CH$_2$-, PC), 3.90 (br s, -COOCH$_2$CH_2-, CP), 3.82 (br s, -CH_2CH$_2$OPO$_3$-, CP), 3.75 (br s, -OPO$_3$CH$_2$CH_2-, PC; -CH_2CH$_2$S-, CP), 3.30 (br s, -N(CH_3)$_2$-, CP; -N(CH_3)$_3$,

PC), 2.52 (br s, -CH_2CH_2S-), 2.04-1.85 (br m, -$CH_2C(CH_3)$-, PC and CP), 1.62-0.97 (br m, -$CH_2C(CH_3)$-, PC and CP); ^{31}P NMR, MeOD, δ (ppm): -0.51 (PC), -0.84 (CP)

*Embedded thiol CP styrene copolymers **4c** and **4d***

In a typical procedure to achieve 20 mol% CP methacrylate content, MPC (300 mg, 1.01 mmol) and **3c** (80 mg, 127 µmol) (or **3d**) were mixed together in methanol (0.5 M) with appropriate amounts of PCTA (9.0 mg, 32 µmol) and ACVA (3.0 mg, 11 µmol) to target a final copolymer molecular weight of 10 kDa. The solution was degassed three hours over ice before being placed at 70°C for ~24 hours, at which point conversion reached >90%. The crude polymer was precipitated in diethyl ether and dialyzed against water (3.5 kDa MWCO) for one days before lyophilization to yield pink solids **4c** (106 mg, 45%) or **4d** (130 mg, 57%). **4c.** ^{1}H NMR (500 MHz), MeOD, δ (ppm): 7.37-7.20 (br m, -$C(C_6H_5)_3$, -C_6H_4-, CP), 6.92-6.90 (br m, -OC_6H_4S-, CP), 4.54 (br s, -$CH_2N(CH_3)_2$-, CP), 4.31 (br s, -$COOCH_2CH_2$-, PC; -$N(CH_3)_2CH_2CH_2OPO_3$-, CP), 4.22 (br s, -$COOCH_2CH_2$, PC), 4.08 (br s, -$OPO_3CH_2CH_2$-, PC), 3.70-3.67 (br m, -$OPO_3CH_2CH_2$-, PC), 3.59 (br s, -$N(CH_3)_2CH_2CH_2OPO_3$-, CP), 3.26 (br s, -$N(CH_3)_3$, PC), 3.05 (br s, $N(CH_3)_2$-, CP), 1.95-1.87 (br m, -$CH_2C(CH_3)$-, PC; -CH_2CH-, CP), 1.29-0.90 (br m, -$CH_2C(CH_3)$-, PC); ^{31}P NMR, MeOD, δ (ppm): -0.49 (PC), -6.20 (CP). **4d.** ^{1}H NMR (500 MHz), MeOD, δ (ppm): 7.39-7.20 (br m, -$C(C_6H_5)_3$, -C_6H_4-, CP), 4.58 (br s, -$CH_2N(CH_3)_2$-, CP), 4.31 (br s, -$COOCH_2CH_2$-, PC; -$N(CH_3)_2CH_2CH_2OPO_3$-, CP), 4.23 (br s, -$COOCH_2CH_2$, PC), 4.08 (br s, -$OPO_3CH_2CH_2$-, PC), 3.75 (br s, -$OPO_3CH_2CH_2$-, CP), 3.70-3.67 (br m, -$OPO_3CH_2CH_2$-, PC), 3.59 (br s, -$N(CH_3)_2CH_2CH_2OPO_3$-, CP), 3.27 (br s, -$N(CH_3)_3$, PC), 3.08 (br s, $N(CH_3)_2$-, CP), 2.50 (br s, -$OPO_3CH_2CH_2$-, CP), 1.97-1.88 (br m, -$CH_2C(CH_3)$-, PC; -

C*H*$_2$C*H*-, CP), 1.12-0.94 (br m, -CH$_2$C(C*H*$_3$)-, PC); ^{31}P NMR, MeOD, δ (ppm): -0.46 (PC), -0.79 (CP)

*Deprotection CP zwitterion copolymers **4a-4d***

Trifluoroacetic acid (10 mL, 57 mmol) was added to **4a** (1.0 g, 53 μmol) (or **4b-d**) copolymers along with triisopropylsilane (280 uL, 2.6 mmol) and water (200 uL, 2.2 mmol). After 1 hour, the solutions were concentrated and the crude polymers were precipitated into diethyl ether, which was subsequently dissolved in an aqueous solution containing TCEP (< 100 μM) and dialyzed (3.5 kDa MWCO) against degassed DI water. The polymer solutions were then lyophilized to yield white solids **5a** (0.66 g, 67%), **5b** (0.32 mg, 72%), **5c** (63 mg, 66%) or **5d** (78 mg, 65%), and the free thiol content in each copolymer was quantified using Ellman's Assay. **5a.** ^{1}H NMR (500 MHz), MeOD, δ (ppm): 7.71-7.08 (br m, -C$_6$*H*$_4$-), 4.49-4.43 (br m, -COOC*H*$_2$CH$_2$-, -CH$_2$C*H*$_2$OPO$_3$-, CP), 4.32 (br s, -COOC*H*$_2$CH$_2$-, PC); 4.32 (br s, -COOCH$_2$C*H*$_2$, PC); 4.23 (br s, -OPO$_3$C*H*$_2$CH$_2$-, PC), 3.88 (br s, -C*H*$_2$CH$_2$OPO$_3$-, -COOCH$_2$C*H*$_2$-, CP), 3.72 (br s, -OPO$_3$CH$_2$C*H*$_2$-, PC), 3.28 (br s, -N(C*H*$_3$)$_2$-, CP; -N(C*H*$_3$)$_3$, PC), 1.96-1.90 (br m, -C*H*$_2$C(CH$_3$)-, PC and CP), 1.66-0.94 (br m, -CH$_2$C(C*H*$_3$)-, PC and CP); ^{31}P NMR, MeOD, δ (ppm): -0.52 (PC), -5.69 (CP-SH), -5.98 (CP-S-S-CP). **5b.** ^{1}H NMR (500 MHz), MeOD, δ (ppm): 4.55 (br s, -COOC*H*$_2$CH$_2$-, CP), 4.33-4.24 (br m, -COOC*H*$_2$C*H*$_2$-, PC; -CH$_2$C*H*$_2$OPO$_3$-, CP), 4.09 (br s, -OPO$_3$C*H*$_2$CH$_2$-, PC), 3.93 (br s, -COOCH$_2$C*H*$_2$-, CP), 3.85 (br s, -C*H*$_2$CH$_2$OPO$_3$-, CP), 3.74 (br s, -OPO$_3$CH$_2$C*H*$_2$-, PC; -C*H*$_2$CH$_2$S-, CP), 3.40 (br s, -CH$_2$C*H*$_2$S-), 3.30 (br s, -N(C*H*$_3$)$_2$-, CP; -N(C*H*$_3$)$_3$, PC), 1.97-1.89 (br m, -C*H*$_2$C(CH$_3$)-, PC and CP), 1.58-0.96 (br m, -CH$_2$C(C*H*$_3$)-, PC and CP); ^{31}P NMR, MeOD, δ (ppm): -0.45 (PC), 0.07 (CP). **5c.** ^{1}H NMR (500 MHz), MeOD, δ (ppm): 7.57-7.08 (br

m, -C_6H_4-, -OC_6H_4S-, CP), 4.57 (br s, -$CH_2N(CH_3)_2$-, CP), 4.51 (br s, -$COOCH_2CH_2$-, -$COOCH_2CH_2$, PC; -$N(CH_3)_2CH_2CH_2OPO_3$-, CP), 4.26 (br s, -$OPO_3CH_2CH_2$-, PC), 3.82-3.81 (br m, -$OPO_3CH_2CH_2$-, PC), 3.72-3.68 (br m, -$N(CH_3)_2CH_2CH_2OPO_3$-, CP), 3.31 (br s, -$N(CH_3)_3$, PC), 3.13 (br s, $N(CH_3)_2$-, CP), 2.01-1.92 (br m, -$CH_2C(CH_3)$-, PC; -CH_2CH-, CP), 1.29-0.94 (br m, -$CH_2C(CH_3)$-, PC); ^{31}P NMR, MeOD, δ (ppm): -1.99 (PC), -6.79 (CP). **5d.** ^{1}H NMR (500 MHz), MeOD, δ (ppm): 7.56-7.27 (br m, -C_6H_4-, CP), 4.71 (br s, -$CH_2N(CH_3)_2$-, CP), 4.53 (br s, -$COOCH_2CH_2$, -$COOCH_2CH_2$-, PC; -$N(CH_3)_2CH_2CH_2OPO_3$-, CP), 4.27-4.05 (br s, -$OPO_3CH_2CH_2$-, CP; -$OPO_3CH_2CH_2$-, PC), 3.85 (br s, -$OPO_3CH_2CH_2$-, PC), 3.76 (br s, -$N(CH_3)_2CH_2CH_2OPO_3$-, CP), 3.34 (br s, -$N(CH_3)_3$, PC), 3.17 (br s, $N(CH_3)_2$-, -$OPO_3CH_2CH_2$-, CP), 2.02-1.92 (br m, -$CH_2C(CH_3)$-, PC; -CH_2CH-, CP), 1.12-0.96 (br m, -$CH_2C(CH_3)$-, PC); ^{31}P NMR, MeOD, δ (ppm): -2.03 (PC), -1.30 (CP)

6.5 RAFT Homopolymerization of CP Zwitterion Monomers

*Homopolymerization of **3a***

In a typical procedure, CP methacrylate **3a** (300 mg, 475 µmol) was dissolved in methanol (0.5 M) along with YCTA (12.3 mg, 30.5 µmol) and ACVA initiator (3.3 mg, 12 µmol). The solution was purged under nitrogen before being heated at 70°C for ~24 hours at which point a viscous orange oil precipitated out of solution. The crude polymer oil was redissolved in DMSO and precipitated from diethyl ether. The crude polymer was further purified by dialysis (1 kDa MWCO) against 50:50 DMSO: MeOH solution (8 hrs, 2x) followed by 50:50 H_2O: MeOH solution (8 hrs, 2X) to remove residual monomer. To precipitate the polymer and remove MeOH, the polymer solution was dialyzed against H_2O

(8 hrs, 3X). After lyophilization, a yellow-orange solid powder was obtained (170 mg, 60%). ^{1}H NMR (500 MHz), DMSO-*d6*, δ (ppm): 7.31-7.22 (br m, -C(C_6H_5)$_3$), 6.82 (br s, -$C_6H_2H_2$-), 6.75-6.73 (br m, -$C_6H_2H_2$-), 4.48 (br s, -COOCH_2CH_2-), 4.06 (br s, -$CH_2CH_2OPO_3$-), 3.81-3.74 (br m, -$COOCH_2CH_2$-), 3.63 (br s, -$OPO_3CH_2CH_2$-), 3.16-3.12 (br m, -N(CH_3)$_2$-), 1.91-1.73 (br m, -CH_2C(CH_3)-), 1.34-0.85 (br m, -CH_2C(CH_3)-); ^{31}P NMR, DMSO-*d6*, δ (ppm): -6.32.

6.6 PZT Post-Polymerization Thiol Functionalization

*Vinyl-sulfone functionalization of CP methacrylate thiol copolymers **5a** and **5b***

Following procedure reported in literature,[4] copolymer **5a** or **5b** (50 mg) was dissolved in 0.5 mL of a 0.1 PBS solution (pH = 7.0, 10 mM TCEP, and 10 mM EDTA). The aqueous polymer solution was then titrated into a divinyl sulfone (DVS) solution in 0.5 mL methanol with enough DVS to achieve 20-30 eq. per pendent copolymer thiol, which was determined from DP as calculated by 1H NMR end group analysis. After 3 hours, the solution was purified using centrifugal dialysis (1 kDa MWCO, 8000 rpm, 5 min) three times before being lyophilized to yield white solids **6a** (33 mg, 88%) or **6b** (30 mg, 70%). Aliphatic **6b-20** copolymers achieved ~1 mol% incorporation of VS functionality onto the pendent thiols of **5b-20 PZTs**, which corresponds to the quantity of free thiol available for reaction (1-2 mol% SH groups, **Table S7**) despite added TCEP. However, aromatic **6a-20** copolymers achieved 5-7 mol% VS modification despite having 13-15 mol% SH groups (**Table S7**) available for reaction. **6a.** ^{1}H NMR (500 MHz), MeOD, δ (ppm): 7.57-7.29 (br m, -C_6H_4-), 6.95 (br s, -SO_2CH=C$H_a$$H_b$), 6.42-6.39 (br d, -$SO_2CH$=$CH_aH_b$), 6.32 (br s, -$SO_2CH$=$CH_aH_b$), 4.47 (br s -COO$CH_2CH_2$-, -$CH_2CH_2OPO_3$-, CP), 4.34 (br s, -

COOC*H*$_2$CH$_2$-, PC); 4.25 (br s, -COOCH$_2$C*H*$_2$, PC); 4.10 (br s, -OPO$_3$C*H*$_2$CH$_2$-, PC), 3.90 (br s, -C*H*$_2$CH$_2$OPO$_3$-, -COOCH$_2$C*H*$_2$-, CP), 3.75 (br s, -OPO$_3$CH$_2$C*H*$_2$-, PC), 3.31 (br s, -N(C*H*$_3$)$_2$-, -S(C*H*$_2$)$_2$-, CP; -N(C*H*$_3$)$_3$, PC), 1.98-1.92 (br m, -C*H*$_2$C(CH$_3$)-, PC and CP), 1.68-0.97 (br m, -CH$_2$C(C*H*$_3$)-, PC and CP); ^{31}P NMR, MeOD, δ (ppm): -0.56 (PC), -6.00 (CP), -6.56 (CP). **6b.** ^{1}H NMR (500 MHz), D$_2$O, δ (ppm): 4.56 (br s, -COOC*H*$_2$CH$_2$-, CP), 4.33 (br m, -COOC*H*$_2$CH$_2$-, PC), 4.26 (br m, -COOCH$_2$C*H*$_2$-, PC; -CH$_2$C*H*$_2$OPO$_3$-, CP); 4.12 (br s, -OPO$_3$C*H*$_2$CH$_2$-, PC), 3.91 (br s, -COOCH$_2$C*H*$_2$-, CP), 3.85 (br s, -C*H*$_2$CH$_2$OPO$_3$-, CP), 3.71 (br s, -OPO$_3$CH$_2$C*H*$_2$-, PC; -C*H*$_2$CH$_2$S-, CP), 3.31 (br s, -CH$_2$C*H*$_2$SC*H*$_2$C*H*$_2$SO3-; CP), 3.26 (br s, -N(C*H*$_3$)$_2$-, CP; -N(C*H*$_3$)$_3$, PC), 2.00-1.84 (br m, -C*H*$_2$C(CH$_3$)-, PC and CP), 1.69-0.94 (br m, -CH$_2$C(C*H*$_3$)-, PC and CP); ^{31}P NMR, D$_2$O, δ (ppm): -0.53 (PC), 2.37 (CP)

*Modification of CP methacrylate thiol copolymers **5a*** and **5*b*** *with dipyridyl disulfide*

The **5a-20** or **5b-20** copolymers (~70 mg) were dissolved in methanol and 0.1 M PBS buffer (pH 8) at a concentration of 5 mM. Enough dipyridyl disulfide was added to obtain 2-70 eq. per pendent copolymer thiol, which was determined from DP as calculated by 1H NMR end group analysis. For solutions containing **5a-20** copolymers, 1 eq. of TCEP was added. After 4-16 hrs, the solution was purified *via* centrifugal dialysis (1 kDa MWCO) against water for 12 hours followed by a 50:50 water: methanol solution for 12 hours. To remove organic solvent, the polymer solution was further dialyzed against water twice for 12 hours each. The polymer solutions were lyophilized to give a white solids **7a-20** (22 mg, ~70%) and **7b-20** (75 mg, >100%), with full integration of pyridyl functionality onto the CP thiol pendant groups by 1H NMR end group analysis. **7a-20.** ^{1}H NMR (500 MHz), MeOD, δ (ppm): 8.45 (br s, -N=C*H*CH-, CP), 7.82 (br s, -SC=C*H*C*H*-, CP), 7.56-7.25 (br

m, -N=CHC*H*-, -C_6H_4-, CP), 4.42 (br m, -COOC$H_2$$CH_2$-, -$CH_2CH_2$$OPO_3$-, CP), 4.32 (br s, -COOC$H_2$$CH_2$-, PC), 4.22 (br s, -COO$CH_2CH_2$, PC); 4.08 (br s, -$OPO_3CH_2$$CH_2$-, PC), 3.87 (br s, -C$H_2$$CH_2$$OPO_3$-, -COO$CH_2CH_2$-, CP), 3.72 (br s, -$OPO_3$$CH_2CH_2$-, PC), 3.28 (br s, -N(C$H_3$)$_2$-, CP; -N(C$H_3$)$_3$, PC), 1.96-1.90 (br m, -CH_2C(CH_3)-, PC and CP), 1.66-0.94 (br m, -CH_2C(CH_3)-, PC and CP); ^{31}P NMR, MeOD, δ (ppm): -0.54 (PC), -5.97 (CP). **7b-20.** ^{1}H NMR (500 MHz), MeOD, δ (ppm): 8.43-8.42 (m, -N=C*H*CH-, CP), 7.78-7.75 (m, -N=CHC*H*-, CP), 7.69-7.67 (m, -SC=C*H*CH-, CP), 7.26-7.23(m, -SC=CHC*H*-, CP), 4.54 (br s -COOC$H_2$$CH_2$-, CP), 4.33-4.23 (br m, -COOCH_2CH_2-, PC; -CH_2C$H_2$$OPO_3$-, CP), 4.09 (br s, -$OPO_3CH_2$$CH_2$-, PC), 3.94 (br s, -COO$CH_2CH_2$-, CP), 3.85 (br s, -C$H_2$$CH_2$$OPO_3$-, CP), 3.74 (br s, -$OPO_3$$CH_2CH_2$-, PC; -$OPO_3$-C$H_2$$CH_2$-, CP), 3.40-3.37 (br s, -OPO_3-CH_2CH_2-, CP), 3.32- 3.30 (br s, -N(CH_3)$_2$-, CP; -N(CH_3)$_3$, PC), 1.96-1.88 (br m, -CH_2C(CH_3)-, PC and CP), 1.56-0.95 (br m, -CH_2C(CH_3)-, PC and CP); ^{31}P NMR, MeOD, δ (ppm): 0.08 (CP), -0.46 (PC).

6.7 Synthesis of Thiol-terminated Poly(MPC)

In a typical procedure, MPC (2.1 g, 7.1 mmol) was dissolved in a methanol (0.5 M) solution containing ACVA initiator (39 mg, 140 umol) and PCTA (100 mg, 370 umol) to target a molecular weight of ~6 kDa. The solution was subjected to three cycles of freeze-pump-thaw before being placed in a pre-heated 70^{o}C for 48 hours. The crude polymer was precipitated in diethyl ether and then dissolved in DI water for purification using dialysis (1 kDa MWCO, 24 hrs, 3x). The polymer solution was lyophilized to yield PMPC as a pink solid (~2 g, 95%). To create thiol-terminated PMPC, *n*-butyl amine (160 uL, 1.6 mmol) was added to aqueous solution (0.1 M PBS, pH 7, 1 mM EDTA, 1 mM TCEP)

containing PMPC (600 mg, 40 umol). After 16 hours, the crude solution was dialyzed against water (1 kDa MWCO, 24 hrs, 3x). The polymer solution was lyophilized to give a white solid (250 mg, 42%). 1H NMR (500 MHz), MeOD, δ (ppm): 4.34 (br s, -COOC*H*$_2$CH$_2$-); 4.23 (br s, -COOCH$_2$C*H*$_2$-); 4.08 (br s, -OPO$_3$C*H*$_2$CH$_2$-), 3.75 (br s, -OPO$_3$CH$_2$C*H*$_2$-), 3.32-3.27 (br s, -N(C*H*$_3$)$_3$-), 2.92- 1.70 (br m, -C*H*$_2$C(CH$_3$)-), 1.63- 0.95 (br m, -CH$_2$C(C*H*$_3$)-); ^{31}P NMR, MeOD, δ (ppm): -0.58.

6.8 Ellman's Assay

In order to quantify the amount of free sulfhydryl in **5a**-**5d PZTs**, thiol-terminated poly(MPC), and native or reduced protein, separate calibration curves were created for each type of thiol: cysteine, mercaptoethanol, and mercaptophenol. For this, enough thiol-containing substrate was added to 20 mL of 0.1 M PBS buffer (pH 8.0) to create a 1.5 mM stock solution. This solution was serially diluted to give solutions of known concentration (0.2-1.2 mM), of which 150 or 250 µL was added to 2.8 or 2.7 mL of 0.1 M PBS buffer (pH 8.0), respectively, to give final thiol concentrations between 10 and 140 µM. Then, 50 µL of 4 mg/ mL of Ellman's reagent (DNTB) in 0.1 M PBS pH 8.0 was added to each of these solutions. After incubating the thiol with DNTB for 15 minutes, the solutions were placed in an UV-Vis spectrophotometer to measure the absorbance at 412 nm, from which a calibration curve was created. A similar procedure was effected to determine the amount of free sulfhydryl in reduced protein, **5a**-**5d** type copolymers, and thiol-terminated poly(MPC). Briefly, a known mass (mg) of protein or polymer was dissolved in 3 mL of 0.1 M PBS buffer (pH 8.0). The absorbance at 412 nm was recorded after 15 minutes and the calibration curves was utilized to determine the amount of free thiol present, which was

then divided by the concentration of protein (or polymer) to give the number of free thiols per protein (or polymer chain). In the case of polymer samples, the number of free thiols per polymer chain was compared against the total number of monomer units containing thiol, calculated in terms of degree of polymerization, which was typically determined using molecular weights from ^{1}H NMR end group analysis.

6.9 Pendant Drop Tensiometry

A 0.5 mg/mL polymer solution was created in pre-filtered HPLC grade water (PES 0.22 microns). Trichlorobenzene (TCB) was likewise filtered (PPTFE 0.22 microns) and loaded into a syringe equipped with an 18 gauge blunt tip needle (1.27 mm), which was utilized to create the pendant drop. The interfacial tension of the trichlorobenzene pendant drop in the polymer solution was measured using a Data Physics model OCA-15 plus tensiometer and the software extracted out interfacial energy (γ) using a Young-Laplace equation.

6.10 Oil-in-Water Emulsion Formation

Aliquots of stock polymer solution (20 mg/mL) created in DI water were diluted to a volume of 500 µL to create solutions at various concentrations (0.5, 1.0, 5.0, and 10 mg/mL). 500 µL of TCB was then added to 500 µL of each copolymer solution and vortexed for one minute to create an emulsion. Optical images of the emulsions were taken using a Cannon EOS 6D Mark II camera to monitor the stability of the emulsion over time.

6.11 Hydrogels

Thiol-Michael Crosslinking

In a typical procedure for photoinitiated thiol-Michael addition, 10 μL of a **5a** copolymer solution (1 mg/uL) was added to a 100 μL sylgard mold. To this solution was added 9 μL of VA-044 (0.25 mg/uL), 14 μL of DI water and 7 μL of PEG700 diacrylate solution (1 mg/uL) to achieve a 20 wt% of **5a** copolymer and a crosslinker:polymer thiol ratio of 2:1, which was calculated based on the theoretical amount of free thiol in **5a** copolymers. All solutions were made using degassed DI water. The final solution was degassed an additional 30 minutes in a nitrogen glove bag before being exposed to 365 nm UV light for 5 minutes. A similar procedure was followed for base-catalyzed thiol-Michael addition, utilizing various bases such as triethylamine (25 wt%) instead of photoinitiator, though with limited success.

Disulfide Crosslinking

In a procedure similar to hydrogels formed *via* UV photocrosslinking, 10 μL of a **5a** copolymer solution (1 mg/uL) was added to a 100 μL sylgard mold. To this solution was added 9 μL of 0.1 M PBS buffer (pH 8, 1 mM EDTA) and 7.6 μL of PEG1000 dithiol solution (1 mg/μL in 0.1 M PBS buffer, pH 8, 1 mM EDTA) to achieve 20 wt% **5a** copolymer and a crosslinker:polymer thiol ratio 3:1, which was calculated based on the theoretical amount of free thiol in **5a** copolymers. Then 5 μL of hydrogen peroxide (50 wt% in water) was added.

Swelling Ratio

The **5a** copolymer hydrogels were swelled in water over the course of three days, replenishing the solution with fresh water every 24 hrs, to obtain its swollen mass. The

hydrogels were then lyophilized to obtain the dry mass of the hydrogel. The swelling ratio (%) of the hydrogels was then calculated by subtracting the dry mass of the hydrogel from its swollen mass, dividing by its dry mass, and multiplying by 100.

6.12 Polymer-Protein Bioconjugation

Reduced Protein

Oxidized cysteine residues were reduced to liberate free thiol in BSA and CAT, as adapted from a reported literature procedure.[5] The proteins were treated with 3-10 mM TCEP in 0.1 M PBS 7.0 (10 mM EDTA) for 4 hours and were extensively dialyzed against water (3.5-25 kMWCO, 24 h, 3 days) before being lyophilized to yield reduced enzyme in 70-100% yield. The number of thiols liberated were quantified using Ellman's Assay to give 14 thiols/protein (BSA-SH) and 16 thiols/enzyme (CAT-SH).

*Disulfide Bioconjugation with **5a** and **5b***

Adapted from a reported literature procedure,[5] a 10 mg/ mL protein (native BSA, HRP, and LYS) solution was created in 0.1 M PBS buffer pH 7.4 (0.14 M NaCl and 2.7 mM KCl) and diluted to 1X in 0.1 M PBS buffer pH 7.4 (0.14 M NaCl and 2.7 mM KCl), 8.0 (1 mM EDTA), or 9.2 (1 mM EDTA). Alternatively, a 10 mg/mL protein solution was created using reduced protein (BSA-SH or CAT-SH). Then, 8-10 µL of protein solution was added to 0.5-1.0 µL of 1 mg/ mL of **5a-20** or (**5b-20**, **5c-20**, or **5d-20**) copolymer solution in PBS buffer (pH 7.4), in addition to 1 µL of DMSO and 10 µL buffer solution. The final concentration of enzyme and polymer was ~50-350 µM and ~0.9-2.0 mM, respectively, or about ~40-1800 eq. of polymer thiol to protein, which was estimated from Ellman's assay based on the amount of free thiol in the **5a-5d PZTs.** After 5-24 hours,

SDS-PAGE was conducted under non-reducing conditions. The reaction solutions corresponding to lanes that demonstrated high molecular weight streaking were purified *via* centrifugal dialysis (50 kDa MWCO, 8000 rpm, 8 min, 4X) against 0.1 M PBS buffer pH 7.4 (0.14 M NaCl and 2.7 mM KCl) to isolate out the polymer-protein bioconjugates. The supernatant (10-40 µL) was diluted to 400 µL before being filtered (PES 0.45 µm) and loaded onto the FPLC.

*Vinyl Sulfone Bioconjugation with **6a** and **6b***

Adapted from a reported procedure,[4] a 10X BSA solution was created by dissolving BSA (10 mg, 150 nmol) in a 0.1 M PBS solution (pH = 6.0, 10 mM EDTA, 10 mM TCEP). 5 µL of this solution was then added to 45 µL of one of five different buffer solutions containing 1 mM TCEP and 1 mM EDTA: (**a**) 0.15 M Phosphate Buffered Saline (pH 9.2); (**b**) Certipur Borate Buffer (pH 9.2); (**c**) 0.1 M Sodium Bicarbonate Buffer (pH 9); (**d**) 0.15 M HEPES buffer (pH 9.2); (**e**) 0.15 M Tris Buffer (pH 9.2). The BSA solutions were allowed to incubate for 1-2 hours. In the meantime, vinyl-sulfone functionalized **6a** (or **6b**) copolymers were dissolved in 20 µL DI water to obtain a concentration of 1 mg/µL. 1 µL of the **5a** (or **5b**) copolymer solution (100-3000 eq. of vinyl sulfone with respect to enzyme, calculated according to mol% VS in the final copolymer) was then added to 10 µL of each of the BSA solutions, in addition to 1 µL DMSO and an additional 10 µL buffer solution to give a total reaction volume of 22 µL. Two control solutions were similarly prepared, one without enzyme and one without copolymer. After ~24 hours, 5 µL of each solution was mixed with 5 µL of 2X Laemmli sample buffer and 0.5 µL of β-mercaptoethanol before denaturing the enzyme at 70^{o}C for 15 minutes. The solutions were analyzed using SDS-PAGE under reducing conditions and imaged at 685/710-730 nm

(excitation/emission) on the LI-COR Odyssey CLx. A similar procedure was used for GOX, HRP and LYS.

6.13 References

1. Zhao, J.; Pan, Z.; Snyder, D.; Stone, H. A.; Emrick, T. Chemically Triggered Coalescence and Reactivity of Droplet Fibers. *J. Am. Chem. Soc.* **2021**, *143* (14), 5558–5564.

2. Tai, C.-H.; Wu, H.-C.; Li, W.-R. Studies on a Novel Safety-Catch Linker Cleaved by Pummerer Rearrangement[1]. *Org. Lett.* **2004**, *6* (17), 2905–2908.

3. Dong, H.; Li, J.; Liu, H.; Lu, S.; Wu, J.; Zhang, Y.; Yin, Y.; Zhao, Y.; Wu, C. Design and Ribosomal Incorporation of Noncanonical Disulfide-Directing Motifs for the Development of Multicyclic Peptide Libraries. *J. Am. Chem. Soc.* **2022**, *144* (11), 5116–5125.

4. Grover, G. N.; Alconcel, S. N. S.; Matsumoto, N. M.; Maynard, H. D. Trapping of Thiol-Terminated Acrylate Polymers with Divinyl Sulfone to Generate Well-Defined Semitelechelic Michael Acceptor Polymers. *Macromolecules* **2009**, *42* (20), 7657–7663.

5. Heredia, K. L.; Bontempo, D.; Ly, T.; Byers, J. T.; Halstenberg, S.; Maynard, H. D. In Situ Preparation of Protein−"Smart" Polymer Conjugates with Retention of Bioactivity. *JACS* **2005**, *127* (48), 16955–16960.

APPENDIX A:
TYROSINASE-MEDIATED OXIDATIVE-ADDITION FOR POLYMER-PROTEIN BIOCONJUGATION

There are multiple bioconjugation strategies to tether biologics/therapeutics to polymers, as was previously highlighted in **Chapter 4**, with maleimide, click and NHS-ester chemistries being most commonly used.[1-10] Departing from these conventional bioconjugation strategies, the recent findings of Francis and coworkers highlight the power of enzyme-induced coupling methods, specifically the utility of tyrosine residues or more generally phenolic groups, in conjunction with tyrosinase enzyme to selectively tag and couple peptides and proteins to suitable reactive partners. These conjugation strategies are proving effective with different partner components, for example: 1) an *ortho*-phenolic moiety, such as catechol or tyrosine, and 2) a nucleophile, such as aniline or the terminal amine of a protein.[11-13] More specifically, in tyrosinase-mediated oxidative addition, the phenolic groups are oxidized to an *o*-quinoid intermediate by tyrosinase (from the *Agaricus bisporus* mushroom), to which the nucleophile is covalently added to ligate the two coupling partners together (**Figure A-1**). By conventional oxidation (*e.g.*, with sodium periodate[13]), *o*-quinoid formation accelerates ligation with nucleophiles on the target

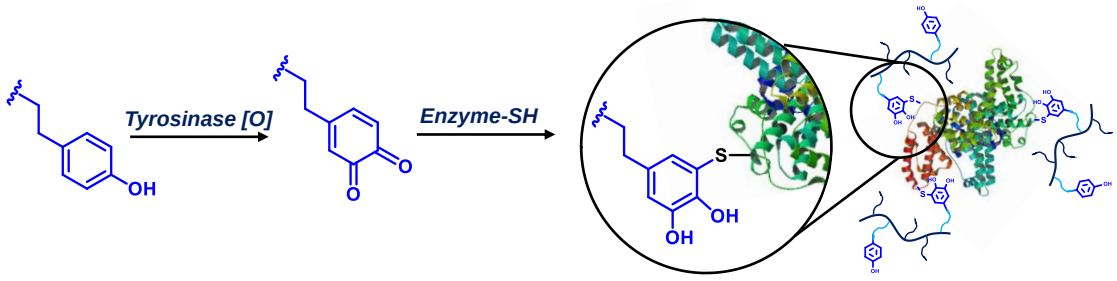

Figure A-1. Overview of tyrosinase-mediated conjugation *via* oxidative-addition, specifically between a phenol-containing polymer coupling partner and the free thiols of protein.

substrate (i.e., peptide or protein). However, enzyme-induced coupling using tyrosinase enhances site-selectivity of the conjugation and precludes the need for chemical purification, such as removal of salts or other by-products.[11,14-17] In addition to oxidizing tyrosine residues of proteins, tyrosinase works well with phenolic components of organic and peptidic structures[11,17] and successfully conjugates thiols, for the substituted catechol as the coupled product.[14] In one example, efficient tyrosinase-mediated oxidative coupling was accomplished on solvent-exposed tyrosine residues (e.g., on α-endorphin) with MS2 viral capsid proteins *via* para-aminophenylalanine groups of the capsids.[18] In another example, site-selective coupling through activation of terminal tyrosine sites using recombinantly expressed tyrosinase produced multiprotein complexes.[11] This conjugation methodology is proving versatile across biological and materials landscapes by granting access to tyrosine-cysteine bond formation,[14] nanobody-cell conjugation,[19] and activation of phenol-functionalized metal NPs.[12] Overall, the site-selectivity and catalytic action of this enzymatic coupling methodology coupled with minimal purification steps is timely for bioconjugation with functional polymers containing either phenolic or thiol moieties; to our knowledge, there is only one reported case using PEG thiol and recombinant GFP protein.[20]

Our strategies in polymer-protein bioconjugation build from these pioneering reports on the versatility of this oxidative coupling methodology,[12-13,15-17] exemplified in surface functionalization of viral capsids with targeting ligands,[15] DNA modification of metal nanoparticles,[12] and protein-labeling with fluorophores.[21] In **Appendix A**, we share preliminary attempts and results exploring the use of tyrosinase in catalyzing polymer-protein bioconjugation, as shown in **Figure A-1**.[14,17] Specifically, we develop a synthetic

route to incorporate pendent phenol groups into MPC copolymers, building off the well-established biocompatibility and immunogenic properties of poly(MPC),[22-31] and then explore their use in tyrosinase bioconjugation methods with thiol-containing reaction partners in the form of reduced protein.

Synthesis of Phenol-Substituted Copolymers

To access polymer-protein bioconjugates through tyrosinase-mediated oxidative addition, a synthetic pathway to phenol-containing MPC copolymers was devised by integrating acetoxy-protected hydroxystyrene into MPC copolymers *via* RAFT polymerization (**Figure A-2**). ^{1}H NMR analysis of the crude polymerization reaction mixtures after ~24 hours revealed full conversion of acetoxystyrene monomers relative to the MPC comonomers, which showed upwards of ~60% conversion as estimated by ^{31}P NMR due to overlapping proton resonances. Following precipitation in THF, the crude polymer solid was purified by dialysis (against water) to remove residual MPC monomer and was then lyophilized. Copolymer **1** was obtained as a white solid in 20-60% yield and

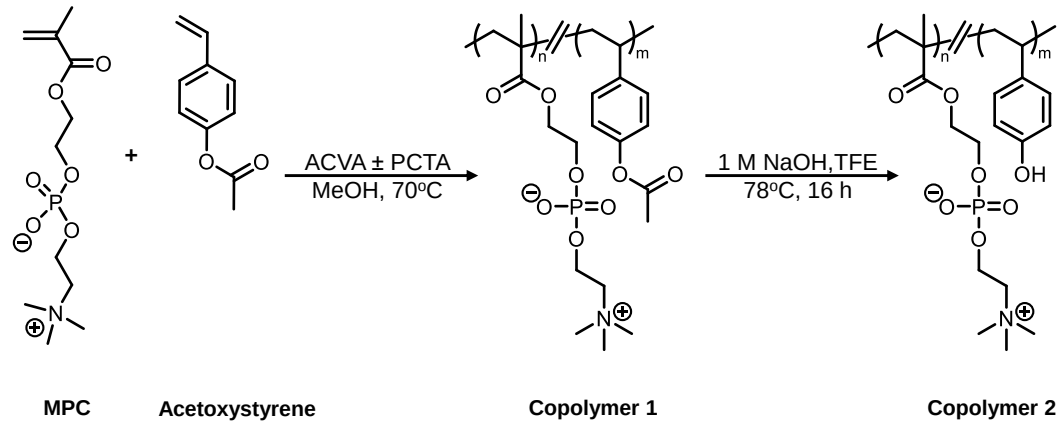

Figure A-2. Synthetic route to phenol-containing MPC copolymers. Acetoxystyrene and MPC are copolymerized using controlled or free radical methods to produce copolymer **1**, which is subsequently deprotected in the presence of base to yield hydroxystyrene-MPC copolymer **2**.

was soluble in polar solvents such as methanol and water. Preliminary optimization of reaction conditions (**Table A-1**) revealed that the highest conversions were obtained in methanol solutions, and that best molecular weight and dispersity control was obtained with dithiobenzoate chain transfer agents. As shown in **Figure A-3**, the ^{1}H NMR spectrum of copolymer **1** in MeOD-*d4* (**Figure A-3a**) has chemical shifts indicative of both MPC and acetoxystyrene monomers: the methyl from the acetoxy protecting group is at ~2.3 ppm while the methylene adjacent to the quaternary ammonium group in MPC is at ~3.7 ppm (**Figure A-3b**). Moreover, ^{31}P NMR displays one resonance at -0.5 ppm, supportive of MPC integration into the copolymer final structure (**Figure A-3c**). ^{1}H NMR analysis end group analysis of copolymer **1** gave an experimental molecular weight (~11 kDa) similar to targeted values (~10 kDa) and confirmed that the incorporation of acetoxystyrene (~25 mol%) into the final copolymer resembled the targeted feed ratio (~20 mol%). GPC estimated molecular weight of copolymer **1** in TFE eluents to be slightly higher (~17 kDa) than the molecular weight calculated by end-group analysis (~11 kDa), and showed moderate dispersity values (~1.3), likely a result of the copolymerization of styrene and methacrylate monomers (**Table A-2**). GPC analysis in aqueous eluents, on the other hand, gave a molecular weight estimate (~5 kDa) lower than the experimental molecular weight.

Table A-1. Optimization of RAFT copolymerization in methanol solutions of MPC with 20 mole percent acetoxystyrene monomer.

Trial	Scale (g)	Solvent	PC:St Ratio		Concentration (M)	CTA:ACVA	Conversion (%)	Yield (mg, %)	Molecular Weight by ^{1}H NMR (kDa)	
			Theo.	*Exp.*					*Theo.*	*Exp.*
1	0.3	MeOH	80:20	74:26	0.5	-	90	163 (55)	-	-
2	0.3	MeOH	80:20	73:27	0.5	2.8:1	90	57 (19)	10.0	11.0
3	0.3	MeOH	80:20	75:25	0.5	3.1:1	90	121 (35)	10.2	14.2
4*	0.3	MeOH	80:20	77:23	0.5	2.9:1	90	80 (23)	10.1	-
5	0.3	TFE	80:20	-	0.5	2.8:1	40	-	10.4	-

**trithiocarbonate chain transfer agent*

Deprotection of copolymer **1** was carried out in the presence of 1 M NaOH in TFE under reflux to give phenol-containing MPC copolymer **2** as a white solid in 50% yield following centrifugal dialysis against water (**Figure A-4a**). ^{1}H NMR analysis confirmed loss of the methyl protons from the acetoxy group (~2.3 ppm) with no further spectral changes (**Figure A-4b,c**). Likewise, GPC analysis in TFE and aqueous eluents revealed little-to-no changes in molecular weight or polydispersity (**Figure A-4d,e**). To confirm that copolymer **2** could serve as substrate for tyrosinase, 5 μL of a 2 mg/mL tyrosinase solution was added to ~ 3 mg of copolymer **2** in 500 μL of a 0.1 M PBS solution (pH 7.4). After

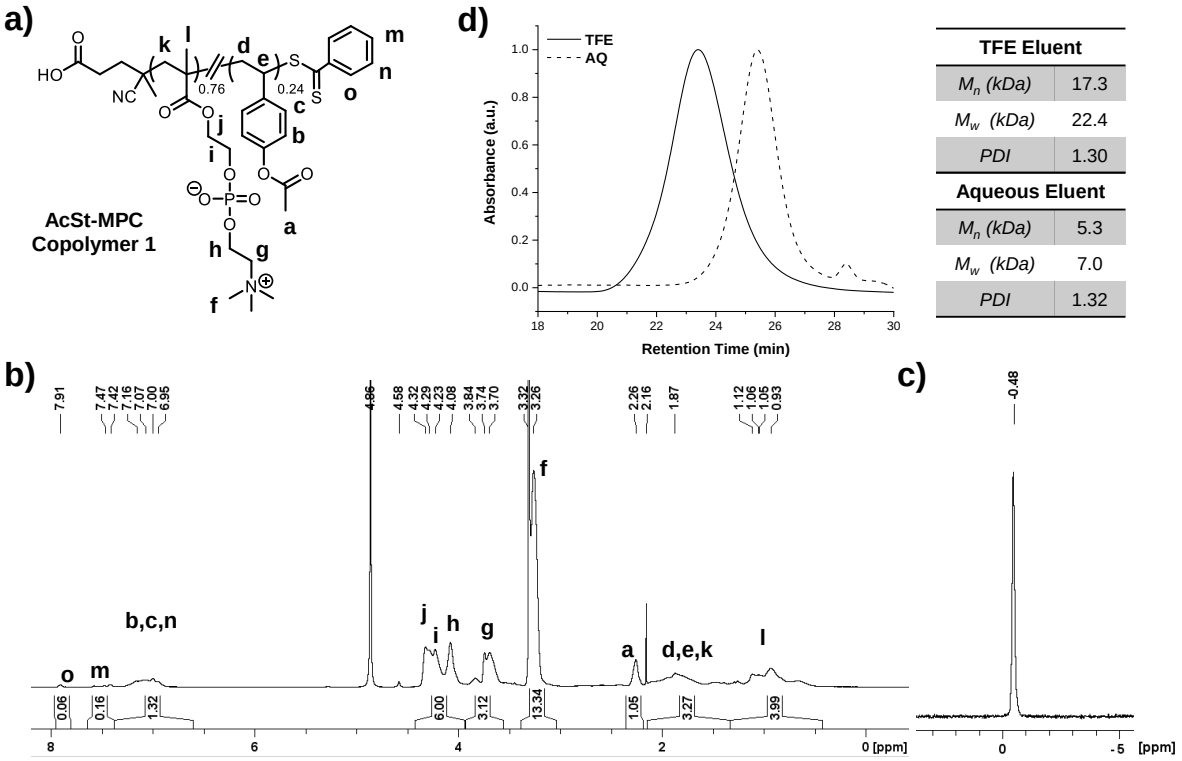

TFE Eluent	
M_n (kDa)	17.3
M_w (kDa)	22.4
PDI	1.30
Aqueous Eluent	
M_n (kDa)	5.3
M_w (kDa)	7.0
PDI	1.32

Figure A-3. (**a**) Synthesis acetoxystyrene copolymers with MPC as comonomer (AcSt-MPC copolymer **1**) *via* RAFT conditions in the presence of a dithiobenzoate chain transfer agent (CTA) and azo initiator (ACVA). (**b**) ^{1}H and (**c**) ^{31}P NMR spectra in MeOD-*d4* and (**c**) representative GPC traces, including estimated molecular weight and PDI values, in TFE and aqueous eluents for copolymer **1** containing 30 mol % acetoxystyrene.

several minutes, the color of the solution changed from colorless to slightly red, which was a positive indication of phenol oxidation by tyrosinase.

Table A-2. Molecular weight estimations by GPC in TFE or aqueous eluents of RAFT copolymerization with MPC of acetoxystyrene copolymer **1** and deprotected hydroxystyrene copolymer **2** at 30 mole percent incorporation.

Sample	Molecular Weight by TFE GPC (kDa)*			Molecular Weight by Aqueous GPC (kDa)ǂ		
	M_n	M_w	PDI	M_n	M_w	PDI
1	17.3	22.4	1.32	5.3	7.0	1.32
2	15.4	20.4	1.32	5.3	7.0	1.32

**calibrated against PMMA standards*
ǂcalibrated against PEO standards

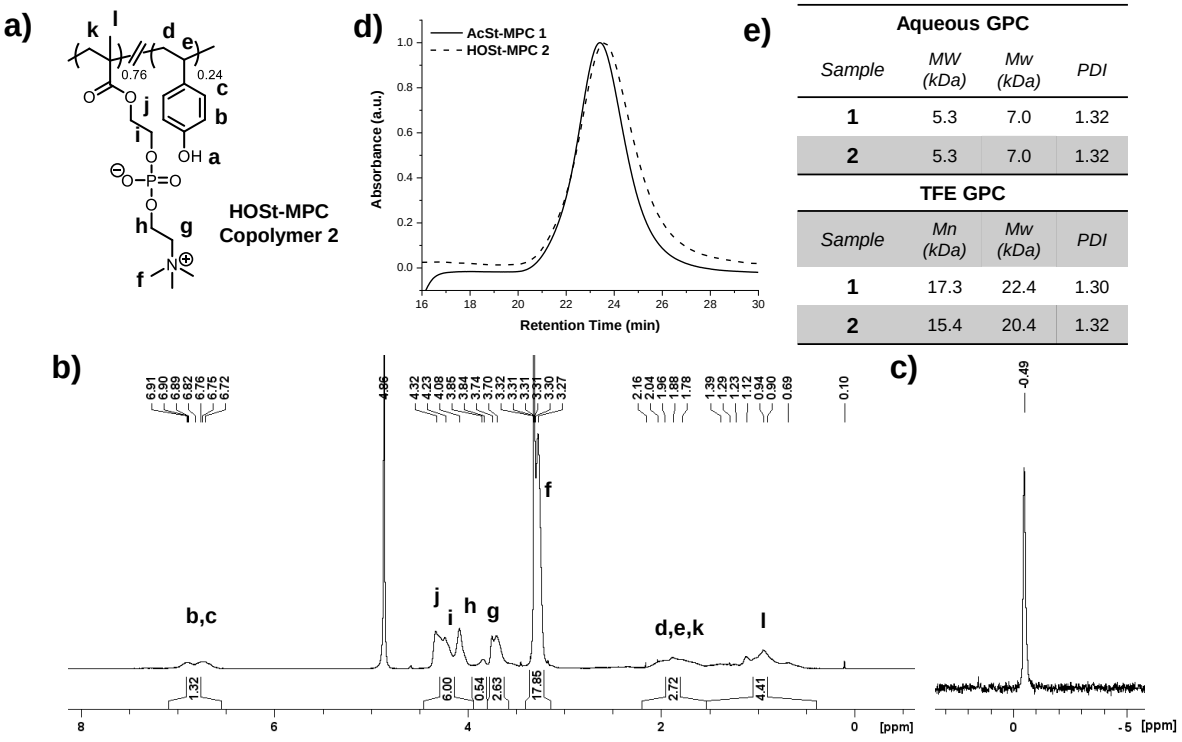

e)

Aqueous GPC

Sample	MW (kDa)	Mw (kDa)	PDI
1	5.3	7.0	1.32
2	5.3	7.0	1.32

TFE GPC

Sample	Mn (kDa)	Mw (kDa)	PDI
1	17.3	22.4	1.30
2	15.4	20.4	1.32

Figure A-4. (**a**) Synthesis hydroxystyrene-MPC copolymers (HOSt-MPC copolymer **2**) following deprotection in sodium hydroxide/trifluoroethanol under reflux. (**b**) ^{1}H and (**c**) ^{31}P NMR spectra in MeOD-*d4* and (**c**) representative GPC traces, including estimated molecular weight and PDI values, in TFE and aqueous eluents for copolymer **2** containing 30 mol % acetoxystyrene.

Tyrosinase Bioconjugation Using Phenol-Containing MPC Copolymers

The phenol-containing MPC copolymer **2** was then evaluated in tyrosinase-mediated bioconjugation following the scheme outlined **Figure A-5a**. For this, reduced BSA or CAT (~2-4 uM), including native BSA, which contains one free cysteine per protein,[32-33] were prepared in various buffer solutions at pH ~7 containing 65 eq. of copolymer **2**, which corresponds to ~36-56 phenol groups per reduced protein thiol or ~1000 eq. phenol for native BSA. After addition of tyrosinase (400 nM), the reactions were incubated at room temperature for 16 hours before being characterized with SDS-PAGE. As shown in **Figure A-5b**, polymer-protein coupling was only observed in experimental conditions containing polymer, protein and tyrosinase, such as in lanes 9 and 10 for reduced BSA, which exhibited a high molecular weight streaking above the protein band. No bioconjugation was observed in reaction mixtures containing polymer and protein without tyrosinase enzyme (lanes 7, 12), nor was any protein-protein coupling observed in lanes containing protein and tyrosinase without polymer (lanes 6, 11). The phenol groups were confirmed to be responsible for the observed bioconjugation in control experiments with unmodified poly(MPC) (**Figure A-6**), and preliminary optimization of reaction conditions revealed that tyrosinase concentration significantly improved extent of bioconjugation. To further explore the role of the buffer solution in BSA-polymer bioconjugation, a variety of buffers from pH 6.7 to 9.0 were evaluated after reacting for 2 hours (**Figure A-7**). Most conditions displayed minor extents of high molecular weight streaking, with condition e having the greatest increase in fluorescence intensity above the protein band; the pH or buffer molarity did not otherwise appear to impact extent of bioconjugation. Unfortunately, despite these promising results, the utilization of phenol-

containing MPC copolymers in post-polymerization modification reactions with small molecule or polymer thiol coupling partners have been unsuccessful to-date.

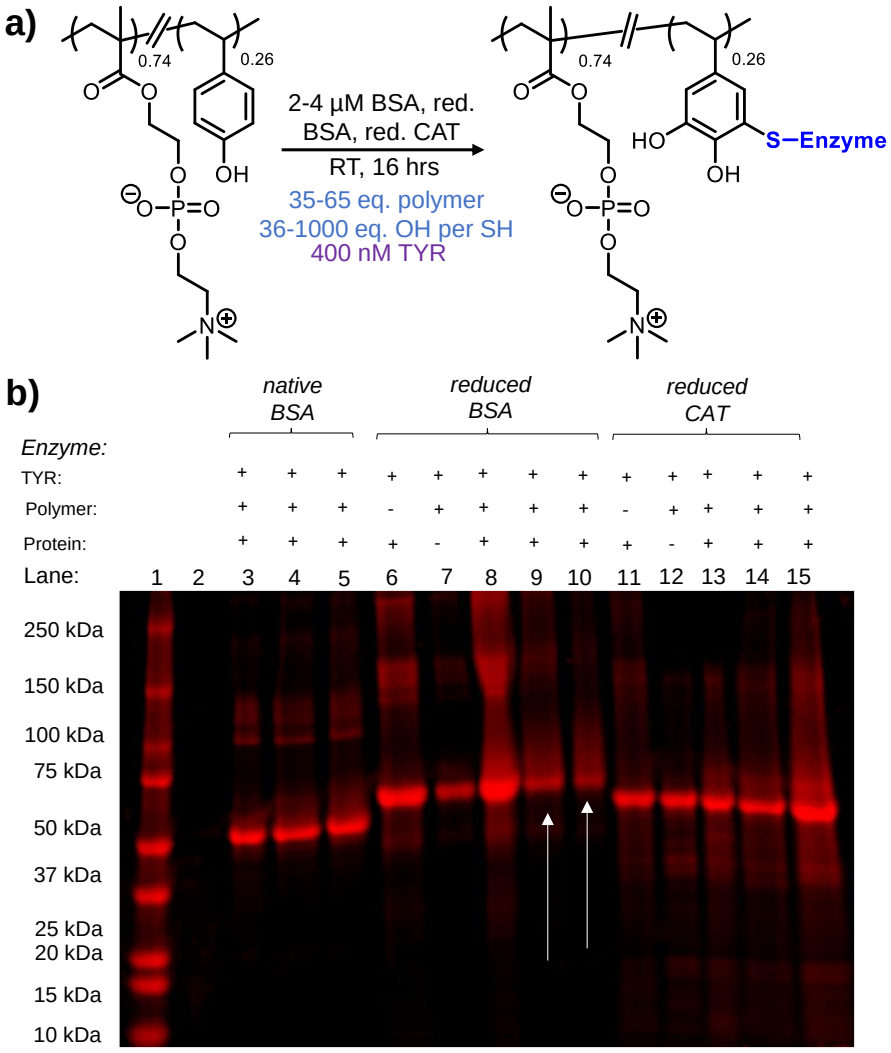

Figure A-5. (**a**) Synthesis of polymer-protein bioconjugates *via* tyrosine-mediated oxidative addition. (**b**) SDS-PAGE gel of bioconjugation reactions after 16 hours between phenol-containing MPC copolymer **2** and native or reduced BSA and reduced CAT in various buffer conditions. Lane 1 is the molecular weight protein ladder and lane 2 is the polymer control. Lanes 6 and 11 are the protein coupling controls with tyrosinase. Lanes 7 and 12 are the polymer-protein bioconjugation controls without tyrosinase. Lanes 3, 8, and 13 are the experimental conditions in Certipur Borate pH 6.7; lanes 4, 9, and 14 are 0.1 M PBS pH 7.4; and lanes 5, 10, and 15 are 0.1 M $NaHCO_3$ pH 6.7. The fluorescence increase in lane 8 is a result of sample/protein overloading, while the consistent streaking in all lanes is likely a result of copolymer **2** streaking during separation. The red arrows indicate lanes where bioconjugation was observed.

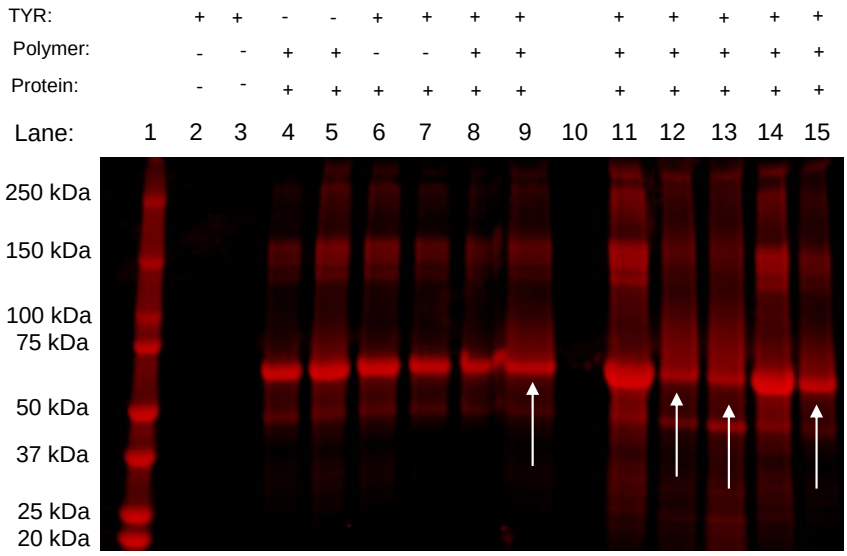

Figure A-6. SDS-PAGE gel of tyrosinase-mediated bioconjugation reactions after 2 hours between phenol-containing MPC copolymer **2** or poly(MPC) and reduced BSA in 0.1 M PBS pH 7.4 (0.14 M NaCl, 2.7 mM KCl). Lane 1 is the molecular weight protein ladder, lane 2 is the poly(MPC) control, and lane 3 is the copolymer **2** control. Lanes 4 and 5 are the polymer-protein bioconjugation controls without tyrosinase for poly(MPC) and copolymer **2**, respectively. Lanes 6 and 7 are the protein coupling controls with tyrosinase. Lanes 8 and 9 are the experimental conditions for poly(MPC) and copolymer 1, respectively. Lanes 11, 12 and 13 have 1/4X, 10X and 30X the typical tyrosinase concentration (400 nM), respectively. Lanes 14 and 15 have 145 and 7 equivalents of phenol to thiol, respectively, compared to lane 9 (36 eq.). The white arrows indicate lanes with observable bioconjugation.

a)

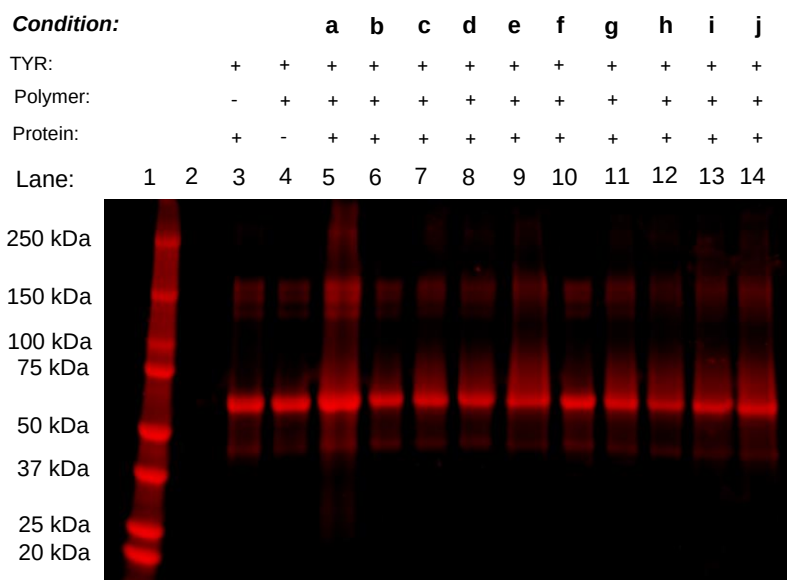

b)

Name	*Condition*	*Name*	*Condition*
a	0.1 M PBS, pH 7.4	**f**	Certipur Borate, pH 8.0
b	Certipur Borate, pH 6.7	**g**	50 mM Tris, pH 8.0
c	0.15 M Tris, pH 7.4	**h**	50 mM HEPES, pH 8.0
d	0.15 M HEPES, pH 7.4	**i**	0.1 M $NaHCO_3$, pH 8.0
e	0.1 M PBS, pH 8.0	**j**	0.1 M PBS, pH 9.0

Figure A-7. (**a**) SDS-PAGE gel of tyrosinase-mediated bioconjugation reactions after 2 hours between phenol-containing MPC copolymer **2** and reduced BSA in (**b**) various buffer conditions. Lane 1 is the molecular weight protein ladder and lane 2 is the polymer control. Lane 3 is the protein coupling control with tyrosinase. Lane 4 is the polymer-protein bioconjugation control without tyrosinase. Lanes 5-14 are the experimental conditions.

Summary & Future Directions

Appendix A discussed synthetic strategies to phenol-containing MPC copolymers for utilization in tyrosinase-mediated bioconjugation. Phenolic groups were integrated into MPC copolymers through RAFT polymerization as acetoxy-protected hydroxystyrene monomers, which gave hydroxystyrene-MPC copolymers following base deprotection. These novel phenol-containing MPC polymers were subsequently evaluated in tyrosinase-

mediated oxidative addition with thiol-containing proteins and resulted in the formation of BSA-polymer bioconjugates across a variety of conditions, following SDS-PAGE analysis. These preliminary results are encouraging and highlight the potential power and versatility of a tyrosinase-mediation bioconjugation platform in setting the stage to improved macromolecular therapeutic conjugation strategies.

References

1. Hong, V.; Presolski, S. I.; Ma, C.; Finn, M. G. Analysis and Optimization of Copper-Catalyzed Azide–Alkyne Cycloaddition for Bioconjugation. *Angew. Chem.* **2009**, *121*, 10063 –10067.

2. Sen Gupta, S.; Kuzelka, J.; Singh, P.; Lewis, W. G.; Manchester, M.; Finn, M. G. Accelerated Bioorthogonal Conjugation: A Practical Method for the Ligation of Diverse Functional Molecules to a Polyvalent Virus Scaffold. *Bioconjugate Chem.* **2005**, *16* (6), 1572–1579.

3. Bays, E.; Tao, L.; Chang, C.-W.; Maynard, H. D. Synthesis of Semitelechelic Maleimide Poly(PEGA) for Protein Conjugation By RAFT Polymerization. *Biomacromolecules* **2009**, *10* (7), 1777–1781.

4. Ravasco, J. M. J. M.; Faustino, H.; Trindade, A.; Gois, P. M. P. Bioconjugation with Maleimides: A Useful Tool for Chemical Biology. Chem. Eur. J. 2019, 25, 43–59.

5. Kalia, D.; Malekar, P. V.; Parthasarathy, M. Exocyclic Olefinic Maleimides: Synthesis and Application for Stable and Thiol-Selective Bioconjugation. *Angew. Chem. Int. Ed.* **2015**, *55* (4), 1432-1435.

6. Jones, M. W.; Strickland, R. A.; Schumacher, F. F.; Caddick, S.; Baker, J. R.; Gibson, M. I.; Haddleton, D. M. Polymeric Dibromomaleimides as Extremely Efficient Disulfide Bridging Bioconjugation and Pegylation Agents. *J. Am. Chem. Soc.* **2012**, *134* (3), 1847–1852.

7. Lu, Z.-P.; Kopečková, P.; Wu, Z.; Kopeček, J. Functionalized Semitelechelic Poly[N-(2-hydroxypropyl)methacrylamide] for Protein Modification. *Bioconjugate Chem.* **1998**, *9* (6), 793–804.

8. Lele, B. S.; Murata, H.; Matyjaszewski, K.; Russell, A. J. Synthesis of Uniform Protein−Polymer Conjugates. *Biomacromolecules* **2005**, *6* (6), 3380–3387.

9. Turecek, P. L.; Bossard, M. J.; Schoetens, F.; Ivens, I. A. PEGylation of Biopharmaceuticals: A Review of Chemistry and Nonclinical Safety Information of Approved Drugs. *J. Pharm. Sci*. **2016**, *105* (2), 460-475.

10. Ko, J. H.; Maynard, H. D. A Guide to Maximizing the Therapeutic Potential of Protein-Polymer Conjugates by Rational Design. *Chem. Soc. Rev.* **2018**, *47*, 8998-9014.

11. Mogilevsky, C. S.; Lobba, M. J.; Brauer, D. D.; Marmelstein, A. M.; Maza, J. C.; Gleason, J. M.; Doudna, J. A.; Francis, M. B. Synthesis of Multi-Protein Complexes through Charge-Directed Sequential Activation of Tyrosine Residues. *J. Am. Chem. Soc.* **2021**, *143* (34), 13538–13547.

12. Ramsey, A. V.; Bischoff, A. J.; Francis, M. B. Enzyme Activated Gold Nanoparticles for Versatile Site-Selective Bioconjugation. *J. Am. Chem. Soc*. **2021**, *143* (19), 7342–7350.

13. ElSohly, A. M.; Francis, M. B. Development of Oxidative Coupling Strategies for Site-Selective Protein Modification. *Acc. Chem. Res.* **2015**, *48* (7), 1971–1978.

14. Lobba. M. J.; Fellmann, C.; Marmelstein, A. M.; Maza, J. C.; Kissman, E. N.; Robinson, S. A.; Staahl, B. T.; Urnes, C.; Lew, R. J.; Mogilevsky, C. S.; Doudna, J. A.; Francis, M. B. Site-Specific Bioconjugation through Enzyme-Catalyzed Tyrosine–Cysteine Bond Formation. *ACS Cent. Sci.* **2020**, *6* (9), 1564–1571.

15. Carrico, Z. M.; Romanini, D. W.; Mehl, R. A.; Francis, M. B. Oxidative Coupling of Peptides to a Virus Capsid Containing Unnatural Amino Acids. *Chem. Commun.* **2008**, 1205–1207.

16. Maza, J. C.; Ramsey, A. V.; Mehare, M.; Krska, S. W.; Parish, C. A.; Francis, M. B. Secondary Modification of Oxidatively-modified Proline N-termini for the Construction of Complex Bioconjugates. *Org. Biomol. Chem.* **2020**, *18*, 1881–1885.

17. Maza, J. C.; Bader, D. L. V.; Xiao, L.; Marmelstein, A. M.; Brauer, D. D.; ElSohly, A. M.; Smith, M. J.; Krska, S. W.; Parish, C. A.; Francis, M. B. Enzymatic Modification of N-Terminal Proline Residues Using Phenol Derivatives. *J. Am. Chem. Soc.* **2019**, *141* (9), 3885–3892.

18. Aanei, I. L.; Huynh, T.; Seo, Y.; Francis, M. B. Vascular Cell Adhesion Molecule-Targeted MS2 Viral Capsids for the Detection of Early-Stage Atherosclerotic Plaques. *Bioconjugate Chem*. **2018**, *29* (8), 2526–2530.

19. Maza, J. C.; García-Almedina, D. M.; Boike, L. E.; Hamlish, N. X.; Nomura, D. K.; Francis, M. B. Tyrosinase-Mediated Synthesis of Nanobody–Cell Conjugates. *ACS Cent. Sci.* **2022**, *8* (7), 955–962.

20. Hong, H.; Lee, U.-J.; Lee, S. H.; Kim, H.; Lim, G.-H.; Lee, S.-H.; Son, H. F.; Kim, B.-G.; Kim, K.-J. Highly Efficient Site-Specific Protein Modification Using Tyrosinase from Streptomyces avermitilis: Structural Insight. *Int. J. Biol. Macromol.* **2024**, *225*, 128313, 11 pages.

21. Marmelstein, A. M.; Lobba, M. J. ; Mogilevsky, C. S. ; Maza, J. C.; Brauer, D. D.; Francis, M. B. Tyrosinase-Mediated Oxidative Coupling of Tyrosine Tags on Peptides and Proteins. *J. Am. Chem. Soc.* **2020**, *142* (11), 5078–5086.

22. Samanta, D.; McRae, S.; Cooper, B.; Hu, Y.; Emrick, T. End-functionalized Phosphorylcholine Methacrylates and their use in Protein Conjugation. *Biomacromolecules* **2008**, *9*, 2891-2897.

23. Chen, XJ.; McRae, S.; Samanta, D.; Emrick, T. Polymer-Protein Conjugation in Ionic Liquids. *Macromolecules* **2010**, *43*, 6261-6263.

24. McRae, S.; Chen, X.; Kratz, K.; Samanta, D.; Henchey, E.; Schneider, S.; Emrick, T. Pentafluorophenyl Ester-Functionalized Phosphorylcholine Polymers: Preparation of Linear, Two-Arm, and Grafted Polymer–Protein Conjugates. *Biomacromolecules* **2012**, *13* (7), 2099–2109.

25. Chen, XJ.; McRae, S.; Parelkar, S.; Emrick, T. Polymeric Phosphorylcholine-Camptothecin Conjugates Prepared by Controlled Free Radical Polymerization and Click Chemistry. *Bioconjugate Chem*. **2009**, *20*, 2331–2341.

26. Wong, K. E.; Mora, M. C.; Skinner, M.; Page, S. M.; Crisi, G. M.; Arenas, R. B.; Schneider, S. S.; Emrick, T. Evaluation of PolyMPC-Dox Prodrugs in a Human Ovarian Tumor Model. *Mol. Pharmaceutics* **2016**, 13(5), 1679–1687

27. McRae Page, S.; Henchey, E.; Chen, X., Schneider, S. and Emrick, T. Efficacy of PolyMPC-DOX Prodrugs in 4T1 Tumor-bearing Mice. *Mol. Pharmaceutics* **2014**, 11(5), 1715–1720.

28. Ward, S.M.; Skinner, M.; Saha, B.; Emrick, T. Polymer - Temozolomide Conjugates as Therapeutics for Treating Glioblastoma. *Mol. Pharmaceutics* **2018**, *15* (11), 5263–5276.

29. Jin, Q.; Chen, Y.; Wang, Y.; Ji, J. Zwitterionic Drug Nanocarriers: A Biomimetic Strategy for Drug Delivery. *Colloids Surf. B Biointerfaces* **2014**, *124*, 80-86.

30. Harijan, M.; Singh, M. Zwitterionic Polymers in Drug Delivery: A Review. *J. Mol. Recognit.* **2021**, *35* (1), e2944, 13 pages.

31. Zeng, Z.; Chen, S.; Chen, Y. Zwitterionic Polymer: A New Paradigm for Protein Conjugation beyond PEG. *ChemMedChem* **2023**, *18* (20), e202300245, 9 pages.

32. 22. Bontempo, D.; Heredi, K. L.; Fish, B. A.; Maynard, H. D. Cysteine-Reactive Polymers Synthesized by Atom Transfer Radical Polymerization for Conjugation to Proteins. *J. Am. Chem. Soc.* **2004**, *126* (47), 15372–15373.

33. 23. Liu, J.; Liu, H.; Bulmus, V.; Tao, L.; Boyer, C.; Davis, T. P. J. A Simple Methodology for the Synthesis of Heterotelechelic Protein–Polymer–Biomolecule Conjugates. *Polym. Sci. A. Polym. Chem.* **2010**, *48* (6), 1399–1405.

APPENDIX B:
PROBING SOLUTION DYNAMICS, CONFIGURATION, AND MOLECULAR WEIGHT OF POLY(MPC) BY DOSY NMR

Polymer zwitterions, such as poly(MPC), are a unique class of hydrophilic polymers with well-known biocompatibility and anti-fouling properties that arise from the interactions between their zwitterion subunits and water molecules, resulting in the formation of a hydration layer.[1-6] Probing the aqueous solution behavior of poly(MPC) with differential scanning calorimetry (DSC)[7] and fluorescence spectroscopy,[8] for example, has revealed that interactions between the phosphate and ammonium charged groups of poly(MPC) with neighboring water molecules are strong enough to inhibit tightly-bound water molecules from freezing at 0 ^{o}C.[7] Moreover, poly(MPC) was found to hydrate an extensive number of water molecules per zwitterionic unit,[7-9] preventing backbone aggregation and precipitation,[10] similar to the PC head group of phospholipid molecules, which was found to hydrate ~20 water molecules using ^{2}H NMR and additionally exhibited restricted mobility.[9] Notably, the diffusion of poly(MPC) in aqueous environments was described as largely independent of salt concentration (up to 1 M), leading to speculation that poly(MPC) chains are fully expanded in an aqueous environment.[11] Unlike their polyelectrolyte counterparts, polymer zwitterions retain solubility in aqueous solutions at elevated salt concentrations and in polar organic solvents such as methanol and trifluoroethanol (TFE).[10,12-14] This is further supported by simulating hydrated poly(MPC) chains, which shows the chains are highly extended.[10] In **Appendix B**, we share a brief summary of our efforts to further explore the solution behavior of

poly(MPC) samples in various solvents (D_2O, MeOD-*d4*, and TFE-*d3*) using the NMR techniques of diffusion-ordered spectroscopy (DOSY) and T_2 relaxation.

Overview of Experimental Procedure. Reversible-addition-fragmentation chain-transfer (RAFT) polymerization was utilized to prepare poly(MPC) with controlled degrees of polymerization (DP), as determined by ^1H NMR end group analysis, and low polydispersity indices (PDI ~ 1.1), as confirmed by GPC characterization. DOSY experiments were conducted using a Bruker Avance III 400 MHz NMR on poly(MPC) solutions at concentrations near the dilute limit (< 1 mg/mL) to determine the diffusion coefficient of poly(MPC) in each solvent, which was then converted to hydrodynamic radius (R_H) using the Stokes-Einstein relation. T_2 relaxation times of selected samples were additionally evaluated, using a Carr-Purcell-Meiboom-Gill (CPMG) pulse sequence. As was necessary, 3 mm NMR tubes were utilized to minimize convection. In cases where the overlap between the target polymer signals and the solvent signals were severe, the first data point of the DOSY decay was discarded and the remaining data points were fitted with a single Gaussian component in OriginPro®.

Impact of Degree of Polymerization on Hydrodynamic Radius. The R_h of a series of poly(MPC) samples at various DP was evaluated by DOSY NMR as solutions in D_2O, MeOD-*d4* and, TFE-*d3*. As can be observed in **Figure B-1**, the R_h in D_2O is smaller than those in MeOD-*d4* and TFE-*d3*; the values of R_h for these samples range between ~ 1 nm for the smallest DP (M_n ~ 3 kDa) to ~ 4 nm for the largest DP (M_n ~ 52 kDa) and were found to be pH independent on the window probed. Linear fits of poly(MPC) yielded slopes of 0.41 for D_2O, 0.37 for MeOD-*d4*, and 0.40 for TFE-*d3*, respectively (R^2 ~ 0.984). In

contrast, PMMA in $CDCl_3$ showed a slope of 0.52 (R^2 = 0.998), which is consistent with what has been reported in the literature.[15] These results suggest that PMMA in $CDCl_3$ is close to a random coil configuration (power law dependence = 0.5) for a standard theta-solvent condition, while those for poly(MPC) in all probed solvents are closer to a collapsed globule configuration (power law dependence = 0.33). It is likely that the attractive force between the electric dipoles of the zwitterionic groups controls the chain dimension: the hydration shells formed by the solvent molecules around the polymer

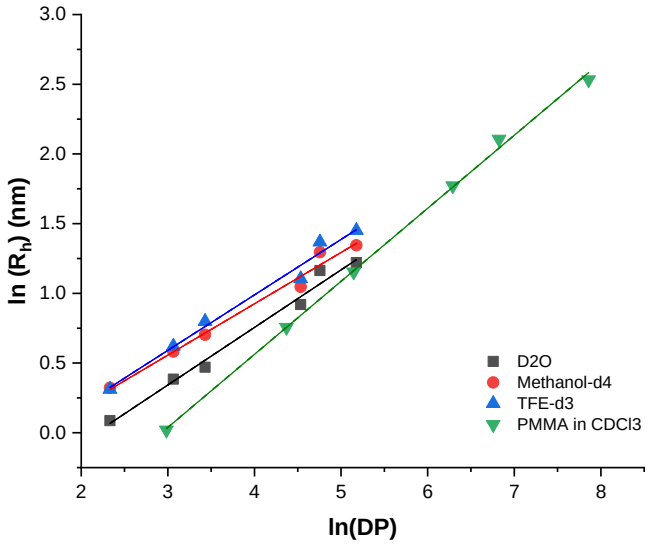

Figure B-1. Logarithmic plot of R_h *vs.* DP of poly(MPC) in D_2O, MeOD-*d4*, and TFE-*d3*, compared to reference PMMA in $CDCl_3$.

zwitterion subunits partially, but not fully, shield the attractions between the dipoles, which creates a relatively tight sphere held together by the residual dipolar attractions.

Impact of Molecular Weight (M_n) on Segmental Relaxation (T_2). Since the ordering of solvent molecules in hydrated poly(MPC) spheres will affect its segmental rotation, the segmental dynamics of poly(MPC) were evaluated with T_2 relaxation experiments. Shown in **Figure B-2** are the ^{1}H NMR T_2 relaxation times of three poly(MPC) samples in all three solvents, including PEO in D_2O for comparison. The poly(MPC) relaxation times (~10-60

ms) are much smaller than PEO (~540 ms) and other small molecules or flexible-chain synthetic polymers dissolved in organic solvents, which are usually between several hundred milliseconds to several seconds. In addition, there is a notable dependence of T_2 on M_n for all three solvents whereas T_2 of PEO is constant on the range tested. **Figure B-2** additionally shows that the T_2 relaxation times are shorter in TFE-*d3* and longer in MeOD-*d4*, which is likely due to the different viscosity of these solvents.

The difference in the T_2 behaviors of poly(MPC) and PEO highlights the different nature of polymer-solvent interactions. For PEO and hydrocarbon polymers in solution, the interaction between the solvent and the solute is weak; thus, the rotation of a given molecular segment is mostly independent of the segments that are >4-5 bonds away, resulting in the M_n-independence of T_2 and causing longer T_2 times. In contrast, the dependence of T_2 on M_n for poly(MPC) indicates that the rotations between different segments of one poly(MPC) chain are not independent and suggests that the solvent

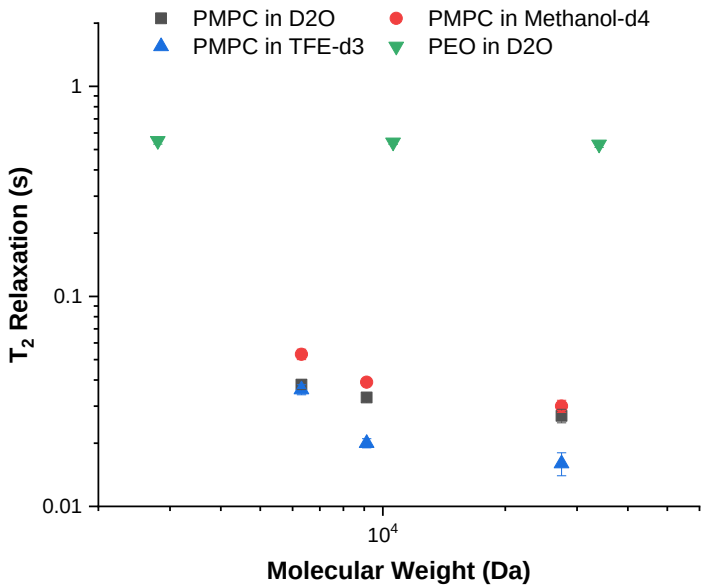

Figure B-2. T_2 relaxation times (s) of poly(MPC) in D_2O, MeOD-*d4*, and TFE-*d3* as a function of molecular weight (M_n , Da). The error bars are standard deviations of single-exponential fittings.

molecules have orientational order and limited mobility around each PC group. As such, the T_2 relaxation is likely driven by the tumbling of the hydrated sphere of poly(MPC) as a whole, like that of a fully folded protein molecule. The larger the M_n, the slower are such tumbling motions, resulting in faster T_2 relaxation.

Summary & Outlook. The relationship between the hydrodynamic radius (R_h) and the molecular weight (M_n) of poly(MPC) in three different solution environments—D_2O, MeOD-*d4*, and TFE-*d3*—was examined by DOSY NMR spectroscopy and T_2 relaxation experiments. In all three solvents, the slopes (~0.4) arising from the logarithmic plots of R_h *v.* DP more closely resembled collapsed globules (~0.33) than random coils (~0.5). T_2 relaxation experiments additionally revealed an M_n dependence of T_2, which suggested that the poly(MPC) macromolecules behave as rigid "ice balls" as a result of the solvent structures that form around the zwitterion subunits. Taken together, the NMR results the highlight the impact of the local rigidity around the PC group (from T_2 experiments), which is most likely caused by zwitterion-water interactions demonstrate an interconnectedness, on the swollen polymer state, *i.e.*, a collapsed globule. Findings such as this provide a foundation to interpret various performance attributes of PMPC, such as its antifouling behavior, while establishment of M_n – R_h correlations will lead to more reliable determination of polymer zwitterion molecular weight *via* diffusion NMR methods.

References

1. Ishihara, K.; Ueda, T.; Nakabayashi, N. Preparation of Phospholipid Polymers and Their Properties as Polymer Hydrogel Membranes. *Polym. J.* **1990**, *22* (5), 355–360.

2. Li, D.; Wei, Q.; Wu, C.; Zhang, X.; Xue, Q.; Zheng, T.; Cao, M. Superhydrophilicity and Strong Salt-Affinity: Zwitterionic Polymer Grafted Surfaces in Biological Systems. *Adv. Colloid Interface Sci.* **2020**, *278*, 102141, 18 pages.

3. Jin, Q.; Chen, Y.; Wang, Y.; Ji, J. Zwitterionic Drug Nanocarriers: A Biomimetic Strategy for Drug Delivery. *Colloids Surf. B: Biointerfaces* **2014**, *124*, 80–86.

4. Ishihara, K., Nomura, H., Mihara, T., Kurita, K., Iwasaki, Y., and Nakabayashi, N. Why do Phospholipid Polymers Reduce Protein Adsorption? *J. Biomed. Mater. Res.* **1998**, 39, 323–330.

5. Mi, L.; Jiang, S. Integrated Antimicrobial and Nonfouling Zwitterionic Polymers. *Angew. Chem. Int. Ed.* **2014**, *53*, 1746–1754.

6. Iwasaki, Y.; Ishihara, K. Phosphorylcholine-Containing Polymers for Biomedical Applications. *Anal. Bioanal. Chem.* **2005**, 381, 534–546.

7. Shiomoto, S.; Inoue, K.; Higuchi, H.; Nishimura, S.-N.; Takaba, H.; Tanaka, M.; Kobayashi, M. Characterization of Hydration Water Bound to Choline Phosphate-Containing Polymers. *Biomacromolecules* **2022**, *23* (7), 2999–3008.

8. Ho, C.; Slater, S. J.; Stubbs, C. D. Hydration and Order in Lipid Bilayers. *Biochemistry* **1995**, *34*, 6188–6195.

9. Hou, J.; Pearce, E. Characterization of Polymer Molecular Weight Distribution by NMR Diffusometry: Experimental Criteria and Findings. *Anal. Chem.* **2021**, *93*, 7958–7964.

10. Ishihara, K.; Mu, Mingwei, M.; Konno, T.; Inoue, Y.; Fukazawa, K. The Unique Hydration State of Poly(2-methacryloyloxyethyl phosphorylcholine). *J. Biomater. Sci. Polym. Ed.* **2017**, *28* (10-12), 884–899.

11. Zhang, Z. J.; Madsen, J.; Warren, N. J.; Mears, M.; Leggett, G. J.; Lewis, A. L.; Geoghegan, M. Influence of Salt on the Solution Dynamics of a Phosphorylcholine-Based Polyzwitterion. *Eur. Polym. J.* **2017**, *87*, 449–457.

12. Lashewsky, A.; Rosenhahn, A. Molecular Design of Zwitterionic Polymer Interfaces: Searching for the Difference. *Langmuir* **2019**, *35* (5), 1056–1071.

13. Brown, M. U.; Triozzi, A.; Emrick, T. Polymer Zwitterions with Phosphonium Cations. *J. Am. Chem. Soc.* **2021**, *143* (17), 6528–6532.

14. Brown, M. U.; Seong, H.-G.; Margossian, K. O.; Bishop, L.; Russell, T. P.; Muthukumar, M.; Emrick, T. Zwitterionic Ammonium Sulfonate Polymers: Synthesis and Properties in Fluids. *Macromol. Rapid Commun.* **2022**, *43*, 2100678, 7 pages.

15. Arnold, K.; Gawrisch, K. Effects of Fusogenic Agents on Membrane Hydration: A Deuterium Nuclear Magnetic Resonance Approach. *Methods Enzymol.* **1993**, *220*, 143–157.

BIBLIOGRAPHY

Abuchowski, A.; McCoy, J. R.; Palczuk, N. C.; van Es, T.; Davis, F. F. Effect of Covalent Attachment of Polyethylene Glycol on Immunogenicity and Circulating Life of Bovine Liver Catalase. *J. Biol. Chem.* **1977**, *252* (11), 3582–3586.

Abuchowski, A.; van Es, T.; Palczuk, N. C.; Davis, F. F. Alteration of Immunological Properties of Bovine Serum Albumin by Covalent Attachment of Polyethylene Glycol. *J. Biol. Chem.* **1977**, *252* (11), 3578–3581.

Alconcel, S. N. S.; Baas, A. A.; Maynard, H. D. FDA-Approved Poly(ethylene glycol)–Protein Conjugate Drugs. *Polym. Chem.* **2011**, *2*, 1442–1448.

Alfonso, I.; Solà, J. Molecular Recognition of Zwitterions with Artificial Receptors. *Chem. Asian J.* **2020**, *15* (7), 986–994.

Altinbasak, I.; Arslan, M.; Sanyal, R.; Sanyal, A. Pyridyl disulfide-based thiol–disulfide exchange reaction: shaping the design of redox-responsive polymeric materials. *Polym. Chem.* **2020**, *11* (48), 7603–7624.

Arnold, K.; Gawrisch, K. Effects of Fusogenic Agents on Membrane Hydration: A Deuterium Nuclear Magnetic Resonance Approach. *Methods Enzymol.* **1993**, *220*, 143–157.

Azcune, I.; Odriozola, I. Aromatic Disulfide Crosslinks in Polymer Systems: Self-Healing, Reprocessability, Recyclability and more. *Eur. Polym. J.* **2016**, *84*, 147–160.

Bader, H.; Ringsdorf, H.; Schmidt, B. Watersoluble Polymers in Medicine. *Angew. Makromol. Chem.* **1984**, *123*, 457–485.

Badescu, G.; Bryant, P.; Swierkosz, J.; Khayrzad, F.; Pawlisz, E.; Farys, M.; Cong, Y.; Muroni, M.; Rumpf, N.; Brocchini, S.; Godwin, A. A New Reagent for Stable Thiol-Specific Conjugation. *Bioconjugate Chem.* **2014**, *25* (3), 460–469.

Baggerman, J.; Smulders, M. M. J.; Zuilhof, H. Romantic Surfaces: A Systematic Overview of Stable, Biospecific, and Antifouling Zwitterionic Surfaces. *Langmuir* **2019**, *35* (5), 1072–1084.

Bai, Y.; Chang, C.-C.; Choudhary, U.; Bolukbasi, I.; Crosby, A. J.; Emrick, T. Functional Droplets that Recognize, Collect, and Transport Debris on Surfaces. *Sci. Adv.* **2016**, *2*, e1601462, 7 pages.

Bai, Y.; Chang, C.-C.; Zhao, X.; Ribbe, A.; Bolukbasi, I.; Szyndler, M. J.; Crosby, A. J.; Emrick, T. Mechanical Restoration of Damaged Polymer Films by "Repair-and-Go". *Adv. Funct. Mater.* **2016**, *26*, 857–863.

Bain, C. D.; Evall, J.; Whitesides, G. M. Formation of Monolayers by the Coadsorption of Thiols on Gold: Variation in the Head Group, Tail Group, and Solvent[1]. *J. Am. Chem. Soc.* **1989**, *111* (18), 7155–7164.

Banno, T.; Asami, A.; Ueno, N.; Kitahata, H.; Koyano, Y.; Asakura, K.; Toyota, T. Deformable Self-Propelled Micro-Object Comprising Underwater Oil Droplets. *Sci. Rep.* **2016**, *6*, 31292, 9 pages.

Barz, M.; Luxenhofer, R.; Zentel, R.; Vincent, M. Overcoming the PEG-Addiction: Well-Defined Alternatives to PEG, from Structure–Property Relationships to Better Defined Therapeutics. *Polym. Chem.* **2011**, *2*, 1900-1918.

Bays, E.; Tao, L.; Chang, C.-W.; Maynard, H. D. Synthesis of Semitelechelic Maleimide Poly(PEGA) for Protein Conjugation By RAFT Polymerization. *Biomacromolecules* **2009**, *10* (7), 1777–1781.

Beaupre, D. M.; Weiss, R. G. Thiol- and Disulfide-Based Stimulus-Responsive Soft Materials and Self-Assembling Systems. *Molecules* **2021**, *26* (11), 3332, 44 pages.

Beinert, H. A Tribute to Sulfur. *Eur. J. Biochem.* **2001**, *267* (18), 5657–5664.

Bontempo, D.; Heredi, K. L.; Fish, B. A.; Maynard, H. D. Cysteine-Reactive Polymers Synthesized by Atom Transfer Radical Polymerization for Conjugation to Proteins. *J. Am. Chem. Soc.* **2004**, *126* (47), 15372–15373.

Bracchi, M. E.; Dura, G.; Fulton, D. A. The Synthesis of Poly(aryl thiols) and Their Utilization in the Preparation of Cross-Linked Dynamic Covalent Polymer Nanoparticles and Hydrogels. *Polym. Chem.* **2019**, *10* (10), 1258–1267.

Brown, M. U.; Triozzi, A.; Emrick, T. Polymer Zwitterions with Phosphonium Cations. *J. Am. Chem. Soc.* **2021**, *143* (17), 6528–6532.

Brown, M. U.; Seong, H.; Russell, T. P.; Emrick, T. Zwitterionic Sulfonium Sulfonate Polymers: Impacts of Substituents and Inverted Dipole. *Macromolecules* **2023**, *56*, 1105–1110.

Brown, M. U.; Seong, H.-G.; Margossian, K. O.; Bishop, L.; Russell, T. P.; Muthukumar, M.; Emrick, T. Zwitterionic Ammonium Sulfonate Polymers: Synthesis and Properties in Fluids. *Macromol. Rapid Commun.* **2022**, *43*, 2100678, 7 pages.

Bulmus, V.; RAFT Polymerization Mediated Bioconjugation Strategies. *Polym. Chem*. **2011**, *2*, 1463–1472.

Caliceti, P.; Veronese, F. M. Pharmacokinetic and Biodistribution Properties of Poly(ethylene glycol)–Protein Conjugates. *Adv. Drug Deliv. Rev.* **2003**, *55*, 1261–1277.

Canadell, J.; Goossens, H.; Klumperman, B. Self-Healing Materials Based on Disulfide Links. *Macromolecules* **2011**, *44* (8), 2536–2541.

Carrico, Z. M.; Romanini, D. W.; Mehl, R. A.; Francis, M. B. Oxidative Coupling of Peptides to a Virus Capsid Containing Unnatural Amino Acids. *Chem. Commun.* **2008**, 1205–1207.

Čejková, J.; Novák, M.; Štěpánek, F.; Hanczyc, M. Dynamics of Chemotactic Droplets in Salt Concentration Gradients. *Langmuir* **2014**, *30* (40), 11937–11944.

Chakma, P.; Konkolewicz, D. Dynamic Covalent Bonds in Polymeric Materials. *Angew. Chem. Int. Ed.* **2019**, *58* (29), 9682–9695.

Chalarca, C. F. S.; Emrick, T. Reactive Polymer Zwitterions: Sulfonium Sulfonates. *J. Polym. Sci. A. Polym. Chem.* **2017**, *55*, 83–92.

Chalarca, C. F. S.; Letteri, R. A.; Perazzo, A.; Stone, H. A.; Emrick, T. Building Supracolloidal Fibers from Zwitterion-Stabilized Adhesive Emulsions. *Adv. Funct. Mater.* **2018**, *28*, 1804325, 10 pages.

Chang, C.-C.; Letteri, R.; Hayward, R. C.; Emrick, T. Functional Sulfobetaine Polymers: Synthesis and Salt-Responsive Stabilization of Oil-in-Water Droplets. *Macromolecules* **2015**, *48* (21), 7843–7850.

Chen, B.-M.; Cheng, T.-L.; Roffler, S. R. Polyethylene Glycol Immunogenicity: Theoretical, Clinical, and Practical Aspects of Anti-Polyethylene Glycol Antibodies. *ACS Nano* **2021**, *15* (9), 14022–14048.

Chen, F.-J.; Gao, J. Fast Cysteine Bioconjugation Chemistry. *Chem. Eur. J.* **2022**, *28* (66), e202201843, 15 pages.

Chen, T.-M.; Wang, Y.-F.; Li, Y.-J.; Nakaya, T.; Sakurai, I. Studies on the Synthesis and Properties of Novel Phospholipid Analogous Polymers. *J. Appl. Polym. Sci.* **1996**, *60* (3), 455–464.

Chen, X.; Lawrence, J.; Parelkar, S.; Emrick, T. Novel Zwitterionic Copolymers with Dihydrolipoic Acid: Synthesis and Preparation of Nonfouling Nanorods. *Macromolecules* **2013**, *46* (1), 119–127.

Chen, X.-J.; McRae, S.; Samanta, D.; Emrick, T. Polymer-Protein Conjugation in Ionic Liquids. *Macromolecules* **2010**, *43*, 6261-6263.

Chen, Y.; Li, J.; Li, Q.; Shen, Y.; Ge, Z.; Zhang, W.; Chen, S. Enhanced Water-Solubility, Antibacterial Activity and Biocompatibility upon Introducing Sulfobetaine and Quaternary Ammonium to Chitosan. *Carbohydr. Polym*. **2016**, *143* (5), 246–253.

Chen, X.-J.; McRae, S.; Parelkar, S.; Emrick, T. Polymeric Phosphorylcholine-Camptothecin Conjugates Prepared by Controlled Free Radical Polymerization and Click Chemistry. *Bioconjugate Chem*. **2009**, *20*, 2331–2341.

Cheng, G.; Li, G.; Xue, H.; Chen, S.; Bryers, J. D.; Jiang, S. Zwitterionic Carboxybetaine Polymer Surfaces and their Resistance to Long-term Biofilm Formation. *Biomaterials* **2009**, *30* (28), 5234–5240.

Cook, A. B.; Novosedlik, S.; van Hest, J. C. M. Complex Coacervate Materials as Artificial Cells. *Acc. Mater. Res.* **2023**, *4* (3), 287–298.

Crooke, S. N.; Zheng, J.; Ganewatta, M. S.; Guldberg, S. M.; Reineke, T. M.; Finn, M. G. Immunological Properties of Protein–Polymer Nanoparticles. *ACS Appl. Bio Mater*. **2019**, *2* (1), 93–103.

Deng, B.; Burns, E.; McNelles, S. A.; Sun, J.; Ortega, J.; Adronov, A. Molecular Sieving with PEGylated Dendron-Protein Conjugates. *Bioconjugate Chem.* **2023**, *34* (8), 1467–1476.

Deng, Z.; Hu, J.; Liu, S. Disulfide-Based Self-Immolative Linkers and Functional Bioconjugates for Biological Applications. *Macromol. Rapid Commun.* **2019**, *41* (1), 1900531, 14 pages.

Deng, Z.; Yuan, S.; Xu, R. S.; Liang, H.; Liu, S. Reduction-Triggered Transformation of Disulfide-Containing Micelles at Chemically Tunable Rates. *Angew. Chem. Int. Ed*. **2018**, *57* (29), 8896–8900.

Dey, K. K.; Zhao, X.; Tansi, B. M.; Méndez-Oritz, W. J.; Córdova-Figueroa, U. M. Golestanian, R.; Sen, A. Micromotors Powered by Enzyme Catalysis. *Nano Lett.* **2015**, *15* (12), 8311–8315.

Dong, H.; Li, J.; Liu, H.; Lu, S.; Wu, J.; Zhang, Y.; Yin, Y.; Zhao, Y.; Wu, C. Design and Ribosomal Incorporation of Noncanonical Disulfide-Directing Motifs for the Development of Multicyclic Peptide Libraries. *J. Am. Chem. Soc.* **2022**, *144* (11), 5116–5125.

Duncan, R. The Dawning Era of Polymer Therapeutics. *Nat. Rev. Drug Discov.* **2003**, *2*, 347–360.

Duncan, R.; Vicent, M. J. Polymer Therapeutics-Prospects for 21st Century: The End of the Beginning. *Adv. Drug Deliv. Rev.* **2013**, *65* (1), 60–70.

Duncan, R. Development of HPMA Copolymer–Anticancer Conjugates: Clinical Experience and Lessons Learnt. *Adv. Drug Deliv. Rev.* **2009**, *61* (13), 1131–1148.

Duro-Castano, A.; Conejos-Sánchez, I.; Vincent, M J. Peptide-Based Polymer Therapeutics. *Polymers* **2014**, *6* (2), 515-551.

Ekladious, I.; Colson, Y. L.; Grinstaff, M. W. Polymer–Drug Conjugate Therapeutics: Advances, Insights and Prospects. *Nat. Rev. Drug Discov.* **2019**, *18*, 273–294.

Elani, Y. Interfacing Living and Synthetic Cells as an Emerging Frontier in Synthetic Biology. *Angew. Chem.* **2020**, *133* (11), 5662–5671.

ElSohly, A. M.; Francis, M. B. Development of Oxidative Coupling Strategies for Site-Selective Protein Modification. *Acc. Chem. Res.* **2015**, *48* (7), 1971–1978.

Fang, J.; Sawa, T.; Akaike, T.; Akuta, T.; Sahoo, S. K.; Khaled, G.; Hamada, A.; Maeda, H. In Vivo Antitumor Activity of Pegylated Zinc Protoporphyrin: Targeted Inhibition of Heme Oxygenase in Solid Tumor. *Cancer Res.* **2003**, *63* (13), 3567–3574.

Frasconi, M.; Mazzei, F.; Ferri, T. Protein Immobilization at Gold-Thiol Surfaces and Potential for Biosensing. *Anal. Bioanal. Chem.* **2010**, *398*, 1545–1564.

Frederix, F.; Bonroy, K.; Laureyn, W.; Reekmans, G.; Campitelli, A.; Dehaen, W.; Maes, G. Enhanced Performance of an Affinity Biosensor Interface Based on Mixed Self-Assembled Monolayers of Thiols on Gold. *Langmuir* **2003**, *19* (10), 4351–4357.

Fontana, A.; Spolaore, B.; Mero, A.; Veronese, F. M. Site-specific Modification and PEGylation of Pharmaceutical Proteins Mediated by Transglutaminase. *Adv. Drug Deliv. Rev.* **2008**, *60* (1), 13–28.

Fried, S. D.; Boxer, S. G. Electric Fields and Enzyme Catalysis. *Annu. Rev. Biochem.* **2017**, *86*, 387-415.

Fuoco, T.; Finne-Wistrand, A.; Pappalardo, D. A Route to Aliphatic Poly(ester)s with Thiol Pendant Groups: From Monomer Design to Editable Porous Scaffolds. *Biomacromolecules* **2016**, *17* (4), 1383–1394.

Gagner, J. E.; Kim, W.; Chaikof, E. L. Designing Protein-Based Biomaterials for Medical Applications. *Acta Biomater.* **2014**, *10* (4), 1542–1557.

Gao, Y.; Joshi, M.; Zhao, Z.; Mitragotri, S. PEGylated Therapeutics in the Clinic. *Bioeng. Transl. Med.* **2020**, *9* (1), e10600, 28 pages.

Gevrek, T. N.; Cosar, M.; Aydin, D.; Kaga, E.; Arslan, M.; Sanyal, R.; Sanyal, R. Facile Fabrication of a Modular "Catch and Release" Hydrogel Interface: Harnessing Thiol–Disulfide Exchange for Reversible Protein Capture and Cell Attachment. *ACS Appl. Mater. Interfaces* **2018**, *10* (17), 14399–14409.

Givetal, N. I.; Ushakov, S. N.; Panarin, E. F.; Popova, G. O. Experimental Studies on Penicillin Polymer Derivatives (in Russian). *Antibiotiki* **1965**, *10*, 701-706.

Gregor, H. P.; Dolar, D.; Hoeschele, G. K. Polythiolstyrene-A New Oxidation-Reduction Ion Exchange Resin. *J. Am. Chem. Soc.* **1955**, *77* (13), 3675–3675.

Grover, G. N.; Alconcel, S. N. S.; Matsumoto, N. M.; Maynard, H. D. Trapping of Thiol-Terminated Acrylate Polymers with Divinyl Sulfone to Generate Well-Defined Semitelechelic Michael Acceptor Polymers. *Macromolecules* **2009**, *42* (20), 7657–7663.

Haller, B.; Jahnke, K.; Weiss, M; Göpfrich, K.; Platzman, I.; Spatz, J. Autonomous Directional Motion of Actin-Containing Cell-Sized Droplets. *Adv. Intell. Syst.* **2021**, *3*, 2000190, 8 pages.

Hanczyc, M. M.; Toyota, T.; Ikegami, T.; Packard, N.; Sugawara, T. Fatty Acid Chemistry at the Oil-Water Interface: Self-Propelled Oil Droplets. *J. Am. Chem. Soc.* **2007**, *129* (30), 9386–9391.

Harijan, M.; Singh, M. Zwitterionic Polymers in Drug Delivery: A Review. *J. Mol. Recognit.* **2021**, *35* (1), e2944, 13 pages.

Harris, J. M.; Chess, R. B. Effect of PEGylation on Pharmaceuticals. *Nat. Rev. Drug Discov.* **2003**, *2*, 214-221.

Heredia, K. L.; Bontempo, D.; Ly, T.; Byers, J. T.; Halstenberg, S.; Maynard, H. D. In Situ Preparation of Protein−"Smart" Polymer Conjugates with Retention of Bioactivity. *J. Am. Chem. Soc.* **2005**, *127* (48), 16955–16960.

Ho, C.; Slater, S. J.; Stubbs, C. D. Hydration and Order in Lipid Bilayers. *Biochemistry* **1995**, *34*, 6188–6195.

Hoang, M. V.; Chung, H.-J.; Elias, A. L. Irreversible Bonding of Polyimide and Polydimethylsiloxane (PDMS) Based on a Thiol-Epoxy Click Reaction. *J. Micromech. Microeng.* **2016**, *26*, 105019, 9 pages.

Hong, H.; Lee, U.-J.; Lee, S. H.; Kim, H.; Lim, G.-H.; Lee, S.-H.; Son, H. F.; Kim, B.-G.; Kim, K.-J. Highly Efficient Site-Specific Protein Modification Using Tyrosinase from Streptomyces avermitilis: Structural Insight. *Int. J. Biol. Macromol.* **2024**, *225*, 128313, 11 pages.

Hong, V.; Presolski, S. I.; Ma, C.; Finn, M. G. Analysis and Optimization of Copper-Catalyzed Azide–Alkyne Cycloaddition for Bioconjugation. *Angew. Chem.* **2009**, *121*, 10063 –10067.

Hoyle, C. E.; Lowe, A.; Bowman, C. N. Thiol-Click Chemistry: A Multifaceted Toolbox for Small Molecule and Polymer Synthesis. *Chem. Soc. Rev.* **2010**, *4*, 1355–1387.

Hu, Y.; Samanta, D.; Parelkar, S. S.; Hong, S. W.; Wang, Q.; Russell, T. P.; Emrick, T. Ferritin–Polymer Conjugates: Grafting Chemistry and Integration into Nanoscale Assemblies. *Adv. Funct. Mater.* **2010**, *20* (20), 3603–3612.

Hu, G. J.; Parelkar, S. S.; Emrick, T. A Facile Approach to Hydrophilic, Reverse Zwitterionic, Choline Phosphate Polymers. *Polym. Chem.* **2015**, *6* (4), 525–530.

Hu, G.; Emrick, T. Functional Choline Phosphate Polymers. *J. Am. Chem. Soc.* **2016**, *138*, 1828–1831.

Huo, M.; Yuan, J.; Tao, L.; Wei, Y. Redox-Responsive Polymers for Drug Delivery: From Molecular Design to Applications. *Polym. Chem.* **2014**, *5*, 1519–1528.

Hou, J.; Pearce, E. Characterization of Polymer Molecular Weight Distribution by NMR Diffusometry: Experimental Criteria and Findings. *Anal. Chem.* **2021**, *93*, 7958–7964.

Isarov, S. A.; Lee, P. W.; Pokorski, J. K. "Graft-to" Protein/Polymer Conjugates Using Polynorbornene Block Copolymers. *Biomacromolecules* **2016**, *17* (2), 641–648.

Ishihara, K.; Ueda, T.; Nakabayashi, N. Preparation of Phospholipid Polymers and Their Properties as Polymer Hydrogel Membranes. *Polym. J.* **1990**, *22* (5), 355–360.

Ishihara, K. Highly Lubricated Polymer Interfaces for Advanced Artificial Hip Joints Through Biomimetic Design. *Polym. J.* **2015**, *47*, 585–597.

Ishihara, K.; Oshida, H.; Endo, Y.; Ueda, T.; Watanabe, A.; Nakabayashi, N. Hemocompatibility of Human Whole Blood on Polymers with a Phospholipid Polar Group and its Mechanism. *J. Biomed. Mater. Res*. **1992**, *26*, 1543–1552.

Ishihara, K.; Tsuji, T.; Kurosaki, T.; Nakabayashi, N. Hemocompatibility on Graft Copolymers Composed of Poly(2-methacryloyloxyethyl phosphorylcholine) Side Chain and Poly(n-butyl methacrylate) Backbone. *J. Biomed. Mater. Res*. **1994**, *28*, 225–232.

Ishihara, K.; Nomura, H.; Mihara, T.; Kurita, K.; Iwasaki, Y.; Nakabayashi, N. Why do Phospholipid Polymers Reduce Protein Adsorption? *J. Biomed. Mater. Res.* **1998**, 39, 323–330.

Ishihara, K.; Mu, Mingwei, M.; Konno, T.; Inoue, Y.; Fukazawa, K. The Unique Hydration State of Poly(2-methacryloyloxyethyl phosphorylcholine). *J. Biomater. Sci. Polym. Ed.* **2017**, *28* (10-12), 884–899.

Ishihara, K. Revolutionary Advances in 2-Methacryloyloxyethyl Phosphorylcholine Polymers as Biomaterials. *J. Biomed. Mater. Res. A* **2019**, *107* (5), 933–943.

Iwasaki, Y.; Ishihara, K. Phosphorylcholine-Containing Polymers for Biomedical Applications. *Anal. Bioanal. Chem.* **2005**, 381, 534–546.

Jackson, M. A.; Werfel, T. A.; Curvino, E. J.; Yu, F.; Kavanaugh, T. E.; Sarett, S. M.; Dockery, M. D.; Kilchrist, K. V.; Jackson, A. N.; Giorgio, T. D.; Duvall, C. L. Zwitterionic Nanocarrier Surface Chemistry Improves siRNA Tumor Delivery and Silencing Activity Relative to Polyethylene Glycol. *ACS Nano* **2017**, *11* (6), 5680–5696.

Jatzkewitz, H. Peptamin (Glycyl-L-leucyl-mescaline) Bound to Blood Plasma Expander (Polyvinylpyrrolidone) as a New Depot form of a Biologically Active Primary Amine (Mescaline) *Z. Naturforsch.* **1955**, *10b*, 27–31.

Jiang, W.; Wu, Z.; Gao, Z.; Wan, M.; Zhou, M.; Mao, C.; Shen, J. Artificial Cells: Past, Present and Future. *ACS Nano* **2022**, *16* (10), 15705–15733.

Jin, C.; Krüger, C.; Maass, C. Chemotaxis and Autochemotaxis of Self-Propelling Droplet Swimmers. *PNAS* **2017**, *114* (20), 5089–5094.

Jin, Q.; Chen, Y.; Wang, Y.; Ji, J. Zwitterionic Drug Nanocarriers: A Biomimetic Strategy for Drug Delivery. *Colloids Surf. B: Biointerfaces* **2014**, *124*, 80–86.

Jones, M. W.; Strickland, R. A.; Schumacher, F. F.; Caddick, S.; Baker, J. R.; Gibson, M. I.; Haddleton, D. M. Polymeric Dibromomaleimides as Extremely Efficient Disulfide Bridging Bioconjugation and Pegylation Agents. *J. Am. Chem. Soc.* **2012**, *134* (3), 1847–1852.

Kalia, D.; Malekar, P. V.; Parthasarathy, M. Exocyclic Olefinic Maleimides: Synthesis and Application for Stable and Thiol-Selective Bioconjugation. *Angew. Chem. Int. Ed.* **2015**, *55* (4), 1432-1435.

Kasuo, Y.; Kitahata, H.; Koyano, Y.; Takinoue, M.; Asakura, K.; Banno, T. Start of Micrometer-Sized Oil Droplet Motion through Generation of Surfactants. *Langmuir* **2019**, *35* (41), 13351–13355.

Keefe, A. J.; Jiang, S. Poly(zwitterionic)protein Conjugates offer Increased Stability without Sacrificing Binding Affinity or Bioactivity. *Nat. Chem.* **2012**, *4*, 59–63.

Kharkar, P. M.; Kloxin, A. M.; Kiick, K. L. Dually Degradable Click Hydrogels for Controlled Degradation and Protein Release. *J. Mater. Chem. B* **2014**, *2* (34), 5511–5521.

Khunsuk, P.; Chawalitpong, S.; Sawutdeechaikul, P.; Palaga, T.; Hoven, V. P. Gold Nanorods Stabilized by Biocompatible and Multifunctional Zwitterionic Copolymer for Synergistic Cancer Therapy. *Mol. Pharmaceutics* **2018**, *15*, 164–174.

Kihara, N.; Kanno, C.; Fukutomi, T. Synthesis and Properties of Microgel Bearing a Mercapto Group. *J. Polym. Sci. A. Polym. Chem.* **1997**, *35* (8), 1443–1451.

Kim, Y. H.; Her, A.-Y.; Rha, S.-W.; Choi, B. G.; Choi, S. Y. ; Byun, J. K. ; Park, Y. ; Kang, D. O.; Jang, W. Y.; Kim, W.; Choi, W. G.; Kang, T. S.; Ahn, J.; Park, S.-H.; Park, J. Y.; Lee, M-H.; Choi, C. U.; Park, C. G.; Seo, H. S. Three-Year Major Clinical Outcomes of Phosphorylcholine Polymer- vs Biolinx Polymer-Zotarolimus-Eluting Stents. *Medicine (Baltimore)* **2019**, *98* (32), e16767, 10 pages.

Kloxin, C. J.; Bowman, C. N. Covalent Adaptable Networks: Smart, Reconfigurable and Responsive Network Systems. *Chem. Soc. Rev.* **2013**, *42*, 7161–7173.

Ko, J. H.; Maynard, H. D. A Guide to Maximizing the Therapeutic Potential of Protein-Polymer Conjugates by Rational Design. *Chem. Soc. Rev.* **2018**, *47*, 8998-9014.

Kolate, A.; Baradia, D.; Patil, S.; Vhora, I.; Kore, G.; Misra, A. PEG — A Versatile Conjugating Ligand for Drugs and Drug Delivery Systems. *J. Cont. Release* **2014**, *192*, 67–81.

Konkolewicz, D.; Gray-Weale, A.; Perrier, S. Hyperbranched Polymers by Thiol−Yne Chemistry: From Small Molecules to Functional Polymers. *J. Am. Chem. Soc*. **2009**, *131* (50), 18075–18077.

Kosif, I.; Chang, C. C.; Bai, Y.; Ribbe, A. E.; Balazs, A. C.; Emrick, T. Picking up Nanoparticles with Functional Droplets. *Adv. Mater. Interfaces* **2014**, *1*, 1400121, 6 pages.

Kopeček, J. Polymer–Drug Conjugates: Origins, Progress To-Date and Future Directions. *Adv. Drug Deliv. Rev.* **2013**, *65* (1), 49–59.

Kopeček, J.; Kopečková, P.; Minko, T.; Lu, Z.-R. HPMA Copolymer–Anticancer Drug Conjugates: Design, Activity, and Mechanism of Action. *Eur. J. Pharm. Biopharm*. **2000**, *50* (1), 61–81.

Kostka, L.; Kotrchová, L.; Šubr, V.; Libánská, A.; Ferreira, C. A.; Malátová, I.; Lee, H. J.; Barnhart, T. E.; Engle, J. W.; Cai, W.; Šírová, M.; Etrych, T. HPMA-based Star Polymer Biomaterials with Tuneable Structure and Biodegradability Tailored for Advanced Drug Delivery to Solid Tumours. *Biomaterials* **2020**, *235*, 119728, 14 pages.

Kovacs, E. W.; Hooker, J. M.; Romanini, D. W.; Holder, P. G.; Berry, K. E.; Francis, M. B. Dual-Surface-Modified Bacteriophage MS2 as an Ideal Scaffold for a Viral Capsid-Based Drug Delivery System. *Bioconjugate Chem.* **2007**, *18* (4), 1140–1147.

Kozma, G. T.; Shimizu, T.; Ishida, T.; Szebeni, J. Anti-PEG Antibodies: Properties, Formation, Testing and Role in Adverse Immune Reactions to PEGylated Nano-biopharmaceuticals. *Adv. Drug Deliv. Rev.* **2020**, *154-155*, 163–175.

Kratz, K.; Narasimhan, A.; Tangirala, R.; Moon, S.; Revanur, R.; Kundu, S.; Kim, H. S.; Crosby, A. J.; Russell, T. P.; Emrick, T.; Kolmakov, G.; Balazs, A. C. Probing and Repairing Damaged Surfaces with Nanoparticle-Containing Microcapsules. *Nat. Nanotechnol.* **2012**, *7*, 87– 90.

Kuo, W.-H.; Wang, M.-J.; Chien, H.-W.; Wei, T.-C.; Lee, C.; Tsai, W.-B. Surface Modification with Poly(sulfobetaine methacrylate-co-acrylic acid) To Reduce Fibrinogen Adsorption, Platelet Adhesion, and Plasma Coagulation. *Biomacromolecules* **2011**, *12* (12), 4348–4356.

Lach, S.; Yoon, S. M.; Gryzbowski, B. A. Tactic, Reactive, and Functional Droplets Outside of Equilibrium. *Chem. Soc. Rev.* **2016**, *45*, 4766–4796.

Lagaraine, C.; Hoarau, C.; Chabot, V.; Velge-Roussel, F.; Lebranchu, Y. *Int. Immunol.* **2005**, *17*, 351–363.

Lalani, R.; Liu, L. Electrospun Zwitterionic Poly(Sulfobetaine Methacrylate) for Nonadherent, Superabsorbent, and Antimicrobial Wound Dressing Applications. *Biomacromolecules* **2012**, *13* (6), 1853–1863.

Lang, Y.; Kiick, K. L. Liposome-Cross-Linked Hybrid Hydrogels for Glutathione-Triggered Delivery of Multiple Cargo Molecules. *Biomacromolecules* **2016**, *17* (2), 601–614.

Laschewsky, A.; Rosenhahn. A. Molecular Design of Zwitterionic Polymer Interfaces: Searching for the Difference. *Langmuir* **2019**, *35* (5), 1056–1071.

Laskar, A.; Shklyaev, O. E.; Balazs, A. C. Designing Self-Propelled, Chemically Active Sheets: Wrappers, Flappers, and Creepers. *Sci. Adv.* **2018**, *4* (12), eaav1745, 11 pages.

Lee, M. H.; Sessler, J. L.; Kim, J. S. Disulfide-Based Multifunctional Conjugates for Targeted Theranostic Drug Delivery. *Acc. Chem. Res.* **2015**, *48* (11), 2935–2946.

Leimkühler, S.; Ogunkola, M. O. 10 - Sulfur Transferases in the Pathways of Molybdenum Cofactor Biosynthesis and tRNA Thiolation in Humans. In *Foundations and Frontiers in Enzymology, Sulfurtransferases* [Online]; Nagahara, N., Ed.; Academic Press: 2023, 207–236.

Lele, B. S.; Murata, H.; Matyjaszewski, K.; Russell, A. J. Synthesis of Uniform Protein−Polymer Conjugates. *Biomacromolecules* **2005**, *6* (6), 3380–3387.

Le Neindre, M.; Nicolaÿ, R. Polythiol Copolymers with Precise Architectures: A Platform for Functional Materials. *Polym. Chem.* **2014**, *5* (16), 4601–4611.

Le Neindre, M.; Nicolaÿ, R. One-pot Deprotection and Functionalization of Polythiol Copolymers via Six Different Thiol–X Reactions. *Polym. Int.* **2013**, *63* (5), 887–893.

Letteri, R. A.; Chalarca, C. F. S.; Bai, Y.; Hayward, R. C.; Emrick, T. Forming Sticky Droplets from Slippery Polymer Zwitterions. *Adv. Mater.* **2017**, *29*, 17002921, 8 pages.

Lewis, A.; Tang, Y.; Brocchini, S.; Choi, J.; Godwin, A. Poly(2-methacryloyloxyethyl phosphorylcholine) for Protein Conjugation. *Bioconjugate Chem*. **2008**, *19* (11), 2144–2155.

Lin, Y.; Wang, L.; Huang, X. Dynamic Behaviour in Microcompartments. *Chem. Eur. J.* **2019**, *25*, 16440–16450.

Li, D.; Wei, Q.; Wu, C.; Zhang, X.; Xue, Q.; Zheng, T.; Cao, M. Superhydrophilicity and Strong Salt-Affinity: Zwitterionic Polymer Grafted Surfaces in Biological Systems. *Adv. Colloid Interface Sci.* **2020**, *278*, 102141, 18 pages.

Li, J.-Y.; Qiu, L.; Xu, X.-F.; Pan, C.-Y.; Hong, C.-Y.; Zhang, W.-J.; Photo-Responsive Camptothecin-Based Polymeric Prodrug Coated Silver Nanoparticles for Drug Release Behaviour Tracking *via* the Nanomaterial Surface Energy Transfer (NSET) Effect. *J. Mater. Chem. B* **2018**, *6*, 1678-1687.

Li, J.; Richardson, J. J.; Ejima, H. Synthesis of Dithiocatechol-Pendant Polymers. *J. Am. Chem. Soc.* **2022**, *144* (6), 2450–2454.

Li, M.; Cheng, F.; Li, H.; Jin, W.; Chen, C.; He, W.; Cheng, W.; Wang, Q. Site-Specific and Covalent Immobilization of His-Tagged Proteins via Surface Vinyl Sulfone–Imidazole Coupling. *Langmuir* **2019**, *35* (50), 16466–16475.

Li, M.; De, P.; Gondi, S. R.; Sumerlin, B. S. End Group Transformations of RAFT-Generated Polymers with Bismaleimides: Functional Telechelics and Modular Block Copolymers. *Polym. Sci. A. Polym. Chem.* **2008**, *46* (15), 5093–5100.

Li, Q.; Wen, C.; Yang, J. Zhou, X.; Zhu, Y.; Zheng, J.; Cheng, G.; Bai, J.; Xu, T.; Ji, J.; Jiang, S.; Zhang, L.; Zhang, P. Zwitterionic Biomaterials. *Chem. Rev.* **2022**, *122* (23), 17073–17154.

Liaw, D.-J.; Huang, C.-C.; Lee, W.-F.; Borbély, J.; Kang, E.-T. Synthesis and Characteristics of the Poly(carboxybetaine)s and the Corresponding Cationic Polymers. *J. Polym. Sci., Part A: Polym. Chem.* **2000**, *35* (16), 3527–3536.

Lin, W.; Ma, G.; Kampf, N.; Yuan, Z.; Chen, S. Development of Long-Circulating Zwitterionic Cross-Linked Micelles for Active-Targeted Drug Delivery. *Biomacromolecules* **2016**, *17* (6), 2010–2018.

Liu, J.; Bulmus, V.; Herlambang, D. L.; Barner-Kowollik, C.; Stenzel, M. H.; Davis, T. P. In Situ Formation of Protein–Polymer Conjugates through Reversible Addition Fragmentation Chain Transfer Polymerization. *Angew. Chem. Int. Ed.* **2007**, *46* (17), 3099-3103.

Liu, Y., Sheri, M., Cole, M. D., Emrick, T. & Russell, T. P. Combining Fullerenes and Zwitterions in Non-Conjugated Polymer Interlayers to Raise Solar Cell Efficiency. *Angew. Chem. Int. Ed.* **2018**, *57*, 9675–9678.

Liang, S.; Liu, Y.; Jin, X.; Liu, G.; Wen, J.; Zhang, L.; Li, J.; Yuan, X.; Chen, I. S. Y.; Chen, W.; Wang, H.; Shi, L.; Zhu, X.; Lu, Y. Phosphorylcholine Polymer Nanocapsules Prolong the Circulation Time and Reduce the Immunogenicity of Therapeutic Proteins. *Nano Res.* **2016**, *9*, 1022-1031.

Lobba. M. J.; Fellmann, C.; Marmelstein, A. M.; Maza, J. C.; Kissman, E. N.; Robinson, S. A.; Staahl, B. T.; Urnes, C.; Lew, R. J.; Mogilevsky, C. S.; Doudna, J. A.; Francis, M. B. Site-Specific Bioconjugation through Enzyme-Catalyzed Tyrosine–Cysteine Bond Formation. *ACS Cent. Sci.* **2020**, *6* (9), 1564–1571.

Lowe, A. B.; Billingham, N. C.; Armes, S. P. Synthesis and Properties of Low-Polydispersity Poly(sulfopropylbetaine)s and Their Block Copolymers. *Macromolecules* **1999**, *32* (7), 2141–2148.

Lowe, A. B. Thiol-ene "Click" Reactions and Recent Applications in Polymer and Materials Synthesis: A First Update. *Polym. Chem.* **2014**, *5*, 4820-4870.

Lu, Z.-P.; Kopečková, P.; Wu, Z.; Kopeček, J. Functionalized Semitelechelic Poly[N-(2-hydroxypropyl)methacrylamide] for Protein Modification. *Bioconjugate Chem.* **1998**, *9* (6), 793–804.

Lurie-Luke, E. Product and Technology Innovation: What can Biomimicry Inspire? *Biotechnol. Adv.* **2014**, *32*, 1494–1505.

Luxenhofer, R.; Han, Y.; Schulz, A.; Tong, J.; Kabanov, A. V.; He, Z.; Jordan, R. Poly(2-oxazoline)s as Polymer Therapeutics. *Macromol. Rapid Commun.* **2012**, *33* (19), 1613-1631.

Maass, C. C.; Krüger, C.; Herminghaus, S.; Bahr, C. Swimming Droplets. *Annu. Rev. Condens. Matter Phys.* **2015**, *7*, 171–193.

Macková, H.; Plichta, Z.; Hlídková, H.; Sedláček, O.; Konefal, R.; Sadakbayeva, Z.; Dušková-Smrčková, M.; Horák, D.; Kubinová, S. Reductively Degradable Poly(2-hydroxyethyl methacrylate) Hydrogels with Oriented Porosity for Tissue Engineering Applications. *ACS Appl. Mater. Interfaces* **2017**, *9*, 10544–10553.

Macková, H.; Hlídková, H.; Kaberova, Z.; Proks, V.; Kučka, J.; Patsula, V.; Vetrik, M.; Janoušková, O.; Podhorská, B.; Pop-Georgievski, O.; Kubinová, S.; Horák, D. Thioated Poly(2-hydroxyethyl methacrylate) Hydrogels as a Degradable Biocompatible Scaffold for Tissue Engineering. *Mater. Sci. Eng. C* **2021**, *131*, 112500, 11 pages.

Maeda, H.; Seymour, L. W.; Miyamoto, Y. Conjugates of Anticancer Agents and Polymers: Advantages of Macromolecular Therapeutics In Vivo. *Bioconjugate Chem.* **1992**, *3* (5), 351–362.

Maeda, H. SMANCS and Polymer-conjugated Macromolecular Drugs: Advantages in Cancer Chemotherapy. *Adv. Drug Deliv. Rev.* **2001**, *46* (1–3), 169–185.

Maiti, S.; Shklyaev, O. E.; Balazs, A. C.; Sen, A. Self-Organization of Fluids in a Multi-enzymatic Pump System. *Langmuir* **2019**, *35*, 3724–3732.

Malik, N.; Evagorou, E. G.; Duncan, R. Dendrimer-Platinate: A Novel Approach to Cancer Chemotherapy. *Anti-Cancer Drugs* **1999**, *10* (8), 767–776.

Marmelstein, A. M.; Lobba, M. J. ; Mogilevsky, C. S. ; Maza, J. C.; Brauer, D. D.; Francis, M. B. Tyrosinase-Mediated Oxidative Coupling of Tyrosine Tags on Peptides and Proteins. *J. Am. Chem. Soc.* **2020**, *142* (11), 5078–5086.

Martin, R.; Rekondo, A.; de Luzuriaga, A. R.; Santamaria, A.; Odriozola, I. Mixing the Immiscible: Blends of Dynamic Polymer Networks. *RCS Adv.* **2015**, *5* (23), 17514–17518.

Mathé, G.; Loc, T. B.; Bernard, J. Effet sur la leucémie 1210 de la Souris d'une combinaison par diazotation d'**A**-méthopterine et de γ-globulines de hamsters porteurs de cette leucémie par hétérogreffe. *C R Hebd. Seances Acad. Sci.* **1958**, *246* (10),1626-1628.

Matsumura, Y.; Maeda, H. A New Concept for Macromolecular Therapeutics in Cancer Chemotherapy: Mechanism of Tumoritropic Accumulation of Proteins and the Antitumor Agent smancs. *Cancer Res.* **1986**, *46* (12:1), 6387–6392.

Maza, J. C.; Ramsey, A. V.; Mehare, M.; Krska, S. W.; Parish, C. A.; Francis, M. B. Secondary Modification of Oxidatively-modified Proline N-termini for the Construction of Complex Bioconjugates. *Org. Biomol. Chem.* **2020**, *18*, 1881–1885.

Maza, J. C.; Bader, D. L. V.; Xiao, L.; Marmelstein, A. M.; Brauer, D. D.; ElSohly, A. M.; Smith, M. J.; Krska, S. W.; Parish, C. A.; Francis, M. B. Enzymatic Modification of N-Terminal Proline Residues Using Phenol Derivatives. *J. Am. Chem. Soc.* **2019**, *141* (9), 3885–3892.

Maza, J. C.; García-Almedina, D. M.; Boike, L. E.; Hamlish, N. X.; Nomura, D. K.; Francis, M. B. Tyrosinase-Mediated Synthesis of Nanobody–Cell Conjugates. *ACS Cent. Sci.* **2022**, *8* (7), 955–962.

McRae, S.; Chen, X.; Kratz, K.; Samanta, D.; Henchey, E.; Schneider, S.; Emrick, T. Pentafluorophenyl Ester-Functionalized Phosphorylcholine Polymers: Preparation of Linear, Two-Arm, and Grafted Polymer–Protein Conjugates. *Biomacromolecules* **2012**, *13* (7), 2099–2109.

Meredith, C. H.; Moerman, P. G.; Groenewold, J.; Chiu, Y.-J.; Kegel, W. K.; van Blaaderen, A.; Zarzar, L. D. Predator–Prey Interactions Between Droplets Driven by Non-Reciprocal Oil Exchange. *Nat. Chem.* **2020**, *12*, 1136–1142.

Mi, L.; Jiang, S. Integrated Antimicrobial and Nonfouling Zwitterionic Polymers. *Angew. Chem. Int. Ed.* **2014**, *53*, 1746–1754.

Michal, B. T.; Jaye, C. A.; Spencer, E. J.; Rowan, S. J. Inherently Photohealable and Thermal Shape-Memory Polydisulfide Networks. *ACS Macro Lett.* **2013**, *2* (8), 694–699.

Mogilevsky, C. S.; Lobba, M. J.; Brauer, D. D.; Marmelstein, A. M.; Maza, J. C.; Gleason, J. M.; Doudna, J. A.; Francis, M. B. Synthesis of Multi-Protein Complexes through Charge-Directed Sequential Activation of Tyrosine Residues. *J. Am. Chem. Soc.* **2021**, *143* (34), 13538–13547.

Morales-Sanfrutos, J.; Lopez-Jaramillo, J.; Ortega-Munoz, M.; Megia-Fernandez, A.; Perez-Balderas, F.; Hernandez-Mateo, F.; Santoyo-Gonzalez, F. Vinyl Sulfone: A Versatile Function for Simple Bioconjugation and Immobilization. Org. Biomol. Chem. 2010, 8 (3), 667–675.

Muiznieks, L. D.; Keeley, F. W. Biomechanical Design of Elastic Protein Biomaterials: A Balance of Protein Structure and Conformational Disorder. *ACS Biomater. Sci. Eng.* **2017**, *3* (5), 661–679.

Mutlu, H.; Ceper, E. B.; Li. X.; Yang, J.; Dong, W.; Ozmen, M. M.; Theato, P. Sulfur Chemistry in Polymer and Materials Science. *Macromol. Rapid. Comm.* **2019**, *40*, 1800650, 51 pages.

Nagasaka, Y.; Tanaka, S.; Nehira, T.; Amimoto, T. Spontaneous Emulsification and Self-Propulsion of Oil Droplets Induced by the Synthesis of Amino Acid-Based Surfactants. *Soft Matter* **2017**, *37*, 6450–6457.

Nair, D. P.; Podgórski, M.; Chatani, S.; Gong, T.; Xi, W.; Fenoli, C. R.; Bowman, C. N. The Thiol-Michael Addition Click Reaction: A Powerful and Widely Used Tool in Materials Chemistry. *Chem. Mater.* **2014**, *26* (1), 724–744.

Nakai, S.; Nakaya, T.; Imoto, M. Polymeric Phospholipid Analog, 10*): Synthesis and Polymerization of 2-(Methacryloyloxy)ethyl 2-Aminoethyl Hydrogen Phosphate. *Makromol. Chem.* **1977**, *178*, 2963–2967.

Nakano, H.; Noguchi, Y.; Kakinoki, S.; Yamakawa, M; Osaka, I.; Iwasaki, Y. Highly Durable Lubricity of Photo-Cross-Linked Zwitterionic Polymer Brushes Supported by Poly(ether ether ketone) Substrate. *ACS Appl. Bio Mater*. **2020**, *3* (2), 1071–1078.

Nguyen, H. N.; Ngo, T. L. H.; Iwasaki, Y.; Huang, C.-J. Biodegradable Phosphocholine Cross-Linker with Ion-Pair Design for Tough Zwitterionic Hydrogel. *Adv. Mater. Interfaces* **2022**, *9* (33), 2201002, 11 pages.

Nijemeisland, M.; Abdelmohsen, L. K. E. A.; Huck, W. T. S.; Wilson, D. A.; van Hest, J. C. M. A Compartmentalized Out-of-Equilibrium Enzymatic Reaction Network for Sustained Autonomous Movement. *ACS Cent. Sci.* **2016**, *2* (11), 843–849.

Nilsson, L.; Csuth, Á.; Storsaeter, J.; Garvey, L. H.; Jenmalm, M. C. Vaccine Allergy: Evidence to Consider for COVID-19 Vaccines. *Curr. Opin. Allergy Clin. Immunol*. **2021**, *21* (4), 401-409.

Nori, A.; Kopeček, J. Intracellular Targeting of Polymer-Bound Drugs for Cancer Chemotherapy. *Adv. Drug Deliv. Rev.* **2005**, *57* (4), 609–636.

Otsuka, H.; Nagano, S.; Kobashi, Y.; Maeda, T.; Takahara, A. A Dynamic Covalent Polymer Driven by Disulfide Metathesis under Photoirradiation. *Chem. Comm.* **2010**, *7*, 1150–1152.

Overberger, C. G.; Lebovits, A. The Synthesis of Poly-p-thiostyrene, An Oxidation Reduction Polymer. *J. Am. Chem. Soc.* **1955**, *77* (13), 3675–3676.

Overberger, C. G.; Lebovits, A. Preparation of p-Vinylphenyl Thioacetate,[1] its Polymers, Copolymers and Hydrolysis Products. Water-Soluble Copolymers Containing Sulfhydryl Groups[2]. *J. Am. Chem. Soc.* **1956**, *78* (18), 4792–4797.

Ozer, I.; Tomak, A.; Zareie, H. M.; Baran, Y.; Bulmus. Effect of Molecular Architecture on Cell Interactions and Stealth Properties of PEG. *Biomacromolecules* **2017**, *18* (9), 2699–2710.

Pagaduan, J. N.; Hight-Huf, N.; Datar, A.; Nagar, Y.; Barnes, M.; Naveh, D.; Ramasubramaniam, A.; Katsumata, R.; Emrick, T. Electronic Tuning of Monolayer Graphene with Polymeric "Zwitterists". *ACS Nano* **2021**, *15* (2), 2762–2770.

Page, S. M.; Martorella, M.; Parelkar, S.; Kosif, I.; Emrick, T. Disulfide Cross-Linked Phosphorylcholine Micelles for Triggered Release of Camptothecin. *Mol. Pharmaceutics* **2013**, *10* (7), 2684–2692.

Page, S. M.; Henchey, E.; Chen, X., Schneider, S. and Emrick, T. Efficacy of PolyMPC-DOX Prodrugs in 4T1 Tumor-bearing Mice. *Mol. Pharmaceutics* **2014**, 11(5), 1715–1720.

Panarin, E. F.; Ushakov, S. N. Synthesis of Polymer Salts and Amidopenicillines (in Russian). *Khim. Pharm. Zhur.* **1968**, *2*, 28-31.

Park, H.; Otte, A.; Park, K. Evolution of Drug Delivery Systems: From 1950 to 2020 and Beyond. *J. Cont. Release* **2022**, *342*, 53-65.

Patino, T.; Porchetta, A.; Jannasch, A.; Lladó, A.; Stumpp, T.; Schäffer, E.; Ricci, F.; Sánchez, S. Self-Sensing Enzyme-Powered Micromotors Equipped with pH-Responsive DNA Nanoswitches. *Nano Lett.* **2019**, *19* (6), 3440–3447.

Pokorski, J. K.; Breitenkamp, K.; Liepold, L. O.; Qazi, S.; Finn, M. G. Functional Virus-Based Polymer–Protein Nanoparticles by Atom Transfer Radical Polymerization. *J. Am. Chem. Soc.* **2011**, *133* (24), 9242–9245.

Poole, L. B. The Basics of Thiols and Cysteines in Redox Biology and Chemistry. *Free Radic. Biol. Med.* **2014**, *0*, 148–157.

Raggatt, L. J.; Partridge, N. C. Cellular and Molecular Mechanisms of Bone Remodeling. *J. Biol. Chem.* **2010,** *285* (33), 25103–25108.

Raja, K. S.; Wang, Q.; Gonzalez, M. J.; Manchester, M.; Johnson, J. E.; Finn, M. G. Hybrid Virus−Polymer Materials. 1. Synthesis and Properties of PEG-Decorated Cowpea Mosaic Virus. *Biomacromolecules* **2003**, *4* (3), 472–476.

Ramsey, A. V.; Bischoff, A. J.; Francis, M. B. Enzyme Activated Gold Nanoparticles for Versatile Site-Selective Bioconjugation. *J. Am. Chem. Soc.* **2021**, *143* (19), 7342–7350.

Ravasco, J. M. J. M.; Faustino, H.; Trindade, A.; Gois, P. M. P. Bioconjugation with Maleimides: A Useful Tool for Chemical Biology. Chem. Eur. J. 2019, 25, 43–59.

Rekondo, A.; Martin, R.; de Luzuriaga, A. R.; Cabañero, G.; Grande, H. J.; Odriozola, I. Catalyst-Free Room-Temperature Self-Healing Elastomers Based on Aromatic Disulfide Metathesis. *Mater. Horiz.* **2014**, *1* (2), 237–240.

Rideau, E.; Dimova, R.; Schwille, P.; Wurm, F.R.; Landfester, K. Liposomes and Polymersomes: A Comparative Review towards Cell Mimicking. Chem. Soc. Rev. **2018**, 47, 8572–8610.

Ringsdorf, H. Structure and Properties of Pharmacologically Active Polymers. J. Polym. Sci., Polym. Symp. **1975**, *51*, 135–153.

Roskoski, R. A Historical Overview of Protein Kinases and Their Targeted Small Molecule Inhibitors. *Pharmacol. Res*. **2015**, *100*, 1–23.

Russell, J. T.; Lin, Y.; Böker, A.; Su, L.; Carl, P.; Zettl, H.; He, J.; Sill, K.; Tangirala, R.; Emrick, T.; Littrell, K.; Thiyagarajan, P.; Cookson, D.; Fery, A.; Wang, Q.; Russell, T. P. Self-Assembly and Cross-Linking of Bionanoparticles at Liquid–Liquid Interfaces. *Angew. Chem.* **2005**, *117* (16), 2472–2478.

Sae-ung, P.; Kolewe, K. W.; Bai, Y.; Rice, E. W.; Schiffman, J. D.; Emrick, T.; Hoven, V. P. Antifouling Stripes Prepared from Clickable Zwitterionic Copolymers. *Langmuir* **2017**, *33* (28), 7028–7035.

Santiago, I.; Simmel, F. C. Self-Propulsion Strategies for Artificial Cell-Like Compartments. *Nanomaterials* **2019**, *9*, 1680, 14 pages.

Samanta, D.; McRae, S.; Cooper, B.; Hu, Y.; Emrick, T. End-functionalized Phosphorylcholine Methacrylates and their use in Protein Conjugation. *Biomacromolecules* **2008**, *9*, 2891-2897.

Sathyan, A.; Yang, Z.; Bai, Y.; Kim, H.; Crosby, A. J.; Emrick, T. Simultaneous "Clean-and-Repair" of Surfaces Using Smart Droplets. *Adv. Funct. Mater*. **2019**, *29*, 1805219, 6 pages.

Sen Gupta, S.; Kuzelka, J.; Singh, P.; Lewis, W. G.; Manchester, M.; Finn, M. G. Accelerated Bioorthogonal Conjugation: A Practical Method for the Ligation of Diverse Functional Molecules to a Polyvalent Virus Scaffold. *Bioconjugate Chem.* **2005**, *16* (6), 1572–1579.

Shahkaramipour, N.; Lai, C. K.; Venna, S. R.; Sun, H.; Cheng, C.; Lin, H. Membrane Surface Modification Using Thiol-Containing Zwitterionic Polymers via Bioadhesive Polydopamine. *Ind. Eng. Chem. Res.* ***2018***, *57* (6), 2336–2345.

Shao, Q.; Jiang, S. Molecular Understanding and Design of Zwitterionic Materials. *Adv. Mater.* **2014**, *27* (1), 15–26.

Shaunak, S.; Godwin, A.; Choi, J.-W.; Balan, S.; Pedone, E.; Vijayarangam, D.; Heidelberger, S.; Teo, I.; Zloh, M.; Brocchini, S. Site-Specific PEGylation of Native Disulfide Bonds in Therapeutic Proteins. *Nat. Chem. Biol.* **2006**, *2*, 312-313.

Shi, D.; Beasock, D.; Fessler, A.; Szebeni, J.; Ljubimova, J. Y.; Afonin, K. A.; Dobrovolskaia, M. A. To PEGylate or not to PEGylate: Immunological Properties of Nanomedicine's Most Popular Component, Polyethylene Glycol and its Alternatives. *Adv. Drug Deliv. Rev.* **2022**, *180*, 114079, 22 pages.

Shiomoto, S.; Inoue, K.; Higuchi, H.; Nishimura, S.-N.; Takaba, H.; Tanaka, M.; Kobayashi, M. Characterization of Hydration Water Bound to Choline Phosphate-Containing Polymers. *Biomacromolecules* **2022**, *23* (7), 2999–3008.

Shklyaev, O. E.; Shum, H.; Sen, A.; Balazs, A. C. Harnessing Surface-Bound Enzymatic Reactions to Organize Microcapsules in Solution. *Sci. Adv.* **2016**, *2* (3), e150183, 13 pages.

Shum, H.; Balazs, A. C. **Flow**-Driven Assembly of Microcapsules into Three-Dimensional Towers. *Langmuir* ***2018***, *34* (8), 2890–2899.

Skinner, M.; Johnston, B. M.; Liu, Y.; Hammer, B.; Selhorst, R.; Xenidou, I.; Perry, S. L.; Emrick, T. Synthesis of Zwitterionic Pluronic Analogs. *Biomacromolecules* **2018**, *19* (8), 3377–3389.

Somasundar, A.; Ghosh, S.; Mohajerani, F.; Massenburg, L.; Yang, T.; Cremer, P.; Velegol, D.; Sen, A. Positive and Negative Chemotaxis of Enzyme-Coated Liposome Motors. *Nat. Nanotechnol.* **2019**, *14*, 1129–1134.

Sonu, K. P.; Zhou, L.; Biswas, S.; Klier, J.; Balazs, A. C.; Emrick, T.; Peyton, S. R. Strain-Stiffening Hydrogels with Dynamic, Secondary Cross-Linking. *Langmuir* **2023**, *39* (7), 2659–2666.

Steinmetz, N. F.; Manchester, M. PEGylated Viral Nanoparticles for Biomedicine: The Impact of PEG Chain Length on VNP Cell Interactions In Vitro and Ex Vivo. *Biomacromolecules* **2009**, *10* (4), 784–792.

Stone, C. A.; Yiwei Liu, Y.; Relling, M. V.; Krantz, M. S.; L. Pratt, A. L.; Abreo, A.; Hemler, J. A.; Phillips, E. J. Immediate Hypersensitivity to Polyethylene Glycols and Polysorbates: More Common Than We Have Recognized. *J. Allergy Clin. Immunol. Pract*. **2019**, *7* (5), 1533–1540.e8.

Strader, R. L.; Shmidov, Y.; Chilkoti, A. Encoding Structure in Intrinsically Disordered Protein Biomaterials. *Acc. Chem. Res.* **2024**. DOI: 10.1021/acs.accounts.3c00624

Suematsu, N. J.; Nakata, S. Evolution of Self-Propelled Objects: From the Viewpoint of Nonlinear Science. *Chem. Eur. J.* **2018**, *24* (24), 6308–6324.

Summonte, S.; Racaniello, G. F.; Lopedota, A.; Denora, N.; Bernkop-Schnürch, A. Thiolated Polymeric Hydrogels for Biomedical Application: Cross-Linking Mechanisms. *J. Control. Release* **2021**, *330* (10), 470–482.

Sun, H.; Chang, M. Y. Z.; Cheng, W.; Wang, Q.; Commisso, A.; Capeling, M.; Wu, Y.; Cheng, C. Biodegradable Zwitterionic Sulfobetaine Polymer and its Conjugate with Paclitaxel for Sustained Drug Delivery. *Acta Biomater.* **2017**, *64*, 290–300.

Sun, H.; Yan, L.; Zhang, R.; Lovell, J. F.; Wu, Y.; Cheng, C. A Sulfobetaine Zwitterionic Polymer-Drug Conjugate for Multivalent Paclitaxel and Gemcitabine Co-Delivery. *Biomater. Sci*. **2021**, *9* (14), 5000-5010.

Suzuki, K.; Sugawara, T. Phototaxis of Oil Droplets Comprising a Caged Fatty Acid Tightly Linked to Internal Convection. *ChemPhysChem.* **2016**, *17* (15), 2300–2303.

Tai, C.-H.; Wu, H.-C.; Li, W.-R. Studies on a Novel Safety-Catch Linker Cleaved by Pummerer Rearrangement[1]. *Org. Lett.* **2004**, *6* (17), 2905–2908.

Toohey, J. I.; Cooper, A. J. L. Thiosulfoxide (Sulfane) Sulfur: New Chemistry and New Regulatory Roles in Biology. *Molecules* **2014**, *19* (8), 12789–12813.

Toyota, T.; Sugiyama, H.; Hiroi, S.; Ito, H.; Kitahata, H. Chemically Artificial Rovers Based on Self-Propelled Droplets in Micrometer-Scale Environment. *Curr. Opin. Colloid Interface Sci.* **2020**, *49*, 60–68.

Turecek, P. L.; Bossard, M. J.; Schoetens, F.; Ivens, I. A. PEGylation of Biopharmaceuticals: A Review of Chemistry and Nonclinical Safety Information of Approved Drugs. *J. Pharm. Sci*. **2016**, *105* (2), 460-475.

Tuten, B. T.; Chao, D.; Lyon, C. K.; Berda, E. B. Single-Chain Polymer Nanoparticles via Reversible Disulfide Bridges. *Polym. Chem*. **2012**, *3* (11), 3068–3071.

Venault, A.; Chang, Y. Designs of Zwitterionic Interfaces and Membranes. *Langmuir* **2019**, *35* (5), 1714–1726.

Veronese, F. M.; Pasut, G. PEGylation, Successful Approach to Drug Delivery. *Drug Discov. Today* **2005**, *10* (21), 1451-1458.

Veronese, F. M.; Schiavon, O.; Pasut, G.; Mendichi, R.; Andersson, L.; Tsirk, A.; Ford, J.; Wu, G.; Kneller, S.; Davies, J.; Duncan, R. PEG−Doxorubicin Conjugates: Influence of Polymer Structure on Drug Release, in Vitro Cytotoxicity, Biodistribution, and Antitumor Activity. *Bioconjugate Chem.* **2005**, *16* (4), 775–784.

Viegas, T. X.; Bentley, M. D.; Harris, J. M.; Fang, Z.; Yoon, K.; Dizman, B.; Weimer, R.; Mero, A.; Pasut, G.; Veronese, F. M. Polyoxazoline: Chemistry, Properties, and Applications in Drug Delivery. *Bioconjugate Chem.* **2011**, *22* (5), 976–986.

Wang. L.; Song, S.; van Hest, J.; Abdelmohsen, L. K. E. A.; Huang, X.; Sanchez, S. Biomimicry of Cellular Motility and Communication Based on Synthetic Soft-Architectures. *Small* **2020**, *16*, 1907680, 19 pages.

Wang, Z.; Ma, G.; Zhang, J.; Lin, W.; Ji, F.; Bernards, M. T.; Chen, S. Development of Zwitterionic Polymer-Based Doxorubicin Conjugates: Tuning the Surface Charge to Prolong the Circulation and Reduce Toxicity. *Langmuir* **2014**, *30* (13), 3764–3774.

Ward, S.M.; Skinner, M.; Saha, B.; Emrick, T. Polymer - Temozolomide Conjugates as Therapeutics for Treating Glioblastoma. *Mol. Pharmaceutics* **2018**, *15* (11), 5263–5276.

Wojtecki, R. J.; Jones, G. O.; Yuen, A. Y.; Chin, W.; Boday, D. J.; Nelson, A.; García, J. M.; Yang, Y. Y.; Hedrick, J. Developments in Dynamic Covalent Chemistries from the Reaction of Thiols with Hexahydrotriazines. *J. Am. Chem. Soc.* **2015**, *137* (45), 14248–14251.

Wong, K. E.; Mora, M. C.; Skinner, M.; Page, S. M.; Crisi, G. M.; Arenas, R. B.; Schneider, S. S.; Emrick, T. Evaluation of PolyMPC-Dox Prodrugs in a Human Ovarian Tumor Model. *Mol. Pharmaceutics* **2016**, 13(5), 1679–1687

Xiang, H.; Yin, J.; Lin, G.; Liu, X.; Rong, M.; Zhang, M. Photo-Crosslinkable, Self-Healable, and Reprocessable Rubbers. *Chem. Eng. J.* **2019**, *358*, 878–890.

Xue, Y.; Li, X.; Li, H.; Zhang, W. Quantifying Thiol-Gold Interactions Towards the Efficient Strength Control. *Nat. Commun.* **2014**, *5*, 4348, 9 pages.

Yang, J.; Kopeček, J. The Light at the End of the Tunnel—Second Generation HPMA Conjugates for Cancer Treatment. *Curr. Opin. Colloid. Interface Sci.* **2017**, *31*, 30–42.

Yang, Q.; Lai, S. K. Anti-PEG Immunity: Emergence, Characteristics, and Unaddressed Questions. *WIREs Nanomed. Nanobiotechnol.* **2015**, *7*, 655–677.

Yang, R.; Liu, X.; Ren, Y.; Xue, W.; Liu, S.; Wang, P.; Zhao, M.; Xu, H.; Chi, B. Injectable Adaptive Self-Healing Hyaluronic Acid/Poly (γ-glutamic acid) Hydrogel for Cutaneous Wound Healing. *Acta Biomaterialia* **2021**, *127*, 102–115.

Yang, W.; Chen, S.; Cheng, G.; Vaisocherová, H.; Xue, H.; Li, W.; Zhang, J.; Jiang, S. Film Thickness Dependence of Protein Adsorption from Blood Serum and Plasma onto Poly(sulfobetaine)-Grafted Surfaces. *Langmuir* **2008**, *24* (17), 9211–9214.

Yang, Z.; Snyder, D.; Pagaduan, J. N.; Waldman, A.; Crosby, A. J.; Emrick, T. Mesoscale Polymer Surfactants: Photolithographic Production and Localization at Droplet Interfaces. *J. Am. Chem. Soc.* **2022**, *144* (48), 22059–22066.

Yang, Z.; Snyder, D.; Sathyan, A.; Balazs, A.C.; Emrick, T. Smart Droplets Stabilized by Designer Surfactants: from Biomimicry to Active Motion to Materials Healing. *Adv. Funct. Mater.* **2023**, 2306819, 31 pages.

Yang, Z.; Zhao, J.; Emrick, T. Functional Polymer Zwitterions as Reactive Surfactants for Nanoparticle Capture. *ACS Appl. Mater. Interfaces* **2021**, *13* (18), 21898–21904.

Yin, Y.; Lee, J. E.; Kim, N. W.; Lee, J. H.; Lim, S. Y.; Kim, E. S.; Park, J. W.; Lee, M. S.; Jeong, J. H. Inhibition of Tumor Growth via Systemic siRNA Delivery Using Reducible Bile Acid-Conjugated Polyethylenimine. *Polymers* **2018**, *10* (9), 953, 16 pages.

Yoon, J. A.; Kamada, J.; Koynov, K.; Mohin, J.; Nicolaÿ, R.; Zhang, Y.; Balazs, A. C.; Kowalewski, T.; Matyjaszewski, K. Self-Healing Polymer Films Based on Thiol-Disulfide Exchange Reactions and Self-Healing Kinetics Measured Using Atomic Force Microscopy. *Macromolecules* **2012**, *45* (1), 142–149.

Young, G.; Bowers, R.; Hall, B.; Port, M. Clinical Comparison of Omafilcon A with Four Control Materials. *CLAO J.* **1997**, *23* (4), 249–58.

Yu, X.; Yang, X.; Horte, S.; Kizhakkedathu, J. N.; Brooks, D. E. ATRP Synthesis of Poly(2-(methacryloyloxy)ethyl choline phosphate): A Multivalent Universal Biomembrane Adhesive. *Chem. Commun.* **2013**, *49*, 6831–6833.

Zarghami, S.; Xiao, Y.; Wagner, P.; Florea, L.; Diamond, D.; Officer, D.; Wagner, K. Dual Droplet Functionality: Phototaxis and Photopolymerization. *ACS Appl. Mater. Interfaces* **2019**, *11* (34), 31484–31489.

Zeng, Z.; Chen, S.; Chen, Y. Zwitterionic Polymer: A New Paradigm for Protein Conjugation beyond PEG. *ChemMedChem* **2023**, *18* (20), e202300245, 9 pages.

Zhai, S.; Ma, Y.; Chen, Y.; Li, D.; Cao, J.; Liu, Y.; Cai, M.; Xie, X.; Chen, Y.; Luo, X. Synthesis of an Amphiphilic Block Copolymer Containing Zwitterionic Sulfobetaine as a Novel pH-Sensitive Drug Carrier. *Polym. Chem.* **2014**, 5, 1285-1297.

Zhang, P.; Sun, F.; Liu, S.; Jiang, S. Anti-PEG Antibodies in the Clinic: Current Issues and Beyond PEGylation. *J. Cont. Release* **2016**, *244* (B), 184–193.

Zhang, P.; Wu, J.; Xiao, F.; Zhao, D.; Luan, Y. Disulfide Bond Based Polymeric Drug Carriers for Cancer Chemotherapy and Relevant Redox Environments in Mammals. *Med. Res. Rev.* **2018**, *38* (5), 1485–1510.

Zhang, Q.; Qu, D.-H.; Feringa, B. L.; Tian. H. Disulfide-Mediated Reversible Polymerization toward Intrinsically Dynamic Smart Materials. *J. Am. Chem. Soc.* **2022**, *144* (5), 2022–2033.

Zhang, Z.; Chao, T.; Chen, S.; Jiang, S. Superlow Fouling Sulfobetaine and Carboxybetaine Polymers on Glass Slides. *Langmuir* **2006**, *22* (24), 10072–10077.

Zhang, Z.; Chen, S.; Jiang, S. Dual-Functional Biomimetic Materials: Nonfouling Poly(carboxybetaine) with Active Functional Groups for Protein Immobilization. *Biomacromolecules* **2006**, *7* (12), 3311–3315.

Zhang, Z. J.; Madsen, J.; Warren, N. J.; Mears, M.; Leggett, G. J.; Lewis, A. L.; Geoghegan, M. Influence of Salt on the Solution Dynamics of a Phosphorylcholine-Based Polyzwitterion. *Eur. Polym. J.* **2017**, *87*, 449–457.

Zhao, G.; Sun, Y.; Dong, X. Zwitterionic Polymer Micelles with Dual Conjugation of Doxorubicin and Curcumin: Synergistically Enhanced Efficacy against Multidrug-Resistant Tumor Cells. *Langmuir* **2020**, *36* (9), 2383–2395.

Zhao, J.; Pan, Z.; Snyder, D.; Stone, H. A.; Emrick, T. Chemically Triggered Coalescence and Reactivity of Droplet Fibers. *J. Am. Chem. Soc.* **2021**, *143* (14), 5558–5564.

Zhao, J.; Chalarca, C. F. S.; Nunes, J. K.; Stone, H. A.; Emrick, T. Self-Propelled Supracolloidal Fibers from Multifunctional Polymer Surfactants and Droplets. *Macromol. Rapid Commun.* **2020**, *41*, 2000334, 7 pages.

Zhou, L.; Triozzi, A.; Figueiredo, M.; Emrick, T. Fluorinated Polymer Zwitterions: Choline Phosphates and Phosphorylcholines. *ACS Macro Lett.* **2021**, *10*, 1204–1209.

Zhou, L.; Yang, Z.; Pagaduan, J. N.; Emrick, T. Fluorinated Zwitterionic Polymers as Dynamic Surface Coatings. *Polym. Chem.* **2023**, *14*, 32–36.

Zupancich, J. A.; Bates, F. S.; Hillmyer, M. A. Synthesis and Self-Assembly of RGD-Functionalized PEO-PB Amphiphiles. *Biomacromolecules* **2009**, *10* (6), 1554–1563.